Development of Bimetallic Emitters for Organic Light Emitting Diodes

Ross Martinscroft

PhD 2018

Development of Bimetallic Emitters for Organic Light Emitting Diodes

Ross Martinscroft

BSc (Hons), AMRSC

A thesis in part-fulfilment of the requirements of the University of Northumbria at Newcastle for the degree of Doctor of Philosophy. Research undertaken in the Department of Applied Sciences in collaboration with Merck KGaA.

November 2018

Abstract

Development of Bimetallic Emitters for Organic Light Emitting Diodes

The chemical and photophysical properties of iridium (III) and platinum (II) complexes make them ideal candidates for dopants in organic light emitting diodes (OLEDs). To date, the majority of documented complexes have contained a single heavy metal atom. Only recently have multinuclear complexes emerged as efficient emitters with the addition of a secondary metal centre having shown to improve the photophysical properties of the complexes.

This project describes the preparation of novel complexes which incorporate iridium (III) and platinum (II) as central metal ions. The work is mainly focused on the synthesis of complexes rigidly linked by heterocycles such as pyrimidine and thiazolo-[5,4-d]-thiazole (TzTz). The use of these linking heterocycles and different auxiliary ligands led to novel complexes that displayed intense luminescence at room temperature.

Chapter 2 describes the adaptation of known dinuclear Ir(III) complexes for application in solution processable OLEDs. In particular the solubility of dinuclear iridium complexes with cyclometalated C^N ligands rigidly linked by pyrimidine was improved by the introduction of the hexamethylated auxiliary ligand (III) and the removal of the fluorine groups from the auxiliary ligand in the previously published complex, (I). The complex (II) shows intense red emission (λ_{max}= 631 nm) with a high quantum yield and a short triplet state lifetime (ϕ_{lum}= 0.87, τ = 0.53 μs). The complex (II) was successfully used in solution processable OLEDs with external quantum efficiency of 8% was recorded and emission centred at λ_{max}= 646 nm.

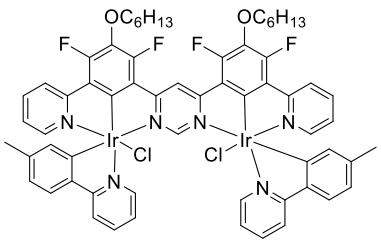

(I)
λ_{max}= 622nm
ϕ= 0.65
τ = 0.70μs

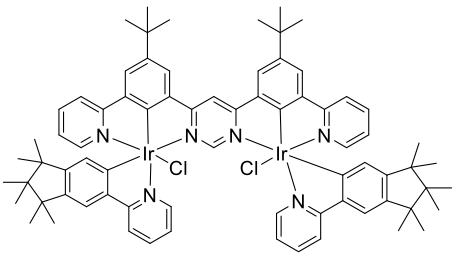

(II)
λ_{max}= 631nm
ϕ= 0.87
τ = 0.53μs

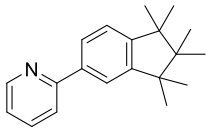

(III)

Chapter 3 describes the preparation of dianionic terdentate cyclometalating phenolate ligands and the associated complexes. These unprecedented phenolate terdentate assemblies have not previously been described in literature. The complexes (IV, V, VI, VII) showed encouraging photoluminescent properties. The mono-iridium complexes prepared showed quantum efficiencies in the range ϕ_{lum}= 0.16-0.19 and short triplet state lifetimes in the range τ = 0.46-0.58μs. The work showed that phenolate coordination is considerably more favourable in comparison to picolinate auxiliary ligands. Several changes to the structure of the O^N^C ligands have been performed do not vastly alter the photophysical properties. Despite the encouraging results, our attempts to prepare dinuclear iridium complexes with O^N^C ligands were not successful.

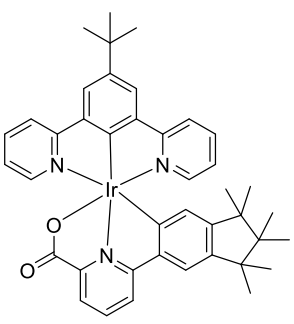

(IV)
λ_{max}= 542nm
ϕ= 0.04
τ =0.16

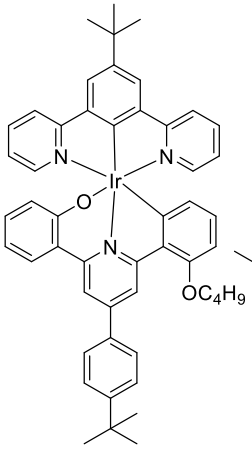

(V)
λ_{max}= 558nm
ϕ= 0.16
τ =0.48

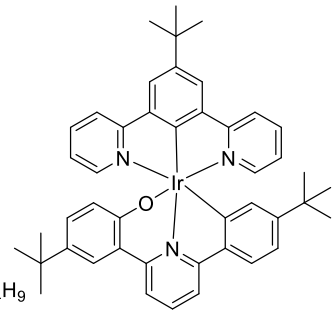

(VI)
λ_{max}= 564nm
ϕ= 0.16
τ =0.56

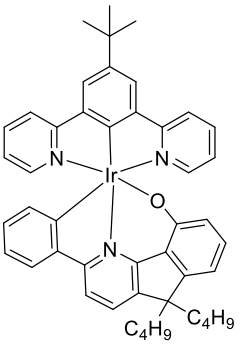

(VII)
λ_{max}= 539nm
ϕ= 0.19
τ =0.48

Chapter 4 describes the preparation of symmetrical complexes as a strategy to remove chirality from the dinuclear structures. Two novel C^N^C cyclometalated di-iridium complexes were prepared with both showing intense luminescence at room temperature. A fluorine containing complex (VIII) and a tert-butylated complex (IX) were prepared showing quantum yields of ϕ= 0.89 and ϕ= 0.74 respectively. The synthetic procedure was optimised to achieve 44% yield. This complex was used in the fabrication of a device showing a peak external quantum efficiency of η_{ext}= 19.7%.

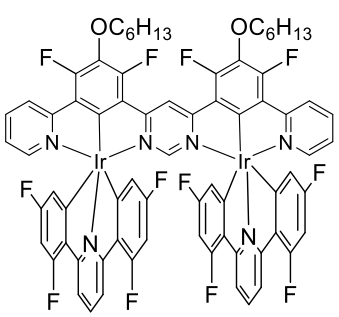

(VIII)
λ_{max}= 637nm
ϕ= 0.89
τ =1.33μs

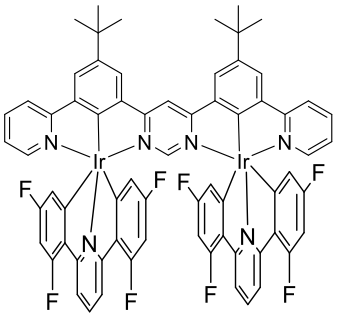

(IX)
λ_{max}= 655nm
ϕ= 0.74
τ =1.30μs

Chapter 5 describes that changing the linking heterocycle from pyrimidine to thiazole-[5,4-d]-thiazole resulted in one of the first examples of a luminescent cyclometalated complex using TzTz as a linking group. Preliminary testing of the complex (X) prepared showed a peak emission wavelength of λ_{max}= 675 nm, highlighting the effect that changing the heterocycle and increasing the π system has on the luminescent properties. Addition of a DMSO group to the dichlorobridged dimer (XI) also displayed luminescence - an abnormal observation in DMSO complexes.

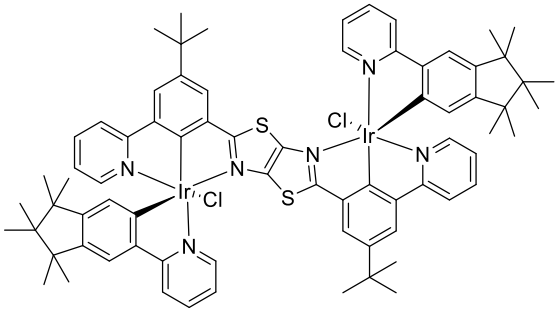

(X)
λ_{max}= 675nm

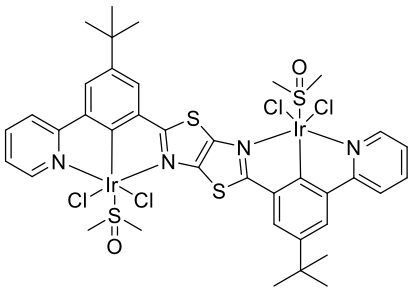

(XI)
λ_{max}= 645nm

Chapter 6 describes how the synthesis of two novel SALEN type platinum (II) complexes (XII, XIII) was investigated using 3,3' and 5,5'-bis-1,2,4-triazines. It was found that the tertiary butyl had little effect on solubility and the position of the cyclopentene ring had a greater effect. A device was fabricated using the tert-butylated complex and showed a device efficiency of η_{ext}= 10.4% and only required one emitter to produce the desired "candlelight" colour. The change of tertiary butyl to mesitylene was also investigated as a means of improving overall solubility.

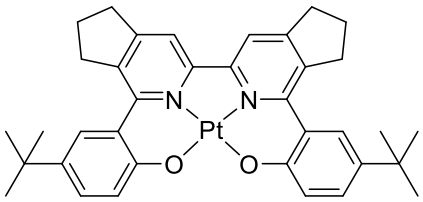

(XII)
λ_{max}= 610nm
ϕ= 0.25
τ =1.42μs

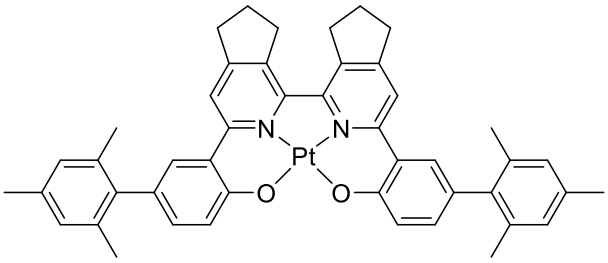

(XIII)
λ_{max}= 613nm

Overall this research shows that although difficult to prepare, the bimetallic emitters are some of the best performing phosphorescent red emitters known to date. As a result show great potential for further development as dopants in OLEDs.

Declaration

I declare that the work contained in this thesis is my own and has not been submitted for another award. The work has been carried out as a collaboration between Northumbria University and Merck KGaA. I declare that the word count of this thesis is 57471 words.

Name: Ross Martinscroft

Signature:

Date: 13/03/19

Acknowledgements

Firstly I would like to thank my supervisor Dr Valery Kozhevnikov for giving me the opportunity to carry out this research project as part of his research group. I would also like to thank him for his unwavering support, enthusiasm, encouragement and guidance throughout.

I would like to thank both Northumbria University and Merck KGaA for funding the project and providing the facilities to carry out the research. An additional thanks to Dr Christian Ehrenreich, Dr Armin Auch and Dr Anna Hayer for their assistance with photophysical testing and analysis but also their guidance during the project.

The staff of Northumbria University deserve special recognition, especially Gordon Forrest and Dr Karen Haggerty for their support and aid during my time in EBA606. I'd like to thank Dr Graeme Turnbull, Dr Kate Nicholson, Samantha Bowerbank and Dr Andrey Zaytsev for sharing their knowledge and teachings when required. I would also like to give a special thanks to Dr Ruth Daniels for imparting a world of knowledge to me during her time as part of the Kozhevnikov group and member of A510.

A huge amount of gratitude and thanks must go to my friends and colleagues in EBA510, for providing some of the best moments of my university life. An extra special thanks must go to Matt Knight, Dr Hannah Sykes, Rachel Bulmer, Dr Ruth Daniels, Dr Alex Twist and Sotiris Kyriakou for their support, reassurance and friendship. I feel I am finishing my time at Northumbria with friends for life.

Finally, I must thank my friends and family for their unfaltering support and reassurance throughout my project. I must thank my Mum and Dad for always being there and making me see sense, despite knowing nothing about what I do, except that it is luminous. All of my friends, you have been more important than you know, so thank you. Extra special mentions go to Kristy, Paul, Matthew, Andrew, Rebecca, Philip, Joe, James, the Bramley family and the Calderwood clan.

Table of Contents

List of Abbreviations

acac	Acetylacetonate
AgOTf	Silver Triflate (Silver trifluoromethanesulfonate)
bpy	2,2'-bipyridine
BpyBph	Bipyridine Bisphenolate
$CDCl_3$	Deuterated chloroform
$CHCl_3$	Chloroform
CIE	Commission Internationale D'Eclairage
C^N	Bidentate coordination by carbon and nitrogen
C^N^C	Terdentate coordinating auxiliary ligand by carbon-nitrogen-carbon
DCM	Dichloromethane
DFT	Density Functional Theory
4,6-dfppy	4,6-difluorophenylpyridine
DMF	*n,n*-dimethylformamide
DMSO	Dimethyl sulfoxide
dpm	Dipivaloylmethane
dpyb	1,3-di(2-pyridyl)benzene
dpyx	1,3-di(2-pyridyl)-4,6-dimethylbenzene
dppym	4,6-di(4-tertbutylphenyl)pyrimidine
EQE	External Quantum Efficiency (η_{ext})
ETL	Electron Transport Layer
EtOAc	Ethyl Acetate
Et_2O	Diethyl ether
fac	Facial
F_2dpyb	1,3-di(2-pyridyl)-4,6-difluorobenzene
FWHM	Full width half maximum
HCl	Hydrochloric Acid

HOMO Highest Occupied Molecular Orbital

HTL Holes transport layer

IC Internal conversion

ISC Intersystem crossing

ITO Indium Tin Oxide

KCN Potassium cyanide

K_2CO_3 Potassium Carbonate

KOAc Potassium Acetate

KOtBu Potassium tert-butoxide

KPF_6 Potassium Hexafluorophosphate

k_r/k_{nr} Radiative/non-radiative rate constants

LC Ligand Centred

LCD Liquid Crystal Display

LMCT Ligand to Metal Charge Transfer

LT_{50} Lifetime measurement to 50% of starting value

LUMO Lowest Unoccupied Molecular Orbital

MC Metal Centred

MeOH Methanol

mer Meridional

Merck1/M1 2-(1,1,2,2,3,3-hexamethyl-2,3-dihydro-1H-inden-5-yl)-4,4,5,5-tetramethyl-1,3,2-dioxaborolane

Merck2/M2 2-(1,1,2,2,3,3-hexamethyl-2,3-dihydro-1H-inden-5-yl)pyridine

Mes Mesitylene

MLCT Metal to Ligand Charge Transfer

mmol Millimoles

nm Nanometre

NMR Nuclear Magnetic Resonance

OLED(s) Organic light emitting diodes

$Pd(PPh)_3$	Tetrakis palladium triphenylphosphine
PE	Petroleum Ether (40/60 or 60/80)
phen	Phenanthroline
pic	Picolinate
piq	Phenylisoquinoline
PLQY/PLQE	Photoluminescent Quantum Yield/Efficiency
ppy	2-phenylpyridine
ppz	2-phenylpyrazole
QE	Quantum Efficiency
R_f	Retention factor
RGB	Red Green Blue
$S_0/S_1/S_n$	Singlet ground/excited state
Sal	*N*-methylsalicylimine
SOC	Spin Orbit Coupling
TD-DFT	Time Dependent-Density Functional Theory
THF	Tetrahydrofuran
tfdpyb	1,3-di(2-pyridyl)-4,6-bis(trifluoromethyl)benzene
tpy	Terpyridine
TzTz	Thiazolo-[5,4-d]-Thiazole
τ	Luminescence lifetime
ϕ	Luminescence efficiency

CHAPTER 1

Introduction

1. Introduction

Organometallic complexes have a wide range of uses including organic light emitting diodes (OLEDs), biological imaging and dye sensitised solar cells.[1-4] A number of research groups worldwide have reported on the photophysical properties, synthesis and the characterisation of a multitude of complexes, which use heavy transition metals such as iridium (III) and platinum (II) as a central metal ion.[5-14]

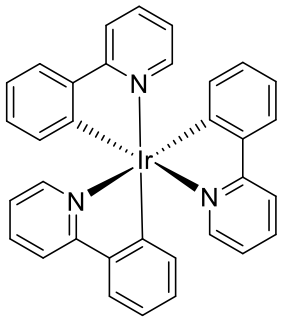

1.0.1
***fac*-Ir(ppy)$_3$**

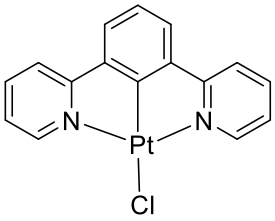

1.0.2
Pt(dpyb)Cl

Figure 1 - An example of well documented Ir(III) and Pt(II) complexes, *fac*-Ir(ppy)$_3$ (left) is one of the first examples of a charge neutral iridium complex used in OLED application. Pt(dpyb)Cl (right), is a prime example of a highly phosphorescent platinum complex.

Over the past century there has been rising interest in organometallic compounds, which has massively increased in the last decade. This is due to their potential as emitters for highly efficient organic light emitting diodes.[15] These devices have been widely studied and are now becoming common place in the technological market with applications in mobile phone and television screens.[16]

The use of OLED screens has increased benefits over liquid crystal displays (LCD's). The presence of the emissive material layer means a white backlight is not required, which has led to the development of ultra-thin products. OLED devices also possess an increased efficiency and better temperature durability whilst also providing a better colour contrast in comparison to LCD products. The design of ultra-thin OLEDs has led to the design of curved and foldable technology.

The use of these metal complexes in devices has been derived from their long excited state lifetimes and high luminescent efficiencies.[1-2, 15] This use of heavy transition metals such as iridium (III), as a central metal ion has stemmed from the high spin-orbit coupling that accompanies the addition of a heavy metal centre. This promotes the radiative triplet-singlet transition which benefits a complex's photophysical properties.[7] The central iridium ion leads to an increased energy in the metal to ligand charge transfers (MLCT) in comparison to previously used ruthenium (II) complexes, a process which will be discussed further. This increased energy is in part due to the increased level of oxidation state of the central iridium ion (Ru^{2+} to Ir^{3+}).[13] The use of heavy central metal ions aids the chemical and photochemical stability of the complex.[10, 13] The increased photochemical stability of charge-neutral complexes makes them excellent candidates as phosphors or dopants in OLED devices. The advantage of using heavy metal complexes is that the emission is tuneable to certain wavelengths of the visible spectrum through manipulation of structural features.[17]

This research project describes the preparation of bi-metallic triplet emitters for OLED application. The majority of OLED complexes currently consist of a single metal centre with coordinated terdentate auxiliary ligands. The focus of the research was the design, synthesis and production of novel bi-metallic terdentate complexes emitting in the red region of the visible spectrum. An area that has significantly fewer investigations in comparison to mono-metallic studies. There has been development of both bidentate and tetradentate complexes which show promising luminescent properties, highlighting the ability to adopt different characteristics to achieve certain wavelengths. The progress and development of highly luminescent metal complexes, covering the development of multimetallic complexes from their mono-metallic analogues will be reviewed. This will cover the synthesis and characterisation of different complexes in a range of studies leading to a detailed description of the advantages of multimetallic complexes over mono-metallic compounds. The use of these complexes in OLED devices will also be discussed in detail.

1.1. Principles of Luminescence

By definition, luminescence is the emission of light without the presence of heat. This emission of light can be differentiated by the external stimulus. Chemical reactions can result in chemiluminescence whilst exposure to electrical energy promotes electroluminescence. The complexes discussed in this project display luminescence following stimulation through absorption of photons (photoluminescence) but electroluminescence can also be displayed in some cases.

Transition metal complexes are highly dependent on and influenced by the metal and ligand components of the structure. These complexes can possess metal or ligand based properties, depending on which specific atomic orbitals are filled. However this is classed as an approximation as the molecular orbitals are spread over the entire molecule. The coupling of these characteristics and the transfer of energy between different states of the molecular orbitals can bear influence over these energy transfers and the overall luminescence.

1.1.1. Absorption

When the molecule absorbs energy in the form of a photon, the molecule is raised to an excited state from the stable and fundamental ground state (S_0). The molecule remains in the excited state (S_n) however undergoes rapid relaxation to the lowest vibrational state (S_1) by the process of internal conversion (10^{-10}-10^{-14} second timescale). This relaxation pathway is supported by Kasha's rule, that an excited molecule will undergo rapid non-radiative relaxation to a lower energy excited state.[18]

The absorbance of a molecule can indicate the capacity of a compound to absorb light, and can be useful tool when calculating or carrying out photophysical testing. The value of absorbance is directly proportional to the concentration of the sample and is a useful tool for calculating the extinction coefficient. The extinction coefficient highlights the ability of a compound to absorb light at a specific wavelength which can be calculated using Beer-Lambert law, as shown in Equation 1.

Equation 1 - The Beer- Lambert equation used to calculate the absorbance (A), using the extinction coefficient (ε), sample concentration (c) and the length of the pathway (L).

$$A = \varepsilon . c . L$$

The extinction coefficient is a useful value as a form of identifying the presence of a typically 'forbidden' process. The use of a heavy metal as a central ion can often change this and facilitate and promote phosphorescence (a typically 'spin forbidden' process).

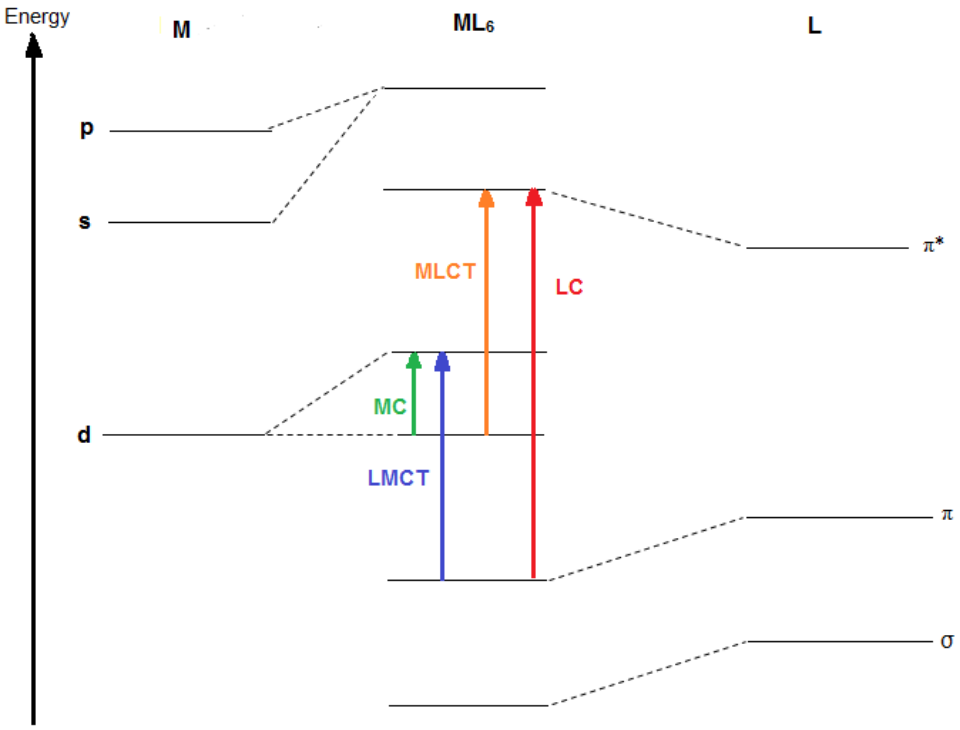

Figure 2 - A diagram highlighting the possible energy transitions upon excitation of an octahedral metal complex. The diagram shows the different transitions with the metal centred (MC) transition taking place between the d-d orbitals on the central metal atom. The ligand-to-metal charge transfer (LMCT) is predominantly between the neutral π orbitals of the ligand and the excited d state of the metal. The metal-to-ligand charge transfer (MLCT) occurs between the ground d state of the metal and the π* orbital of the ligand. The ligand centred (LC) transition takes place exclusively between the π and the π* orbitals on the ligand moieties. There are few transitions that take place from the σ orbital of the ligand.

When exposed to an external stimulus, energy is absorbed and the resulting transition between orbitals can aid in the characterisation of the excited state.[19] The transition of energy can often be denoted as charge transfer (CT), this describes the movement of an electronic charge between ligand to metal or metal to ligand, the charge can also remain on the metal or ligand

components. An example of these transitions is the metal to ligand charge transfer (MLCT), which is defined as the transfer of an electron from the d orbital of the metal centre to the π* orbital of the ligand.[20] The process of ligand-to-metal charge transfer (LMCT), is the electronic movement of an electron from an orbital on the ligand to an orbital on the central metal ion. Transitions of energy between two orbitals centred on the metal are called metal centred transitions (MC) and the transitions located on the ligand orbitals are ligand centred (LC). The nature of the lowest excited stated is defined by the ordering of the molecular orbitals which is in turn dependent on the structure of the molecule. Alterations to the ordering of the molecular orbitals can be achieved through modifications to the structure which will be described further.

The use of iridium (III) as a central metal ion is attributed to the encouraging luminescent properties. The lowest excited state emission is typically triplet in nature for iridium complexes. Phosphorescent emission from the singlet excited state is forbidden and therefore the complexes rely on intersystem crossing and spin-orbit coupling for triplet state emission.[21] The emissive state has been shown to be predominantly ^{3}MLCT in nature, using the occupied 5d electrons of the iridium atom and the unoccupied π* orbitals of the cyclometalated 2-phenylpyridine ligand.[22-25] For systems with a high level of ^{3}MLCT character in the emissive state, the required process of intersystem crossing has been determined to be approximately 50 femtoseconds (fs).[26] For instance, the process of intersystem crossing for the complex, $Ir(ppy)_3$ is approximately 100 fs.[27] Most iridium complexes have an emissive state of ^{3}MLCT character. The emission states can be split into spin levels in the absence of a magnetic field, this is called zero-field splitting. This process is more common in transition metal complexes due to the presence of unpaired electrons. The sub-states as described have a direct effect on the emission properties at ambient temperatures. A large zero field splitting constant indicates efficient spin-orbit coupling (SOC) which can lead to a rapid and emissive decay time. This can also result in a decrease in the population of the highest thermal sub-state which can be identified as a limiting factor. Efficient SOC can directly result in effective intersystem

crossing between the excited singlet state and the excited triplet state which allows harvesting of the triplet states and provides the basis for high efficiencies in OLED devices.[21, 28] The mechanisms of emission will be discussed further.

1.1.2. Emission

Once the energy has relaxed to a lower excited state (S_1), the energy can be released through different processes, depending on the excited state. There are two main forms of energetic release, radiative decay refers to the release of photons as energy from either the singlet or triplet excited states. Radiative decay can often manifest as luminescence which can be separated into fluorescence and phosphorescence. Non-radiative decay refers to the release or dispersion of energy across and between the molecular structure of surrounding molecules and solvent.

Fluorescence is the short-lived release of radiative energy from the excited singlet state (S_1) to the singlet ground state (S_0) with a typical relaxation within the nanosecond range (10^{-9} to 10^{-8} seconds). In order for a compound to emit light, the complex must absorb a photon of a specific energy. The electrons of the molecule are then increased to an excited singlet state (S_1, S_2 and S_n). Once the electron is in an excited state, the energy dissipates in different ways; one of the main process is vibrational relaxation; a rapid non-radiative process where the energy from the excited molecule is transferred to surrounding molecules. If the vibrational energy levels overlap with the electronic energy levels, it is possible for the excited electron to transfer to a different vibration level in a lower electronic excited state; this is internal conversion (labelled in Figure 3). The higher the level of overlap increases the likelihood of the conversion taking place. From this point the energy can take two routes, the energy can either be released as a photon which can be termed 'Fluorescence'.[29] This emission of light from the singlet excited state does not require a change in the spin multiplicity, as the electrons are anti-parallel (as seen in the ground state). The emission of energy as fluorescence takes place at lower frequencies as some energy has been lost through vibrational relaxation.

An alternative route that can be taken is intersystem crossing (labelled in Figure 3), the conversion of an electron from the excited singlet state to the excited triplet state.[18] The introduction of a heavy metal centre produces strong spin-orbit coupling which results in efficient intersystem crossing.[30] From this point the energy is often released as phosphorescence through the transition of energy from the excited triplet state (T_1) to the singlet ground state (S_0).[31]

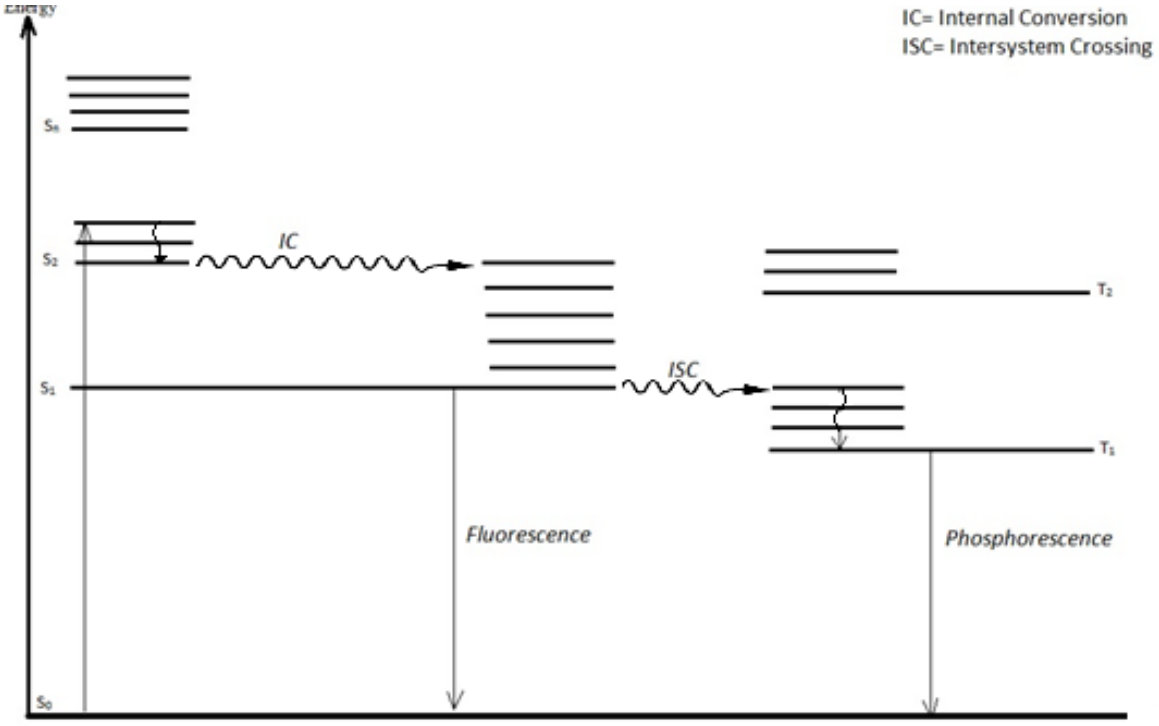

Figure 3 - A Jablonski diagram to show the transfer of energy through the excited states, resulting in different types of energy release back to the singlet ground state. The radiative processes are depicted by solid downward arrows. The "wavy" arrows represent non-radiative transitions.

The process of intersystem crossing to phosphorescence is often considered "spin forbidden" however the inclusion of a metal centre facilitates this process by producing strong spin orbit coupling, this will then increase the efficiency of the crossing from S_1 to T_1.

Phosphorescence is the release of energy from the excited triplet state which is often a longer lived emission in comparison to fluorescence. It is thought to be forbidden due to the change in spin required during intersystem crossing (the change from S_1 to T_1).[31] Typical lifetimes of phosphorescence are generally in the microsecond range (10^{-6} to 10^{-4} seconds).[32] Due to the

crossing from the singlet excited state to the excited triplet state, the phosphorescent emission is often a longer lived process and this transfer results in a large shift of emission from the absorption wavelength. This is the Stokes shift, the difference between the absorption and emission wavelengths. This difference is typically larger for phosphorescence than fluorescence.

Phosphorescent emission is highly advantageous for technological application, the release of light from the triplet state can be harvested and this results in a theoretical device quantum efficiency of 100% (fluorescence based devices are often limited to 25%), a process which is further benefitted by the inclusion of a heavy metal.[28] This is extremely beneficial to OLED devices as highly efficient emitters are desirable for use as dopants in the emissive layer.

1.1.3. Measurements of Luminescence

The lifetime of emission (τ_{obs}) and the quantum yield (ϕ) of a compound can be measured experimentally and are related in the form of rate constants that measure the radiative (k_r) and non-radiative (k_{nr}) rates of decay. The equation used to calculate the lifetime of emission is shown in Equation 2 below.

Equation 2 - The equation used to quantify the observed lifetime of luminescence from a complex.

$$\tau_{obs} = \frac{1}{(k_r + k_{nr})}$$

The efficiency of the emission can be associated with and defined by the luminescent quantum yield. This can be calculated by using Equation 3 as described by Friend and coworkers.[33] In support, as part of Kasha's rule, Vavilov's rule states that the quantum yield of a compound is independent of emission wavelength.[34]

Equation 3 - The quantum yield equation outlined by Friend and co-workers.

$$\phi = \frac{number\ of\ photons\ emitted}{number\ of\ photons\ absorbed}$$

Equation 3 can be used to calculate the quantum yield uses the lifetime of emission rate constant (τ_{obs}). The relationship stands between the observed lifetime and the radiative rate constant which gives a more accurate insight into the quantum yield of the compound than the equation outlined above. The below equation highlights the relationship between the quantum yield and radiative rate constants.[20] The overall equation can be simplified by using the observed luminescent lifetime equation as shown below.

Equation 4- The equations below show the relationship between the radiative rate constant and the quantum efficiency (left). The equation can be simplified to a linear equation by using the luminescent lifetime equation (τ).

$$\phi = \frac{k_r}{(k_r + k_{nr})} \quad or \quad \phi = k_r \tau$$

Red emitters typically have lower quantum efficiencies due to the decreased energy gap between the highest occupied molecular orbital (HOMO) and the lowest unoccupied molecular orbital (LUMO). This decrease of the energy gap can result in vibrational deactivation of complexes close to the near infra-red region.[35] The energy gap increases in the blue region of the spectrum, the MLCT state becomes close in energy to the lower lying MC ground state which is deactivating and often leads to the loss of energy from the excited state.

1.2. Metal Complexes of Iridium (III) and Platinum (II)

Heavy metal complexes that contain a single metal centre are typically accompanied by chelating auxiliary and ancillary ligands. These ligands often take similar forms using pyridyl or phenyl based moieties and have been widely studied by numerous research groups. As an example, some typical cyclometalating and coordinating ligands are highlighted in Figure 4.

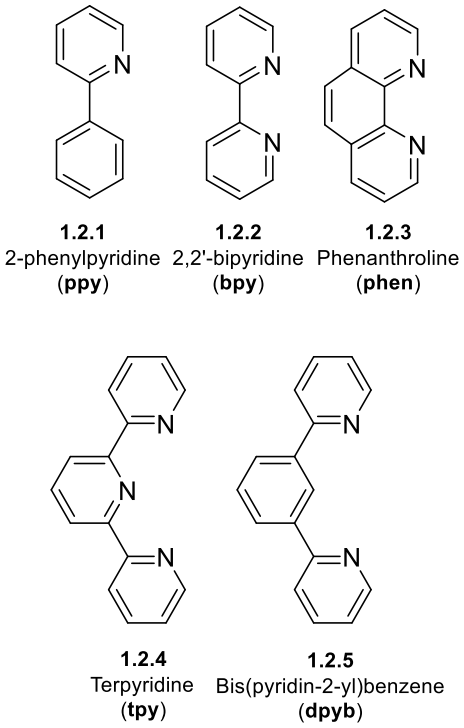

Figure 4- A selection of the typical bidentate and terdentate ligands used to generate luminescent metal complexes used as either auxiliary or ancillary ligands. Often the ligands developed are analogues of the above compounds.

The first recorded luminescent heavy metal complex utilised ruthenium(II) as a central metal ion and was discovered by Brandt and co-workers in 1959. The complex used a tris-coordinated assembly with 2,2'-bipyridine (bpy).[36] The $[Ru(bpy)_3]^{2+}$ complex has been extensively researched and has been applied to oxygen sensing and photocatalysis. The dicationic charge meant that the poor solubility limits the use of this complex in some applications such as OLEDs.[37-38]

Over time the use of transition metals has increased and iridium (III), rhodium (III), platinum (II) and osmium (II) have been used to form luminescent complexes. This development has led to the intense focus on platinum (II) and iridium (III) complexes using ligands outlined in Figure 4 such as 2,2'-bipyridine (bpy) and phenanthroline (phen). As complexes using these ligands often lead to a charged compound, alterations to the structures resulted in the focus on similar cyclometalating ligands such as 2-phenylpyridine (ppy) and its terdentate analogue 1, 3-dipyridylbenzene (dpyb).[2, 10, 12-13, 39-42]

Cyclometalation is the binding of a multidentate ligand to a central metal ion via a metal-carbon bond. The remaining groups bind with the metal through coordination using groups such as N, O or S. The use of cyclometalating ligands such as ppy are highly advantageous in comparison to the analogous polypyridyl ligands like bpy due to their overall negative charge. The ppy ligand can bind to 2nd and 3rd row transition metals (such as ruthenium (II) or iridium (III)) as a C^N coordinating ligand. The use of an anionic ligand is beneficial due to the deprotonation of the aromatic C-H on the phenyl ring. Following the deprotonation, the resulting C^- is a very strong σ donor and this is synergistic with the π-accepting pyridyl moiety.[43] These cyclometalating ligands raise the energy level of d-d excited states on the metal centre and these act as a pathway for non-radiative deactivation. Due to the increase in energy the d-d states are less likely to be populated at low temperatures. As a result, there is an increased likelihood that the excited state will release energy radiatively and allow for the quantum yield to be measured for the cyclometalated luminescent metal complexes.[43-44]

The effect of changing the cyclometalating ligand can be displayed by square planar Pt(II) complexes that utilise terdentate tpy and dpyb ligands. The terpyridyl complex (**1.2.6**) has no visible emission and this can be attributed to the lack of a metal-carbon bond, in contrast Pt(dpyb)Cl is one of the brightest platinum complexes known to date with ϕ= 0.6 and τ= 7.2 μs.[45]

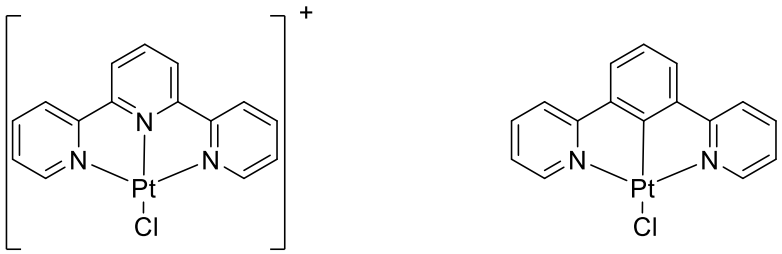

1.2.6
$[Pt(tpy)Cl]^+$
No visible
emission (RT)

1.0.2
Pt(dpyb)Cl
ϕ_{lum}= 0.6
τ : 7.2us

Figure 5 - Two known square planar Pt(II) complexes, $[Pt(tpy)Cl]^+$ has no visible emission at room temperature (RT) however alteration to the central pyridyl moeity results in the highly luminescent Pt(dpyb)Cl. The quantum yield (ϕ_{lum}) and triplet state decay time (τ) is shown for Pt(dpyb)Cl.

The process of complex tuning typically involves the substitution of either π-donating or π-accepting groups to the structure of the ligands. The tuning of a complex can be simplified or facilitated if the HOMO and LUMO are localised within the structure which will be discussed in detail.

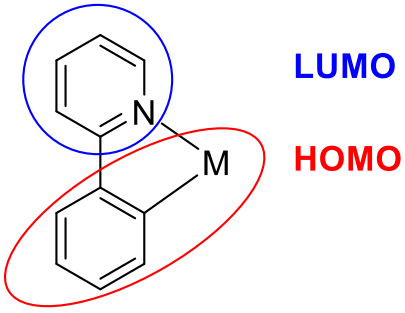

Figure 6- The HOMO and LUMO locations in the widely documented 2-phenylpyridine ligand. Typically the HOMO is located on the central metal ion and across the cyclometalated phenyl moiety of the ligand. The LUMO is generally located on the pyridyl group of the ligand.

The structure in Figure 6 highlights the typical locations of the highest occupied and lowest unoccupied molecular orbitals for a metal-coordinated ppy ligand. This separation is typical with the HOMO being localised to the metal and aryl group of the phenyl ring on the ligand as this is a strong σ donor and the C^- forms a strong bond with the central metal ion.

The separation of the different orbitals can also be demonstrated by the use of terdentate ligands such as 1,3-di(2-pyridyl)-4,6-dimethylbenzene (dpyx) with 2-phenylpyridine (shown in Figure 7) and a monodentate chloride ligand. Brulatti and co-workers studied this and displayed the separation of the orbitals and the effects that different substituents had on the localisation of the HOMO.[10]

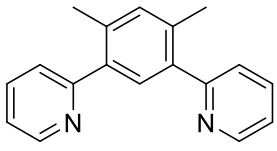

1.2.7
1,3-di(2-pyridyl)-4,6-dimethylbenzene
(dpyx)

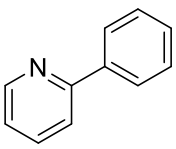

1.2.1
2-phenylpyridine
(ppy)

Figure 7 - Examples of the ligands dpyx and ppy used in complexes by Brulatti *et al.*[10]

It was shown that the inclusion of an increasing amount of fluorine groups or fluorine dominant groups resulted in a migration of the electrons when comparing the HOMO and the lower energy orbital HOMO-1. Using the complex, Ir(dpyx)(ppy)Cl, density functional theory (DFT) showed that the HOMO was delocalised predominantly across the central metal ion, the monodentate chlorine and the N^C^N cycle of the cyclometalated dpyx ligand. However when the energy of the frontier orbitals was decreased to HOMO-1, the electron density became delocalised across the metal, halide and the aryl moiety of the N^C ppy ligand. The inclusion of fluorine atoms as 1,3-di(2-pyridyl)-4,6-difluorobenzene (F_2dpyb) or trifluoromethyl groups as 1,3-di(2-pyridyl)-4,6-bis-(trifluoromethyl)benzene (tfdpyb) in the place of the methyl groups resulted in the inversion of the localisation of electron density. The HOMO showed the electrons are delocalised across the aryl group, halide and central metal. However, the lowering of energy resulted in the electrons being predominantly delocalised across the cyclometalating N^C^N group and the central metal.

	HOMO–1	HOMO	LUMO	LUMO+1
1a	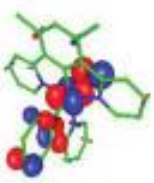	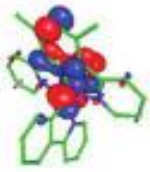	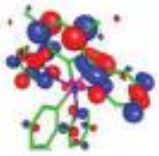	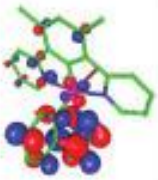
E / eV	–4.990	–4.980	–1.453	–1.295
% contribution				
Ir	25	33	0	0
N^C^N	20	37	89	18
Cl	32	23	0	0
N^C	23	7	11	82
2a	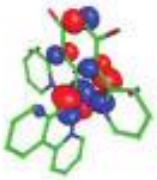	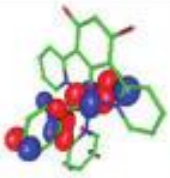		
E / eV	–5.373	–5.269	–1.731	–1.565
% contribution				
Ir	45	45	2	7
N^C^N	21	8	93	88
Cl	27	27	0	4
N^C	7	20	5	1
3a	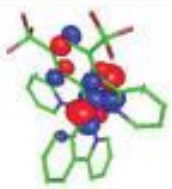	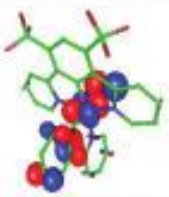		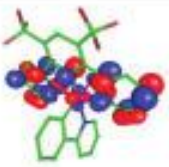
E / eV	–5.608	–5.491	–2.527	–1.787
% contribution				
Ir	42	43	3	6
N^C^N	19	6	96	89
Cl	32	31	0	4
N^C	7	20	1	1

Figure 8 - A figure showing the electron density for the complexes in the study by Brulatti and co-workers. The energy levels of each orbital are detailed with the HOMO decreasing upon the increased inclusion of fluorine. The percentage contribution to each orbital of the different groups is also detailed.[10] **1a**=Ir(dpyx)(ppy)Cl, **2a**= Ir(F_2dpyb)(ppy)Cl and **3a**= Ir(tfdpyb)(ppy)Cl. The figure is taken directly from the study by Brulatti *et al.*[10]

The table in Figure 8 shows how the electron density changes between the different frontier orbitals. The complexes also displayed no discernible difference in the LUMO with electron density being delocalised across the N^C^N moiety of the terdentate ligand in all complexes. The percentage contribution does not change from the LUMO to the higher energy LUMO+1 in the fluorinated complexes (**2a**/**3a**) however the electron density migrates from the N^C^N group almost entirely to the N^C ppy ligand in the non-fluorinated dpyx compound (**1a**).[10]

The use of cyclometalating ligands is now widely researched due to the promising structural and chemical properties of the derived metal complexes. The work described in this section will investigate and describe the previous work that has been carried out using known ligands such as 2-phenylpyridine and 1,3-di(2-pyridyl)benzene including any associated analogues. As these groups are easily adaptable, this has facilitated the tuning of complexes to reach a wider range of colours in the visible spectrum for use in optoelectronic applications such as organic light emitting diodes (OLED's). The strategies of complex development will be discussed and the further benefits of incorporating a secondary metal centre. The use of a multinuclear complex will be discussed and the reasons why these complexes show promise for the development and increase in device efficiency of OLEDs.

1.2.1. Mononuclear Metal Complexes of Iridium(III) and Platinum(II)

The use of iridium (III) and platinum (II) in cyclometalated complexes has been widely researched and the use of these as central metal ions with bidentate ligands has developed over time using 2-phenylpyridine and similar derivatives from which highly luminescent and tunable complexes have been observed.[44, 46] The development of homoleptic and heteroleptic complexes has accelerated with tuning resulting in a multitude different complexes. In tris-cyclometalated complexes, a homoleptic complex can be described as possessing 3 coordinated cyclometalating ligands, a heteroleptic complex has at least 2 cyclometalating ligands and a different ancillary group such as acetylacetonate (acac) or picolinate (pic).[47]

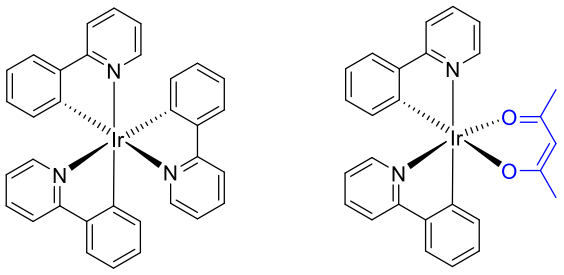

1.0.1
fac-Ir(ppy)$_3$
Homoleptic

1.2.8
Ir(ppy)$_2$(acac)
Heteroleptic

Figure 9 - A figure showing the difference between typical homoleptic and heteroleptic complexes, *fac*-Ir(ppy)$_3$ and Ir(ppy)$_2$(acac) respectively.

The initial work in the field of heavy transition metal complexes focused predominantly on the formation of the tris-coordinated ruthenium (II) complexes, for example $[Ru(bpy)_3]^{2+}$. The complexes synthesised offered little to no emission tuning as a result of thermal occupation of the non-emissive metal centred state (^{3}MC).[48] Due to the low emissive nature of the ruthenium complexes, focus moved to the use of iridium (III) as a central metal ion, which would facilitate the colour tuning due to a stronger and more stable ligand field.

Prior to 1986, bright luminescence from square planar d^8 complexes was relatively uncommon, with complexes displaying luminescence at low temperatures (~77K).[49-51] The luminescence displayed by these compounds could be associated with intraligand interactions (π-π^*). A study by Von Zelewsky and co-workers documented a Pt(II) complex that exhibited metal to ligand interactions within the excited state.[52] Further developments to Pt(II) compounds showed their luminescence in solution at room temperature an added benefit of the square planar complexes.[53] Cyclometalated Pt(II) complexes often display high quantum yields and a long lived emission from the excited electronic states which originate from a ^{3}LC (ligand centred) state and influences from the MLCT states provided by the strong spin-orbit coupling from the heavy metal central ion.[14]

Von Zelewsky and co-workers developed a library of bis-cyclometalated complexes using a series of analogous ligands of 2-phenylpyridine.[54] The ligands prepared used cyclometalating C^N ligands and exploited the tuning capabilities of transition metal complexes by altering the different moieties present in the structure.[55] Some of the complexes developed by Von Zelewksy and co-workers are shown in Figure 10.[54-55]

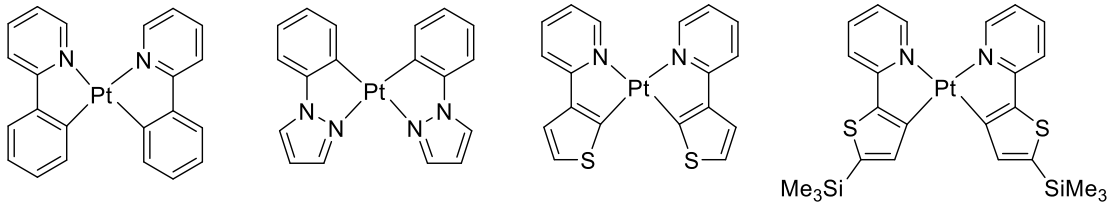

1.2.9 **$Pt(ppy)_2$**

1.2.10 **$Pt(ppz)_2$**

1.2.11 **$Pt(thpy)_2$**

1.2.12 **$Pt(thpy\text{-}SiMe_3)_2$**

Figure 10 - Examples of the bis-cyclometalated C^N platinum(II) complexes, $Pt(ppy)_2$, $Pt(ppz)_2$, $Pt(thpy)_2$ and $Pt(thpy\text{-}SiMe_3)$ synthesised by Von Zelewsky and co-workers.

The synthesis of the complexes (**1.2.9**-**1.2.12**) shown in Figure 10 were not achieved through the traditional route of heating under reflux in 2-ethoxyethanol and water with potassium tetrachloroplatinate (K_2PtCl_4). This strategy yielded complexes with the general formula, Pt(C^N)(HC^N)Cl in high yields due to the lack of cyclometalation of one of the aryl rings resulting in the presence of a monodentate chloride ligand, displayed in complex **1.2.13**.[56]

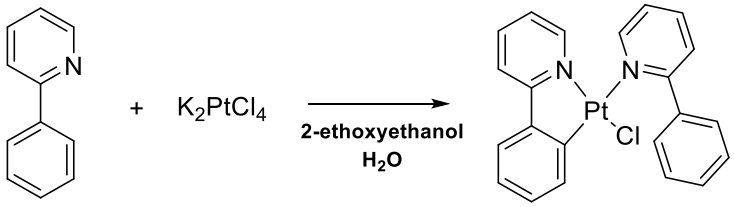

1.2.1 **ppy**

1.2.13 **Pt(ppy)(ppyH)Cl**

Scheme 1- The reaction scheme showing the outcome of using 2-ethoxyethanol with potassium tetrachloroplatinate to form the square planar platinum complex as investigated by Cho and co-workers. This example uses 2-phenylpyridine as an example of an ancillary ligand.

A method to avoid the formation of the Pt(C^N)(HC^N)Cl species (**1.2.13**) was displayed by Gianini and co-workers.[57] This was done by lithiation of the coordinating C^N ligand using *tert*-butyllithium, a procedure previously described by Kaufmann.[58] In place of K_2PtCl_4, the platinum precursor used was $Pt(SEt_2)Cl_2$, resulting in the synthesis of bis-cyclometalated Pt(II) complexes with a predetermined chirality.[57]

Typically the luminescence of homoleptic platinum (II) complexes is poor, typically showing low quantum yields. Due to this, studies typically began to investigate the design and synthesis of heteroleptic complexes.[59-62] By using accompanying ancillary ligands such as acetylacetonate (*acac*) and picolinate (*pic*) to further tune the emission profile. The design of heteroleptic complexes was thought to yield complexes with more promising luminescent properties, the general formula of these complexes is [Pt(C^N)(L)], with L denoting the ancillary ligand. The benefits of heteroleptic complexes is that through the tuning and alteration of the ancillary ligand, inclusion of additional or different functional groups will lead to varying levels of electron density surrounding the central metal ion. The varied levels of electron density results in a change to the MLCT state and this directly affects the emission and wavelength of the resulting complex.[59]

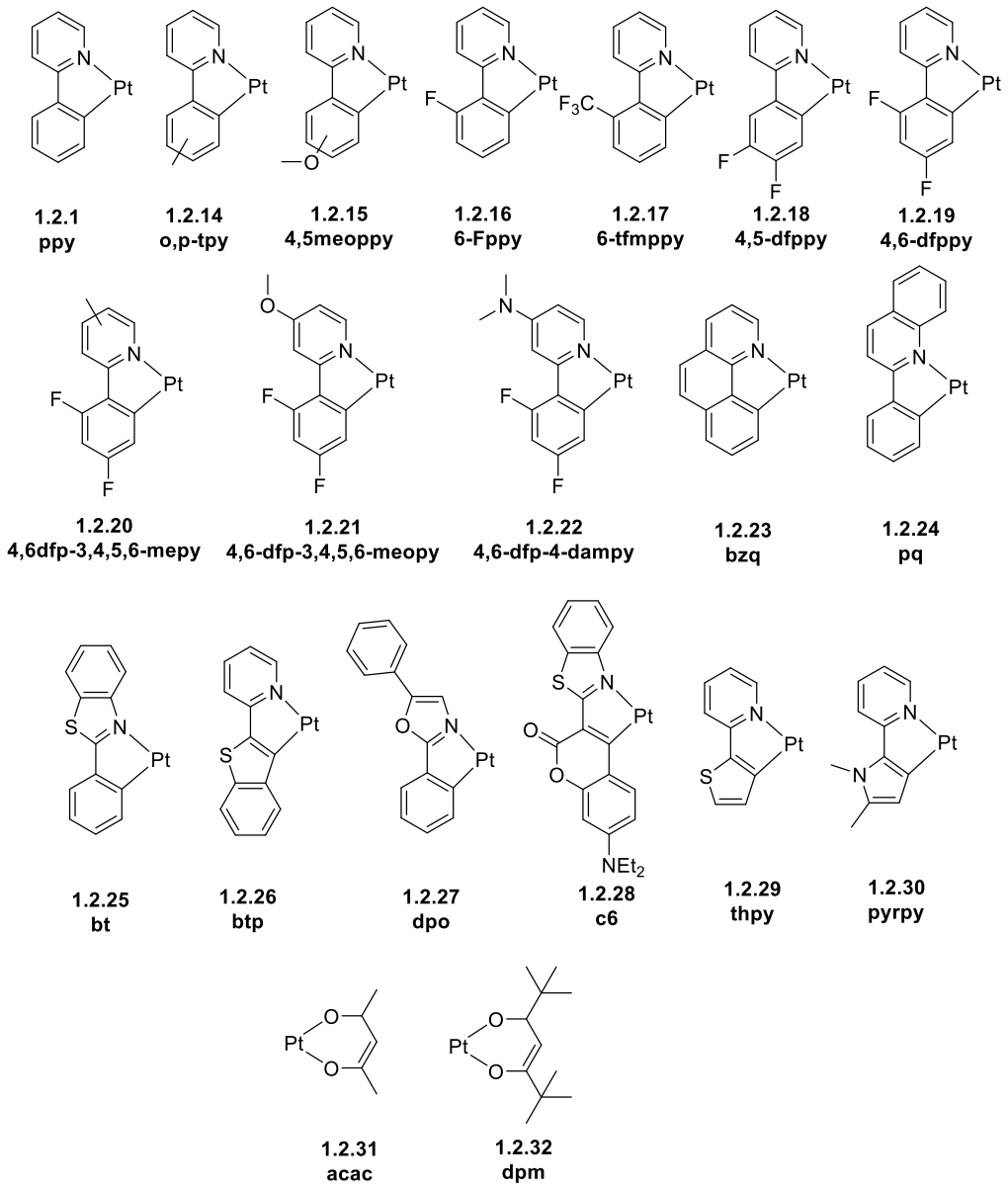

Figure 11 - The bidentate cyclometalating C^N ligands studied by Brooks and co-workers with the associated abbreviations. The ancillary ligands used in the study, acetylacetonate (**1.2.31**) and 2,2,6,6-Tetramethyl-3,5-heptanedione (**1.2.32**) are shown at the bottom with the platinum metal centre.[59]

Brooks and co-workers developed a library of cyclometalating bidentate C^N ligands for use with β-diketonate ancillary ligands, acetylacetonate (acac) and dipivaloylmethane (dpm).[59] The study highlighted that changes to the structure did result in changes in the emission. Changes to the conjugation of the C^N system, decreased the ligand centred transitions (^{3}LC) by simultaneously lowering the LUMO level and raising the HOMO level, resulting in a red shift of the emission. This can be seen with the structures displayed in Figure 11, as the compounds Pt(bpy)(dpm), Pt(pq)(dpm) and Pt(btp)(acac) all emit in the yellow-red region, in

contrast to Pt(ppy)(dpm) which emits in the green region.[59] The different complexes showed promising luminescent properties with peak quantum yields in the range ϕ= 0.02-0.25 at room temperature. This data is shown in Table 1.

Table 1 - The table of photophysical properties displayed by the square planar Pt(II) complexes synthesised by Brooks and co-workers.

Cyclometalating C^N Ligand	**Ancillary Ligand**	**Emission, λ_{max}, nm**	**Lifetime, τ_{298} (RT), µs.**	**Φ_{PL}, Quantum Yield.**
ppy	acac	**486**	**2.6**	**0.15**
p-tpy	acac	**485**	**4.5**	**0.22**
6fppy	dpm	**476**	**<1.0**	**0.06**
4,5-dfppy	acac	**484**	**3.0**	**0.22**
4,6-dfppy	acac	**466**	**<1.0**	**0.02**
4,6-dfppy	dpm	**466**	**<1.0**	**0.02**
4,6-dfp-5-mepy	dpm	**472**	**<1.0**	**0.05**
4,6-dfp-4-meopy	dpm	**456**	**<1.0**	**-**
4,6-dfp-4-dmapy	dpm	**447**	**<1.0**	**-**
4-meoppy	dpm	**490**	**7.4**	**0.20**
c-6	acac	**589**	**27.9**	**0.25**
Btp	acac	**612**	**3.4**	**0.08**
thpy	acac	**575**	**4.5**	**0.11**
pyrpy	acac	**603**	**7.1**	**0.02**

The data highlights that groups using more polarisable atoms such as sulfur or nitrogen within the ring system have displayed lower transition energy values and emit in the orange region of the visible spectrum, as displayed by ***c-6, btp, thpy*** and ***pyrpy***.[59] It can also be concluded

that the variation of the cyclometalating ligands had a more significant effect on the photophysical properties in comparison to the alteration of the β-diketonate ancillary ligands.

A study in 2009 by Tsujimoto *et al*, built on previous work investigating Pt(C^N)(O^O) complexes described by Brooks and co-workers. The study showed that changing the ancillary ligand and alterations to the cyclometalating ligand can result in significant increases in the quantum yield of the resulting complexes. The changes put forward displayed highly promising quantum yield values for each complex (ϕ= 0.02-0.59) at room temperature.[60]

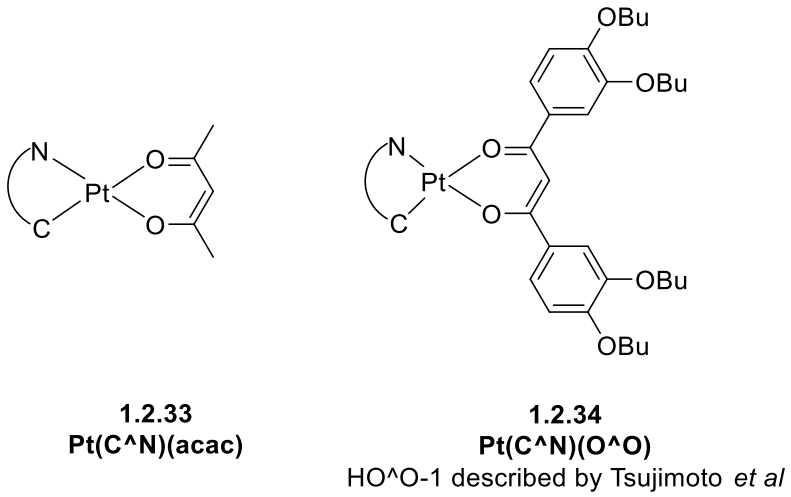

1.2.33
Pt(C^N)(acac)

1.2.34
Pt(C^N)(O^O)
HO^O-1 described by Tsujimoto *et al*

Figure 12 - The typical platinum(II) complex using acetylacetonate as an auxiliary ligand (left), one of the typical structures of a complex and β-diketonate ligand (HO^O-1) described by Tsujimoto and co-workers (right). [60]

The study showed the effects of changing the cyclometalating ligand. It was found that the phosphorescence lifetimes were decreased and the quantum yields increased by using the O^O based ligand displayed in Figure 12. The quantum yields were also shown to decrease as the wavelength became red shifted further (>620 nm). This decrease can be attributed to vibrational decay and possible triplet-triplet annihilation, a common issue in platinum complexes.[60]

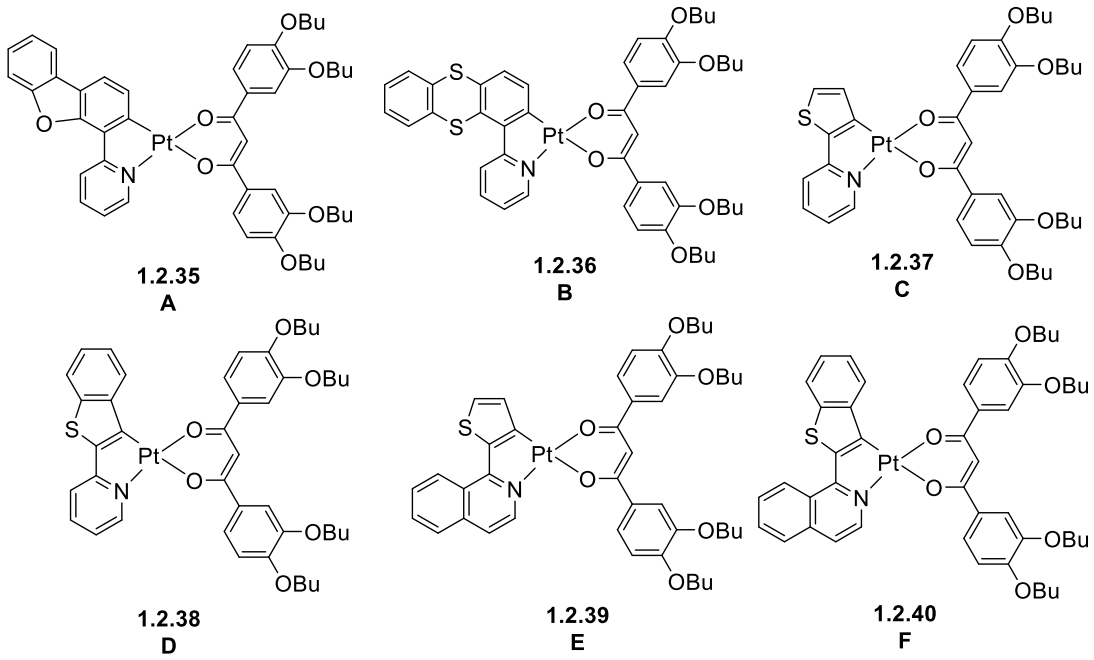

Figure 13 - The Pt(II) complexes (**1.2.35-1.2.40**) synthesised by Tsujimoto and co-workers with peak quantum efficiencies of ϕ= 0.59, the changes to the cyclometalating ligand resulted in the red shift of emission, likely due to the decreasing in the energy gap between the HOMO and LUMO.[60]

In addition to the development of bidentate platinum complexes, there has been movements toward the development of mononuclear platinum complexes that employ tridentate ligands. As previously mentioned, Pt(dpyb)Cl was shown by Rausch *et al* to display moderate quantum yields of ϕ= ~0.60 and average lifetimes τ= 7.2μs in deoxygenated conditions.[45] There are benefits of using a terdentate ligand such as 1,3-di(2-pyridyl)benzene (dpybH), for instance the efficient emissive states are predominantly ^{3}MLCT in character and not a ligand centred (^{3}LC) transition. The use of this ligand adds to the conjugated system which increases the stability and reduces the HOMO level. This reduction often results in a red shift in the emission of the complex.[15, 62] Adaptations to the terdentate ligand have been carried out by Koo *et al*.[61, 63] The study described that a pyridyl group was substituted for a pyrazole ring. This change resulted in an N^N^C coordination to the central platinum (II) ion. The developed complexes were poorly luminescent with quantum yield values peaking at ϕ=0.3. However each complex showed relatively long lifetimes of τ= 0.57-2.00μs.[61, 63]

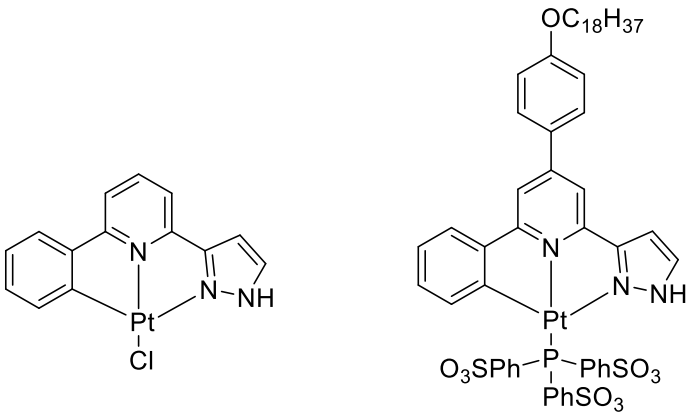

1.2.41
10
ϕ= 0.10
τ= 0.57μs

1.2.42
11
ϕ= 0.30
τ= 1.95μs

Figure 14 – The structures of two of the terdentate Pt (II) complexes synthesised by Koo and co-workers for use in bioimaging applications. Compounds 10 and 11 in the review by Mauro and co-workers.[61, 63-64]

The design and synthesis of homoleptic and heteroleptic complexes is not exclusive to platinum (II). The use of iridium (III) as a central metal ion with cyclometalating bidentate ligands has been a major focus of study. Notably one of the first developed highly luminescent complexes was the tris-cyclometalated $Ir(ppy)_3$ which can exist in two optical isomers, facial (*fac*) and meridional (*mer*). Watts *et al* prepared $Ir(ppy)_3$ in 1985, which consequently stimulated a large amount of research by Forrest *et al*.[65-67] The study of the green emitting complex indicated a high level of thermal stability (stable to ~380°C).[68-69] As these properties showed promise, Kido and co-workers fabricated an OLED device using *fac*-$Ir(ppy)_3$ which displayed intense green phosphorescence and high levels of device efficiency (η_{ext}= 0.29).[70]

The tris-cyclometallated complex of *fac*-$Ir(ppy)_3$ has been shown to display a phosphorescence typical ^{3}MLCT character as previously discussed, and Watts *et al* primarily reported a luminescence quantum yield ϕ= 0.4 (±0.1) in deoxygenated conditions. The quantum yield of *fac*-$Ir(ppy)_3$ has since been revised to be approximately ϕ= 0.97 by Kawamura and co-workers.[71] The synthesis of *fac*-$Ir(ppy)_3$ initially began due to its production as a side product from the fabrication of the dimer $(Ir(ppy)_2Cl)_2$.[25] Advancements in the synthesis have resulted in the development of the homoleptic complex in higher yields. This

has been achieved by using $Ir(acac)_3$ and heating in glycerol with an excess of the cyclometalating ligand ppyH, as initially described by Watts *et al*.[67, 72] King and co-workers described the synthesis of this complex using iridium chloride hydrate in place of the more expensive $Ir(acac)_3$. The *facial* isomer was synthesised by heating in glycerol and washing with methanol in a 10% yield.[67] Watts and co-workers outlined a methodology to further increase the reaction yield from 10% to 45-75% using $Ir(acac)_3$ as a starting material. The starting iridium material and the ligand, ppyH were dissolved in degassed glycerol and the mixture was heated under reflux over 10 hours. The addition of 1 molar hydrochloric acid then resulted in the formation of precipitate, this precipitate was filtered and purified via chromatographic column with methanol prior to recrystallization from dichloromethane. This recrystallization yielded the yellow crystals of *fac*-$Ir(ppy)_3$ at ~45%, considerably higher than previously outlined procedures.[73]

Method A

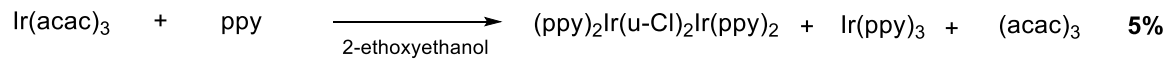

Method B

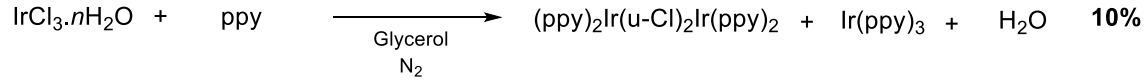

Method C

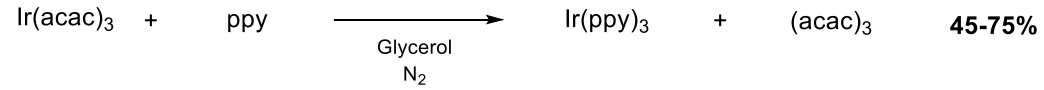

Figure 15- The reactions of the formation of $Ir(ppy)_3$ trialled over time with Method C being the most successful strategy for developing the tris-cyclometalated complex.[67, 72-73] The yield of the $Ir(ppy)_3$ is shown by the percentage values.

By looking at the synthetic methodologies described in Figure 15, it can be seen that the use of $Ir(acac)_3$ was considerably more favourable than the use of iridium chloride hydrate.[73]

The investigation into the use of bidentate ligands has been studied extensively. Tamayo and co-workers outlined a series of complexes and the synthesis of both *facial* and *meridional* isomers. The complexes were synthesised using the methods outlined in Figure 16.

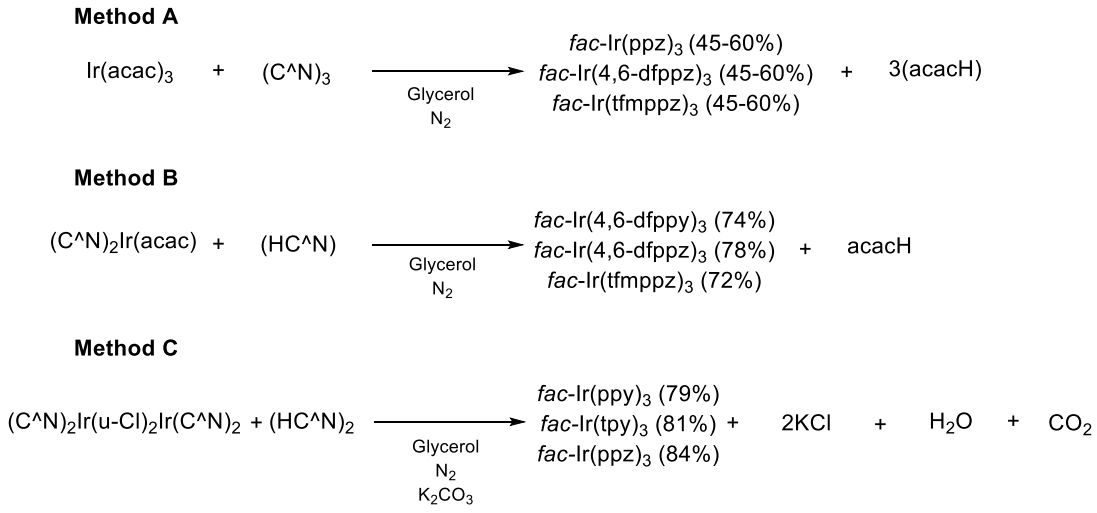

Figure 16 - The reaction conditions used for the synthesis of the facial isomers of the tris-cyclometalated complexes detailed by Tamayo and co-workers.[73-74] The reaction yields for each complex are shown, Tamayo *et al* did not quote specific yields of the complexes synthesised using Method A.

The complexes are similar to those of the platinum complexes detailed previously. The ligands use a bidentate C^N coordination and included an increase in the amount of fluorine atoms, in addition to the inclusion of 'softer' groups such as nitrogen or sulphur. The structures of the ligands are detailed below in Figure 17.

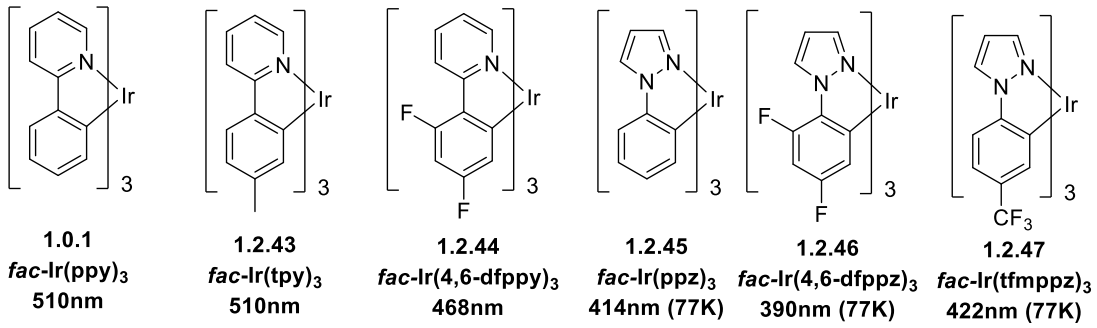

Figure 17- The structures of the cyclometalating C^N ligands (**1.0.1, 1.2.43-1.2.47**) used in the study by Tamayo and co-workers. The use of these complexes has also been documented by other research groups due to the promising chemical and photophysical properties in a complex.[74]The pyridyl based complexes display the values at an ambient temperature (298K) whilst those with a pyrazole moiety have been cooled to 77K.

The study showed that the formation of both isomers takes place during the synthesis but also described the distinct effect the change in isomerism had on the photoluminescent properties. The *facial* isomer displayed more impressive values of overall quantum yield and triplet state lifetime. The inclusion of different groups such as fluorine and pyrazole moieties has resulted in a shift in the emission. The inclusion of fluorine results in a blue shift of emission, likely due to the strong π-accepting nature of the fluorine atom. Complexes with pyrazole moieties were cooled to 77K and showed a blue shift of emission. The shift in emission was of an order of ~40nm. The inclusion of an additional methyl had no effect on the emission of the tris-cyclometalated complex. The photophysical data for the tris-cyclometalated complexes, *fac*-Ir(ppy)$_3$, *fac*-Ir(tpy)$_3$ and *fac*-Ir(4,6-dfppy)$_3$, is shown in comparison to the *meridional* isomers synthesised in the same study in Table 2.

Table 2 - The photophysical data for the facial and meridional isomers of cyclometalating bidentate C^N ligands that increase in the level of fluorine or substituent presence. The inclusion of a methyl group does not drastically effect the values however the inclusion of fluorine atoms increases the k_r values slightly but does not affect the k_{nr}.[74]

Complex	**Quantum Yield (ϕ_{PL})**	**Lifetime (μs)**	**Radiative rate of decay (k_r)**	**Non-radiative rate of decay (k_{nr})**
***fac*-Ir(ppy)$_3$**	**0.40**	**1.9**	2.1×10^5	3.2×10^5
***mer*-Ir(ppy)$_3$**	**0.036**	**0.15**	2.4×10^5	6.4×10^6
***fac*-Ir(tpy)$_3$**	**0.50**	**2.0**	2.5×10^5	2.5×10^5
***mer*-Ir(tpy)$_3$**	**0.051**	**0.26**	2.0×10^5	3.6×10^6
***fac*-Ir(4,6-dfppy)$_3$**	**0.43**	**1.6**	2.7×10^5	3.6×10^5
***mer*-Ir(4,6-dfppy)$_3$**	**0.053**	**0.21**	2.5×10^5	4.5×10^6

A study in 2003 by Tsuboyama and co-workers developed a library of tris-cyclometalated complexes with similar properties to those shown in Table 2. The series also developed other complexes with additional substituents that increased the overall conjugation of the system. The aryl group of the cyclometalating ligand that provides the crucial C^- atom to the structure was substituted with a thiazole group in the majority of the complexes synthesised.[30]

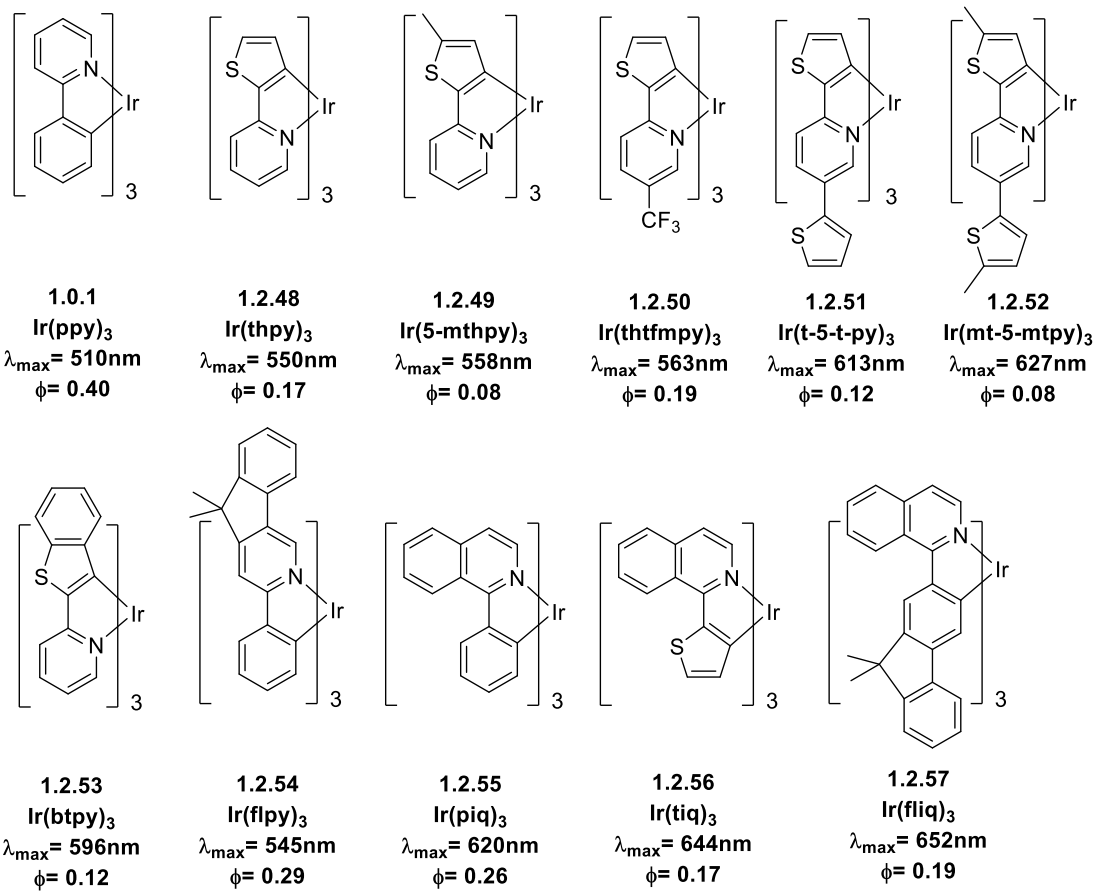

Figure 18 - The structures of the ligands tested by Tsuboyama et al, using the substitution of fluorene and thiophene groups, increasing the conjugation of the system which in turn increases the overall complex stability. The photophysical data for the complexes (**1.0.1**, **1.2.48-1.2.57)** are also described.[30]

The study by Tsuboyama and co-workers specifically targeted complexes that were red emitters and emitted from a ^{3}MLCT excited state, but also possessed high quantum yields. This is relatively difficult due to the decreasing quantum yields as the emission peak wavelength increases as a result of the energy gap law.[75-76] The inclusion of the thiophene moiety results in a red shift of peak emission wavelength approximately 40nm, shown by Ir(thpy)$_3$ (**1.2.48**) with an emission of λ_{max}= 550nm, however this group drastically reduced the quantum yield as this complex shows a value ϕ= 0.17, considerably lower than the model compound, *fac*-Ir(ppy)$_3$. The addition of an extra thiophene displayed an emission of λ_{max}=610nm, a considerable 100nm shift in the emission when compared to Ir(ppy)$_3$ (**1.0.1**). However this inclusion further reduced the quantum yield to ϕ= 0.12. The reduction is also displayed by the isoquinoline based complexes, which showed a red shift in emission in

comparison to $Ir(ppy)_3$, increasing from λ_{max}= 510nm to λ_{max}= 620nm. This could be attributed to the increase in conjugation of both systems. However the phenylisoquinoline complex, **1.2.55**, showed a lower decrease in quantum yield (ϕ=0.26) when compared to the thiophene based complexes and $Ir(ppy)_3$.[30]

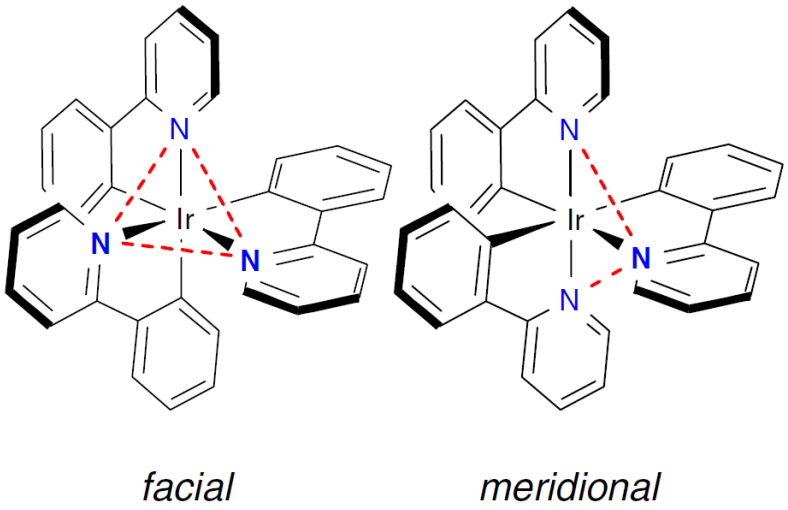

Figure 19 - The depiction of the geometrical isomers of **1.0.1** shown in the study by Ide and co-workers.[77]

The arrangement of the ligands is depicted by Ide *et al* in Figure 19, showing the difference between the two geometrical isomers using $Ir(ppy)_3$ as an example.[77] The study by Thompson *et al* investigated the isomeric selection of the tris-cyclometalated complexes and found that the formation of the *facial* isomer predominantly was formed at higher temperatures (>200°C). The *meridional* isomer is typically formed at lower temperatures (<150°C). The *meridional* isomer can be converted to the *facial* isomer with additional heating, therefore suggesting that the *meridional* isomer is in fact an intermediate product.[74] The *facial* isomer is preferred due to higher quantum yields and luminescence lifetimes in comparison to the *meridional* isomer.

The formation of homoleptic Ir(III) complexes has shown significant progress in the development of efficient optoelectronic devices and intensely luminescent red, green and blue emitters. This is due to the easily tuned cyclometalating ligands which directly affect the emission wavelength due to the separation of the HOMO and LUMO orbitals. This ability to

tune the wavelength makes these complexes excellent candidates for phosphors in devices such as OLEDs.

As the developments of homoleptic complexes have advanced, the formation of heteroleptic Ir(III) compounds has also made improvements. This has resulted in the formation of highly efficient and luminescent complexes. The typical structure of a heteroleptic Ir(III) complex consists of two cyclometalating C^N ligands with an additional ancillary ligand such as acetylacetonate or picolinate. The formation of homoleptic tris-cyclometalated complexes is difficult due to the method of coordinating the final ligand. This difficulty is not present in heteroleptic complexes. Heteroleptic complexes with the formula $[Ir(C^N)_2(LX)]$ typically show intense luminescence at room temperature which is often a mixture of the emissive LC-MLCT states, which is similar to the tris-cyclometalated analogues. The choice of the ancillary ligand can lead to different characteristics, selection of a β-diketonate ligand like acac typically results in a neutral complex. However the inclusion of a bidentate diimine group will produce a cationic complex as a result of the N^N coordination.[44]

A study by Lamansky *et al* investigated the synthesis of heteroleptic complexes using a series of cyclometalating ligands and a series of known ancillary ligands including *acac* and *pic*. The study outlined the synthesis of the iridium dimers in consistent high yields (>75%) and the formation of the complexes which have ranged quantum yields of ϕ= 0.10-0.34 with different ancillary ligands.[78] The luminescent complexes that utilise the assembly, $Ir(C^N)_2(LX)$, can be prepared at yields of approximately 80% and are emissive at room temperature between the wavelengths λ_{max}= 510-610nm.The photophysical properties were noted to be similar to the *fac*-$Ir(C^N)_3$ analogues and the emission spectra match for the ligands *ppy, tpy* and *bzq.* The series of ligands both cyclometalating and ancillary are depicted in Figure 20.

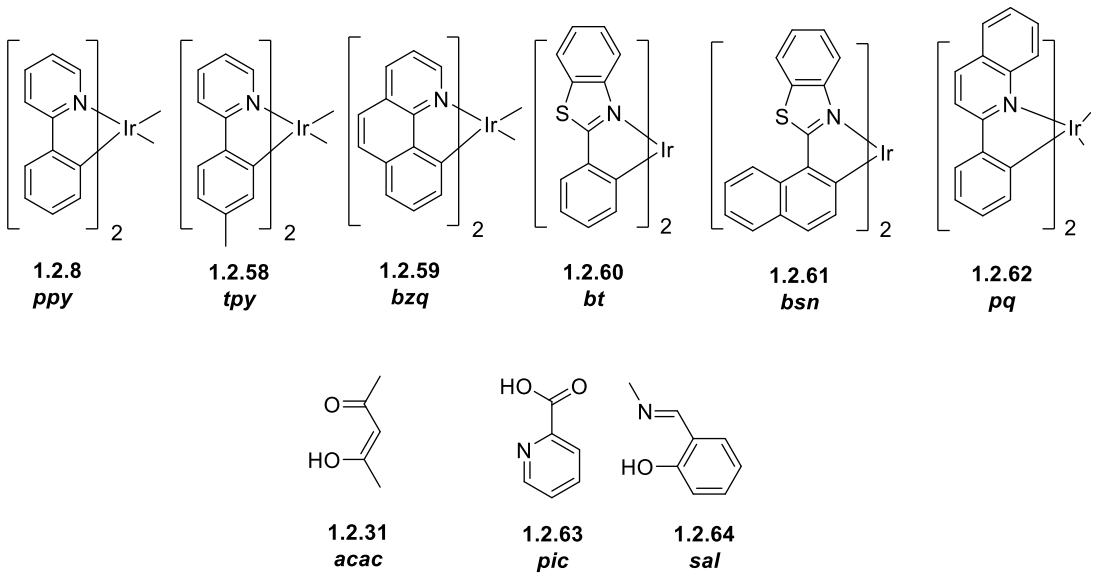

Figure 20 - The series of cyclometalating heteroleptic C^N complexes (top) used in the study by Lamansky et al.[78] The series of ancillary ligands acetylacetonate (acac), picolinate (pic) and N-methylsalicylimine (sal) used is shown below the cyclometalating ligands.

Table 3 - The photophysical data for the complexes synthesised by Lamansky et al.[78] The cyclometalating ligands are listed with the accompanying ancillary ligands.

Cyclometalating Ligand (C^N)	**Ancillary Ligand (LX)**	**Emission λ_{max} (nm)**	**Lifetime (µs)**		**Quantum Efficiency (2-MeTHF)**
			77K	298K	
ppy	Acac	**516**	**3.2**	**1.6**	**0.34**
tpy	Acac	**512**	**4.5**	**3.1**	**0.31**
bzq	Acac	**548**	**23.3**	**4.5**	**0.27**
bt	Acac	**557**	**4.4**	**1.8**	**0.26**
bt	Pic	**541**	**3.6**	**2.3**	**0.37**
bt	Sal	**562**	**3.1**	**1.4**	**0.22**
bsn	Acac	**606**	**2.5**	**1.8**	**0.22**
pq	Acac	**597**	**-**	**2.0**	**0.10**

The results shown in Table 3 show that the inclusion of a thiazole group on the cyclometalating ligand results in a significant red shift of the emission wavelength in comparison to the pyridyl moieties. When the conjugation of the system was increased using a naphthalene moiety, the emission wavelength is increased by an order of ~100nm. The use of this ligand reduces the overall quantum efficiency of the complex. The best combination in the study was the use of the benzylthiazole (*bt*) based cyclometalating ligand which showed a red shift of emission of approximately 50nm and a slight increase in efficiency to ϕ_{lum}= 0.37 when compared to $Ir(ppy)_2(acac)$.[78] The changes in the emission properties of the complexes can be attributed to the addition of groups with an increased electron donating nature and the increased conjugation of the system. Changing of the ancillary ligand is not an effective method of tuning with these complexes as very little change to the emission properties is noted. The use of *bt* showed that an increase in donor capability of the ancillary ligand results in a slight increase of emission wavelength (pic < sal≈acac). The development of these heteroleptic complexes by Lamansky *et al* was followed by a number of other research groups developing complexes that emit across the visible light spectrum.[79-82]

The development of charged heteroleptic complexes has been investigated by multiple research groups, predominantly the cationic complexes were constructed using two cyclometalating C^N ligands and the ancillary ligand was a neutral N^N group. The preparation of the cationic complexes were similar to the neutral analogues. In some cases similar procedures were used to prepare the dimer and complex. The dimer is produced in the same manner by heating the cyclometalating ligand with iridium chloride hydrate which is known as the Nonoyama reaction.[83-84] The dimer was cleaved using the diimine to produce the tris-cyclometalated cationic structure.

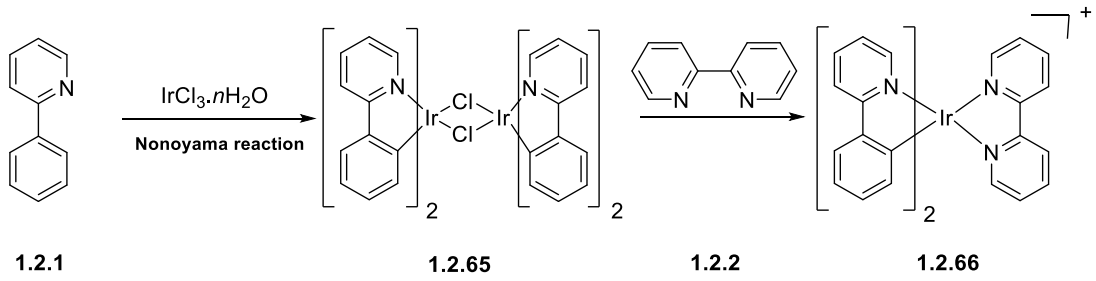

Scheme 2 - The reaction scheme depicting the formation of the cationic heteroleptic Ir(III) complex. The cyclometalating ligand used in this example is 2-phenylpyridine (ppy) and the diimine ligand is 2,2'-bipyridine.

The isolation differs from the typical procedure and involves the use of potassium hexafluorophosphate (KPF_6) to form the complex as a salt using counter ion exchange.

A study by Bolink *et al* showed the development of a blue emitting heteroleptic complex that used a phenanthroline diimine group as the ancillary ligand.[85] The complex synthesised had a maximum emission wavelength of λ_{max}= 476nm and a peak quantum efficiency of ϕ=0.52. This quantum efficiency was concentration dependent and showed a ϕ= 0.02 photoluminescent quantum yield (PLQY) at high concentrations of the complex. Low concentrations showed higher quantum efficiencies. It was noted that the emission was ^{3}LC in nature, and the absorption process was typically a MLCT transition.[85]

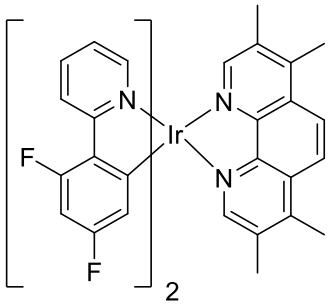

1.2.67
Ir(4,6-dfppy)$_2$(Me$_4$Phen)
λ_{max}= 476nm
ϕ_{lum}= 0.52 (2% conc.)

Figure 21 - The structure of the complex documented and described by Bolink and co-workers. The blue emitter has a PLQY that is concentration dependent, with higher ϕ values at lower doping concentrations (~2%).[85]

A further study by Nazeeruddin and co-workers resulted in the fabrication of cationic complexes that emitted in the blue/green region of the visible spectrum.[2] The investigation documented the synthesis and photophysical properties of three complexes. The cyclometalating ligands were changed between each complex and the ancillary ligands for only one of the complexes. The ancillary ligand was bipyridine with dimethylamine and tertiary-butyl substituents.

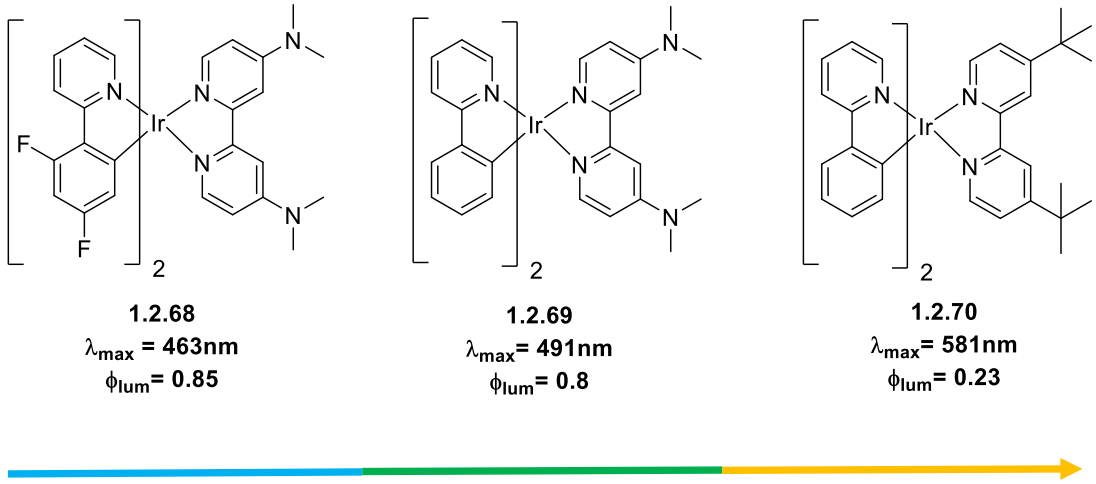

Figure 22 - The complexes detailed by De Angelis et al, highly luminescent cationic Ir(III) complexes using a series of cyclometalating and ancillary ligands. The arrow depicts the typical colour of each complex as the wavelength increases due to structural changes.

The inclusion of the fluorinated analogue of 2-phenylpyridine, *4,6-dfppy* (shown by **1.2.68**), resulted in a blue shift of emission. The ancillary ligand bears strong electron donating groups in the form of amines. This results in the destabilisation of the LUMO and the electron accepting fluorine groups stabilised the metal centred HOMO orbital and results in a large energy gap. A large difference in energy levels of the HOMO and LUMO typically results in a blue emission. As these moieties were removed the quantum yield decreased. This also results in the reduction of the energy gap between the HOMO and LUMO and therefore an increase in the emission wavelength. The substitution of amine for *tert*-butyl groups on the ancillary ligand between **1.2.69** and **1.2.70** respectively, resulted in a shift in emission by ~90nm. Thus, highlighting the effect of the ancillary ligand on the photophysical properties.[86]

A study by Duan *et al* focused on the development of white emitting optoelectronic devices and the synthesis of red, green and blue emitting cationic complexes. Imidazole groups were used to form ancillary ligands, with the aim of destabilising the LUMO and initiating a blue shift of emission wavelength. The PLQY values of the complexes peaked at ϕ=0.34. The emission was found to be of predominantly ligand centred π-π* transitions which is accompanied by MLCT and LLCT transitions.[87]

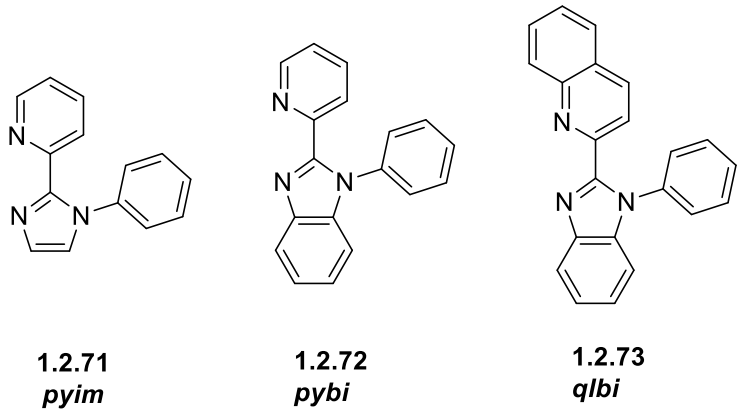

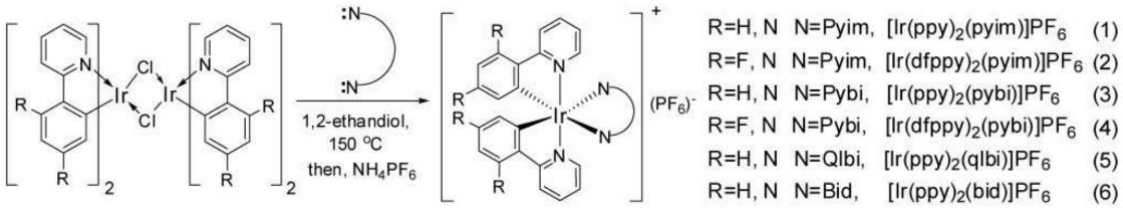

Scheme 3 - The reaction scheme depicting the synthesis of a series of cationic complexes developed by Duan and co-workers.[87] The diimine ancillary ligands are shown above the reaction scheme.

The synthesis of both homoleptic and heteroleptic complexes has shown that the ability to tune individual structures to manipulate emission properties can be facilitated with the use of a heavy central metal ion. The stability of Ir(III) as a central ion is one of the major benefits. As bidentate complexes have been extensively studied, the use of tridentate complexes has been applied to platinum (II). This displayed an overall increase in the stability of the prepared complexes. The increase in the conjugation of the π system resulted in a red shift of the emission. In one of the first instances, tridentate coordination was presented as part of cationic mononuclear and dinuclear Ir(III) complexes for use in oxygen quenching by Di Marco *et al*.

The complexes exhibited maximum luminescence wavelengths in the range 500-650nm in the orange-red region of the visible spectrum.[88]

Following the development of these complexes, the use of terdentate ligands began to become more prominent. Most notably was a study by Williams *et al* which investigated the use of a bis-cyclometalated arrangement.[12] The study showed that the coordination of the Ir(III) atom to the N^C^N ligand could be done successfully at high yields (>80%), at the time, a reaction not yet documented for Ir(III). The coordinating auxiliary ligand coordinated through a C^N^C binding method and proved difficult in comparison to the formation of the dimer. This difficulty was likely due to the presence of the *trans* effect as a result of the cyclometalating carbons on the auxiliary ligand. This prevents the Ir-C bond forming, and results in a complex with the general formula Ir(N^C^N)(HC^N) rather than the targeted Ir(N^C^N)(C^N^C). This study also found a method for forming this complex suggesting the use of molten silver triflate as a solvent with the ligand. This lead to the isolation of the complex and further testing showed a peak emission of λ_{max}= 585nm with a PLQY of ϕ=0.21 in acetonitrile at room temperature, shown in Figure 23 (**1.2.76**).[12] A study by Polson and co-workers prior to these findings investigated the use of terpyridyl N^N^N ligands with a coordinated N^C^N cyclometalated ligand but showed that this resulted in poorly luminescent complexes (ϕ=0.032), an example is shown in Figure 23 (**1.2.74**).[89] This finding was also supported by Williams *et al* which displayed a complex (**1.2.75**) based on a similar arrangement, however once again this displayed poor photophysical properties (ϕ=0.003).[12] The complexes show that as the overall charge of the system is changed to neutral the peak quantum yield can increase by at least ten fold. The low quantum yield of the complex presented by Polson *et al* can be attributed to the emission being in the near-IR region of the visible spectrum.

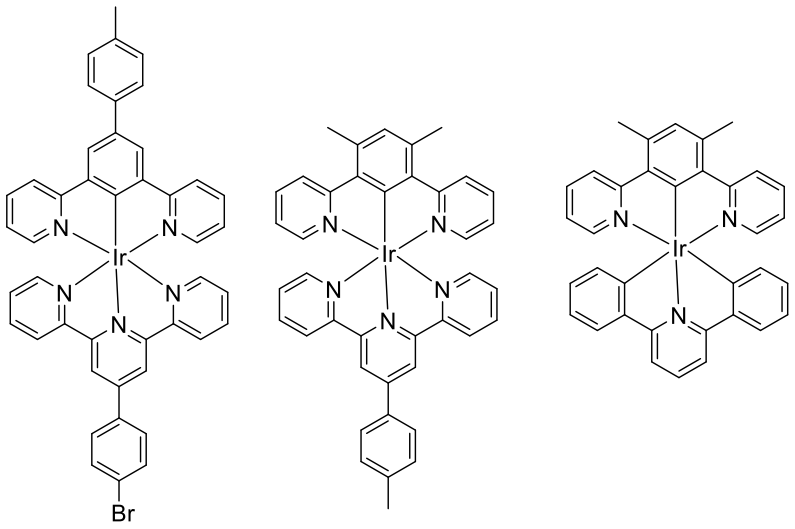

Figure 23- The structures of the complexes detailed by Polson *et al* and Williams *et al*. These complexes are described as the some of the first examples of cyclometalating N^C^N terdentate ligands being used in luminescent metal complexes.[12, 89]

The studies shown above were followed by a important study by Williams *et al* in 2006, this study described the synthesis of 4 possible cyclometalating auxiliary ligands to support the use of the cyclometalating N^C^N ligand. The study detailed the use of three tridentate coordination types, C^N^C, O^N^C and N^N^N (with a counterbalancing charged group). The study also used bidentate C^N ligands as a comparison against the tridentate analogues.[12] The investigation detailed complexes that displayed a peak quantum efficiencies in the range of ϕ= 0.001-0.76, and luminescent lifetimes in the range of τ=0.1-3.8μs. One of the most prominent complexes detailed is a C^N^C based complex, Ir(dpyx)(F_4dppy) which showed a doubling of the quantum yield (ϕ=0.41) in comparison to the non-fluorinated parent complex (ϕ=0.21) in the 2004 study by Williams *et al*.[12-13] The study also detailed the pairing of the cyclometalating N^C^N ligand with the well documented C^N cyclometalating auxiliary ligand, 2-phenylpyridine (*ppy*). This complex showed very intense luminescence and a high quantum yield in degassed acetonitrile (ϕ=0.76). The lifetime (τ=1.6μs) is half that of the C^N^C coordinated complex (τ =3.2μs). A weakness in the use of C^N groups with terdentate

cyclometalating ligands is that this results in the presence of a monodentate labile chlorine ligand, which is often detrimental to the lifetime of a potential device.

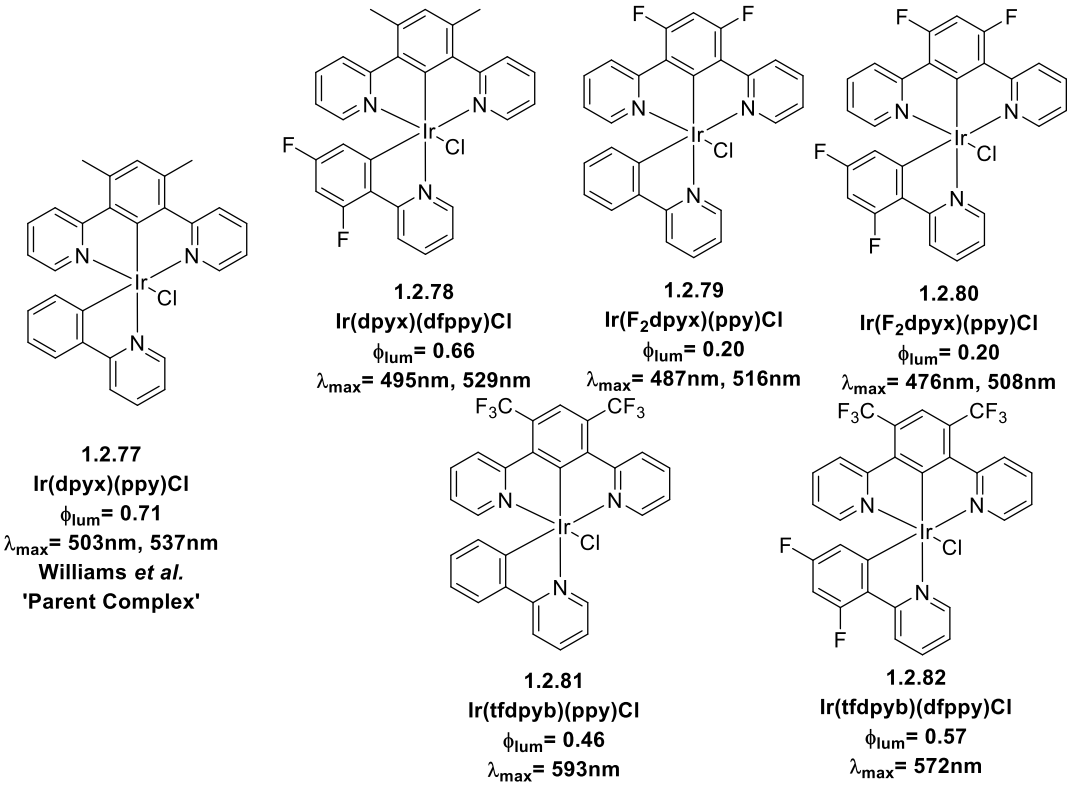

Figure 24 - The different coordination types of the complexes suggested by Williams *et al* and Brulatti *et al*. the coordination modes that show the most promising and highest values are C^N^C and C^N/Cl due to their high quantum yields and relatively low luminescent lifetimes.

A study in 2012 by Brulatti and co-workers examined the development of bis-cyclometalated complexes with the general formula Ir(N^C^N)(C^N)Cl, shown by complex **1.2.77**.[10] This builds on the work described by Williams *et al* and describes the synthesis of highly luminescent complexes. The investigation once again showed that the addition of the iridium metal centre to the cyclometalating N^C^N ligand is possible in high yields (~77%). The peak quantum yield achieved was ϕ=0.66, which was analogue **1.2.78** of the parent complex described by Williams *et al*, Ir(dpyx)(ppy)Cl, the structure is shown in Figure 24. Previous studies of tris-bidentate complexes have shown intense luminescence and it has been theorised that this is due to the large contribution from the metal centre which leads to their emissive nature.

The findings of the investigation have shown that the inclusion of fluorine on the C^N cyclometalating ligand leads to a slight decrease in quantum yield in comparison to the parent complex. This is accompanied by a slight blue shift in emission which is caused by the electron accepting nature of the fluorine groups. The relocation of the fluorine groups to the N^C^N group (Ir(F_2dpyx)(ppy)Cl) leads to a drastic decrease in PLQY (ϕ = 0.20) in comparison to both the parent complex and Ir(dpyx)(dfppy)Cl. The large decrease was attributed to the large amount of non-radiative decay present, which was caused by the reduced gap between the excited state and the deactivating d-d state, a common issue in blue emitting Ir(III) complexes.[90] The inclusion of the trifluoromethyl group resulted in orange/red emitting complexes, despite only a slight decrease in quantum yields (ϕ = 0.46-0.57). The complexes display long excited state lifetimes this was likely due to inefficient SOC. Therefore the emission is likely ligand centred and has little contribution from the central metal ion.[10, 13]

The development of tridentate bis-cyclometalated complexes has led to further development in the area. The use of these ligands increases the stability through a higher level of rigidity. This increased rigidity prevents the detrimental vibration that can quench the emission of the complex. The tuning capabilities of the complexes outlined have shown that the separation of the HOMO and LUMO is highly beneficial and can result in the development of highly luminescent complexes across the visible spectrum.

1.2.2. Multinuclear Metal Complexes of Iridium (III) and Platinum (II)

The majority of complexes used for organic light emitting diodes comprise of structures that include one iridium atom per molecule. In 1974, Nonoyama showed the development of dinuclear compounds by heating $Na_3[IrCl_6]$ with benzoquinoline (bzq) in 2-methoxyethanol. The process yielded a complex bound by two chlorine groups and contained two cyclometalated *bzq* groups on each metal centre and this showed one of the primary examples of multinuclear complexes.[91-92] The formation of the intermediary dimers often lead to the formation of an isomeric mixture, which typically contained a *meso* form and a racemic pair of isomers.

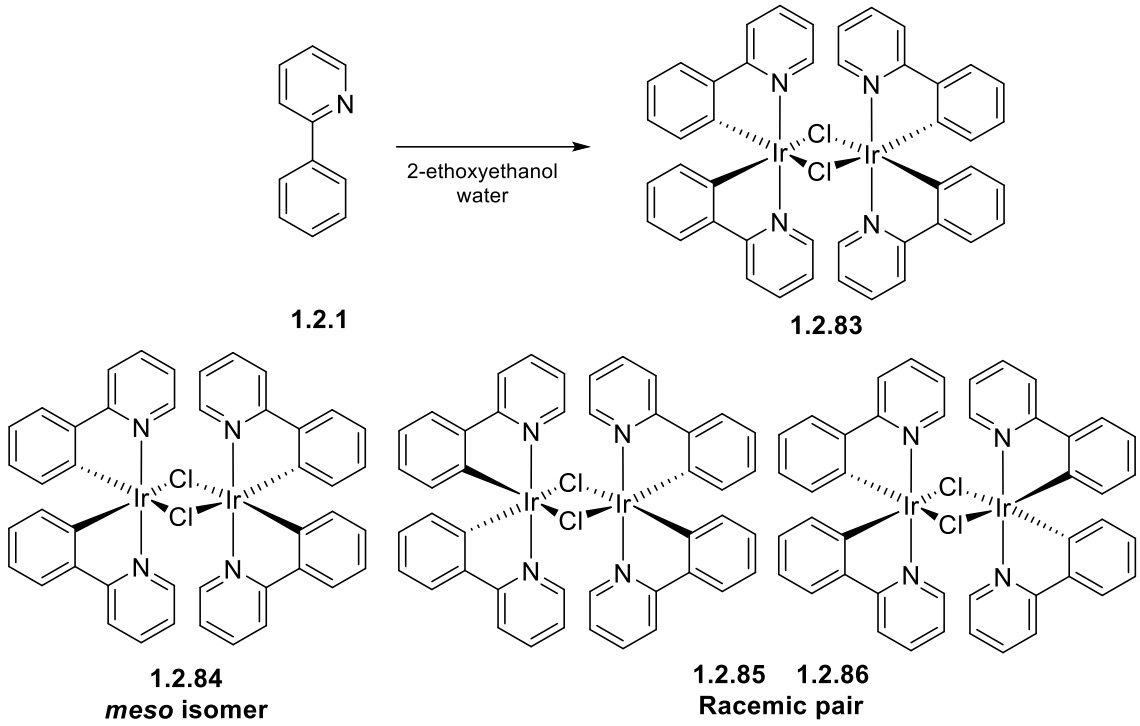

Scheme 4 - The reaction scheme depicted shows the current generally accepted synthetic conditions for generating the dichlorobridged compounds. The possible isomers of this reaction are shown below the reaction method described by Nonoyama *et al.*[91]

The complexes that typically employ a chlorine bridge between the metal centres have shown poor luminescence ($\phi = 0.005$), however this is due to the weak ligand field presented by the chloride bridge. This is considerably lower than that of the tris-cyclometalated *fac*-Ir(ppy)$_3$, an example of a highly luminescent Ir(III) complex.[93] An important characteristic of complexes is a strong ligand field as this aids in the generation of intense luminescence.[94]

The syntheses of these complexes developed as the bridging mode was adapted to using sterically hindered pyrazole and oxygen based bridging groups. This strategy was described by Chandrasekhar and co-workers. Their study showed that the use of the hindered pyrazole groups would disfavour the formation of mono-nuclear analogues and promote the formation of pyrazole bridged dimers.[95] The development of the dinuclear systems exhibit the typical red shift displayed by multimetallic complexes. This is highlighted by the absorption bands showing a ~50nm shift in peak wavelength. The reason for this shift is due to the π-donating nature of the bridging ligands which push electron density toward the central Ir(III) ions. This

destabilises the HOMO and raises the orbital level and closes the energy gap. This reduction of the energy gap accounts for the red shift in absorption and emission.[95]

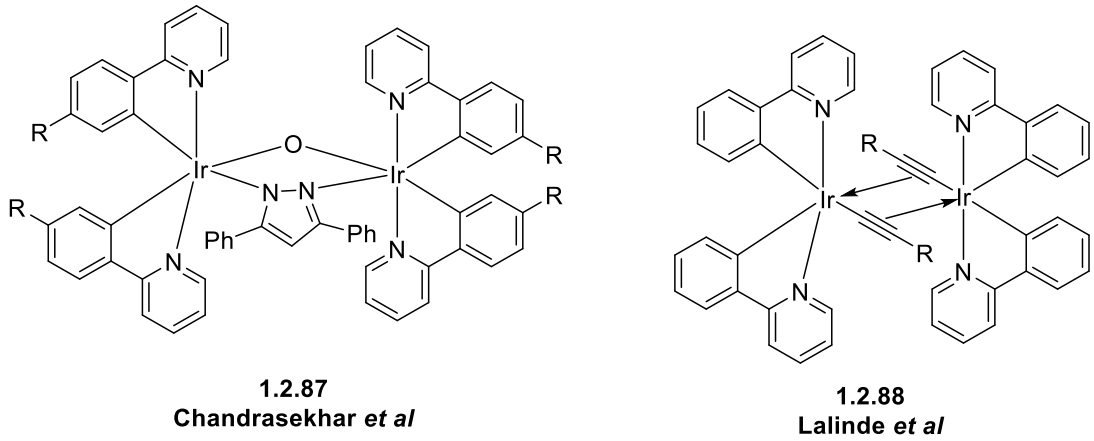

Figure 25 - The dinuclear complexes using different bridging modes. The complex proposed by Chandrasekhar and co-workers is shown (left). The complex described Lalinde *et al* is shown (right).

Lalinde and co-workers proposed the use of acetylide bridged molecules as an alternative to previous methods such as hydroxyl or chloride based bridging.[96] The study proposed the first example of alkynyl bridged di-iridium complexes which also used cyclometalated ppy based ligands. As this bridging mode is rare, the C≡C bond was identified using an array of analytical methods. The alkyne group typically shows a distinct IR peak and this was identified at ~1950cm^{-1} for each complex described. The binding method is achieved through the strong π donation of the alkyne and backbinding to the Ir(III) centre (denoted by the arrows in Figure 25). The complexes described utilised different groups in order to achieve different emission properties. The substitution of electron donating and accepting groups resulted in varying peak emission wavelengths. Despite the use of different functional groups, all of the quantum efficiencies were low (ϕ=0.007-0.024).[96]

Table 4 - The photophysical data from the analysis of the complexes synthesised by Lalinde et al.[96] All values shown are those recorded at ambient temperature (298K).

Complex	λ_{max}	**Lifetime, τ (μs)**	**PLQY, ϕ**
$[Ir(ppy)_2(\mu\text{-}C{\equiv}CTol)]_2$	505	0.07	**0.007**
$[Ir(ppy)_2(\mu\text{-}C{\equiv}CC_6H_4OMe\text{-}4)]_2$	510	0.2	**0.012**
$[Ir(ppy)_2(\mu\text{-}C{\equiv}C\text{-}1\text{-}Np)]_2$	515	0.37	**0.024**
$[Ir(ppy)_2(\mu\text{-}C{\equiv}CSiMe_3)]_2$	512, 536	1.36	**0.01**
$[Ir(ppy)_2(\mu\text{-}C{\equiv}C^t\text{-}Bu)]_2$	512, 545, 590	1.0	**0.009**

The study has shown that the use of alkynyl bridges is a novel but under researched approach, as there is little benefit to the use of this strategy. The complexes displayed low quantum yields and were accompanied by low radiative rate constants and high levels of non-radiative decay. The most promising complex in the study used a naphthyl substituent on the alkynyl bridge. However this was shown to be mainly an emission that is predominantly ^{3}LC in nature leading to low PLQY values.

Development of complexes later incorporated the use of heterocycles to link the metal centres which typically used nitrogen atoms; with common heterocycles being pyrimidine, pyrazine or triazoles. Often the coordinating method of the bridging ligand will be similar to bidentate cyclometalating and bipyridyl ligands, using C^N and N^N binding methods respectively.[97-98]

Serroni *et al* reported a multinuclear complex that used iridium (III), osmium (III) and ruthenium (II) as metal centres using a ligand with a pyrazine heterocycle (2,3-di(2-pyridyl)pyrazine). The emission of the complexes described peak wavelength emission in the near-infrared region (λ_{max}= ~812-825nm). However once complexes begin to emit in this region, the quantum yields are drastically decreased which can be attributed to the energy gap law and vibrational releases of energy. The complexes showed an emissive nature arising from

the energy transfer from one metal centre to another (Ru→Ir, Ir→Os).[98] The study showed that the excited state was located on a single metal centre. However this could only be determined at low temperatures (77K).

Similar to the 2,3-di(2-pyridyl)pyrazine (*dpp*), a study was carried out on multinuclear complexes using HAT (1,4,5,8,9,12-hexaazaphenanthrene) which offers three N^N binding sites for coordination of multiple metal centres. Kirsch-De Mesmaeker *et al* studied the development of both homonuclear and heteronuclear complexes using iridium (III), rhodium (III) and ruthenium (II). However these complexes were found to be unstable. The photophysical properties of the complexes described showed an average emission at ambient temperatures λ_{max}= ~770nm, this near-IR wavelength is also accompanied by a very short luminescence lifetime (τ= ~0.1μs) which indicates a high level of non-radiative emission.[97]

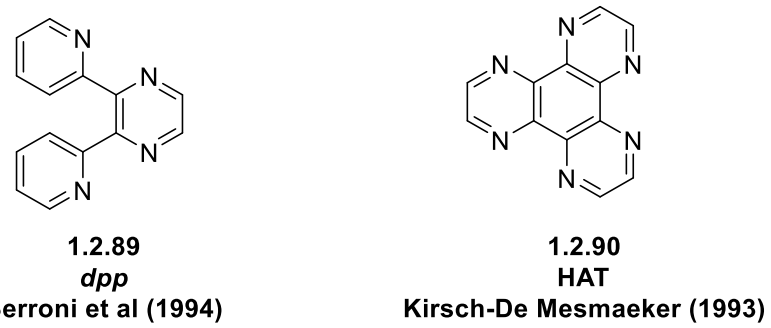

Figure 26 - The bridging ligands described by Serroni and co-workers (left) and Kirsch-De Mesmaeker and co-workers (right) in the development of multinuclear complexes.

The field developed further as Chandrasekhar *et al* developed highly luminescent tri-nuclear and mono-nuclear Ir(III) complexes with cyclometalated ligands.[99] The peak emission of the complexes described was 685nm with PLQY value of ϕ= 0.58, considerably higher than previous attempts to develop emissive complexes. The increase in quantum yield can be attributed or ascribed to the decrease in emission wavelength, which is a result of a slight increase in the energy gap between HOMO and LUMO orbitals. The use of a triazole based bridging group led to a lower lying triplet excited state. This is supported by the increased luminescence lifetime (τ= 6.55μs).[99] Whilst the emissive state of the trinuclear complex is located almost solely on the bridging ligand.

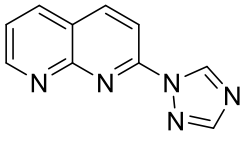

1.2.91
L1

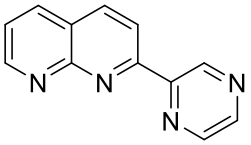

1.2.92
L2

Figure 27 - The structures of the bridging ligands described by Chandresekhar *et al*. These ligands bind the metal centres using the 1,2,4-triazole and pyrazine moieties. The complexes used ppy ligands as the accompanying groups.

As described previously the use of cyclometalating ligands can distinctly benefit the photophysical and chemical properties of a metal complex. An investigation by Auffrant *et al,* used a bis(N^N) bridging ligand with the cyclometalating *ppy* ligand, resulting in charged complexes that showed a luminescence in the red region λ_{max} 654nm. However showed a low quantum yield (ϕ= 0.05) in comparison to previously described studies. The use of the bidentate C^N ligands resulted in the formation of stereoisomers with similar properties ($\Delta\Delta$, $\Delta\Lambda$, $\Lambda\Lambda$). Each isomer displayed similar properties when converted to phosphate salts, and resulted in difficult separation by column chromatography. The different isomers showed unique photophysical properties, and were weakly luminescent in the red region. The cyclometalated isomers in the study showed average wavelengths λ_{max}= ~654nm and relatively short lifetimes (τ = ~0.047μs) at room temperature. At 77K the lifetimes of the luminescence increases to τ = ~3.0μs which indicates a distinct reduction in the degree of non-radiative decay.[100]

Subsequent studies into di-nuclear complexes encompassed the use of ditopic cyclometalating bridging ligands. The difficulty of introducing a third cyclometalation means that conditions are typically quite forcing in contrast to that of N^N coordination.[92] Tsuboyama *et al* described this difficulty during the synthesis of the dinuclear complex, $Ir(ppy)_2(bpb)$ which utilised the bridging ligand, 1,4-bis(2-dipyridyl)benzene (*bpb*). The conditions described involved heating the iridium acetylacetonate dimer in glycerol at 290°C. The use of these conditions led to the formation of other iridium complexes which included the formation of the target complex at low yields (~3%). The complex described is technically a luminescent charge neutral analogue

of a complex described by Donato *et al*.[101] The complex described by Tsuboyama and co-workers was considerably red shifted when compared to $Ir(ppy)_3$ and this could be associated with the addition of the second metal centre. The photophysical properties displayed are λ_{max} 665nm and a quantum yield ϕ= 0.04. The low quantum yield was associated with little contribution from the metal centres and considerable contribution from the ligand centred HOMO which would result in an inefficient spin-orbit coupling.[102]

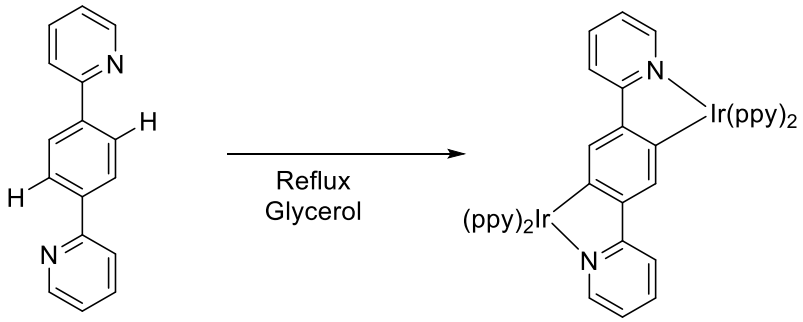

1.2.93 **1.2.94**

Scheme 5 - The cyclometalating ligand described by Tsuboyama *et al*. The protons lost in the cyclometalation are shown. The 2-phenylpyridine groups are not explicitly drawn.

The development of dinuclear and multimetallic systems was significantly progressed by the Kozhevnikov group in 2011. The advances described the use of platinum (II) and iridium (III) coordinated to the 4,6-di-(4-tert-butylphenyl)-pyrimidine (**1.2.95**) bridging ligand. The initial study by the group described the formation of the heterotrimetallic complex, **1.2.98**. The platinum was coordinated to the bridging ligand by heating with potassium tetrachloroplatinate (K_2PtCl_4) in acetic acid. This was followed by coordination with sodium acetylacetonate to produce the mono-platinum complex, Pt(dppym)(acac), **1.2.97**. The formation of this complex was followed by the cyclometalation of the iridium complex using iridium chloride hydrate. The addition of the acetylacetonate was carried out again before the addition of the secondary Pt(dppym)(acac) unit resulred in the heterotrimetallic complex.[103]

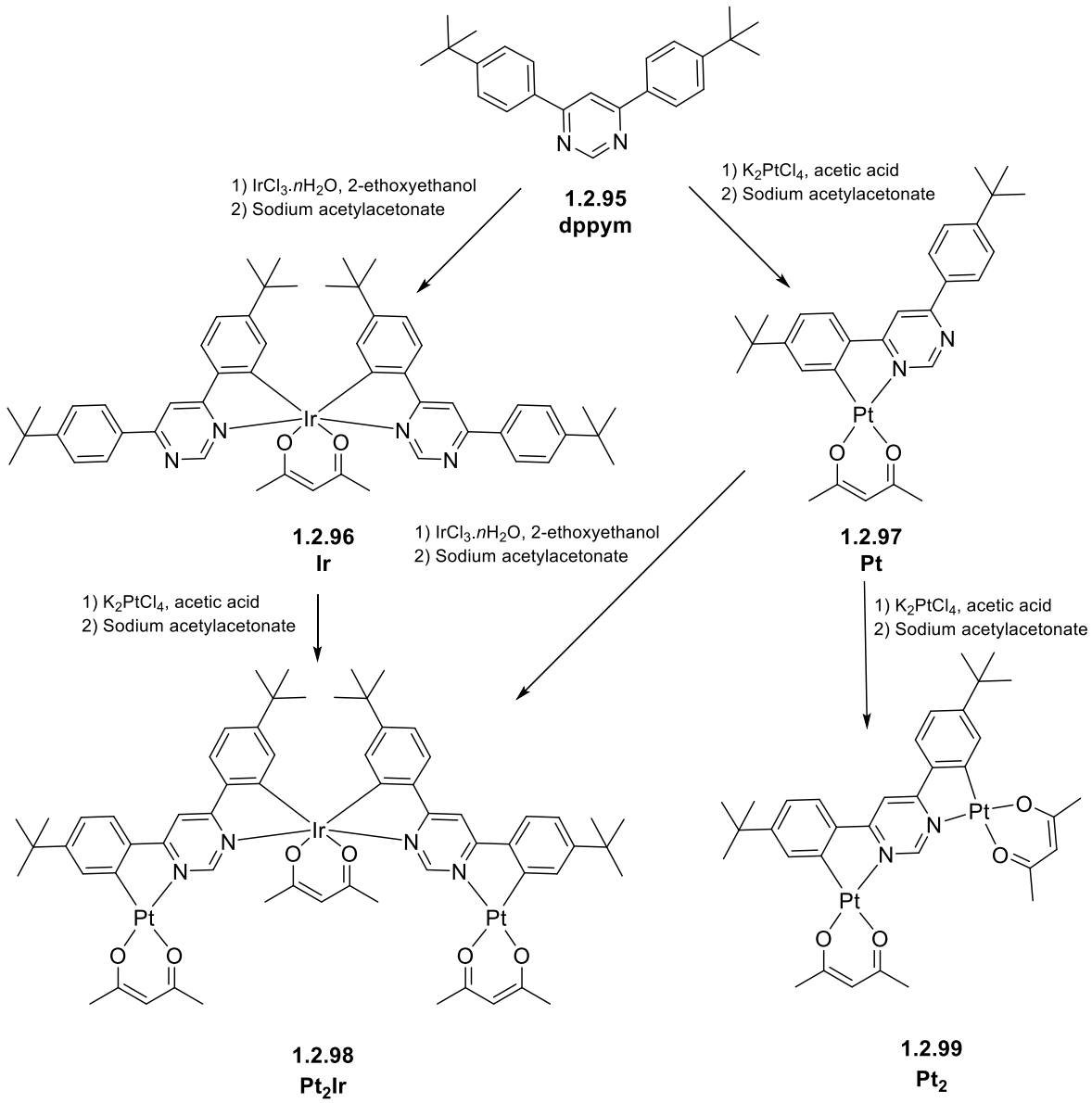

Figure 28 - The structures of the heterotrimetallic complex, **1.2.98** and the di-platinum complex, **1.2.99** which can be formed by heating **1.2.97** with K_2PtCl_4. The structures of the mono-metallic analogues are shown above the multi-metallic derivatives.

Another complex described in the study is the monometallic iridium analogue using the bridging ligand, which resulted in the complex Ir(dppym)(acac) (**1.2.96**) and is used as a comparison. Each of the complexes described are highly luminescent and highlights the effect of adding additional metal centres.

Table 5 - The photophysical data for the complexes described by Kozhevnikov et al. The measurements are taken at 298K and 77K in chloroform.

Compound	**Emission at 298K**			**Emission at 77K**	
	Emission, λ_{max}, nm	Φ_{lum}/PLQE	τ, μs	Emission, λ_{max}, nm	τ, μs
Pt_2Ir (1.2.98)	513, 536	0.31	2.1	494, 531, 569, 616	5.6
Pt_2 (1.2.99)	550, 591, 647	0.54	1.7	540, 561, 575, 585, 631	5.8
Pt (1.2.97)	585	0.39	1.0	554, 595	16
Ir (1.2.96)	626	0.41	0.58	596, 643	12

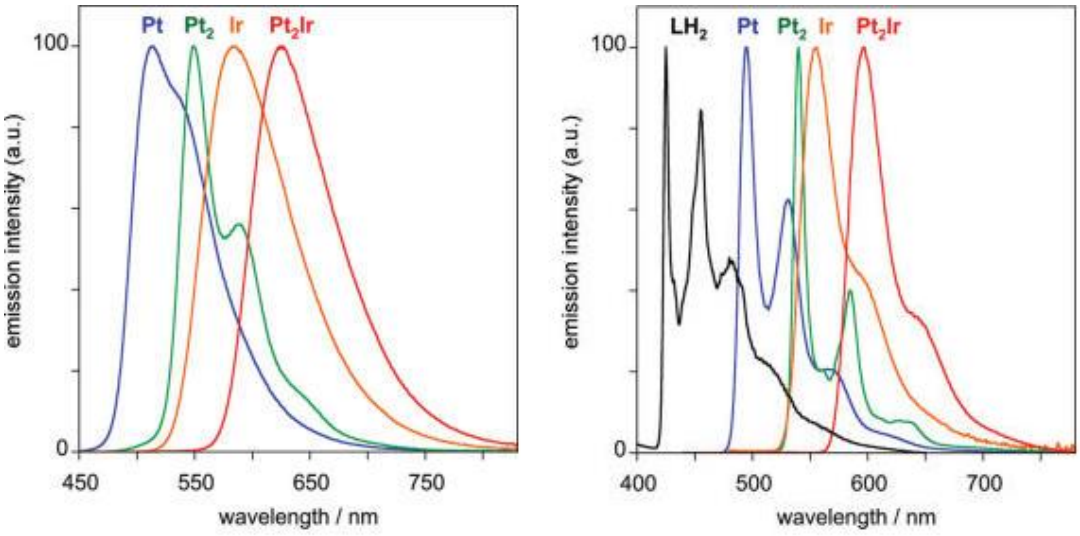

Figure 29 - The luminescence spectra for the complexes (**1.2.96-1.2.99**) described by Kozhevnikov *et al*, the spectra shown are at temperatures 298K (left) and 77K (right) and highlight the red shift induced as the level of metal centres increases. There is also a significant red shift when the central metal is changed from Pt(II) to Ir(III). The spectra are taken from the paper by Kozhevnikov *et al*.[103]

The complexes showed similar PLQY (ϕ= 0.39-0.54) values throughout the series and showed that the inclusion of heterometallic centres does not necessarily lead to an increase in quantum yield. The use of homologous metal centres (Pt_2), ϕ_{lum}= 0.54, lead to a distinct increase in quantum yield over the mono-metallic analogue, ϕ_{lum}= 0.39. The addition of the iridium centre

to this structure reduced the quantum yield (ϕ_{lum}= 0.31) to lower than the monometallic analogue, $Ir(dppym)_2(acac)$.

Building on previous work, Kozhevnikov and co-workers also developed a series of di-platinum complexes that incorporated different bridging ligands that were derivatives of the pyrimidine based bridging ligand described previously. The bridging ligands incorporated pyrimidine, pyrazine and quinoxaline moieties, and the eventual complexes were analogues of the acetylacetonate (acac) platinum complexes previously described, using dipivaloylmethane (dpm) in the place of acac. The study presented complexes with peak quantum efficiencies of ϕ_{lum}= 0.41 for the dinuclear structures, which had a peak emission λ_{max}= 628nm. The complex with the most promising photophysical properties used a dibenzopyrazine bridging ligand with Pt(II). The use of this ligand removed the possibility of sterical hindrances, which likely lead to the increased quantum yield.[5]

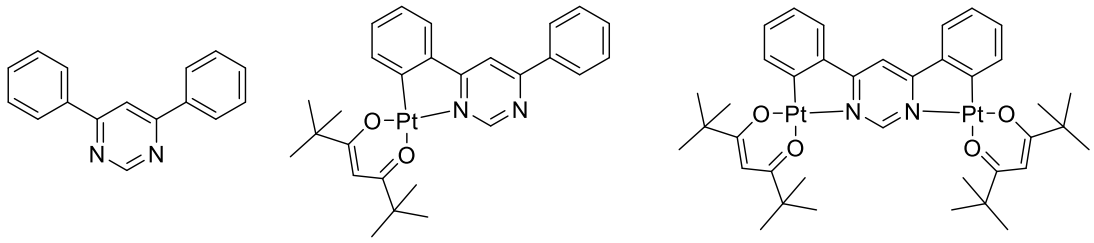

1.2.100 L^1H_2 | **1.2.101** PtL^1H | **1.2.102** Pt_2L^1

Figure 30 - An example structure of the pyrimidine ligand, mono-platinum complex and di-platinum complex described by Kozhevnikov *et al*. The complex shown had a PLQY of ϕ=0.36. The most promising complex used pyrazine as the linking heterocycle (ϕ=0.41).

Complementing previous studies, Kozhevnikov *et al* began the development of bis-tridentate N^C^N complexes. These complexes have been shown to display additional benefits of bidentate analogues. This is due to the increased rigidity which minimises the prevalence of non-radiative decay.[10, 39, 104] The bridging ligand, **1.2.103**, used to create the ditopic ligand uses pyrimidine as a linking heterocycle and this allows for two laterally connected metal centres. The structure of the ligand is shown in Figure 31.

The bridging ligand formed a dichlorobridged dimer (**1.2.104**) in high yields, similar to previously described mono-metallic dimers, by heating the proligand with iridium chloride hydrate. The resultant dimer was coordinated to 2-(4-methylphenyl)pyridine (Meppy) which in turn results in the formation of a mixture of isomers. Unlike the other complexes described, the isomerism was relative to the location of the monodentate chloride ligands with the isomers showing *meso* and racemic forms. In this instance all isomers were isolated in yields around 25%. Sometimes this is not possible if the isomers have similar properties. The photophysical properties of both the *meso* (**1.2.105**) and *rac* isomers (**1.2.106-1.2.107**) are similar with the peak emission wavelength only separated by ~3nm, λ_{max} 625 and 622nm respectively. The quantum yields were considerably higher than other red emitting complexes, ϕ_{lum}= 0.65 and a lifetime unmatched by previously synthesised complexes, τ= 0.7μs.[105] The findings of the paper also showed that the inclusion of a secondary metal centre (of the same nature) increases the emission wavelength of the complex by an order of λ_{max} ~80-100nm, which was a result of the stabilisation caused by the coordination of the Ir(III) to the secondary N atom in the pyridine heterocycle. This effect had been documented previously in bis-bidentate diphenylpyridine complexes and dipyridylpyrimidine ruthenium (II) complexes.[98, 103]

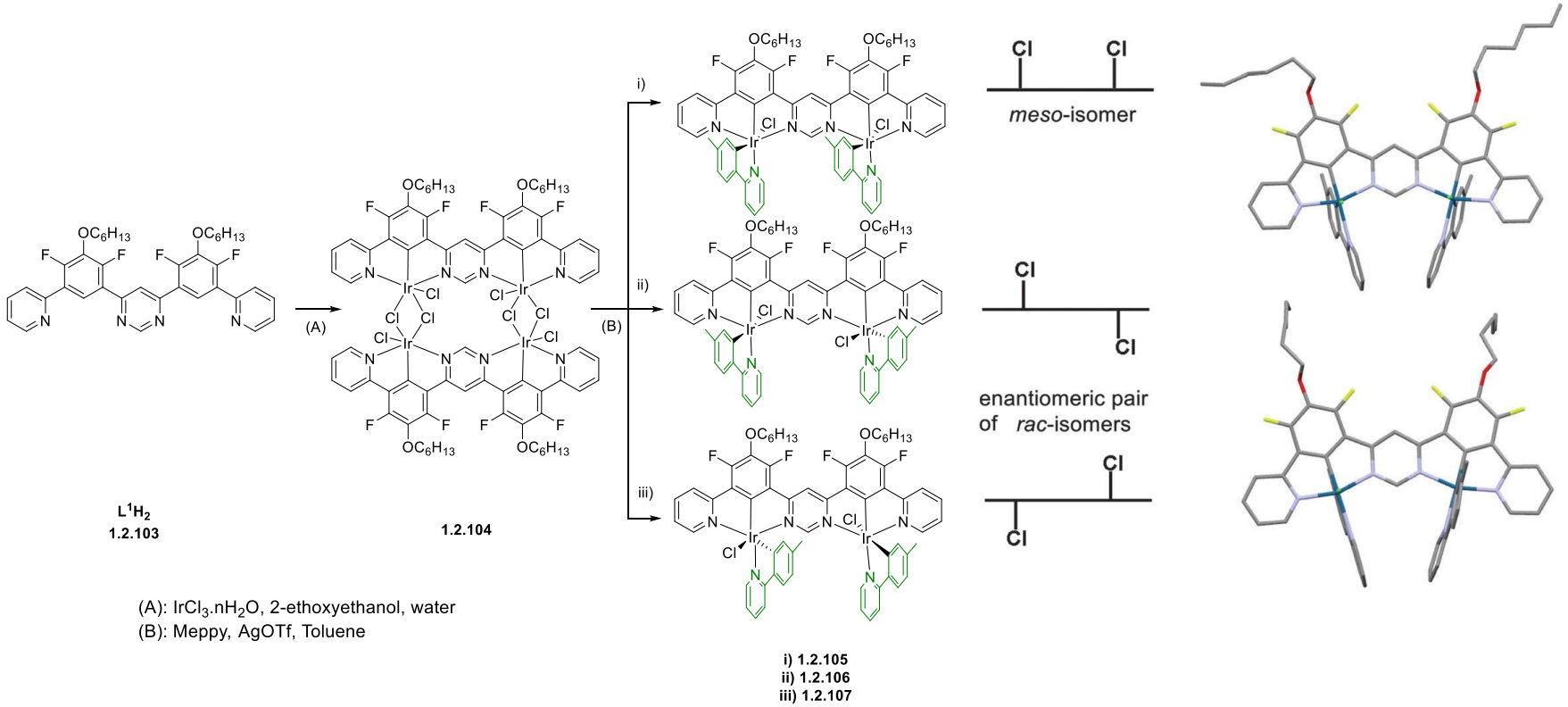

Figure 31 - The depiction of the position of the monodentate chloride ligands in the complexes **1.2.105-1.2.107** described by Kozhevnikov *et al*. The different isomers formed from the tetranuclear dichlorobridged dimer forms the three highly luminescent isomers when cyclometalated to the ligand, the image also shows that the isomerism is dependent on the positioning of the chloride groups.[92] The image was taken directly from the study by Kozhevnikov *et al.*[105]

The quantum yields of red emitting complexes typically decrease at high wavelengths (>600nm) as excited state energy gives way to non-radiative decay and emission. Considering the radiative and non-radiative rates of decay (k_r and $k_{nr,}$ respectively), the addition of the second metal centre led to a 4-fold increase in the radiative rate of decay which significantly overshadowed the increase in the non-radiative rate of decay. The development of the di-nuclear compound was shown to have added benefits to the luminescent properties. The secondary metal centre increased the spin-orbit coupling constant and in turn amplified the spin-orbit coupling effect, which led to a more efficient intersystem crossing. This would explain the high quantum yields displayed by the dinuclear systems.[105] At the time of publication, the complexes detailed were amongst the best and most efficient red emitters.[20, 30, 106-107]

Daniels *et al* further developed the work outlined by Kozhevnikov *et al*, using two iridium centres with a *dppym* bridging ligand and N^C^N coordinating terdentate ligands (shown in Figure 32 as **1.2.108-1.2.115**). Through this study a series of complexes was outlined that showed peak wavelengths in the orange/red region (λ_{max}=517-572nm) and intense luminescence with quantum efficiencies nearing unity (ϕ= 0.88-1.0). All of the complexes described in the study showed luminescence lifetimes in a range of τ= 0.36-4.0μs which was dependent on the bridging ligand used. All measurements were taken at room temperature under deoxygenated conditions in chloroform, due to the complexes being quenched in oxygenated conditions. The study showed that the strong *trans* effect induced by the cyclometalating carbons led to the formation of one product and that the substituents on the bridging ligand had a strong influence over the quantum efficiency displayed. As the lifetime is quite short this can be attributed to the presence of fluorine groups and alkoxy chains in the structure which are known to be detrimental to the luminescent properties. With complexes that display quantum efficiencies near unity the compounds shown in the study can be used as a benchmark for future work and be optimised for use in highly efficient OLED devices or other uses such as water splitting catalysis or bio-imaging.[6]

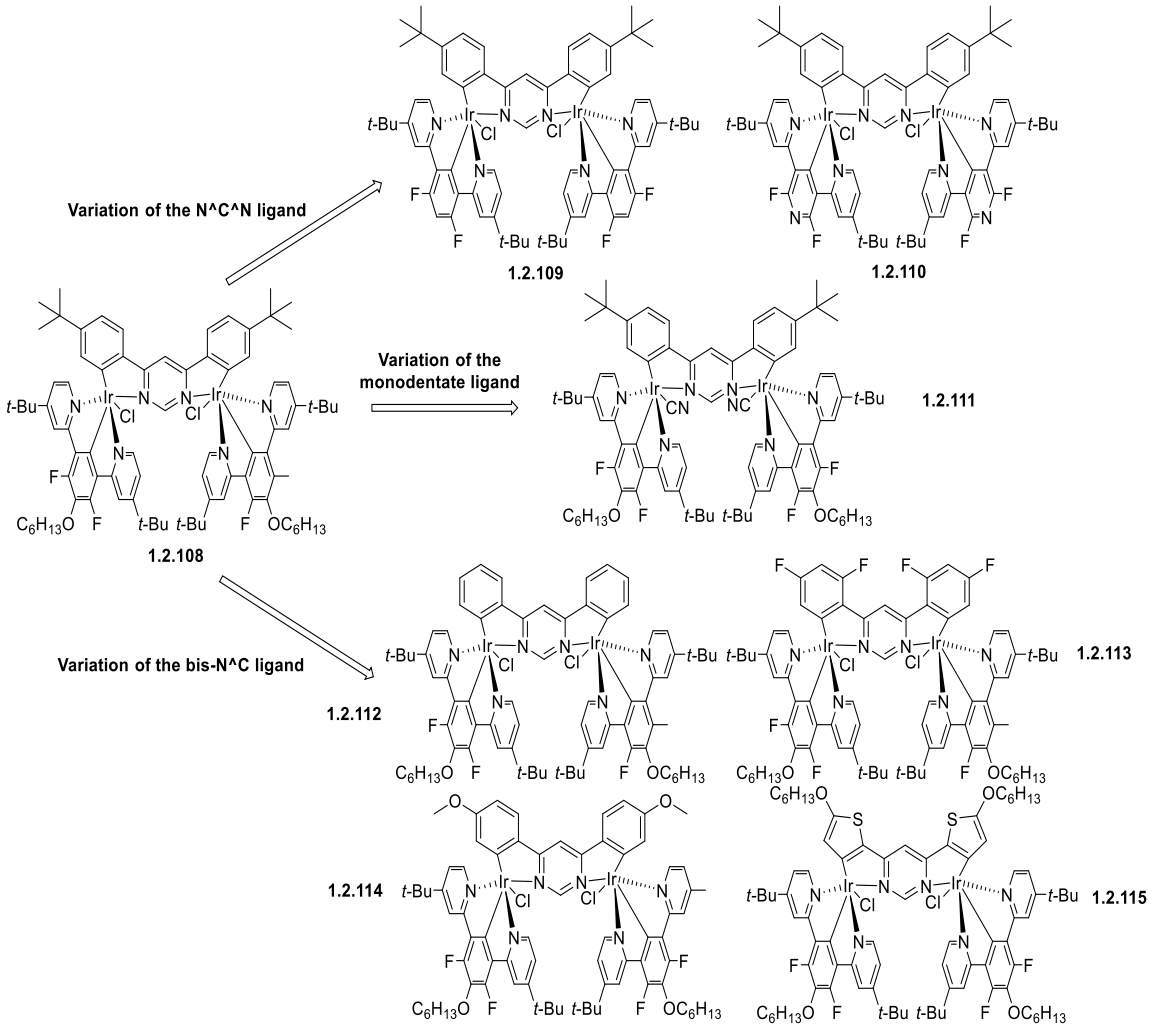

Figure 32 - The entire series of highly luminescent complexes detailed by Daniels *et al* which display high quantum efficiencies. The figure shows the changes made to the bridging ligands, mondentate ligands and the N^C^N coordinated group. The scheme was taken directly from the paper written by Daniels *et al.*[6]

The work detailed by Kozhevnikov *et al* formed the basis for the development of the complexes prepared in this project.

1.2.3. Tetradentate Coordinating Ligands and their Complexes

As described previously the use of terdentate ligands increases the level of stability by increasing the rigidity across the entire structure. Predominantly the development of tetradentate complexes have incorporated the use of platinum (II) as the central metal atom and taken advantage of the square planar arrangement commonly seen in Pt(II) complexes. The use of these square planar complexes has led to the development and fabrication of white emitting organic light emitting diodes (WOLEDs).[108-109]

A study by Kui *et al* in 2013 outlined the development of a series of tetradentate platinum complexes that utilised O^N^C^N coordination. The complexes were developed into efficient WOLED devices. The study outlines that whilst use of symmetrical ligands results in highly efficient luminescence with a range of peak quantum efficiencies ϕ_{lum}= 0.05-0.76.[110-113] The use of asymmetrical groups show an improved level of quantum efficiency, ϕ_{lum}= 0.93 and show a high level of thermal stability to temperatures >400°C.[114]

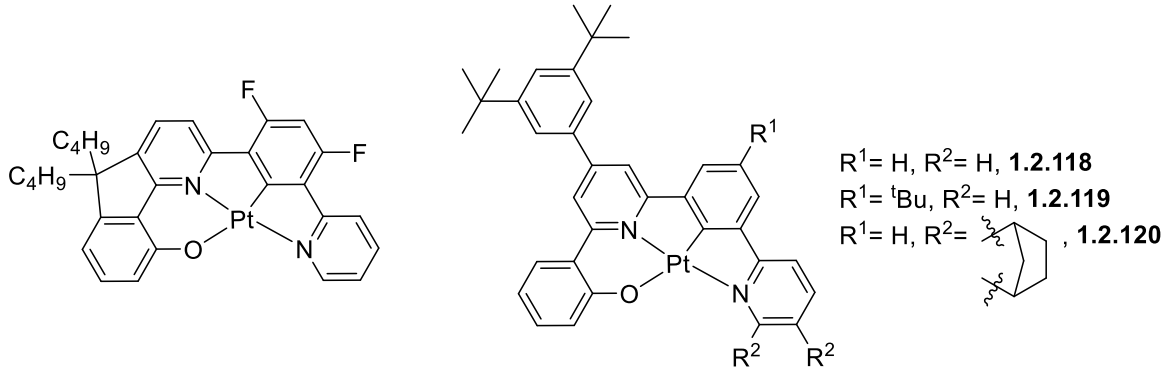

1.2.116
Kui *et al*, 2013

1.2.117
Kui *et al*, 2013

Figure 33 - The structures of the tetradentate complexes described Kui and co-workers in two seperate studies.

Another study by Kui *et al* investigated the use of different substituents on the O^N^C^N bridged ligand. By incorporating the large groups such as tertiary butyl or the norborane group, this will increase the overall solubility by reducing the level of intermolecular interactions. This addition will prevent the stacking of molecules, of which platinum complexes are susceptible.[43]

The introduction of the solubilising groups result in a slight decrease in the quantum efficiencies resulting in a range between ϕ_{lum}= 0.73, 0.84, 0.90 for the complexes **1.2.118**, **1.2.119** and **1.2.120** respectively, shown in Figure 33. In comparison to the previous study by Kui *et al*, the thermal stabilities of all complexes developed exceed 400°C making them candidates for OLED emitters. The study showed that their previous attempts at efficient emitters were more effective at low dopant concentrations which is not desirable in industry.

The inclusion of the norbornane group shown in Figure 33 (**1.2.120**) removes this concern and allows for higher concentrations whilst maintaining a high efficiency.[113-114]

Che *et al* described the use of Schiff base ligands in the development of tetradentate complexes for white emitting OLED devices. Using an ethylene diamine bridge to the link the phenolate groups, this provided the basis future studies using bisphenolate bipyridine coordination. The study by Che *et al* emphasized that the use of tetradentate ligands showed promise in platinum complexes (highlighted by **1.2.121**). The peak emission wavelengths were λ_{max}= 541-592nm and showed an average quantum yield ϕ_{lum}= ~0.19, which was much higher than previously described platinum emitters.[115-116]

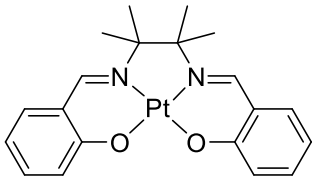

1.2.121
Che *et al*, 2004

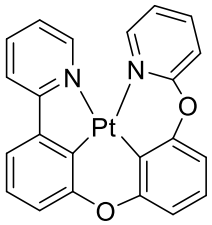

1.2.122
Turner *et al*, 2013

Figure 34 - The structures of the tetradentate complexes described by Che *et al* (left), and one of the complexes exhibited by Turner *et al* (right) both displaying high levels of luminescence.

Turner *et al* described the use of tetradentate Pt(II) complexes which coordinated to the central metal using N^C^C^N binding and displayed intense luminescence and high quantum yields. The study investigated the use of different nitrogen containing cycles such as pyridine and imidazole in order to induce different effects on the emission of the resulting complex. The peak properties shown were by PtOO3 (**1.2.125**) in the study in which the structure was comprised of pyridine and phenolic moieties. The complex displayed a peak wavelength of λ_{max}= 512nm and a quantum efficiency of ϕ_{lum}= 0.63 (ϕ_{lum}= 0.97, in a thin film), the luminescence lifetime was τ= 2.0μs. Whilst the complex, **1.2.124**, showed a higher quantum efficiency (ϕ_{lum}= 0.64), the luminescence lifetime was considerably longer. When comparing the k_r and k_{nr} values of both complexes, it can be seen that the radiative rate of PtOO3 is considerably higher than PtOO2 (**1.2.124**). In addition to the photophysical properties, the

molecular orbitals have been shown to lie in similar locations in each complex. The LUMO was predominantly localised on the pyridyl-phenolate (pypo) moiety in each complex described, whereas the HOMO was located on the aryl phenolate moieties with contribution from the central metal ion in each complex.[117]

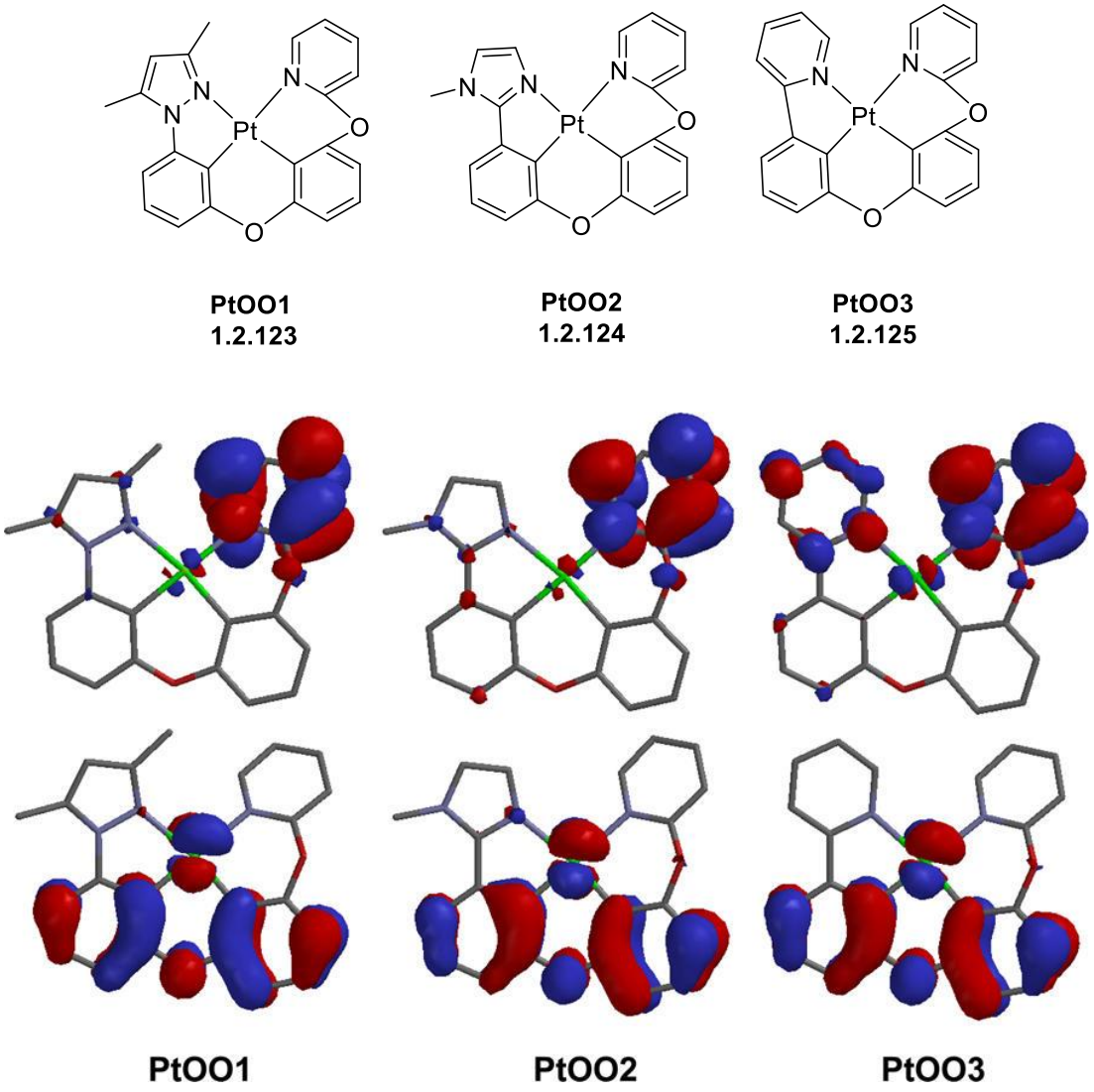

Figure 35 – The structures of the complexes **1.2.123-1.2.125** and the HOMO (bottom) and LUMO (top) of the three complexes described by Turner *et al*. The image has been taken from this paper to give an accurate depiction of the molecular orbitals.[117]

A further study by Fleetham *et al* explored the combination of previous efforts by other research groups. The structures described included the use of phenylpyrazole or phenylimidazole moieties, and this was then paired (by oxygen bridge) with a pyridyl carbazole group. The resulting complexes showed promise for "pure" blue OLED devices

with peak emission wavelengths λ_{max}= 452(±3) nm and the photoluminescent quantum yields of all the complexes mentioned being above ϕ_{lum}= 0.70. Namely, the complexes that showed the best photoluminescent quantum yields were PtON1 (**1.2.126**) and PtON1-tBu (**1.2.127**), which showed ϕ= 0.85 and 0.88 respectively.[118] The complexes described are shown in Figure 34.

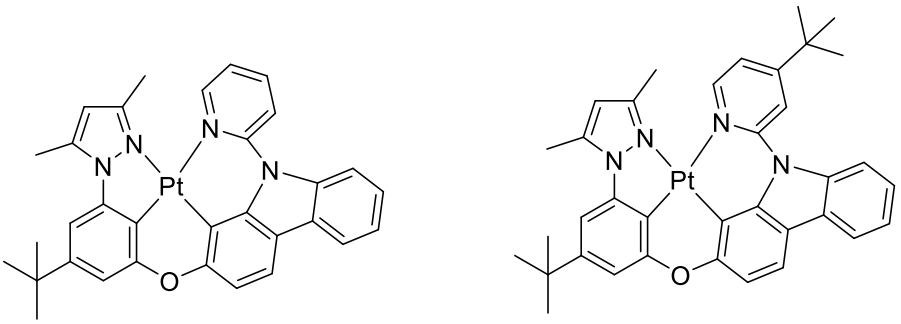

1.2.126
PtON1
ϕ_{lum}= 0.85

1.2.127
PtON1-tBu
ϕ_{lum}= 0.88

Figure 36 - The structures of the two complexes from the study by Fleetham *et al* that showed the highest quantum efficiencies, these highlight that the inclusion of the tertiary butyl substituent led to an increase in the quantum yield.

At this current time, there are few papers that detail the use of tetradentate ligands being used with iridium as a central metal ion. Chen *et al* developed one of the first examples of a luminescent tetradentate iridium complex which was based on the tetradentate complexes developed using platinum (II). The study showed a series of complexes that coordinated to the central iridium atom and generated the general formula Ir(O^N^C^O)X_2. As the study is one of few, the quantum yields can be considered to be high with the peak efficiency of ϕ_{lum}=0.18. However when this is compared with the analogous Pt(II) complexes this is a relatively low quantum efficiency.[109, 113-114, 118] The emission of the complexes described is in the orange-red region and show a range λ_{max}= 564-626nm. This emission was dependent on the substituents and the monodentate ligands used. The emission in the majority of complexes was found to be mainly ^{3}MLCT or ^{3}ILCT (inter-ligand charge transfer) and the red shifted emission is attributed to the strong field ligands used.[119]

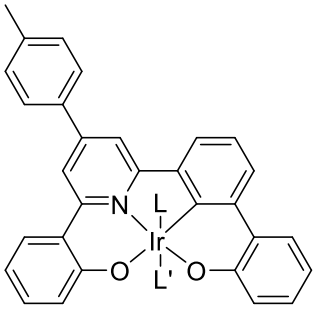

L= Methyl imidazole, pyridine, pyridazine, PPh_3, NHC
L'= Aniline, Methyl imidazole, pyridine, PPh_3

1.2.128
Chen *et al*, 2017

Figure 37 - The general structure of the complex described by Chen *et al* which described complexes with peak quantum efficiencies ϕ_{lum}=0.18.[119]

A different study detailed the use of porphyrin style tetradentate ligands in Ir(III) complexes for use in anti-microbial applications however these complexes did not display luminescence and were not tested as such.[120] The general structure of the tetradentate iridium complex is shown in Figure 37.

The development of tetradentate complexes shows a considerable level of promise for future applications in optoelectronic devices, whilst the current complexes emit in the red region further cyclometalation would remove the monodentate ligands which likely reduce or hinder the photoluminescent properties. The cyclometalation of a C^N ligand would increase the stability of the complex and induce a further red shift, so theoretically the development of tetradentate iridium complexes could be used in the development of near-IR emitting complexes.

1.2.4. Tuning of Photophysical Properties of Metal Complexes

The tuning of photophysical properties is an advantageous strategy that is used to obtain the wide range of colours in the visible spectrum. The colour tuning of the absorption and emission of cyclometalated heavy metal complexes is possible and facilitated by the localisation of the HOMO and LUMO on distinct moieties within the complex. The emission tunability is a direct result of changes to the highest occupied molecular orbital (HOMO) and

the lowest unoccupied molecular orbital (LUMO) levels. Changes to the energy gap between these orbitals can lead to different emission wavelengths.[2-3, 10, 43-45, 121]

Typically the HOMO is centred on and across the central metal ion and the aryl cyclometalated carbon. Whilst the LUMO is often delocalised across the heterocycle within the structure. By changing the substituents on the aryl ring often alters the energy level of the HOMO orbital and substituents introduced on the heterocycle will influence the energy level of the LUMO.

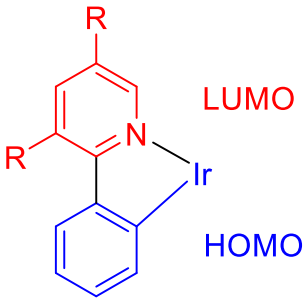

Figure 38 - A depiction of the localisation of the HOMO and LUMO orbitals on a 2-phenylpyridine derivative. HOMO is depicted in blue whilst the LUMO is shown in red.

The groups introduced on these moieties have induction effects and the inclusion of these groups will have different results. The use of electron withdrawing groups, EWG (such as $–CF_3$, -C≡N and –COOR) will stabilise the molecular orbitals, whereas use of electron donating groups, EDG (such as –R, -OR and –OH) will result in a destabilisation. This idea is simplistic in terms of describing the effects of substituents on the emission of metal complexes, nonetheless does suggest strategies for developing compounds using iridium (III) and platinum (II) that emit across the visible spectrum.

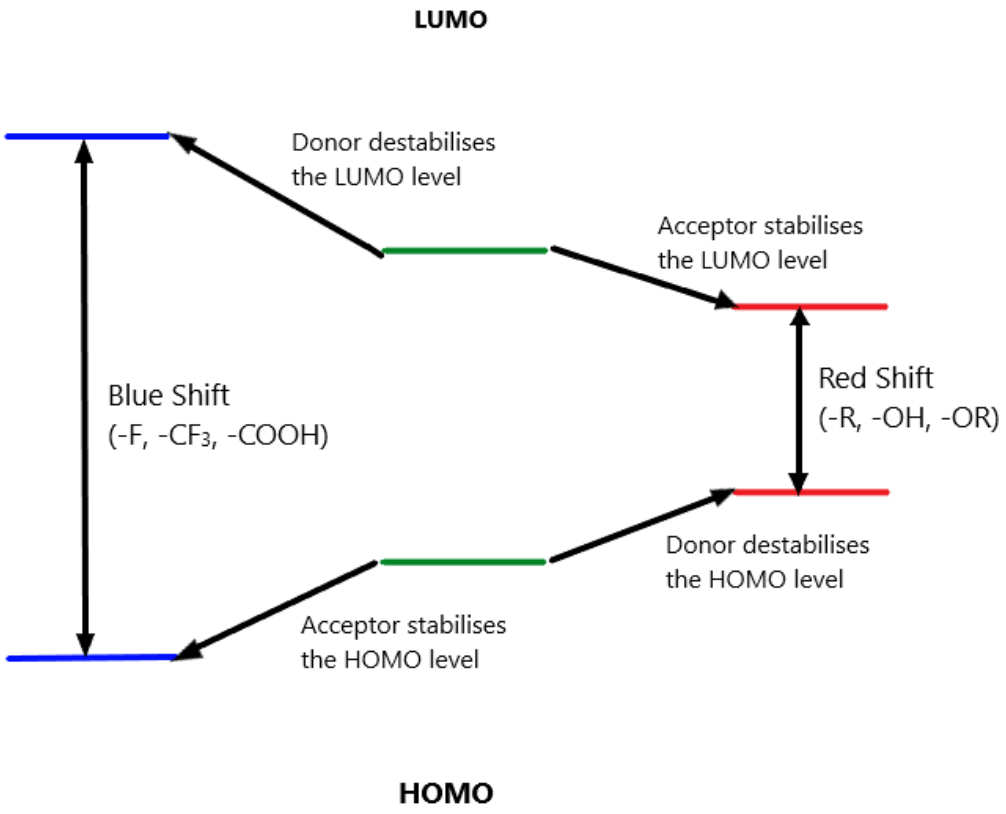

Figure 39 - The effect of EWG and EDG groups on the HOMO and LUMO levels within a compound which leads to emission wavelength changes.

The figure above shows how the inclusion of different ligand substituents can influence the level of the molecular orbitals which results in a change in the emission. Including electron accepting groups on the aryl moiety will stabilise the HOMO and reduce the energy level. When this is paired with electron donors on the heterocycle, the orbital is destabilised and the energy level is increased resulting in a blue shift of emission. If this was reversed and an acceptor was placed on the heterocycle, the orbital stabilises and the energy level decreases. Introducing a donor to the aryl group, will destabilise the HOMO and increase the energy level resulting in a red shift in emission. The blue shift can often be achieved by substituting more electron withdrawing groups onto the ligand, such as introducing a pyrazole in place of pyridine in 2-phenylpyridine.

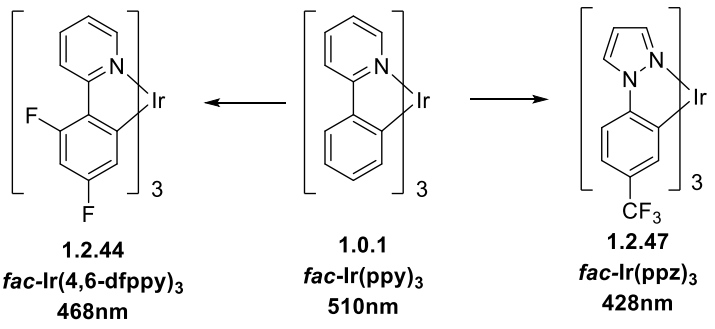

Figure 40 – Examples of complexes displaying the effect of altering the energy levels of the HOMO and LUMO. These examples show the expected blue shift caused by including electron withdrawing groups. The depiction uses **1.0.1** as a starting point.

The effect of including electron acceptors on the heterocycle and aryl moieties can induce different degrees of blue shift of emission, when paired together this strategy is an effective method for inducing significant blue shifts.

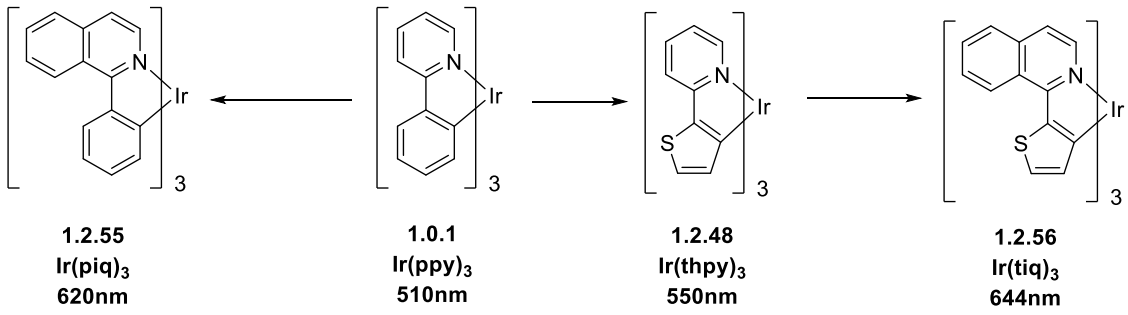

Figure 41 - The effect of inducing a red shift on the emission of the complexes, this is done by introducing electron donating groups to different moieties of the ligands using $Ir(ppy)_3$ as a starting point.

To induce a red shift in emission, the energy gap between the HOMO and LUMO must be reduced and there are many methods for achieving this reduction in orbital energy. The typical strategy for reducing the energy gap between the HOMO and LUMO is often to introduce donor groups to the HOMO and electron accepting groups to the LUMO, which stabilises and destabilises the orbitals, respectively.

Whilst the substituents used in the structure of the ligands is important, the ligand field also plays a critical role in luminescent complexes. Often this makes the difference between intense or no luminescence. This has been evidenced by the formation of blue emitting complexes, as the energy gap in blue emitters is considerably larger, the emissive state is in close proximity

to the non-emissive deactivating MC d-d states. Due to this, the addition of rigid ligands is important in the development of efficient blue emitting complexes.

This was displayed in platinum complexes investigated by Murphy *et al*, in which electron withdrawing and donating groups were used to develop analogues of $Ir(ppy)_2(acac)$. The acetylacetonate ligand was substituted for dipivaloylmethane (dpm), electron withdrawing groups were introduced on the 2-phenylpyridine derivatives. The bidentate Pt (II) complex shows a decreased quantum yield compared to other analogues such as Pt(ppy)(dpm) which has a peak quantum efficiency ϕ_{lum}= 0.15, significantly higher than that shown in Figure 42.[122]

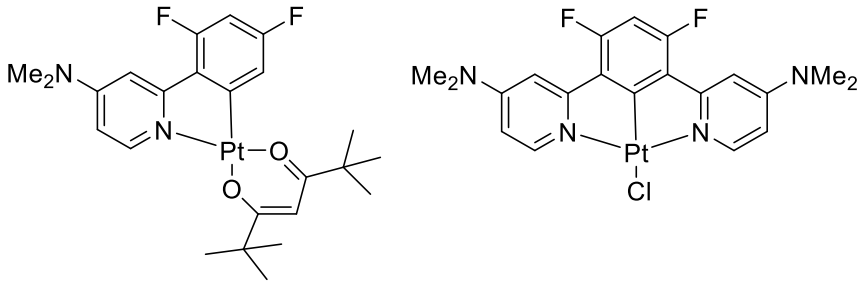

1.2.129
λ_{max} **440nm, 77K**
ϕ_{lum}= **< 10^{-3}**

1.2.130
λ_{max} **453nm, 298K**
ϕ_{lum}= **0.66**

Figure 42 - The structures described by Murphy *et al* highlighting the effect of a strong ligand field on the luminescent properties. The use of the N^C^N ligand increases the rigidity of the complex which in turn stabilises the LUMO and leads to a decrease in orbital energy.

When compared to the N^C^N coordinated complex, the tridentate coordination incorporates an increased level of rigidity imposed by the short Pt-C bond, in effect leading to a more efficient blue emission.[122]

1.3. Organic Light Emitting Diodes (OLEDs)

1.3.1. Fundamental Structure and Requirements of OLEDs

The development of electroluminescent devices such as organic light emitting diodes, has increased over recent decades. This time period coincides with the development of highly luminescent metal complexes suitable for use in these applications.[15] The use of electroluminescent devices such as OLED's show promise for use in large area displays and

solid state lighting. OLED's that incorporate phosphorescent metal complexes have also gathered an increased interest due to a higher level of efficiency and device lifetime. Efficient OLED devices have shown promise in the technological market and have advantages over their predecessors, liquid crystal displays (LCD's). The increased colour contrast, lifetime and temperate stability show that the use of OLED's is more preferable.

Electroluminescence in devices arises from an electronic stimulus and the radiative decay of the excited singlet and triplet states. These excited states are the result of charge recombination, the injection of holes and electrons which are introduced into the system from the anode and cathode respectively. The introduction of a heavy metal ensures that the emission from both singlet and triplet excited states can be harvested.

Electroluminescence of an organic compound was first reported in 1955 by Bernanose in Nancy, France.[123] The first examples of OLED devices were reported by Tang and Van Slyke in 1987 with efficient brightness at low voltages.[124] As OLED devices have developed, the use of different heavy metals in complexes has varied with complexes using both iridium (III) and platinum (II) as central metal ions. A notable complex used for technological application is the ruthenium complex, $[Ru(bpy)_3]^{2+}$. However this complex is cationic and is not preferred for use in OLED devices but may be suitable for other applications such as bioimaging or as a photosensitizer.[125] The use of highly luminescent and efficient charge neutral emitters are desirable for use in OLED devices. This has been a main focus point with complexes starting with a single metal centre and developing to multi-nuclear structures.[5, 105]

A promising use of platinum as a central metal ion was reported as part of a porphyrin structure by Baldo and coworkers in 1998, which resulted with platinum (II) octaethylporphyrin (PtOEP). The study described the formation of device showing an external quantum efficiency η_{ext}= 4%.[115] Further work was carried out and the tuning the capabilities were explored by Baldo and co-workers. This study showed that minor changes to the structure did not result in a significant change to the device efficiency. Additions to the conjugation of the system were revealed to be detrimental to the photophysical properties of the complex.[66]

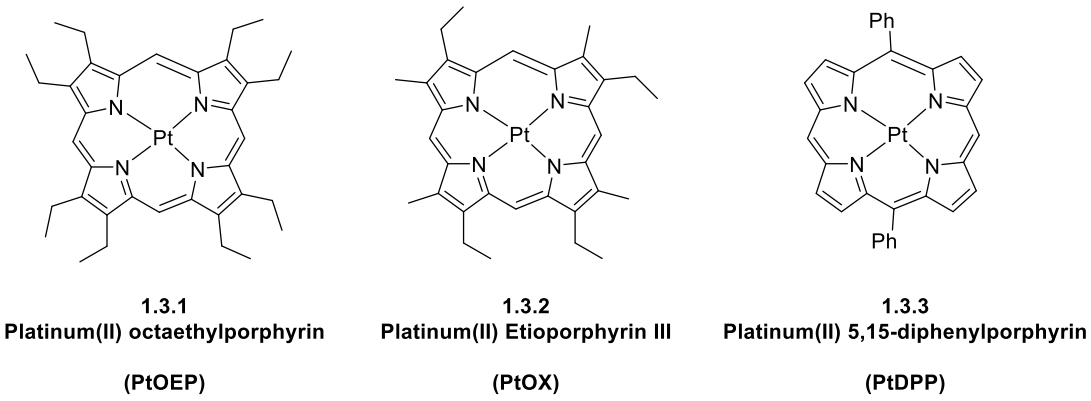

1.3.1
Platinum(II) octaethylporphyrin

(PtOEP)

1.3.2
Platinum(II) Etioporphyrin III

(PtOX)

1.3.3
Platinum(II) 5,15-diphenylporphyrin

(PtDPP)

Figure 43 - The structures of the platinum porphyrin complexes synthesised by Baldo and coworkers.[66, 115]

Complexes that incorporated iridium(III) as the central metal ion were synthesised by Forrest and co-workers using cyclometalating bidentate auxiliary ligands. One of these complexes was notably *fac*-Ir(ppy)$_3$, which employed the use of a tris(2-phenylpyridine) arrangement.[126] The use of 2-phenylpyridine (*ppy*) as a cyclometalating ligand in complexes for highly efficient devices is well documented. This ligand was reported by Thompson and co-workers in Ir(ppy)$_2$(acac), a complex that showed similar photophysical properties to the tris-cyclometalated structure, *fac*-Ir(ppy)$_3$.[65, 78, 127] Kido and co-workers fabricated an OLED device using *fac*-Ir(ppy)$_3$ which showed an external quantum efficiency of η_{ext}= ~29%. The device also showed luminous efficiencies of 133 lm W^{-1} and 100 cd m^{-2}, which highlights the high level of luminous efficacy across the device.[70]

An OLED device typically consists of a conducting and emissive layer between an anode and a cathode, the conducting layer transports ‘holes’ from the anode whilst the emissive layer transports electrons from the cathode and consists of a film of organic material.[128] The emissive layer emits light in response to the stimulus of the electrical current.

The anode used in OLED devices is typically made of indium tin oxide (ITO) whilst the cathode is often made from metals such as aluminium or barium. This is because they have a lower work function than the anode facilitating the release of electrons into an electron transport layer.[128-129] The injection of the electrons and holes from the electrodes move toward the electrode of opposing current via hopping mechanism from molecule to molecule. Upon

recombination in the emissive layer, in a spatially close environment, an exciton is formed and this results in a radiative release of energy.[128] The structure of different OLED devices is shown below with the mechanism of the movement of electrons and holes through the device.[130-132]

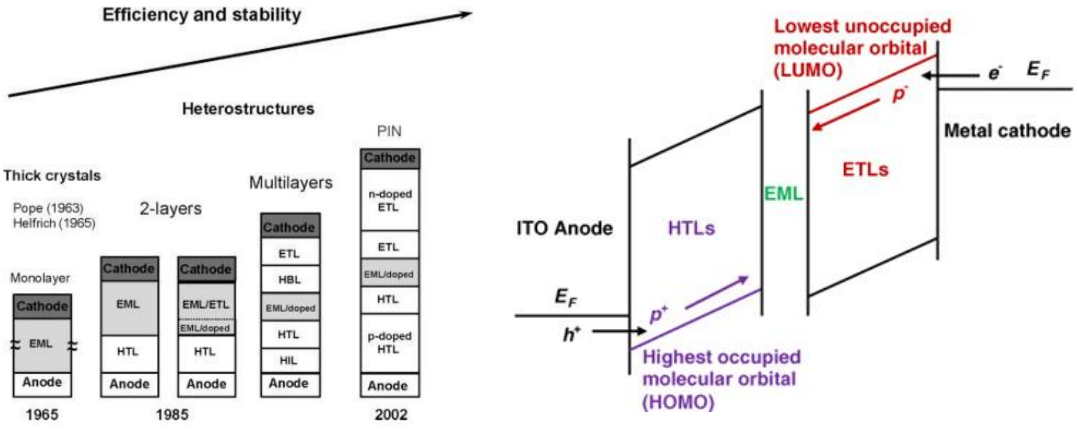

Figure 44- A diagram showing the advances made in the development of OLED devices, showing the first known OLED structure by Pope and Helfrich. (left). EML= emissive layer, HTL= holes transport layer, ETL= electron transport layer. The mechanism of action of an OLED device upon the excitation by electronic current, the holes from the anode move through the HOMO of the molecules whilst the electrons move through the LUMO of the molecules (right).

Of these arrangements, the most important aspect of the structure is the emissive layer which contains the heavy metal or transition metal complex as the emitter. The emitter used for the device can be placed between the transport layers, or more commonly, the emissive layer and emitter are doped with a host compound. The host compound is useful to determine the overall device performance and typically possess a high level of triplet energy and appropriate HOMO and LUMO levels. It is desirable that the host compound has a spectral overlap with the emitter applied to the device.[133] An example host compound is 4,4'-bis(9-carbazolyl)biphenyl (CBP), has been one of the most widely used host materials due to high triplet energies and good hole transporting qualities. However use of this host has led to poor device efficiencies.[134] Changes to the host material from CBP showed promise and the overall internal efficiency of the device. For example the change from a carbazole based host to a triazole based host material resulted in distinctly increased device efficiency.[15, 135] Simplistic changes to the structure of

the host material such as the addition of nitrile groups resulted in an increase of overall device efficiency.[136]

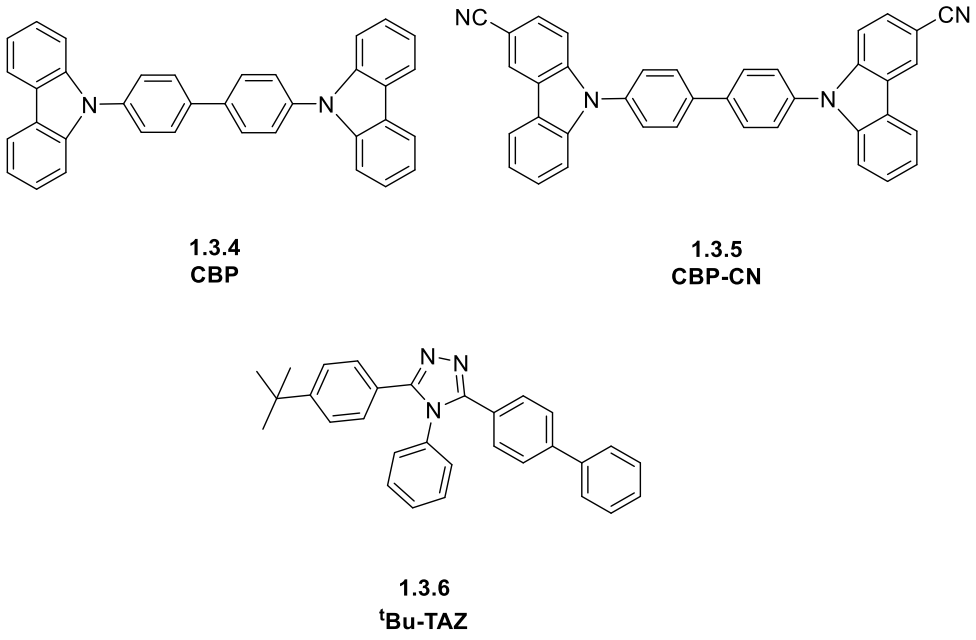

1.3.4
CBP

1.3.5
CBP-CN

1.3.6
^{t}Bu-TAZ

Figure 45- The structure of CBP, a well-documented and commonly used host material in OLED devices (top left), Zhang and coworkers showed that changes to the host compound can dramatically improve the overall device efficiency (top right). By changing the host material to a triazole based compound also had benefits on the device efficiency in comparison to CBP, a notable compound (bottom), 3-(Biphenyl-4-yl)-5-(4-tert-butylphenyl)-4-phenyl-4H-1,2,4-triazole (TAZ).

1.3.2. OLED Device Studies Using Mononuclear Iridium(III) Complexes

For an efficient multi-coloured display, OLEDs using emitters of each colour emission are required. The obligatory emitters for these displays are those that show blue (~450-470nm), green (~500-550nm) and red (~620-700nm) emission.[137] There have been many examples of complexes that emit across the visible spectrum range, each of the complexes utilised different ancillary bidentate ligands to achieve shift in the emission wavelength. The tuning capabilities of complexes will be discussed further in this review. Green emitters typically display a higher level of efficiency in comparison to red and blue emitters. As a result of this, the fabrication of devices using red and blue emitters has proved difficult. The difficulty of fabricating red emitters can be attributed to the energy gap law and the small energy gap between the HOMO and LUMO of the complexes utilised.

Hisamatsu and Aoki developed blue emitting cyclometalating Ir(III) complexes using tris-bidentate ligands based on the previously studied *fac*-Ir(ppy)$_3$ which uses 2-phenylpyridine. The substitution of electron accepting/withdrawing groups such as nitriles and amines were used to induce a blue shift of emission similar to known FIrpic complexes. The study showed the development of potential emitters in the blue region with quantum yields in the range ϕ=0.21-0.68. The complexes synthesised did not include the presence of fluorine a potentially detrimental group to the lifetime of a device.[138-140]

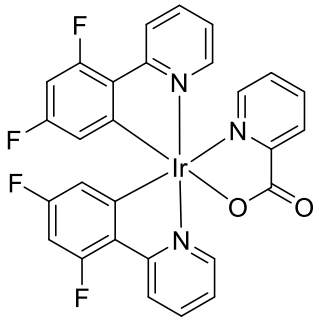

1.3.7
FIrpic

Figure 46 - The structure of FIrpic, a well documented blue emitter that has been used in the development of OLED devices.

Byun *et al* developed devices using analogues of the known blue emitting FIrpic using the substitution of nitriles and the use of supplementary ancillary ligand in place of a tris-bidentate structure. The ancillary ligand used was 3,5-dimethylpyrazole-*N*-carboxamide and resulted in the formation of deep blue emission (λ_{max}= 465nm) and a device external quantum efficiency η_{ext}= ~4%.[141] The findings of this study were developed further by Jeon *et al* and devices were fabricated with external quantum efficiencies η_{ext}= ~20% for sky blue phosphorescent OLEDs (PhOLEDs). A seemingly difficult task due to the requirement of high triplet energy from the host.[142] The study showed the external quantum efficiencies of the sky blue PhOLEDs (FCNIrpic) were barely altered when the doping concentration was changed at a current density of 500 cd m^{-2} with values ranging between 18-21%. The power efficiency of the device ranged between 13-22 lm W^{-1} at the same current density.[142] A study carried out by Tsuzuki

et al in 2003 investigated the use pentafluorophenyl groups in the fabrication of blue emitting PhOLED devices which showed the development of green and blue emitters. The best emitter developed showed external quantum efficiency close to that of the model green emitter $Ir(ppy)_2(acac)$ around η_{ext}= 8-10% and an emission in the low green region λ_{max}= 513nm.[143] The shift of emission to the green region was likely due to the inclusion of the acetoacetonate group. The figure below shows the development of potential emitters for use in the fabrication of blue and green PhOLED devices showing the effect of changing the ancillary ligand has on the resulting external quantum efficiency.

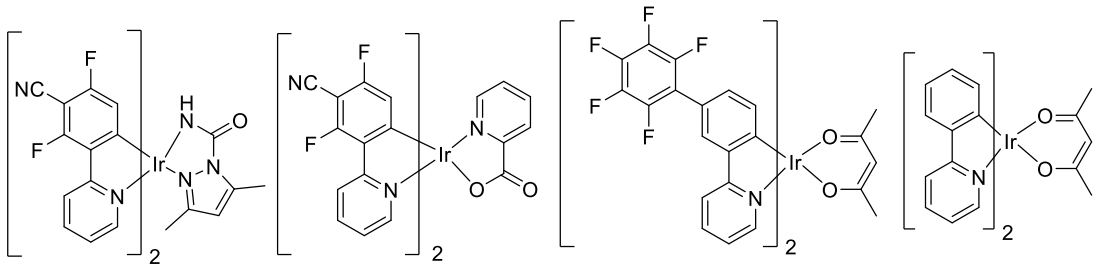

Figure 47 - An example of the complexes developed organised in increasing order of wavelength (blue to green), highlighting the changes in the complexes can result in detrimental effects on the external quantum efficiency of devices. The ZN ligand is 3,5-dimethylpyrazole-1-carboxamide.

Green emitters are typically higher in efficiency than red or blue emitters, Adachi and co-workers reported the fabrication of a device using $Ir(ppy)_2(acac)$ as the green emitter which achieved near 100% internal quantum efficiency. The emitter showed a maximum OLED external quantum efficiency η_{ext}=19% and a luminance power efficiency of ~60 lm W^{-1}, the high efficiencies are due to the high level of calculated internal efficiency (~87%) and a balanced hole and electron injection within the emissive layer.[65]

As the fabrication of efficient red emitters is a greater challenge than efficient green emitters, there has been a larger focus on the complexes that emit in the red region of the visible spectrum. A good example of a deep red OLED device was synthesised Li and co-workers and showed a good EQE values and power efficiency using a tris-cyclometalated system. The

complex, $Ir(piq)_3$ was used with an emissive layer containing a triphenylamine/oxadiazole mixture and this resulted in η_{ext}= ~21% and a power efficiency (η_p) of ~16 lm W^{-1}.[144] The tuning capabilities of metal complexes allowed for adaptations to the structure of $Ir(piq)_3$. These changes were made by Wu *et al* and the phenylisoquinoline group (piq) was substituted for a benzoxazole based ancillary ligand. The result was a shift in the efficiency of the resulting OLED device. The deep red emitting device showed a power efficiency of 9.1 lm W^{-1}, a decrease in comparison to the emitter synthesised by Li and co-workers. The complex also showed luminescence efficiencies of 10.3 cd A^{-1} and a CIE (Commission Internationale d'Eclairage) coordination of (0.67,0.33) which indicates a deep red colour.[145] Complexes using the (piq) ancillary ligand have a typical emission of λ_{max}= ~620nm. The work carried out by Wu *et al* showed a slight improvement of luminescent efficiency at low concentrations (1wt %). In comparison to Li and co-workers, in which the complexes displayed power efficiencies of η_p= 10.62 lm W^{-1}. However the luminescent efficiency (η_L) of η_L =9.44 cd A^{-1} showed a decrease in comparison. There is no difference in the CIE chromaticity coordinates as Li and coworkers reported (0.67,0.33) for $Ir(piq_3)$ at low concentrations.[144-145] At low concentrations there is very little difference despite the changes to the structure of the emitter. The CIE chromaticity chart is shown in Figure 49 and highlights that every colour in the visible spectrum can be defined by specific coordinates.[146]

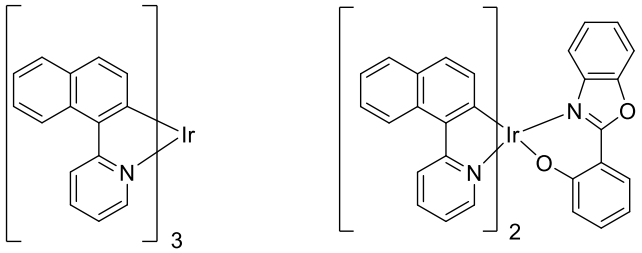

1.2.55
$Ir(piq)_3$
λ_{max} **620nm**
Li *et al*, 2014

1.3.12
$Ir(piq)_2(bop)$
λ_{max} **624nm**
Wu *et al*, 2013

Figure 48 - The structures for known deep red emitters used in PhOLED devices in tris-cyclometalated arrangements. The alteration to the structure of $Ir(piq)_3$ to $Ir(piq)_2$bop did not result in a distinct change in properties.

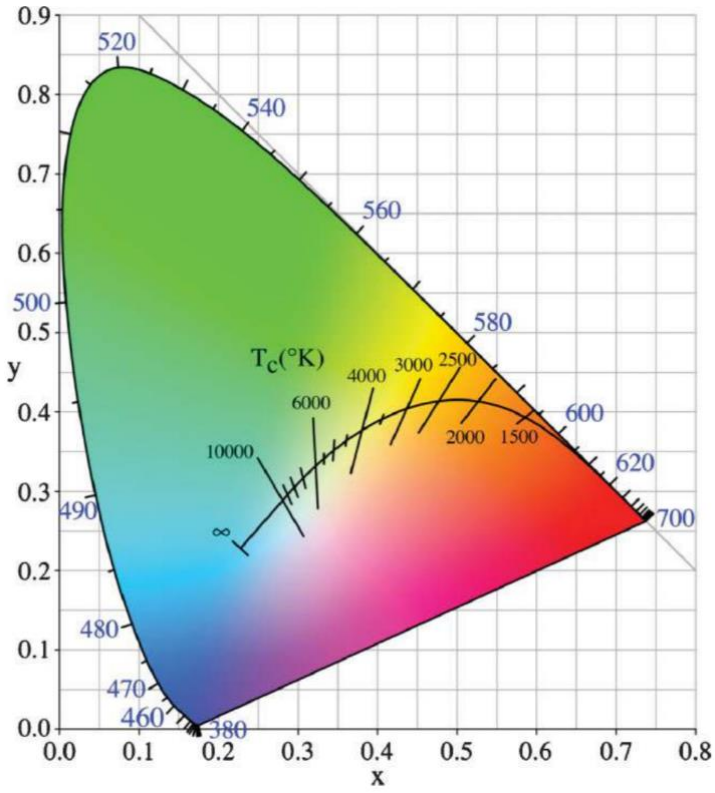

Figure 49 - The CIE chromaticity chart, every colour of the visible light spectrum is defined by specific coordinates within or on the boundary of this chart. The black curve is the optimum colours for lighting in relation to black body radiation.[147]

In addition to the fabrication of red, green and blue emitters there has been an increasing interest in the development of white emitting OLED devices. Bryce and co-workers outlined that an efficient white OLED (WOLED) are bound by three parameters, i) the CIE chromaticity coordinates, ii) the colour temperature (CT) and iii) the colour reference index (CRI). The CRI is measured relative to the CT, for example a black body radiator has a CRI value of 100. Whilst the primary parameter states the typical coordinates of white light is (0.33, 0.33), the most ideal conditions for lighting lie on the black curve between ~3000-10,000°K.[146] As the parameters provide an outline for the development of the WOLEDs, there are also additional requirements for the fabrication of the device, two methods can be used. The first is to use separate layers of each colour of emitter to form the typical RGB format (red-green-blue) or to use both orange and blue emitters (OB) with both methodologies offering a balanced source of white light.

A study carried out by Kanno and co-workers used the OB strategy of only using two emitters in the WOLED device. The two emitters used are [Ir(4,6-dfppy)$_3$] for blue emission and [Ir(PQ)$_2$(acac)] as the red phosphor, the combination of these emitters resulted in a white emitting OLED device with peak EQE and power efficiencies at 10.5% and 9.8 lm W^{-1}. The emission of the device was CIE characterised with coordinates (0.42, 0.39), which is close to the ideal region for white light.[148]

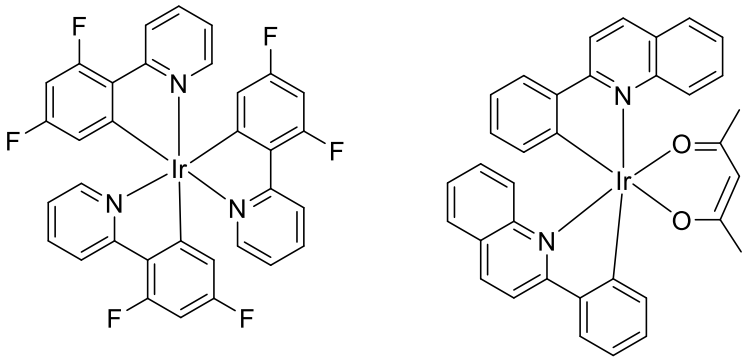

1.2.44
Ir(4,6-dfppy)$_3$

1.3.13
Ir(PQ)$_2$(acac)

Figure 50 - The structures of the complexes used as emitters in WOLED devices described by Kanno *et al*.[148] Ir(4,6-dfppy)$_3$ was used as the blue phosphor, whilst Ir(PQ)$_2$(acac) was the red emitter in the device.

Forrest and Sun developed a white emitting OLED that utilised the RGB strategy of three separate emissive layers. The emitters used were Ir(III) bis-(2-phenylquinolyl-N,C$^{2'}$) acetylacetonate (PQIr), tris-(2-phenylpyridine)iridium [Ir(ppy)$_3$] and bis-(4',6'-difluorophenylpyridinato) tetrakis(1-pyrazolyl) borate (FIr6) for the red, green and blue emitters respectively. The use of the three emissive layers resulted in the fabrication of a device that peaked at a total EQE of 28% and a power efficiency of 54 lm W^{-1}, a significant increase in efficiency in comparison to the OB type OLED devices.[149] It can be noted that the use of the OB method for the fabrication of devices is beneficial in comparison to the use of the RGB strategy, this is because the use of less dopant material reduces the overall cost of production and increases the simplicity of the device manufacture.

1.3.3. OLED Device Studies Using Mononuclear Platinum(II) complexes

The use of platinum (II) as a central metal ion with terdentate auxiliary ligands has been employed as a strategy to blue shift the emission wavelength of a phosphor. Williams and coworkers described that the wavelength of emission changes upon alteration to the doping concentration of the emitter. The blue shift of the emission does not pose any detrimental decreases in the quantum efficiencies displayed by complexes utilising bidentate ligands. The tridentate complex shown in Figure 51, incorporated a strongly donating amine group and electron accepting fluorine groups. This resulted in very low quantum yield values but desirable emission wavelengths. The study showed the use of a planar N^C^N Pt(II) complex resulted in a dramatic increase and improvement in the photophysical properties and therefore increased the benefit for the fabrication of OLED devices. The complex was doped at concentrations ranging from 3-100%. The increase in concentration resulted in the shift of emission to the red region which can be attributed to aggregates formed by Pt-Pt interactions and the formation of triplet state excimers.[122]

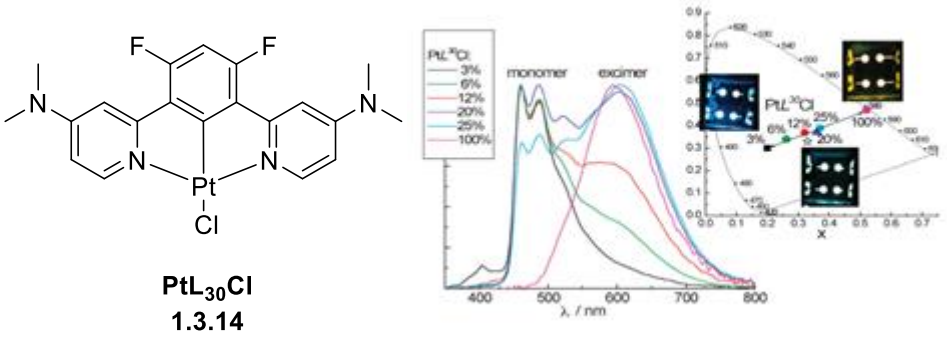

Figure 51- The structure of the Pt(II) terdentate complex described by Williams and coworkers (left). The diagram shows that an increasing doping concentration results in the red shift of the emission and disappearance of the blue colour. The emission spectra shown is taken from the study by Williams *et al.*[122]

The use of terdentate bridging ligands can be highly beneficial to the chemical and luminescent properties of a complex. An increase in coordination to tetradentate ligands furthered the benefits displayed by terdentate complexes by increasing stability and removing the potentially detrimental Cl^- monodentate ligand. An example of this was exhibited by

Fleetham *et al*, who developed a series of tetradentate Pt(II) complexes as a strategy to avoid the use of multiple dopants as a means of targeting bright and efficient WOLED devices. The study displays the development of complexes which resulted in devices with peak EQE values ~24% and a power efficiencies of ~48 lm W^{-1}, these values are also supported by strong device lifetimes >200 hours, making them ideal for solid state white lighting.[109]

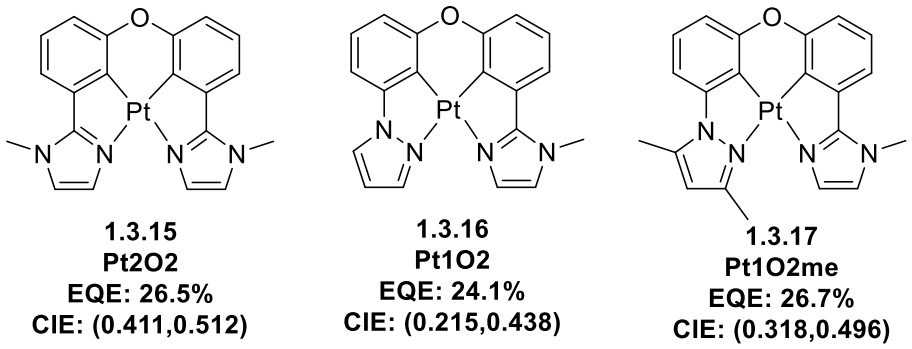

Figure 52 - The tetradentate complexes described by Fleetham and co-workers, the complexes emit in the blue-green region (~490-530nm) however the CIE coordinates show some are present in the white region of the colour matrix.

Developments of non-porphyrin tetradentate complexes using Pt(II) (similar to the complexes in Figure 52 and Figure 53) has vastly increased due to highly desirable emissive excited states and high thermal stability.[150] The development of salen type complexes was first described Che *et al* using dianionic bis(phenoxy)diimine (N_2O_2) ligands, which displayed a high level of stability >500°C and desirable properties for use in multi-layered OLED devices.[112]

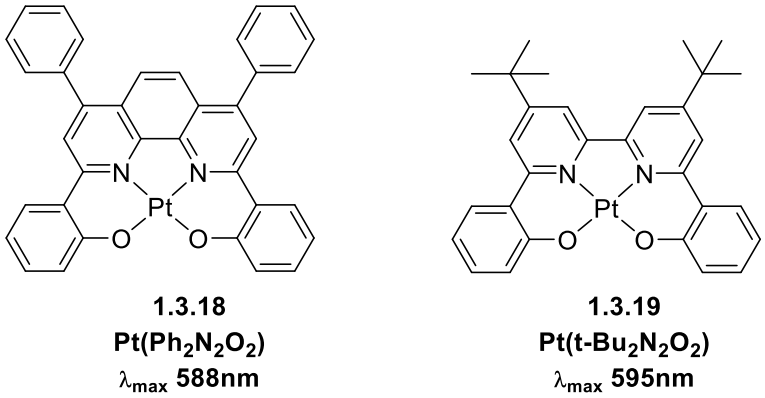

Figure 53- The structures of the complexes described by Che *et al* as principle examples of salen type luminescent Pt(II) complexes.

The tuning capabilities of heavy metal complexes means that these structures can be changed to achieve different emission wavelengths, a strategy that has been discussed previously. Building on the findings of Che and co-workers, a study by Zhang *et al* employed the same O^N^N^O coordination but utilised a Schiff base structure of the ligand. The use of the Schiff base can reduce the conjugation of the π-system and expand the energy gap whilst increasing the overall device efficiency.[151] The study showed that the use of this type of ligand with a central Pt(II) metal ion resulted in peak EQE of 8.3% and power efficiency of 17 lm W^{-1} which is similar to porphyrin type Pt(II) complexes previously discussed. The use of these ligands with bulky substituents prevented aggregation, a known problem with platinum complexes and resulted in a single EML white emitting OLED device.

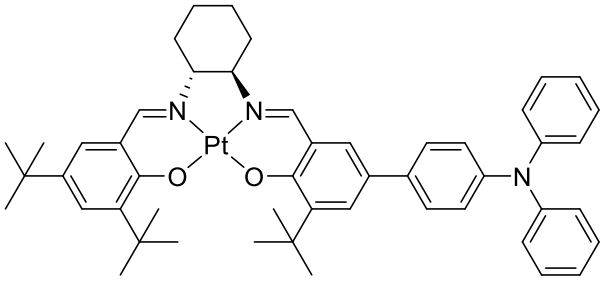

1.3.20
Complex **2g**
λ_{max} **568nm**
η_{ext}: **8.3%**
CIE: **(0.50, 0.50)**

Figure 54 - The structure of the Schiff base salen complex with the peak device properties as a single dopant displayed by Zhang and coworkers.

The use of platinum (II) complexes with tetradentate ligands have displayed desirable properties for use in OLED devices. In addition to the described O^N^N^O coordinating ligands, Che and co-workers developed highly luminescent complexes (ϕ= 0.76-0.90) using O^N^C^N coordination. The complexes developed showed a maximum EQE of ~18% with a luminescence efficiency of 66.7 cd A^{-1} and displaying excellent green phosphorescence.[114]

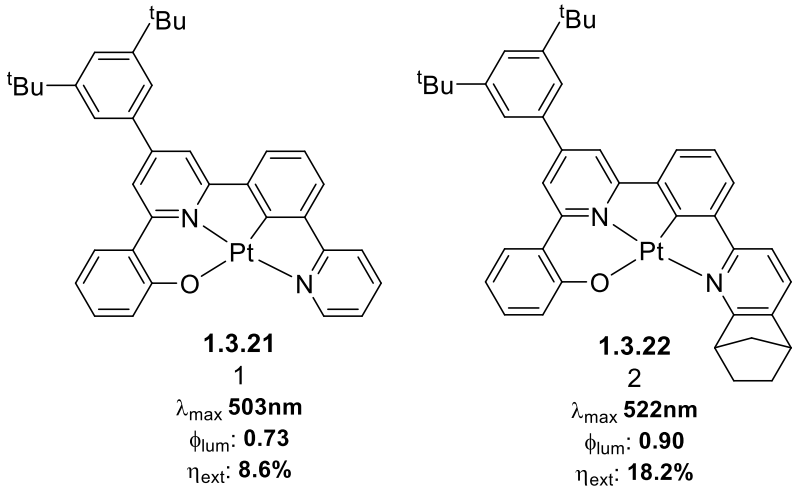

Figure 55- The complexes developed by Che and co-workers displaying high quantum yields and high efficiency green emitting OLED devices.

The complexes in this section have shown that the increasing use of iridium (III) and platinum (II) as central metal ions is gaining traction due to their high thermal and chemical stability and the capability to be used in highly efficient OLED devices. Further investigation into the use of these complexes will lead to the development of devices with improved device stability and longer lifetimes. Through the advancements in the area the device efficiencies will improve and will lead to a higher level of colour purity.

1.4. Aims and Objectives

Throughout the progression of this review, examples of highly luminescent transition metal complexes have been described. The described complexes have shown that the structure of the ligand and the central metal can have significant effects on the luminescent properties. The development of mono-nuclear iridium (III) complexes has been a well-documented topic and has shown advantages for uses in organic light emitting diodes.

In this current field, there are advances in the development of highly efficient multi-nuclear complexes, those described in this review have highlighted that many of the di-iridium complexes are highly efficient but few are applied for use in OLEDs. The design of efficient red emitters must account for the smaller energy gap between the HOMO and LUMO which can lead to non-emissive decay. Current leading complexes developed by Kozhevnikov and

co-workers incorporate cyclometalating bridging ligands and dinuclear terdentate coordination resulting in highly luminescent complexes with quantum efficiencies exceeding ϕ_{lum}= 0.65.

The aim of this project is to develop novel charge neutral di-nuclear Ir(III) complexes that are excellent candidates for use as dopants in OLED devices. There will be more detailed aims in the following sections.

1.4.1. Increasing the Solubility of Previously Synthesised Complexes.

A recent study by Kozhevnikov *et al* in 2014 described the development of novel bis-N^C^N ligands to be used for ditopic Ir(III) complexes.[105] The synthesis of ligands such as those shown in Figure 56 resulted in complexes with the general formula $Ir(N^C^NN^C^N)(C^N)_2Cl_2$ and showed promising luminescent properties.

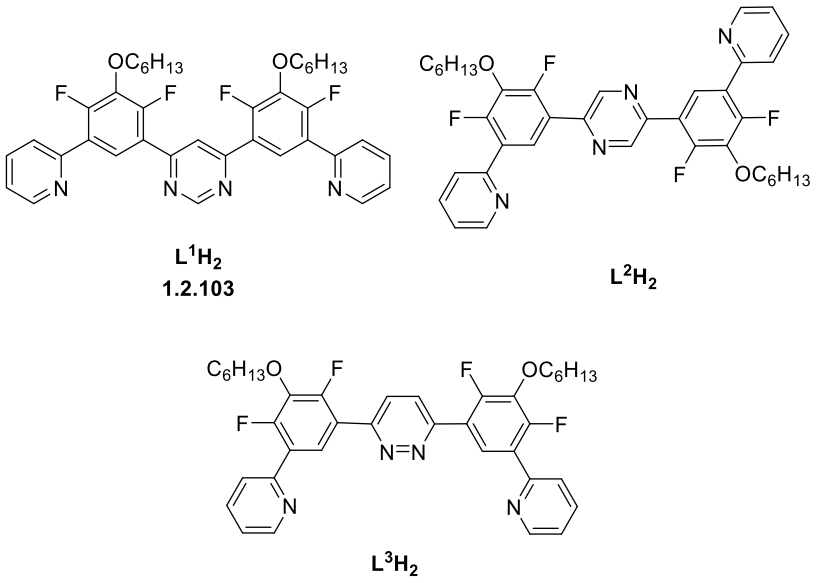

Figure 56 - The ditopic ligands described by Kozhevnikov *et al*, the different heterocycles lead to different levels of luminescence with the pyrimidine linker showing the highest level of promise when coordinate to the iridium metal centres.

Complementing previous work, the solubility of the complexes is dramatically reduced due to the rigidity of the bridging ligands, a known drawback of tridentate coordinating complexes. In order to combat the poor solubility, the auxiliary ligands will be altered and the substituents

changed from the methylated *ppy* analogue (shown in Figure 31) to a hexamethylated cyclopentene derivative (shown in Figure 57).

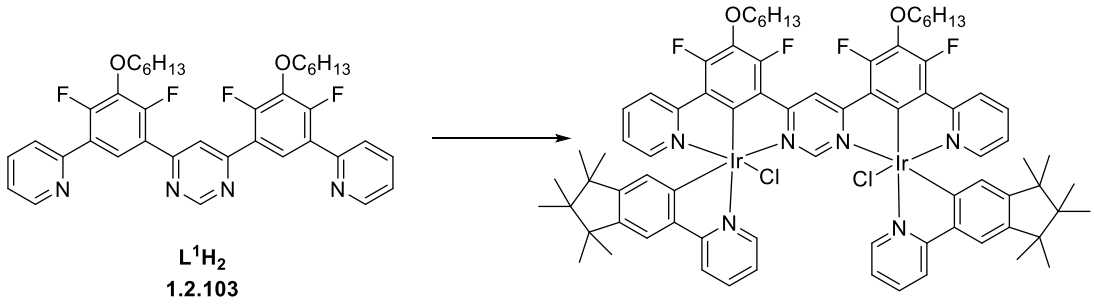

Figure 57 - The complex to be synthesised using the bridging ligand described by Kozhevnikov *et al*.[105]Whilst maintaining the 2-phenylpyridine analogue, a hexamethylated cyclopentene ring will be added to the aryl moiety to investigate the effect of an increased level of solubilising groups. This also decreases the frequency of fluorine groups present within the complex. The removal of these additional fluorine groups will be investigated in the next section.

1.4.2. Removing Fluorine from the Structure of Di-iridium Complexes.

The work carried out by Kozhevnikov *et al* and Daniels *et al* showed the formation of highly luminescent multi-nuclear complexes with high quantum efficiencies (ϕ_{lum}= 0.7-1.0). The complexes described show excellent potential for optoelectronic devices however the presence of fluorine as a substituent can be detrimental to the lifetime of these applications. The cleavage of the fluorine in the devices can lead to charge migration and the overall reduction of the efficiency and longevity of the device lifetime.[6, 105]

As a result the removal of these fluorine groups is of the upmost priority, this is achieved by substituting the halogen and alkoxy groups for a tertiary butyl substituent. The inclusion of the tertiary butyl is to prevent the competitive cyclometalation and increase the level of solubility by preventing intermolecular interaction. The solubility of the complex will be further benefitted by the inclusion of the hexa-methylated C^N ligand.

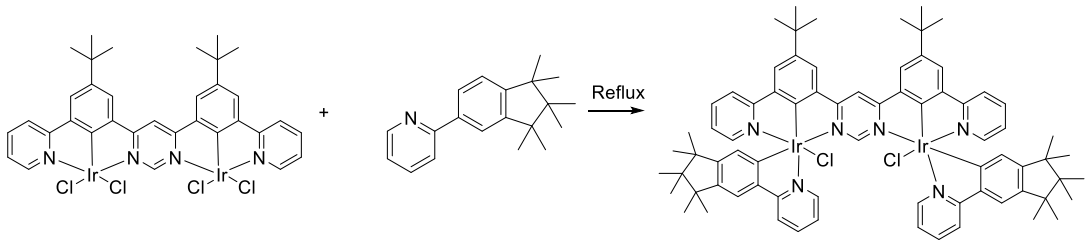

Scheme 6 - The proposed reaction scheme for the development of the novel fluorine free di-topic complex.

Using the work described in the previous section, the removal of the fluorine and alkoxy groups is expected to result in a red shift of emission. The tertiary butyl group is electron donating and the removal of the electron accepting fluorine groups is likely to result in a reduction of the energy gap and therefore inducing a red shift of the emission wavelength.

1.4.3. The use of Di-anionic Asymmetric O^N^C Auxiliary Ligands in Mono-Iridium (III) complexes.

The synthesis of O^N^C coordinating ligands and the associated complexes was described by Williams *et al* however the complexes utilised picolinate binding and was shown to be poorly luminescent (ϕ_{lum}= 0.04). The poor luminescence was attributed to the reversible cleavage of the weak Ir-O coordinated bond.[13]

Unlike the use of picolinate, phenolate coordination is not widely investigated and could bear importance in the development of oxygen containing auxiliary ligands. As phenolic coordination has not been investigated, a series of complexes will be developed in order to observe the changes to the photoluminescent properties when the structure of the auxiliary ligand is changed.

The proposed alterations to the structures include the addition of aromatic cycles and substitution of solubilising groups. Increasing the rigidity of the ligand will also be trialled to monitor the potential effects.

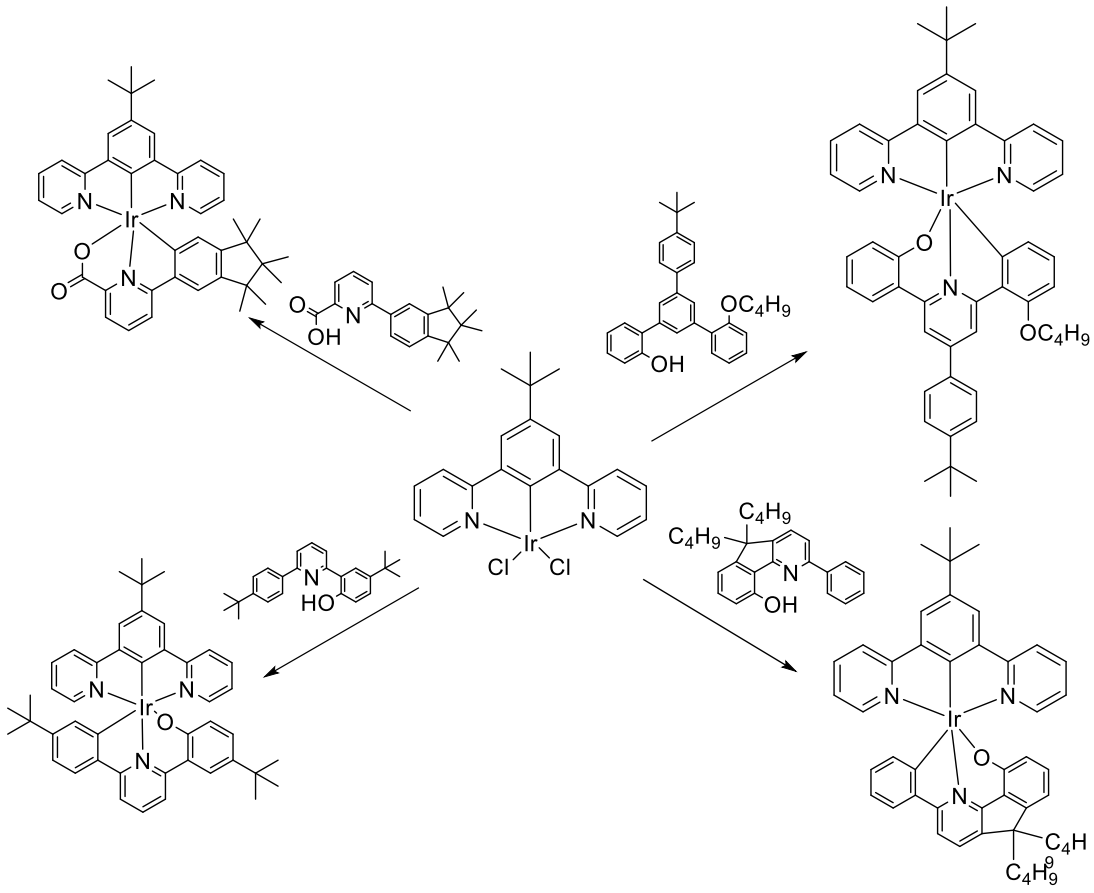

Figure 58 - The proposed complexes to be developed as a series of novel phenolate based mono-iridium complexes.

1.4.4. Development of Symmetrical Di-anionic Tridentate ligands and associated Complexes

In the synthesis of metal complexes, the use of C^N coordinating ligands can lead to the formation of an enantiomeric mix which can often be difficult to separate. This is a considerable issue in the design and synthesis of multi-nuclear complexes and can lead to an inseparable mixture due to the similar properties of individual isomers, a problem described by Kozhevnikov *et al.*[105]

Whilst considering the previous studies and observations, different symmetrical coordination modes will be tried and tested to discover the different effects on the photophysical properties of the resulting complexes. Adjusting the phenolate coordinating tridentate complex, an

additional phenolate coordination will be added to develop an unprecedented coordination type not yet documented for Ir (III) complexes.

Further utilising the coordination modes detailed by Williams *et al*, a symmetrical N^N^N ligand will be tested. In order to make further improvements in the development of symmetrical complexes, the replication of C^N^C cyclometalating complexes will be carried out using the dichlorobridged dimer in this project. Using the same auxiliary ligand detailed by Williams *et al*, the complex methodology will be replicated and then adapted for use in di-iridium structures.[12-13, 39] The fluorine atoms on the ligands require removal and therefore different auxiliary ligands will be designed to produce a novel series of C^N^C complexes.

The chemistry adaptation from mono-nuclear to di-nuclear complexes can prove to be problematic and this project will detail the conditions altered and tested in order to synthesise two novel C^N^C di-nuclear complexes. The project will also detail the attempts to remove fluorine from the auxiliary C^N^C ligands and produce fluorine-free derivatives using electron accepting groups such as pyrimidine and pyridine moieties.

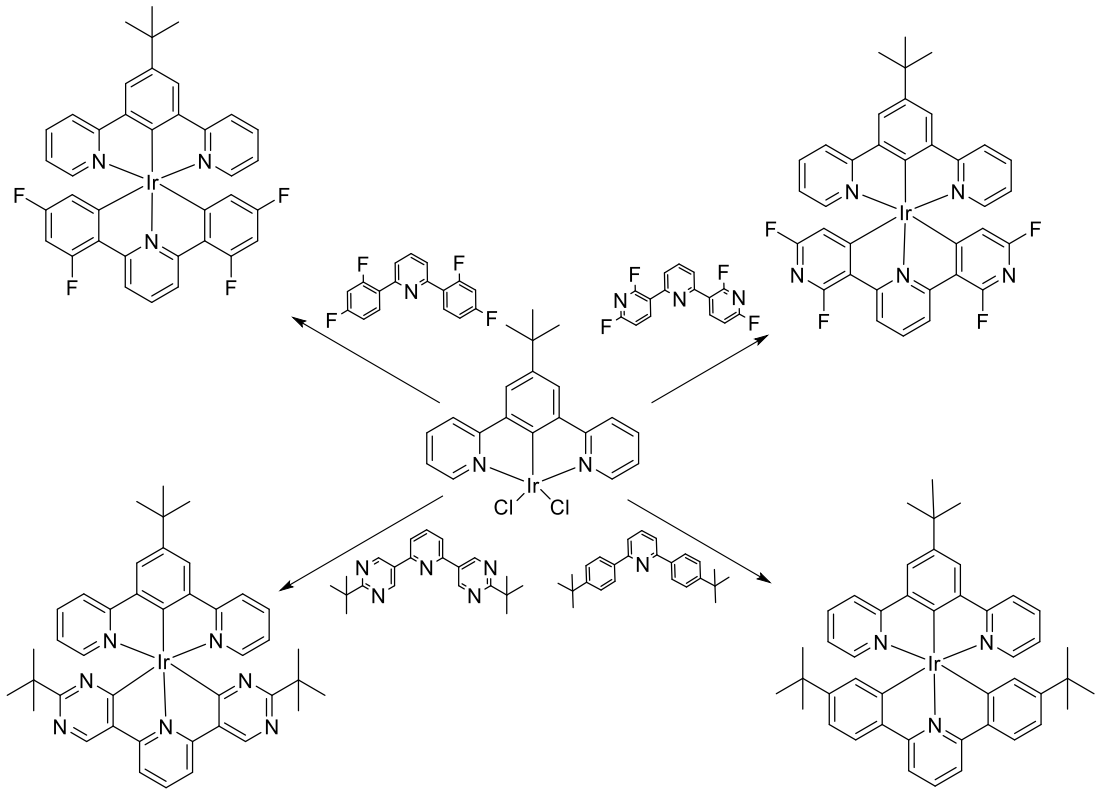

Scheme 7 - The proposed structures of complexes to be tested using a series of C^N^C coordinating auxiliary ligands.

1.4.5. Alteration to the Linking Heterocycle from Pyrimidine to Thiazolo-[5,4-d]-thiazole

Previous studies within the Kozhevnikov group have investigated the use of Thiazolo-[5,4-d]-thiazole (TzTz) as a linking heterocycle. This group was first described by Ephraim in 1891 and was the first example of this being used as a core structure.[152] Johnson *et al* reported on the structure and developed a series of analogues with respect to Ephraim's work.[153]

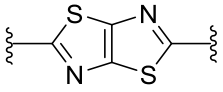

Figure 59 - The general structure of the linking TzTz heterocycle. This group will be formed from a benzaldehyde derivative and dithiooxamide.

The benefits of using this linking heterocycle results in the removal of possible steric hindrance between the coordinating auxiliary ligands. This is due to the coordination of the metal centres being on opposite sides of the molecule.

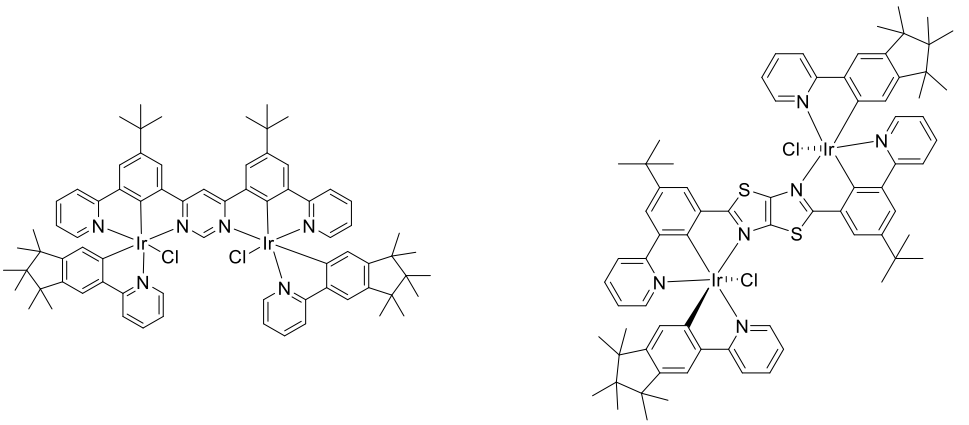

Figure 60 - The differences between the pyrimidine and TzTz heterocycles. There is likely to be a distinct lack of intramolecular interactions between the auxiliary ligands in the TzTz linked complex (right) than the pyrimidine linked complex (left).

As the use of this linking heterocycle has only been used to develop bidentate complexes, the development of bis-tridentate coordinating bridging ligands will be building on work by Dr Ruth Daniels who first developed a similar bridging ligand as part of the Kozhevnikov group. The complex to be targeted in this work is shown in Figure 60. Using this as a target molecule, the ultimate goal will be to coordinate a terdentate auxiliary ligand resulting in a complex not previously described.

The use of the TzTz linking heterocycle dramatically reduces the solubility of the bridging ligand. To combat this, a new bridging ligand will be developed to which a two mono-iridium dimer molecules will be coordinated, resulting in the formation of a di-iridium complex.

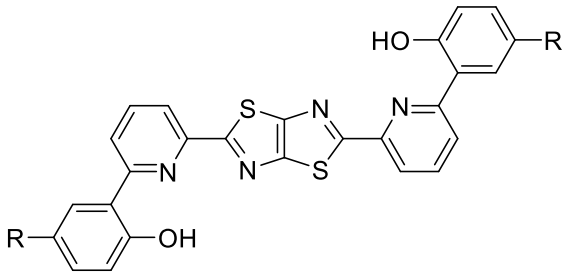

Figure 61 - The general structure of the new bridging ligand which coordinates via O^N^N binding. This example can either have R= H or R= Mesitylene (Mes).

The aim of this work is to develop a novel complex in which the bridging ligand utilises the TzTz linking heterocycle with the mono-nuclear dimers. The work will describe the strategies used to accommodate for the lower level of solubility.

1.4.6. SALEN type tetradentate ligands and the analogous Pt(II) complexes

Following work done on tetradentate Pt(II) complexes by Kui *et al*, highly luminescent complexes are shown to be achievable through both symmetrical and asymmetrical ligands.[113-114] A different study by Lin *et al* demonstrated the formation of bipyridine bis-phenolate structures of the ligands and forms the basis for the work to be developed in this section. Using the general coordination of the bipyridine bisphenolate (N_2O_2), this work will describe and detail the development of two novel complexes from readily available starting materials. The aim is the substitution of the tertiary butyl groups described in complexes by Lin *et al* with cyclopentene rings.[112] This can be done through the use of the Boger reaction, which results in the addition of cyclopentene and the conversion of triazine to pyridine.

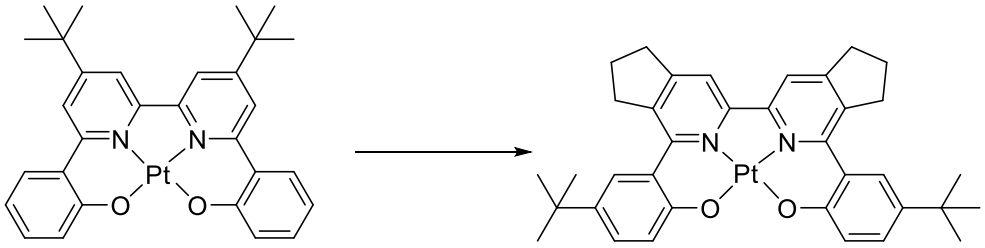

1.3.18
Lin *et al*, 2003

Pander *et al*, 2018

Figure 62 - The previously synthesised SALEN type complex with N2O2 coordination by Lin *et al* (left). The proposed structure of one of the complexes in the publication in this project, Pander *et al* (right).

The study will be focusing on the development of 3,3' and 5,5' triazines and the resulting pyridines, and the effect of including tertiary butyl to the phenolate moieties. By doing this a platinum complex can be developed and can be used in the fabrication of white/ambient OLED devices. The alteration of the cyclopentene ring will also indicate the involvement of the tertiary butyl in the level of solubility of the platinum complexes, which are known to stack and form aggregates.

There will be further investigations into the changing of the tertiary butyl substituent on the phenolate group to the more sizeable mesitylene group. This will further increase the solubility from the previous tetradentate ligand and could be beneficial to the photophysical properties.

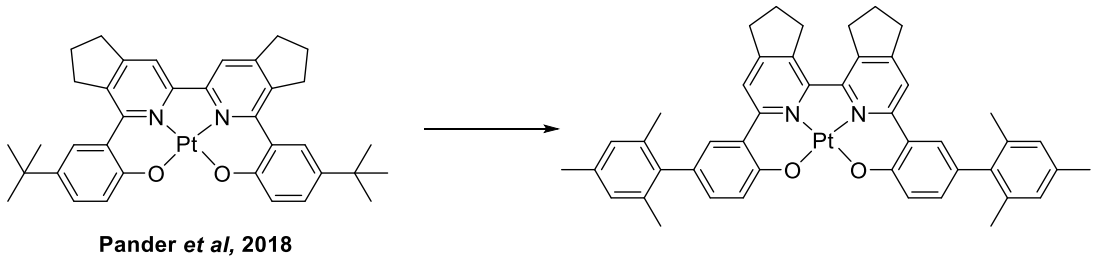

Pander *et al*, 2018

Figure 63 - The proposed changes to the structure of the published complex, the addition of the mesityl groups should increase the level of solubility of the platinum complex as a whole.

The aim is to increase the solubility of the complex. The increased level of rigidity of complexes with tetradentate coordinating ligands results in a drastic reduction of the solubility.

CHAPTER 2

Increasing the Solubility of Di-iridium C^N Complexes

2. Development of Fluorine-free Di-nuclear Ir(III) Complexes for Solution Processable OLEDs

This chapter describes dinuclear iridium(III) complexes, which are composed of two metal centres rigidly linked by a cyclometalating bridging ligand. The bridging ligand which joins the two metal centres is integral to the chemical and photophysical properties of the complexes. Previously most Ir(III) complexes utilised polypyridine bridging ligands and incorporated a spacer unit. As a result the two metal centres were discrete and had no influence over the other. This resulted in bi-metallic complexes displaying similar properties to their mono-metallic counterparts.[103, 154-157]

In our group we are interested in systems where two metal centres are rigidly linked. The approach proposed is to fuse well performing mono-Ir (III) complexes together by a linking heterocycle. The rigid linking of two metal centres in this way leads to the electronic interaction of both metal ions. Photophysical properties of di-nuclear complexes are often vastly different to the mono-nuclear analogues.[103] Di-nuclear complexes typically display higher quantum efficiencies, shorter excited triplet state lifetimes and a significant red shift in emission wavelength that their mono-metallic analogues.

Williams *et al* reported a series of mono-iridium complexes, in which 1,3-di(2-pyridyl)benzene was used in cyclometalating terdentate N^C^N ligands. This ligand was paired with 2-phenylpyridine analogues, resulting in a general complex formula of Ir(N^C^N)(C^N)X shown in Figure 64.[10, 13] The X denotes a mono-dentate ligand which is coordinated to the central iridium ion and is typically a chloride atom which balances the overall charge. The promising luminescent properties of these complexes showed quantum efficiencies as high as 0.71 (complete range: Φ= 0.2-0.71), which indicates a promising potential for use as dopants in OLED devices.[10]

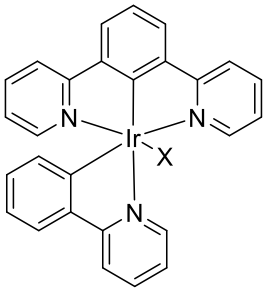

2.0.1
Williams *et al*, 2004

Figure 64 - The general structure of the complexes described by Williams *et al* which showed promising luminescent properties.

Using this motif, Kozhevnikov and co-workers prepared a series of di-iridium complexes in which heterocycles such as pyrimidine and pyrazine groups rigidly link the metal centres. The use of these groups rigidly links the metal centres and was outlined by Steel and Caygill.[158] The use of similar bridging ligands was described by Daniels *et al* in the binding of multi-centred Ir(III) complexes, with the metal centres bound by a ditopic bisbidentate pyrimidine linked bridging ligand, an examples is shown in Figure 65.[5, 103] The green-orange emitting complexes showed high quantum efficiencies at room temperature (ϕ_{lum}= 0.88-1.0) with excited state lifetimes between τ = 0.36-0.59μs.

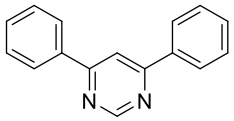

2.0.2
Steel and Caygill, 1990

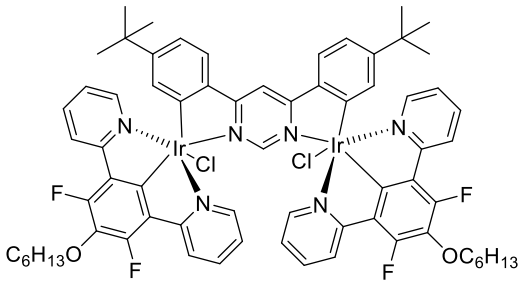

2.0.3
Daniels *et al*, 2016

Figure 65 - The ligand described by Steel and Caygill in 1990 (left). The bisbidentate linked di-iridium (III) complex described by Daniels *et al* (right).

The use of rigidly linked metal centres was further developed by Kozhevnikov and co-workers in 2014, linking two iridium metal centres via a cyclometalating bis-terdentate bridging ligand using a pyrimidine.[105] The combined use of the bis-terdentate bridging ligand and cyclometalated C^N auxiliary ligands resulted in one of the most efficient red emitting phosphorescent complexes at the time.[20, 105]

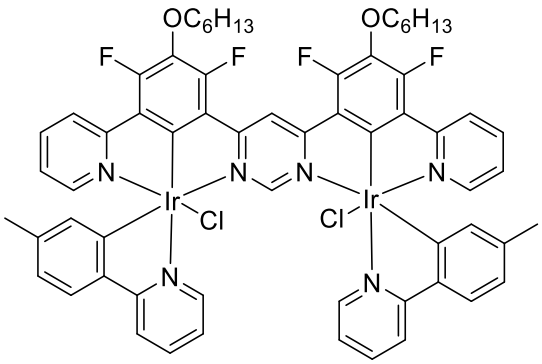

2.0.4

Figure 66 – One of the complexes described by Kozhevnikov *et al* which is the first example of a highly luminescent complex with a pyrimidine bridged bis-terdentate ligand. The structure shown displayed poor levels of solubility and required optimisation.

The study by Kozhevnikov and co-workers described that the use of the rigid bis-N^C^N coordination inhibits non-radiative decay and promotes efficient spin-orbit coupling pathways for triplet phosphorescence.[159-160] The ditopic N^C^N ligand promotes a planar conformation upon the coordination of the Ir(III) cations and the resulting Ir-Cl are nearly perpendicular to the plane of the ligand. The study also highlights that the shift from a mono-nuclear structure to a di-nuclear analogue often results in a considerable red shift (~80nm) in the emission wavelength. This red shift is attributed to the increased stabilisation of the pyrimidine based π^* orbital by the coordination of the second Ir(III) atom to the second N atom of the central pyrimidine. This is similar to previous studies by Kozhevnikov and co-workers.[5, 103]

The aim of this research is to develop bimetallic complexes as phosphorescent dopants in solution processable OLEDs. These alterations aimed to tune the photophysical properties of the final complexes but also to improve solubility and stability. This was done by introducing solubilising groups such as tertiary butyl and altering the structures of the coordinating C^N

auxiliary ligands. The synthesis of the ditopic bridging ligand will be discussed and the characterisation will be outlined. The effect of the structural changes on the photophysical and chemical properties will also be investigated in detail. With the presence of the undesirable fluorine groups on the bridging outer ligand, there is scope to change or remove these groups, in order to further benefit the complex when applied to an OLED device.

2.1. Improving Solubility of Bis-terdentate Ir(III) complexes using solubilising C^N auxiliary ligand.

The use of bis-terdentate structures has largely been overlooked in previous investigations, however over time the use terdentate ligands has gained an increased level of interest. Williams and co-workers outlined monometallic structures using N^C^N coordinating, 1,3-di(2-pyridyl)-4,6-dimethylbenzene as an outer ligand. When paired with varying auxiliary ligands, highly luminescent monometallic Ir(III) complexes were synthesised (Φ=0.21-0.76).[13] The use of terdentate ligands in complexes was documented prior to this study by Yutaka *et al* in 2005, using tridentate benzimidazole groups as outer ligands. The photophysical properties of these complexes did not show promising quantum yields (Φ= 0.037-0.19).[161]

As the use of a rigid ditopic bis-terdentate outer ligand had not been greatly explored, the study, discussed previously, carried out by Kozhevnikov and co-workers showed the first case of highly luminescent complexes. Despite the promising results of the complex and benefits of a rigid ditopic ligand.[9] The reported structures were not suitable for solution processable OLED devices due to low solubility.[105]

In previous studies, mono-metallic dimers were coordinated to a single ancillary ligand, however this work focused on the synthesis of a single multi-centred dimer which utilises supplementary auxiliary ligands. Building on the findings of the study carried out by Kozhevnikov and co-workers in 2011, as one of the primary examples of hexadentate ditopic bridging ligands utilised in multi-nuclear complexes, the quantum yields displayed by the

complexes show that the use of bidentate C^N auxiliary ligands result in promising photophysical properties (Φ=0.65, λ_{max}= 625nm).[105] As previously discussed, there are benefits of using a bis-N^C^N bridging ligand, which consist of an increased chemical stability and the capability of producing achiral molecules and preventing the formation of diastereomers in multimetallic structures.[12, 39, 105, 162]

This work focuses on the tuning and the synthesis of the outer bridging ligand, and the preparation of the final complex. The main aims of the synthesis of these compounds was to increase the stability and solubility of bi-metallic complexes. As the first step in the project, in order to improve the solubility of the complexes, the auxiliary ligand was changed from the group in the published structures, to the one recommended by the Merck team.[163] Merck2, (shown in Scheme 8 as **M2**) was used as the presence of a hexamethylcyclopentene unit would improve overall solubility through the prevention of intermolecular interaction. Using **2.1.3**, which was previously described in literature, the dinuclear Ir(III) complex **2.1.5** was synthesised. Only one, presumably the *rac* isomer of **2.1.5** was isolated. The complex showed significant improvement of solubility in toluene compared to previously published complexes. As toluene is used in the photophysical testing, the level of solubility in this solvent is crucial. The improvement therefore meant M2 was used in further studies as a suitable and effective solubilising motif.

The synthetic route used to develop **2.1.5** was the 'typical' method for the generation of iridium complexes. The dichlorobridged dimer utilised was formed through heating the auxiliary ligand with iridium chloride hydrate in 2-ethoxyethanol and heated under reflux overnight.

To generate the complex, **2.1.5**, the dimer was heated under reflux with silver triflate (AgOTf) in toluene prior to the addition of the ligand. The ligand, **M2**, was added and the reaction was heated under reflux overnight. After the reaction, 2M hydrochloric acid was added to introduce the chloride ions. The product was isolated by column chromatography (DCM/MeOH, 20:1). The retention factor of the most easily separated isomer (R_f = 0.8) is much higher than that of

the stronger retained mixture (R_f = 0.2-0.3). Only the high R_f (0.8) product was isolated. The aromatic region of the ^{1}H NMR of **2.1.5** is shown in Figure 67 and is consistent with the proposed structure.

It should be noted that the mixture of the *meso* form and a racemic (*rac*) pair of isomers forms during the reaction.[74] The diastereomers can typically be separated by column chromatography and in this study only one isomer was isolated.[100, 102, 164-165] In order to determine the identification of these isomers (distinguish between the *meso* and *rac* forms) the best and most accurate method would be X-Ray crystallography. This would show the crystal structure of the complex isolated and identifies the form of the isomer.

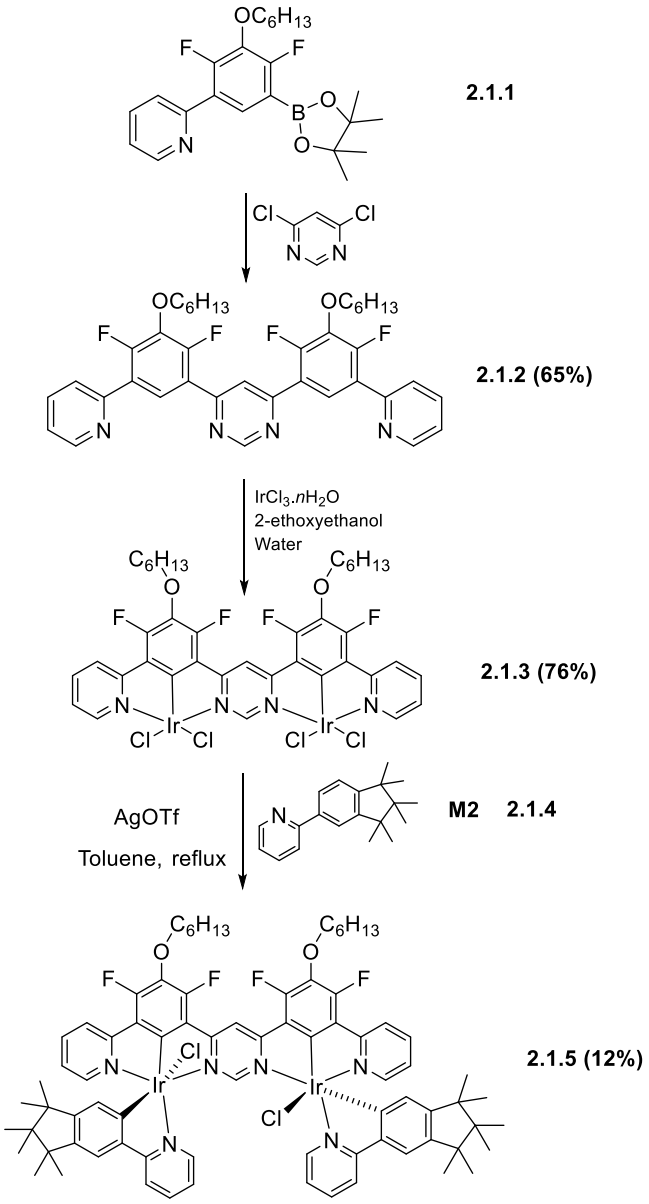

Scheme 8 - The complete synthetic route of **2.1.5**, using silver triflate as a chloride scavenger, the complexes were dissolved in toluene and heated under reflux overnight.

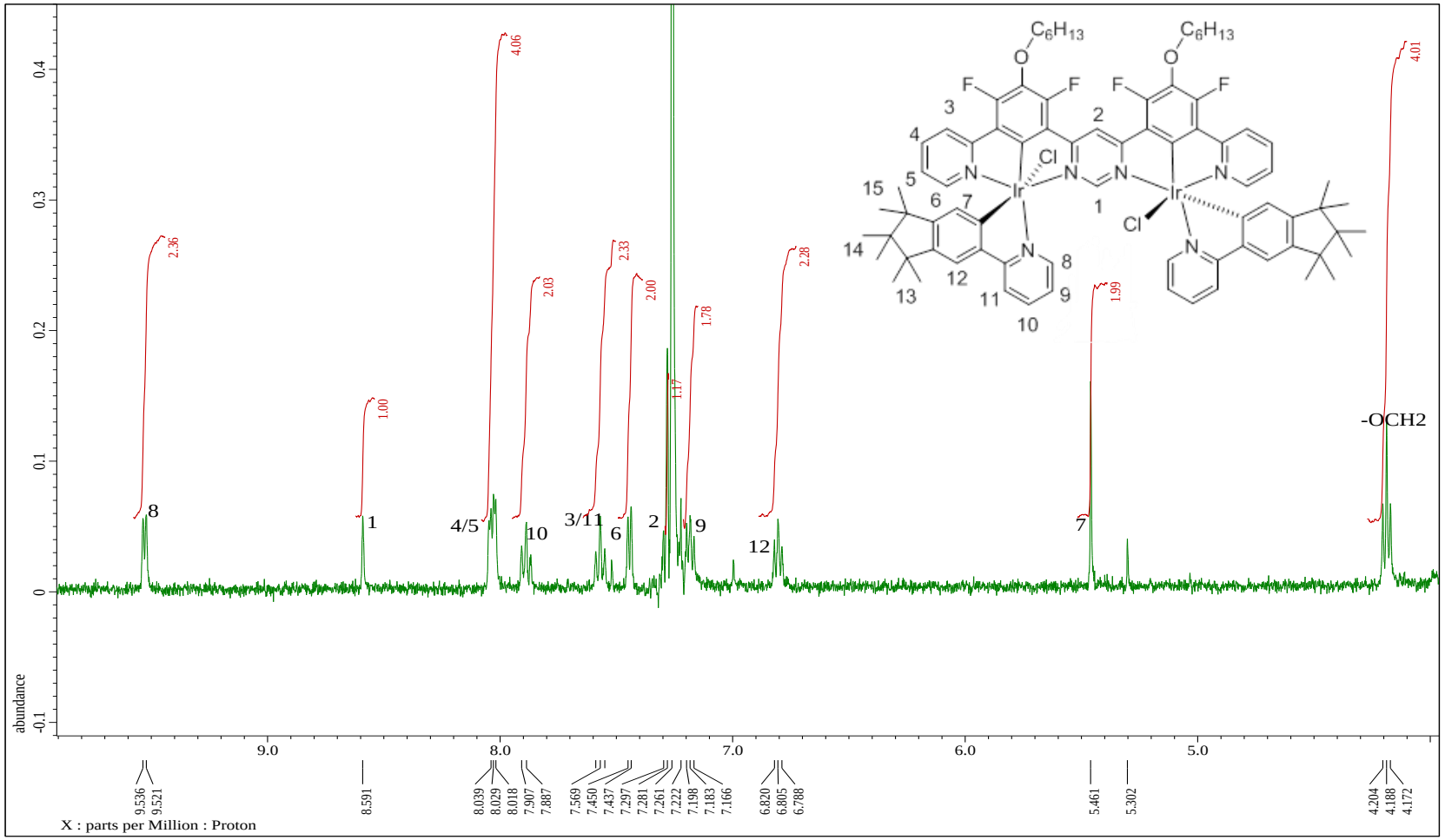

Figure 67 - The aromatic region of the ^{1}H NMR in $CDCl_3$, for the complex **2.1.5**. The overlaid structure corresponds to the numbered peaks. The peak integrations are consistent with the structure and described in the experimental.

The preparation of **2.1.5** showed that the use of previously described dichlorobridged dimer successfully improves solubility. The fluorine groups and alkoxy chains required substitution with different functional groups due to being undesirable in the fabrication and operation of OLED devices.

2.2. Development of Fluorine free Bridging Ligands and Complexes

In the development of OLED emitters, the presence of fluorine groups is not desirable due to the low stability of the dopants under electroluminescent conditions. We therefore targeted two structures, **2.2.1** and **2.2.2**, which do not contain fluorine or alkoxy groups. The role of the tertiary butyl and hexamethylcyclopenteno groups, is to increase the solubility and to prevent competitive cyclometalation.

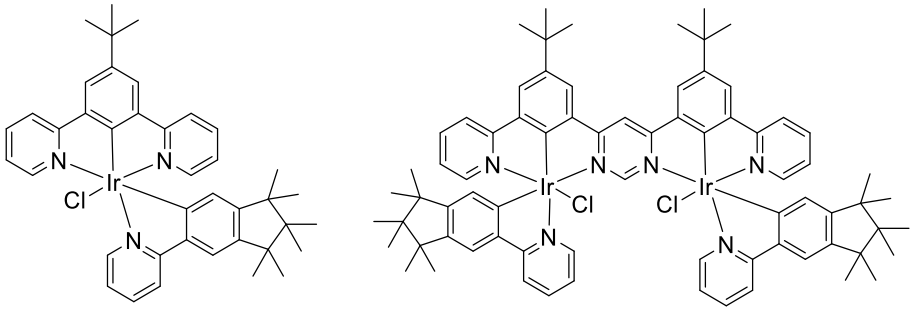

2.2.1 **2.2.2**

Figure 68 - The structures of the fluorine free Ir(III) charge neutral complexes, **2.2.1** and **2.2.2**. The mono-metallic analogue, **2.2.1**, serves as a model compound to ensure that the compound shows promising photoluminescent properties.

The mono-metallic complex **2.2.1** was synthesised as a model compound to ensure that the metalation chemistry was reproducible and reliable. Monometallic complexes are also a good model compound for identifying the influence of the secondary metal centre on the photophysical properties.

2.2.1. Synthesis of Auxiliary Ligands

To synthesise the mono-metallic complex, a Stille cross-coupling reaction was carried out, using the commercially available 1,3-dibromo-5-tertbutylbenzene and 2-(tributylstannyl)pyridine. Typically this reaction forms two products, the mono-brominated

derivative and the N^C^N based cyclometalating ligand, **2.2.6**. As these are easily separated by column chromatography, the preparation of the N^C^N ligand and the bromo derivative required for the synthesis of ditopic ligands is simplified. Stille cross coupling is often complicated by the formation of large quantities of tin based by-products that are difficult to remove.[166] It has been proposed that the use of caesium based compounds such as caesium fluoride can aid in the reduction of harmful tin by-products.[167-168]

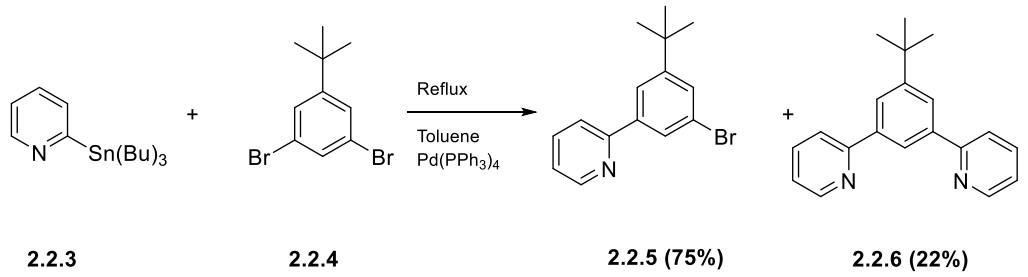

2.2.3 **2.2.4** **2.2.5 (75%)** **2.2.6 (22%)**

Scheme 9 - The Stille cross coupling of 2-(tributylstannyl)pyridine and 1,3-dibromo-5-tertbutylbenzene. The formation of the brominated derivative can be carried forward and used in the synthesis of the bis-terdentate ligand. The secondary product is used to form the mono-nuclear iridium dichloro-bridged dimer.

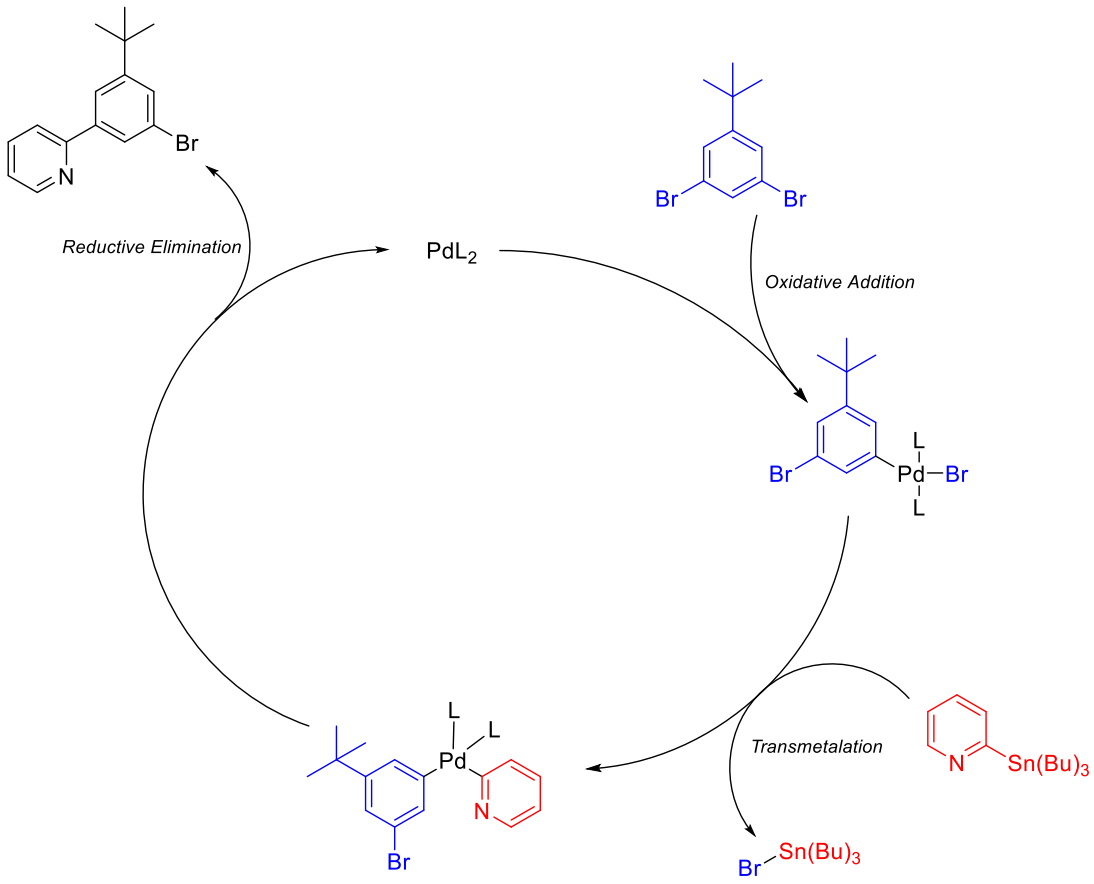

Scheme 10 - The reaction mechanism of the Stille cross coupling using **2.2.5** as an example. The secondary bromine atom then undergoes the same mechanistic procedure to produce the N^C^N based ligand.

The Negishi cross coupling method was also used using commercially available 2-pyridylzinc chloride. However the reaction resulted in lower yields than the Stille cross coupling. Suzuki-Miyaura cross coupling can also potentially be used but would require an additional step to prepare a corresponding boronic acid and was not used.

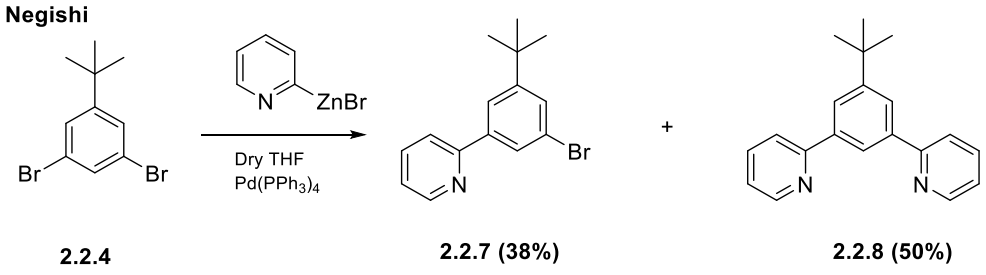

Figure 69 - The synthetic procedures used to develop the N^C^N cyclometalating outer ligand. The reaction conditions are detailed and the reactants required are shown.

The *tert*-butyl functional group was introduced to increase the solubility of the complex. Due to the bulk of the functional group, this prevents the stacking of the molecules and ensures the complex is more soluble.[169] The *tert*-butyl group can prevent competitive cyclometalation of the metal atom at either the positions 2 or 4 of the central phenyl group, highlighted in Figure 70.[13]

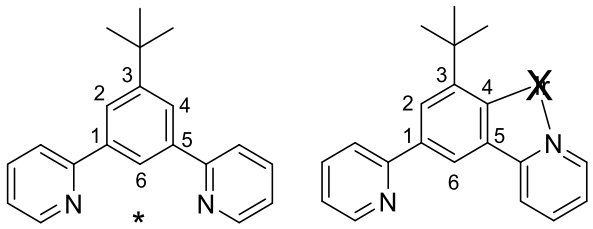

Figure 70 - An illustration of the tert-butyl preventing the competitive cyclometalation of iridium (III) at position 4 of the central phenyl group and the nitrogen of the pyridine.

The synthesis of the ditopic bis terdentate bridging ligand is depicted in Scheme 11. As mentioned previously, the use of the brominated product from the Stille cross coupling can be used in the formation of the ditopic N^C^N ligand. The bromo derivative was used to prepare a boronic ester using Miyaura borylation or through lithium halogen exchange. It was found that the Miyaura borylation resulted in higher yields and this methodology was then primarily used.[170] The boronic acid was then used in a Suzuki cross coupling reaction with 4,6-dichloropyrimidine to give the desired ditopic ligand **2.2.12** in a 76% yield.

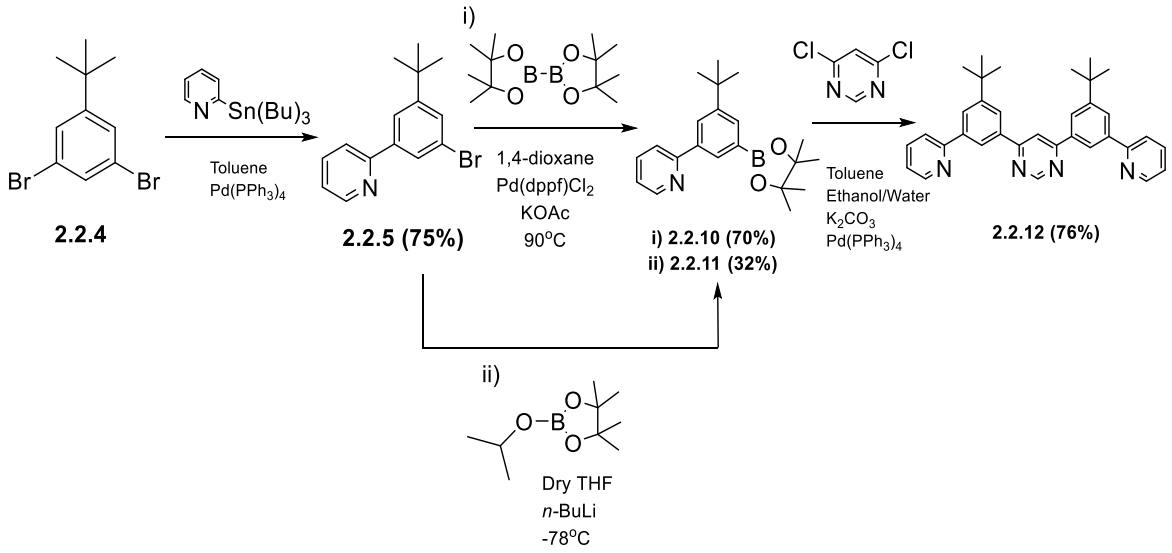

Scheme 11- The reaction pathway followed to develop the di-topic bis-terdentate ligand, both methods have been described with conditions. i) $Pd(dppf)Cl_2$, KOAc, 1,4-dioxane, 90°C. ii) Dry THF, n-*BuLi*, -78°C.

2.2.2. Synthesis of Metal Complexes

Both mononuclear and dinuclear complexes were prepared by the method described previously.[10, 12-13, 39] Similar to the Nonoyama reaction, **2.2.6** was heated under reflux in 2-ethoxyethanol with iridium chloride hydrate to give **2.2.13** in good yield (~75%).[83-84, 171] **2.2.13** is not sufficiently soluble in $CDCl_3$ to obtain a spectrum. However, the NMR can be acquired in DMSO-D_6. During the heating in DMSO-D_6 the dimer is cleaved to give the corresponding DMSO-D_6 complex.[172] The NMR spectrum clearly showed that cyclometalation took place.

To synthesise the model complex **2.2.1**, the mixture of the dimer, M2 and AgOTf in toluene was heated under reflux overnight. After the reaction, 2M aqueous HCl was added to scavenge Ag^- ions and reinstall Cl ligand on the iridium centre. The complex was purified by column chromatography (DCM/MeOH, 20:1) to give **2.2.1**. Unfortunately, the yield of the final step was only 19%.

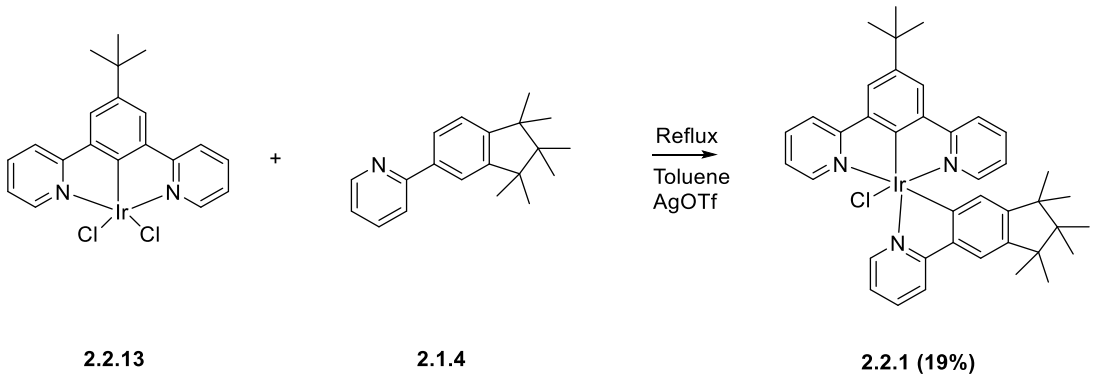

Scheme 12 - The reaction scheme depicting the synthesis of the mono-iridium complex **2.2.1**.

The synthesis of the dinuclear iridium complex **2.2.2** was carried out under similar conditions to one used to prepare the model compound **2.2.1**. Again, the dichloro-bridged dimer was obtained in good yield (86%), unfortunately the final step was low-yielding (20%).

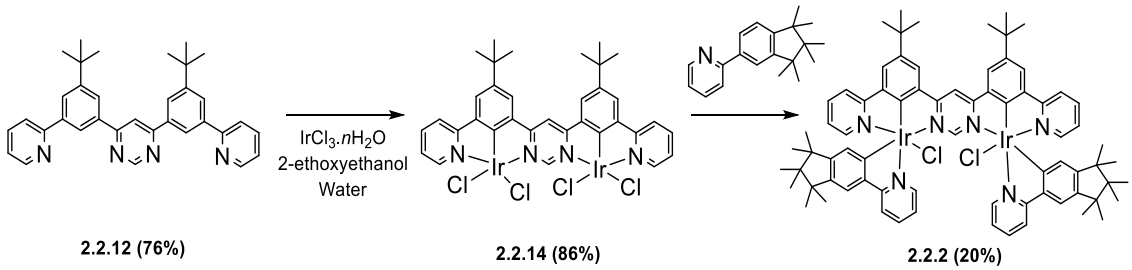

Scheme 13 - The synthetic pathway for the preparation of **2.2.2** from the ditopic ligand. The preparation of the dichlorobridged dimer is also shown.

The resulting solid was purified by column chromatography (DCM/EtOAc, 10:1). It should be mentioned that while it is expected that two diastereomers form during the reaction, we only isolated one isomer. This, of course, does not mean that the second isomer did not form and this phenomenon would require additional studies. The NMR spectrum of **2.2.2** is shown in Figure 71 and is fully consistent with the structure.

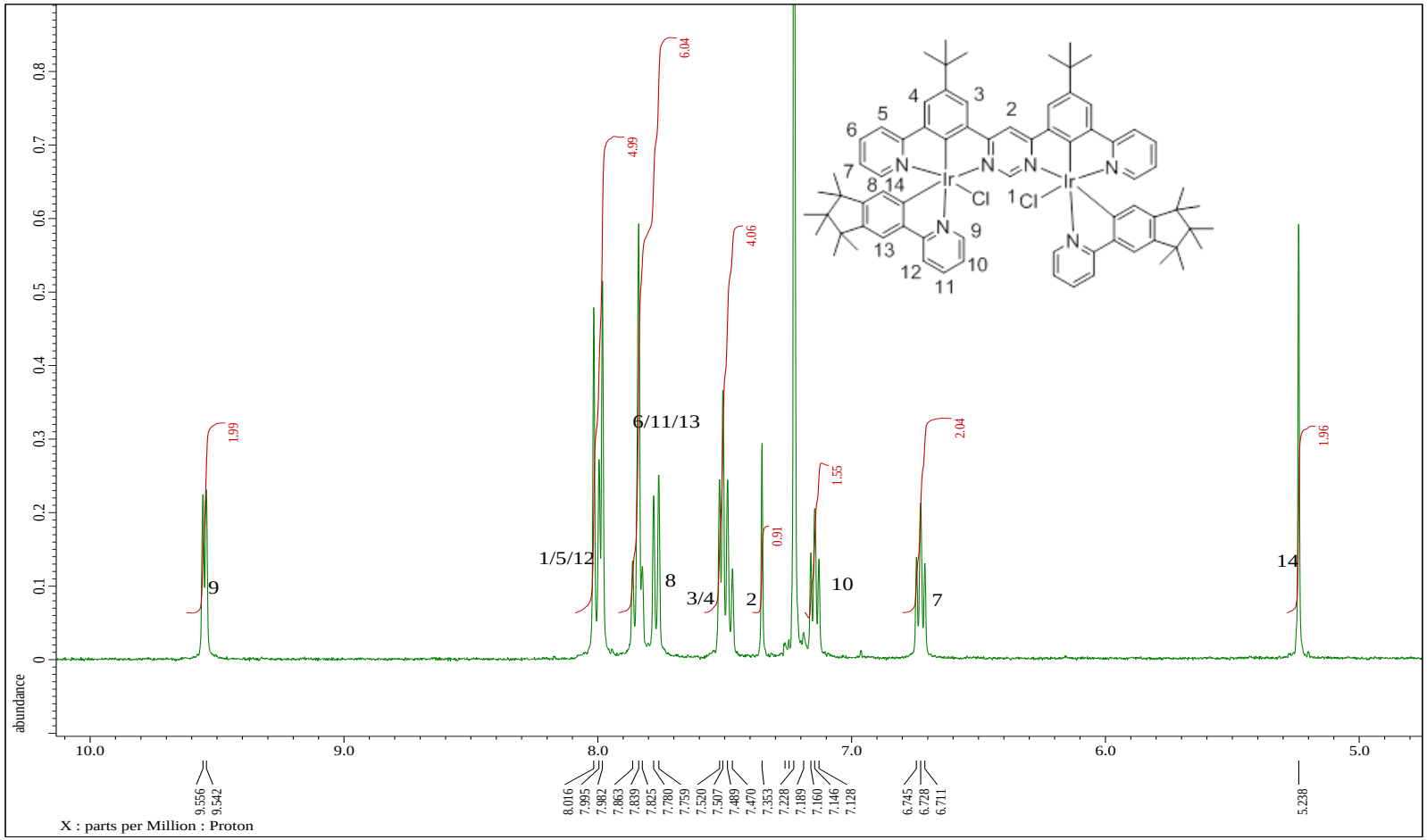

Figure 71 - The aromatic region of the ^{1}H NMR for complex **2.2.2** in $CDCl_3$, the numbered structure is overlaid. The tertiary butyl peak is shown in the aliphatic region as a singlet at δ 1.56ppm, the methyl groups on the auxiliary ligand are shown as singlets at δ 1.04, 0.99 and 0.70ppm. The peak integrations are consistent with the structure and as described in the experimental procedure.

2.2.3. Photophysical Properties

Photophysical characterisation of both complexes was carried out by Dr Anna Hayer at Merck. The complexes are brightly phosphorescent. Photophysical data is summarised in Table 6. It can be seen that upon the addition of the secondary metal centre there is a red-shift of emission maximum by ~110nm. Similar behaviour was previously registered for other multimetallic complexes.[105]

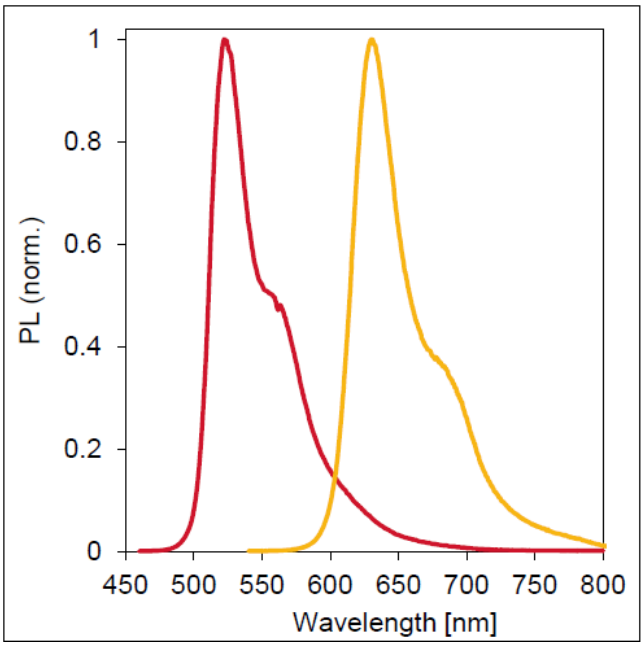

Figure 72 - The emission spectra displaying the emission wavelengths of the mono-metallic complex **2.2.1** (red) and the bi-metallic analogue, **2.2.2** (yellow).

In order to understand the nature of the red-shifted emission in dinuclear complexes, computational studies were performed at Merck. Both the complexes, **2.2.1** and **2.2.2** were analysed using density functional theory (DFT) and time dependent- density functional theory (TD-DFT) to image the location of the HOMO and LUMO orbitals for both the mono-nuclear and the di-nuclear analogues. The calculations are consistent with the experimental results and show that the energy gap for **2.2.2** is considerably lower than for **2.2.1**. The energy gap of the *rac* and *meso* isomers shows no difference between them, which indicates that both isomers have similar properties. The energy gaps of the HOMO and LUMO orbitals are depicted in Figure 73 for both the *rac/meso* isomers of **2.2.2** alongside those for **2.2.1**.

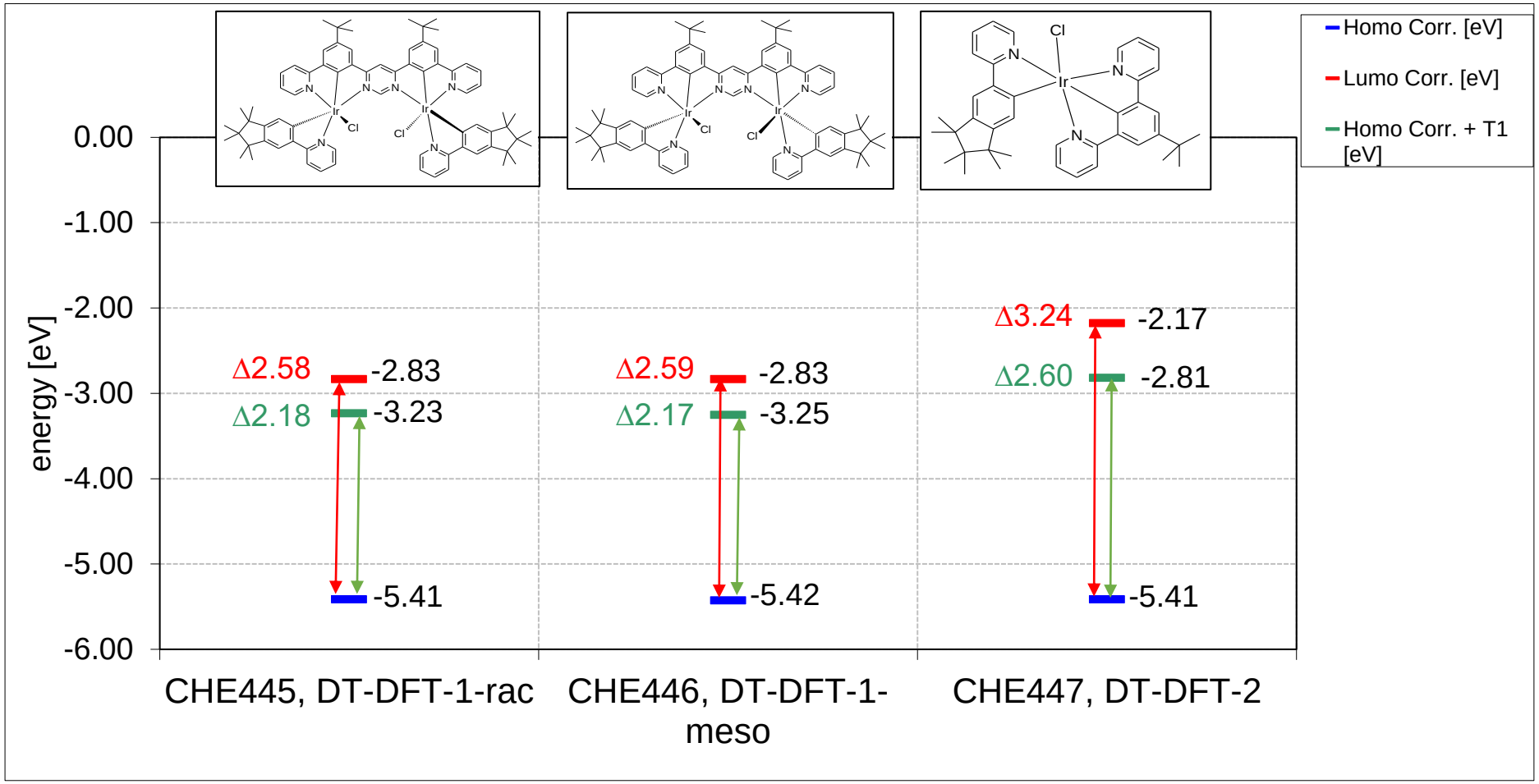

Figure 73- The HOMO and LUMO values of **2.2.2** (di-nuclear), both rac and meso isomers. The energy gap for the mononuclear **2.2.1** is shown on the right. All TD-DFT was calculated at Merck KGaA. The black numbers denote the energy gap between the HOMO and LUMO values.

By going from monometallic to bimetallic complex, HOMO levels are not affected, while the LUMO is significantly stabilised. As a result the HOMO-LUMO energy gap is significantly reduced hence a red-shifted emission.

The ideal emission maximum for a phosphorescent-red emitter should be around 618 nm due to the ideal energy gap between the molecular orbitals. **2.2.2** clearly falls outside this range (λ_{em}= 631 nm) and additional "tuning" is required. Because monodentate ligand (chloride) contributes significantly to the HOMO orbital, by replacing chloride with more electron-withdrawing ligands the HOMO level can be stabilised increasing the energy gap. We therefore, tried to install CN groups instead of chlorides. Unfortunately, our attempts were unsuccessful and this part of the project will be revisited in follow-up studies.

The most exciting result is that, despite such a very big red-shift in emission, the quantum yield is not reduced but actually increased by ~2.5 times. Therefore, this shows the benefit of a secondary metal ion within the complex in particular for the design of low energy phosphorescent complexes. Another important feature of the bimetallic complex **2.2.2** is that life-time of emission decreased from the mono-metallic **2.2.1** to bi-metallic **2.2.2**. The introduction of the *tert*-butyl group reduces the energy band gap in iridium complexes in comparison with published fluorinated examples.[173]

Table 6 - The photophysical properties of the fluorine-free C^N cyclometalating complexes, **2.2.1** and **2.2.2**.

Sample	**λ_{max} (nm)**	**PL-QE (toluene)**	**Decay time (µs)**
2.2.1	523	0.37	0.94
2.2.2	631	0.87	0.53

The photophysical results in Table 6 show that the red shift of emission occurs upon the addition of the secondary metal centre. The resulting emission wavelength was shifted by ~110nm, following the literature trend shown by Kozhevnikov *et al*.[105] The introduction of an additional iridium centre also increased the quantum yield by 4-fold which was also displayed

in the study by Kozhevnikov *et al*. Therefore, this shows the benefit of a secondary metal ion within the complex. The triplet state decay time of the complex decreased from the mono-metallic **2.2.1** to bi-metallic **2.2.2** indicating a more rapid rate of radiative decay.

2.2.2 was used to fabricate a solution processable OLED device at Merck. Several modifications of the device structure have been performed but the device showed an overall efficiency of only η_{ext}= 8%. Much higher efficiency was expected for compounds with PLQY as high as 87%. Further optimisation of OLED devices is required.

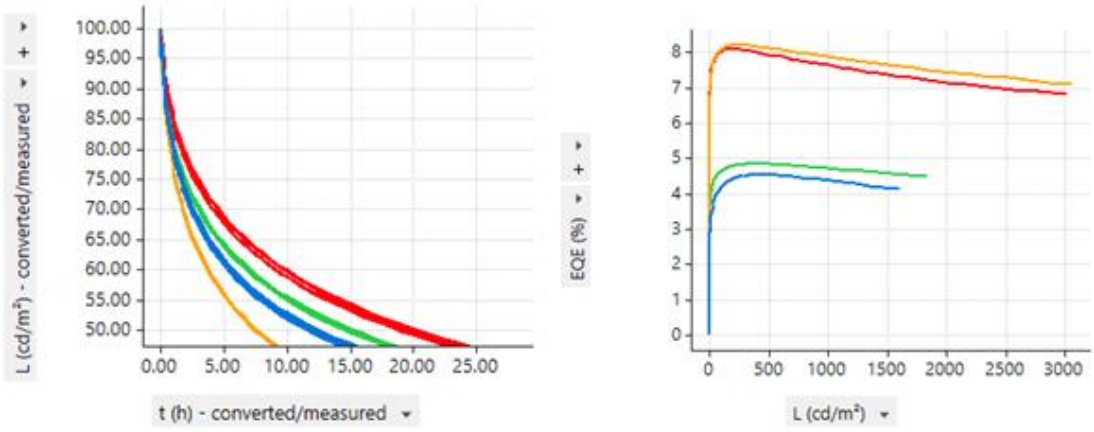

Figure 74 - The graphs showing the short lifetime of the device for **2.2.2**. The graph on the left indicates that the best combination of emitter dopant (**2.2.2**) and host compound displays a peak lifetime (t) of ~22hours. The graph on the right shows that the maximum EQE value of the combinations is η_{ext}= ~8% which is considerably lower than the device fabricated for **2.2.17**, a previously tested complex.

The graph on the left shows the LT_{50} values measured over time, showing that at 50% of the maximum, the best configuration only achieves an efficient device time of a maximum of 22 hours when combined with a mixture of hosts and co-dopants. This is well below sufficient device standards. The reason for the poor device qualities could be attributed to the presence of the monodentate chloride ligands. These groups are likely extremely detrimental to the lifetime of the device in a similar manner to the detrimental presence of fluorine.[140, 174]

Table 7 - The table displaying the localisation of the frontier orbitals in the monometallic **2.2.1** and the bimetallic **2.2.2**.

Complex	**Orbitals**			
	HOMO-1	**HOMO**	**LUMO**	**LUMO+1**
2.2.2-*rac*	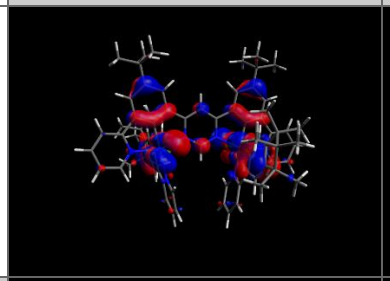	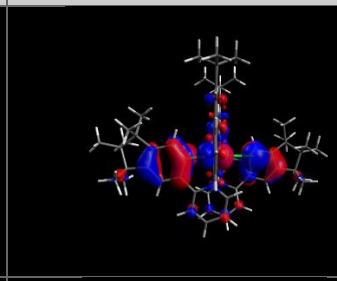	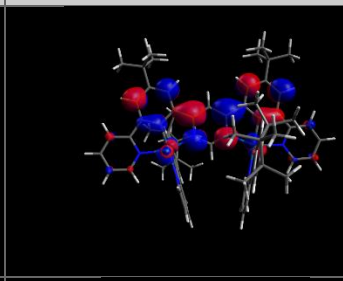	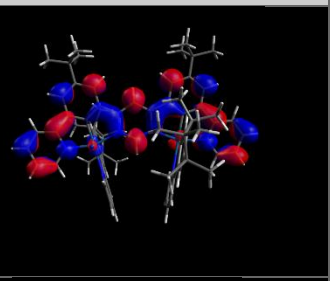
2.2.1	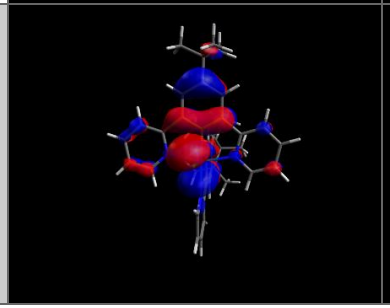	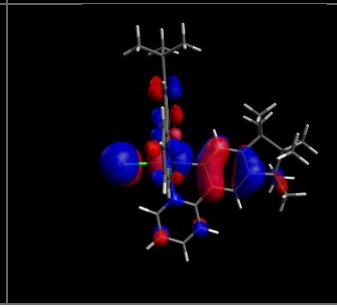	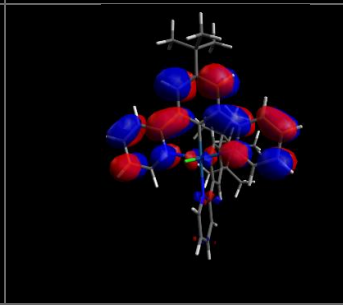	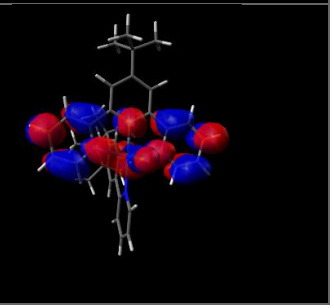

The orbitals are depicted above. In the monometallic complex, **2.2.1**, the HOMO is predominantly localised to the metal centre, and the cyclometalating unit of the outer ligand. In HOMO-1, the electron density is delocalised across the aryl ring of the cyclometalated bidentate ligand. The chloride ligand is not innocent and contributes significantly to the HOMO orbital. The LUMO and LUMO+1 of **2.2.1** is predominately located on pyridine rings of NCN ligand. To a large extent, the bidentate cyclometalating ligands do not contribute much to the LUMO. In the bimetallic complex, **2.2.2**, the LUMO orbital is spread across the pyrimidine heterocycle, metal centre and the central phenyl rings of the N^C^N moieties. LUMO+1 is even further delocalised to involve pyridine rings of the bridging ligand. Such high degree of localisation is probably responsible for the significant stabilisation of LUMO. Interestingly cyclometalating bidentate auxiliary ligands do not contribute much to LUMO and LUMO+1 orbitals.

2.3. Conclusions

The synthesis of the complex **2.1.5** showed that the cyclometalation of the ligand M2 can significantly improve solubility of dinuclear complexes.

Highly soluble, fluorine-free compounds were synthesised. The synthesis of **2.2.2** highlighted that the solubility of the complex could be improved through the introduction of additional solubilising groups to the auxiliary ligand. Removing electron-withdrawing groups resulted in a red shift of emission, away from the ideal λ_{max}= 615 nm to λ_{max}= 631nm. Despite the red-shift of emission, the PLQY values are high (~87%). The OLED devices fabricated using **2.2.2** showed low efficiencies (η_{ext}= <8%) and poor operational lifetime (LT_{50}= 22 hours). This was probably due to the presence of the chloride ligands. A realistic approach for further development of the bimetallic emitters will be to use of dianionic terdentate auxiliary ligands in order to eliminate the detrimental mono-dentate chloride ligands.

2.4. Experimental

2.4.1. Di-topic Bis-terdentate Ligands

2.4.1.1. Synthesis of **2.1.2**.[105]

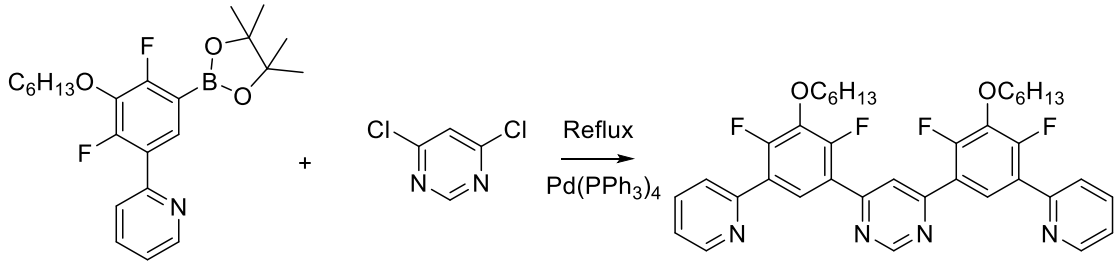

Potassium carbonate (1.66 g, 12 mmol), 2,4-difluoro-3- hexyloxy-5-(2-pyridyl)phenyl boronic acid (1.00 g, 3 mmol) and 4,6- dichloropyrimidine (0.186 g, 1.25 mmol) were added to a water (6mL), toluene (10mL) and ethanol (4mL) mixture. This was deoxygenated with argon for 20 minutes. $Pd(PPh_3)_4$ (0.103g, 0.1 mmol) was added and the mixture was heated under reflux for 15 hours. The reaction was separated with brine (15ml). The product was extracted into ethyl acetate (3 x 10 mL). The combined organic layers were dried over $MgSO_4$, and filtered. The solvent was removed under reduced pressure. The product was triturated with petroleum ether and filtered. Yield (0.54g, 65%). ^{1}H NMR (400MHz, $CDCl_3$, ppm), δ 9.38 (s, 1H), 8.76 (m, 2H), 8.49 (t, 2H, J = 8.2 Hz), 8.30 (s, 1H), 7.76-7.83 (4H, m), 7.31(2H, ddd, J = 6.3, 4.9, 2.7 Hz), 4.24 (4H, t, J = 6.6 Hz), 1.85 (4H, br.q, J= 7.0 Hz), 1.53 (m, 4H), 1.33-1.40 (8H, m), 0.90 (6H, t, J =7.0 Hz).*

*^{1}H NMR agrees with literature values.

2.4.1.2. Synthesis of **2.2.5**.[175]

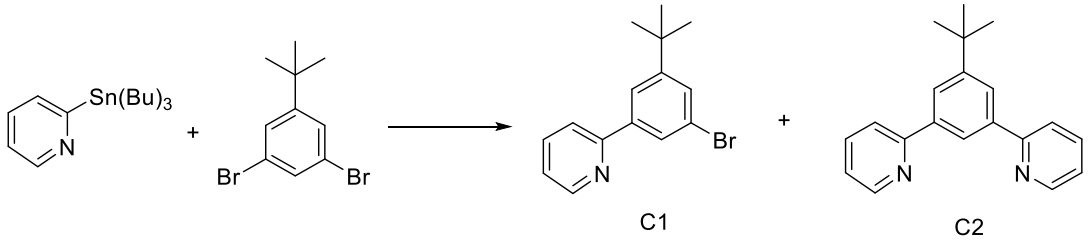

A mixture of 2-(tributylstannane)pyridine (8.66g, 20 mmol), 1,3-dibromo-5-*tert*-butylbenzene (6.40g, 22mmol) and toluene (20 ml) was deoxygenated by bubbling argon through the mixture for 5 minutes. Palladium tetrakis-triphenylphosphine (0.53 g, 0.5 mmol) was added to the mixture and the deoxygenation was continued for a further 5 minutes. The mixture was stirred and heated under reflux for 4.5 hours. The solvent was then removed under reduced pressure. The product was then purified by column chromatography (fine silica, petrol ether/ethyl acetate, 4:1) giving C1 (4.34g, 75%) as a yellowish oil. The by-product (C2) has a lower Rf value, was eluted next. Yield (1.13g, 20%). ^{1}H NMR (400MHz, $CDCl_3$), δ 8.71 (d, *J* = 5.0Hz, 1H), 7.95 (dd, *J* = 3.2, 1.6 Hz, 1H), 7.93 (d, *J*= 1.8 Hz, 1H), 7.76 (ddd, *J*= 8.0, 2.0 Hz, 1H), 7.70 (d, *J*= 8.0Hz, 1H), 7.57 (dd, *J*= 3.2, 1.2 Hz, 1H), 7.27 (ddd, *J*= 5.2, 0.8Hz, 1H), 1.36 (s, 9H). ^{13}C NMR (100MHz, $CDCl_3$), δ 156.7, 154.0, 149.8, 141.2, 136.9, 129.2, 127.3, 122.9, 122.6, 120.9, 35.0, 31.3. ***C2***: ^{1}H NMR (400MHz, $CDCl_3$), δ 8.74 (d, *J*= 4.8Hz, 2H), 8.36 (t, *J*= 3.2, 1.8 Hz, 1H), 8.1 (d, *J*=1.4 Hz, 2H), 7.85 (d, *J*= 8.0 Hz, 2H), 7.77 (ddd, *J*= 9.1, 1.3Hz, 2H), 1.47 (s, 9H). ^{13}C NMR (100MHz, $CDCl_3$), δ 157.9, 153.4, 149.7, 139.8, 136.8, 124.9, 123.1, 122.2, 121.0, 35.2, 31.6.

2.4.1.3. Synthesis of **2.2.7**.

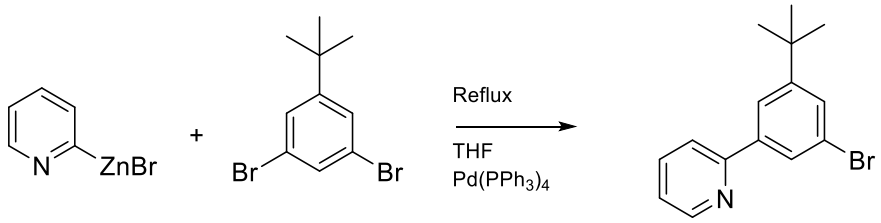

A round bottom flask was flushed with argon. Dry THF (50ml) was then added. The THF was degassed with argon for 10 minutes prior to the addition of 1,3-dibromo-5-tertbutylbenzene (5.00g, 17.1mmol). The solution was stirred and degassed further until complete dissolution. 2-pyridylzinc bromide (24.40g/25mL, 11.40mmol) was then added and the reaction was degassed for a further 15minutes. $Pd(PPh_3)_4$ was added (1.05g, 0.91mmol) and the reaction was heated under reflux for 18 hours. The reaction was cooled to room temperature and separated with brine. The product was extracted into EtOAc and the organic layers were collected. The organic layers were dried over $MgSO_4$ and the solvent was removed under reduced pressure. The resulting residue was then purified by column chromatography (silica, PE/EtOAc, 3:1). Solvent was removed under reduced pressure resulting in an orange crystalline solid. (1.29g, 38%). ^{1}H NMR (400MHz, $CDCl_3$), δ 8.70 (d, *J*= 4.4Hz, 1H), 7.94 (d, *J*= 2.8Hz, 2H), 7.76 (t, *J*= 7.8Hz, 1H), 7.68 (d, *J*= 8.4Hz, 1H), 7.55 (s, 1H), 1.37 (s, 9H).

2.4.1.4. Synthesis of **2.2.10**.[176]

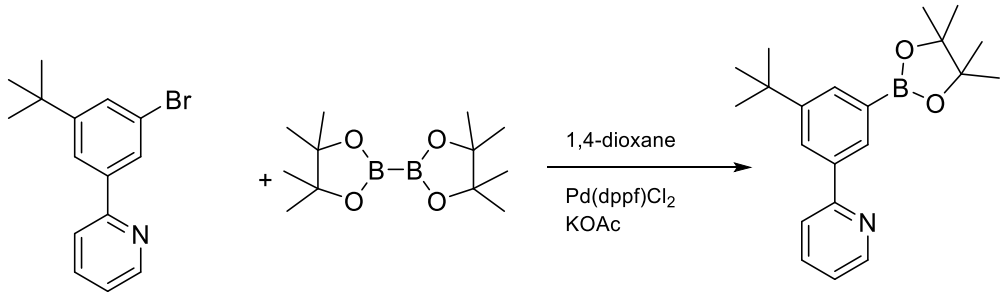

A sample of 2-(3-bromo-5-tertbutyl-phenyl) pyridine (1.50g, 5.17mmol) was added to a dry round bottom flask flushed with argon. 1,4-dioxane (50ml) was added to the flask and argon was bubbled through. Bispinacol diboron (1.96g, 7.76mmol) and KOAc (1.00g, 10.34mmol) were added to the flask and the mixture was degassed further. $Pd(dppf)Cl_2$ (0.21g, 0.259mmol) was added and the reaction was degassed for a further 15minutes before being heated at 80°C for 18hrs. The reaction was cooled to room temperature and separated with Et_2O and water (40ml each). The product was extracted into Et_2O (2 x 20ml). The organic layers were collected and dried over $MgSO_4$ before being filtered and evaporated to dryness *in vacuo*. The resulting oil was then purified by column chromatography (fine silica, DCM/$CHCl_3$, 5:1). Solvent was removed under reduced pressure and white solid was obtained (1.20g, 69%). ^1H NMR (400MHz, $CDCl_3$, ppm), δ 8.68 (d, *J*= 6.0Hz, 1H), 8.16 (d, *J*= 7.0Hz, 2H), 7.87 (d, *J*= 1.0Hz, 1H), 7.75 (d, *J*= 8.0Hz, 1H,), 7.72 (t, *J*= 9.0, 1.0Hz, 1H,), 7.20 (t, *J*=6.0, 1.0Hz, 1H), 1.40 (s, 9H), 1.33 (s, 12H). ^{13}C NMR (100MHz, $CDCl_3$), δ 158.2, 151.0, 149.7, 138.7, 136.6, 132.3, 130.7, 127.2, 121.9, 121.1, 83.9, 34.9, 31.6, 25.0.

2.4.1.5. Synthesis of **2.2.11**. [175]

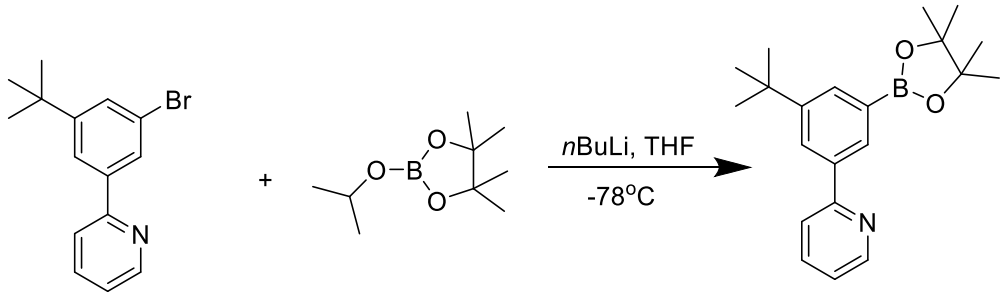

A sample of 2-(3-bromo-5-tertbutyl-phenyl)pyridine (2.00g, 6.9mmol) was added to a dry 3-neck flask. The sample was stirred and anhydrous THF (50ml) was added to the sample under argon. The mixture was cooled to -78°C. Whilst maintaining an excessive Ar atmosphere, *n*Bu-Li (5ml) was added drop wise and left to stir for 1 hour. 2-isopropoxy-4,4,5,5-tetramethyl-1,3,2-dioxaborolane (1.54g, 8.27mmol). The mixture was left overnight to stir at room temperature. The mixture was quenched with water (10ml) and the product was extracted into chloroform. The organic layer was washed with water and dried over $MgSO_4$. Petroleum ether was added to the filtrate and cooled. White crystals were obtained. Yield (0.74g, 32%). ^{1}H NMR (400MHz, $CDCl_3$, ppm), δ 8.68(d, *J*= 6.0Hz, 1H), 8.16(d, *J*= 7.0Hz, 2H), 7.87(d, *J*=1.2Hz, 1H,), 7.75 (d, *J*=8.0Hz, 1H), 7.72 (t, *J*=9.0, 1.2Hz, 1H), 7.20 (t, *J*=6.0, 1.2Hz, 1H), 1.40 (s, 9H), 1.33 (s, 12H). ^{13}C NMR (100MHz, $CDCl_3$), δ 158.2, 151.0, 149.7, 138.7, 136.6, 132.3, 130.7, 127.2, 121.9, 121.1, 83.9, 34.9, 31.6, 25.0.

2.4.1.6. Synthesis of **2.2.12**

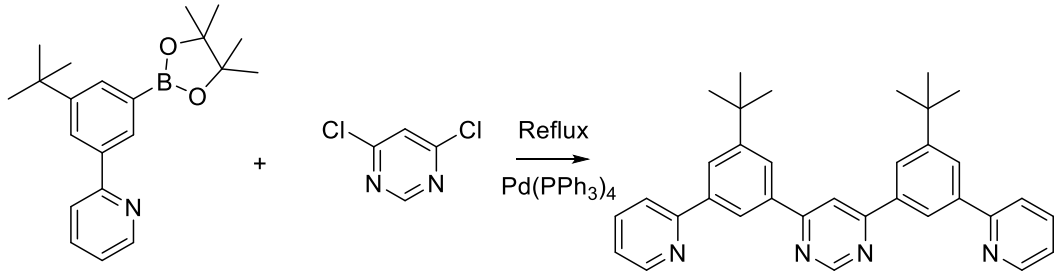

A mixture of K_2CO_3 (1.66g, 2M, 12mmol) was dissolved in water (6ml) and was then bubbled in an Ar atmosphere. Toluene (30ml) and ethanol (5ml) were then added and degassed under argon. 2-(3-tert-butyl-5-(tetramethyl-1,3,2-dioxaborolan-2-yl)phenyl)pyridine (1.05g, 3.11mmol) and 4,6-dichloropyrimidine (0.23g, 1.55mmol) were added to the mixture and degassed for a further 10minutes. $Pd(PPh_3)_4$ (0.10g, 0.1mmol) was added and the reaction was heated under reflux for 18hours. The mixture was separated using brine (15ml) and extracted into ethyl acetate (3x10ml). The organic layer was dried over $MgSO_4$ and filtered. The resulting solution was evaporated to dryness under reduced pressure. The product was purified using column chromatography (fine silica, Hexane/ EtOAc, 3:1). The solvent was removed under reduced pressure resulting in a colourless oil. Yield (0.59g, 76%). ^{1}H NMR (400MHz, $CDCl_3$, ppm), δ 9.37 (s, 1H), 8.71(t, *J*= 5.0, 1.8Hz, 2H), 8.47(s, 2H), 8.28 (d, *J*= 9.0Hz, 2H), 8.18 (s, 2H), 7.87(d, *J*= 8.0Hz, 2H), 7.81(ddd, J=7.8, 1.8Hz, 2H), 7.29 (t, *J*= 0.8Hz, 2H), 1.36 (s, 9H). HRMS (ESI) calculated for $C_{34}H_{34}N_4$ ($[M+H]^+$)= 499.28563. Found m/z= 499.28583.

2.4.2. Mono and Di-iridium Complexes

2.4.2.1. Synthesis of **2.1.3**. [105]

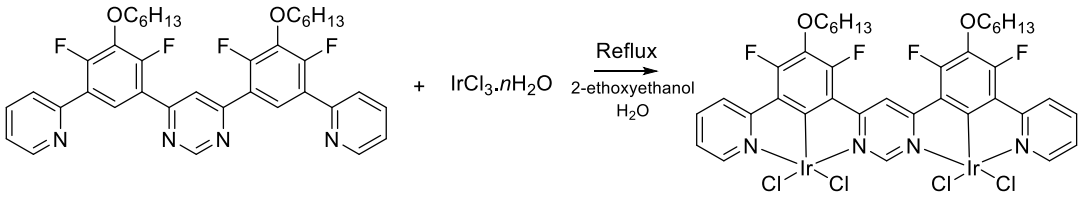

2.1.2 (1.10g, 1.67mmol) was added to a mixture of 2-ethoxyethanol (30ml) and water (10ml) and heated. Iridium chloride hydrate (1.10g, 3.68mmol) was added and the reaction was heated under reflux for 18hours. Water (50ml) was added to the flask and a red precipitate formed upon cooling. The precipitate was filtered and washed with water. Yield (1.60g, 76%). ^{1}H NMR (400MHz, $CDCl_3$, ppm), δ 9.84 (s, 2H), 8.95 (s, 2H), 8.27 (d, *J*= 5.4Hz, 4H), 8.19 (d, *J*= 8.2 Hz, 4H), 7.65 (t, *J*= 7.8Hz, 4H), 6.60 (t, *J*= 7.6 Hz, 4H), 4.24 (t, *J*= 6.6 Hz, 8H), 1.93 (q, *J*= 6.8 Hz, 8H), 1.53-1.63 (m, 8H), 1.40-1.45 (m, 16H), 0.97 (t, *J*= 6.6 Hz, 12H).*

*^{1}H NMR agrees with the literature values.

2.4.2.2. Synthesis of **2.1.5**

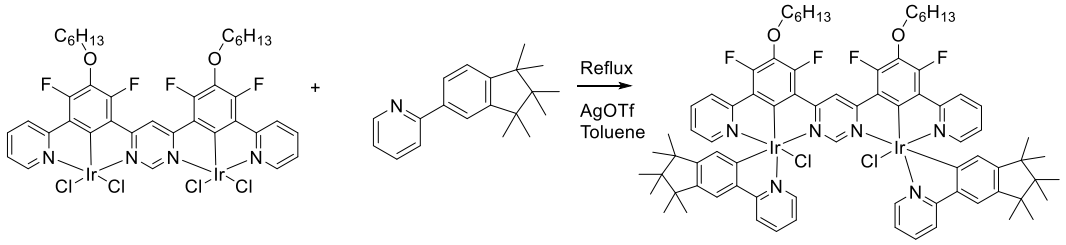

2.1.3 (0.12g, 0.10mmol) was added to a flask with toluene (20ml), 2-(1,1,2,2,3,3-hexamethyl-2,3-dihydro-1H-inden-5-yl)pyridine (0.067g, 0.24mmol) and silver triflate solution (3ml, 0.3mmol, 0.1M) were added to the mixture. The mixture was heated under reflux for 18 hours. Dilute HCl (10ml, 2M) was added and the reaction was stirred. The mixture was filtered through celite and washed with DCM. The solvent was removed under reduced pressure. The product was purified using column chromatography (fine silica, DCM/MeOH, 20:1). The solvent was removed under reduced pressure giving a deep red solid. Yield (0.0175g, 11%). ^{1}H NMR (400MHz, $CDCl_3$, ppm), δ 9.50 (d, *J*=6.0Hz, 2H), 8.56 (s, 1H), 7.99 (t, *J*= 4.2Hz,

4H), 7.86 (t, *J*= 7.8Hz, 2H), 7.54 (t, *J*= 7.8Hz, 2H), 7.41 (d, *J*= 5.5Hz, 2H), 7.25 (s, 2H), 7.15 (t, *J*= 6.4Hz, 2H), 6.77 (t, *J*=6.4Hz, 2H), 5.43 (s, 2H), 4.19 (t, *J*= 6.4Hz, 4H), 1.89 (quin, *J*= 7.8Hz, 4H), 1.58-1.52 (m, 4H), 1.38-1.37 (m, 8H), 1.08 (s, 6H), 1.01 (s, 6H), 0.93 (t, *J*= 6.8Hz, 6H), 0.85 (s, 1H), 0.80 (s, 6H), 0.67 (d, *J*= 8.2Hz, 12H), 0.60 (s, 6H).

2.4.2.3. Synthesis of **2.2.1**

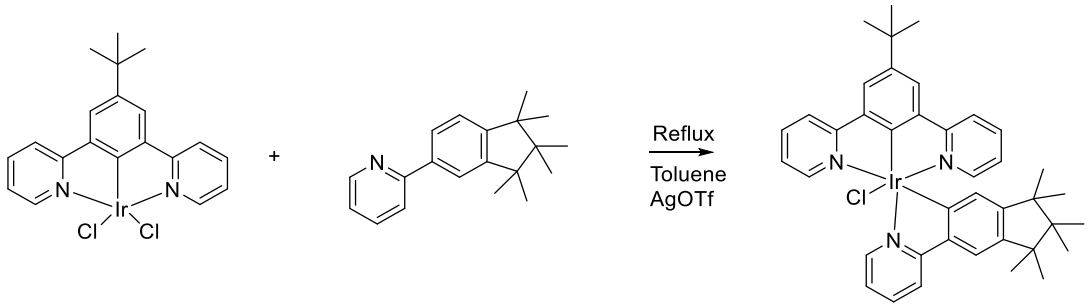

2.2.13 (0.10g, 0.181mmol) and 2-(1,1,2,2,3,3-hexamethyl-2,3-dihydro-1H-inden-5-yl)pyridine (0.071g, 0.212mmol) were added to toluene (30ml). Silver triflate (0.10, 0.40mmol) was added and the reaction was heated under reflux for 5 hours. Dilute HCl (2M, 5ml) was added upon cooling, producing a yellow solution. The mixture was filtered through celite and purified by column chromatography (fine silica, DCM/EtOAc/MeOH, 5:1:1). The solvent was removed under reduced pressure. The resulting yellow/orange solid was washed with diethyl ether and filtered. Yield (0.090g, 38%). ^{1}H NMR (400MHz, $CDCl_3$, ppm), δ 10.06 (d, *J*= 5.2Hz, 1H), 8.01 (d, *J*= 8.2Hz, 1H), 7.91-7.78 (m, 6H), 7.68 (d, *J*= 5Hz, 2H), 7.52 (t, *J*= 7.2Hz, 2H), 7.43 (t, *J*= 6.6Hz, 1H), 6.77 (t, *J*=6.7Hz, 2H), 5.45 (s, 1H), 1.51 (s, 9H), 1.03 (s, 6H), 0.66 (s, 6H), 0.61 (s, 6H).

2.4.2.4. Synthesis of **2.2.2**

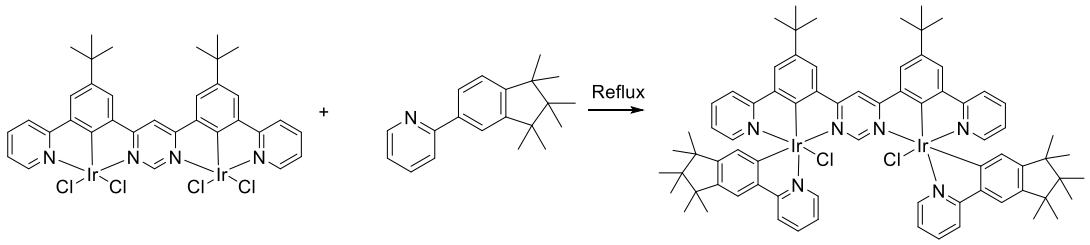

2.2.14 (0.050g, 0.049mmol) and 2-(1,1,2,2,3,3-hexamethyl-2,3-dihydro-1H-inden-5-yl)pyridine (0.033g, 0.12mmol) were added to a silver triflate (0.055g, 0.22mmol) and toluene (25ml) solution. The mixture was heated under reflux for 18 hours. Dilute HCl (2M, 5ml) was added and the resulting red solution was filtered through celite. The solvent was removed under reduced pressure. The resulting solid was purified using column chromatography (fine silica, DCM/EtOAc, 10:1). The solvent was removed under reduced pressure and the resulting deep red solid was filtered. Yield (0.15g, 20%). ^{1}H NMR (400MHz, $CDCl_3$, ppm), δ 9.56 (d, *J*= 4.6Hz, 2H), 8.04 (s, 2H), 8.02-8.00 (m, 3H), 7.86 (td, *J*= 8.3, 1.4Hz, 4H), 7.79 (d, *J*= 8.2Hz, 2H), 7.54-7.49 (m, 4H), 7.37 (s, 1H), 7.16 (t, *J*= 6.0Hz, 2H), 6.75 (td, *J*= 6.2, 1.1Hz, 2H), 5.26 (s, 2H), 1.53 (s, 18H), 1.06 (s, 6H), 1.01 (s, 6H), 0.72 (s, 6H), 0.64 (s, 6H), 0.61 (s, 6H), 0.59 (s, 6H). ^{13}C NMR (100MHz, $CDCl_3$), δ 168.7, 153.5, 152.9, 151.7, 148.6, 144.2, 141.1, 136.8, 136.2, 129.0, 124.1, 123.5, 122.4, 121.5, 119.2, 118.4, 48.1, 46.9, 35.5, 32.0, 27.7, 27.1, 26.5, 21.6. LC-MS (ESI): calculated for $C_{74}H_{80}Cl_2Ir_2N_6$: 1508.5079, Found: 1508.5103.

2.4.2.5. Synthesis of **2.2.13**

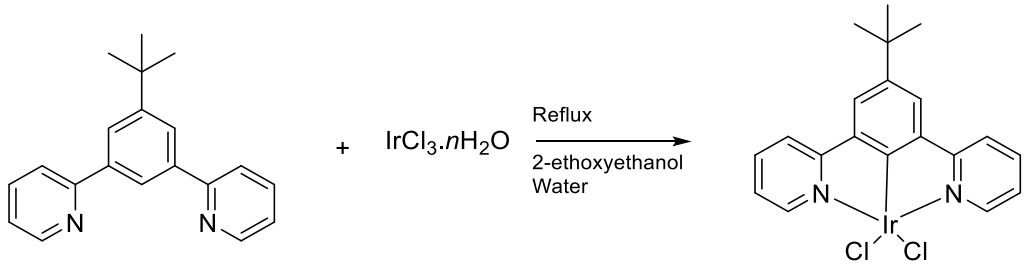

1,3-di(pyridine-2-yl)-5-tert-butylbenzene (0.50g, 1.71mmol) was dissolved in warm 2-ethoxyethanol (30ml) and water (10ml). This solution was stirred and iridium chloride hydrate (0.75g, 2.05mmol) was added. The reaction was heated under reflux for 18 hours. Water was added producing an orange precipitate. The solid was filtered and washed with water (20ml). Yield (0.71g, 75%). ^{1}H NMR (400MHz, DMSO-d6, ppm), δ 8.95 (d, *J*= 4.8Hz, 2H), 8.35 (d, *J*= 7.6Hz, 2H), 8.05 (t, *J*= 7.8Hz, 2H), 7.99 (s, 2H), 7.50 (t, *J*= 6.4Hz, 2H), 1.38 (s, 9H).

2.4.2.6. Synthesis of **2.2.14**

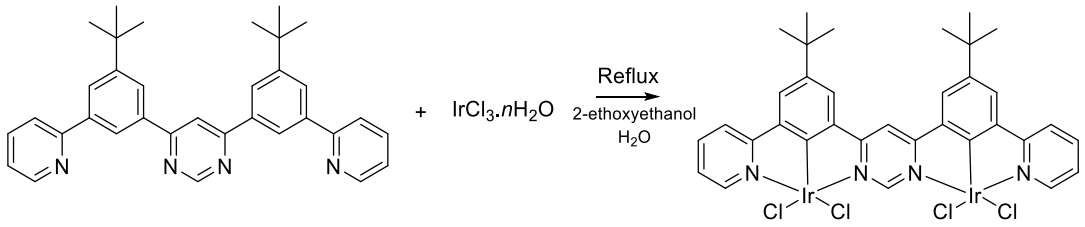

4,6-bis(3-tert-butyl-5-(pyridin-2-yl)phenyl)pyrimidine (0.10g, 0.201mmol) was added to a flask of 2-ethoxyethanol (15ml) and water (5ml) and was heated gradually. The iridium chloride hydrate (0.16g, 0.44mmol) was added to the mixture and heated under reflux for 18 hours. Water (50ml) was added to the mixture, forming a red precipitate which was filtered and washed with water. The dark red solid formed was then dried. Yield (0.18g, 86%). ^{1}H NMR (400MHz, DMSO-d6, ppm), δ 9.77 (s, 1H), 9.07 (d, *J*= 2Hz, 2H), 9.01 (t, *J*= 6, 4.4Hz, 2H), 8.46 (d, *J*= 8Hz, 2H), 8.39 (s, 2H), 8.35 (s, 2H), 8.11 (t, *J*= 7.8Hz, 2H), 7.58 (t, *J*=6.8Hz, 2H), 1.51 (s, 18H).

2.4.2.7. Synthesis of **2.2.15**

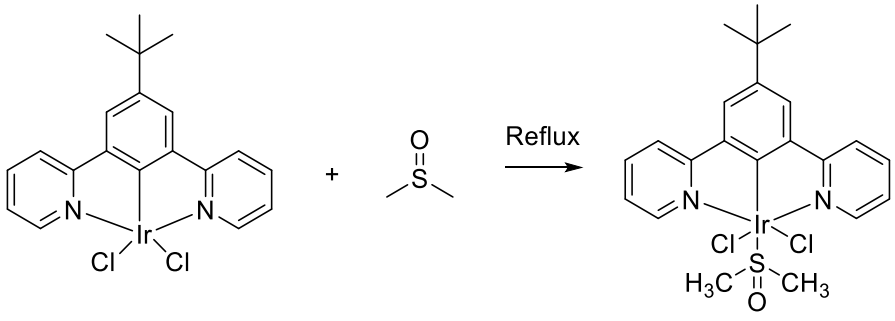

2.2.13 (0.20g, 0.363mmol) was added to a test tube with DMSO (2ml) and the test tube was heated under reflux. The mixture was filtered and water was added. A solid crashed out to form a hydrogel. This mixture was heated to break up the hydrogel and the mixture was filtered to give **2.2.15** (0.15g, 65%). ^{1}H NMR (400MHz, DMSO-d6, ppm), δ 8.95 (d, *J*= 4.6Hz, 2H), 8.34 (d, *J*= 7.8Hz, 2H), 8.03 (ddd, *J*= 7.8, 1.4Hz, 2H), 7.99 (s, 2H), 7.47 (t, *J*= 6.0Hz, 2H), 2.68 (s, 6H), 1.41 (s, 9H).

2.4.2.8. Synthesis of **2.2.16**

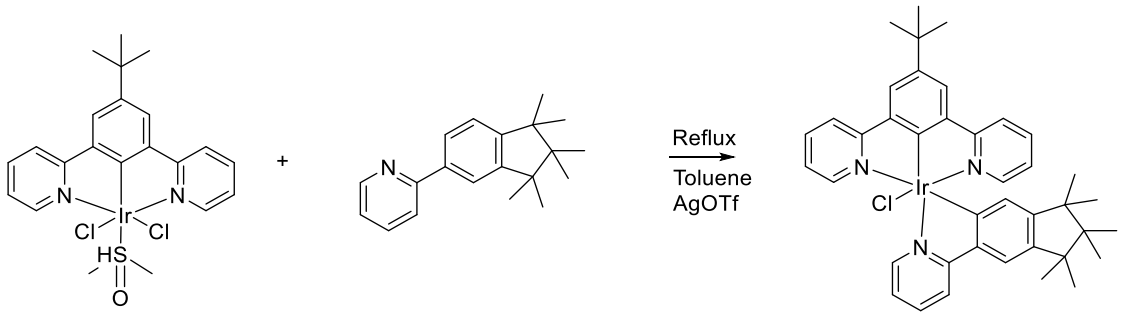

2.2.15 (0.13g, 0.206mmol) was added to a flask with toluene (30ml). Silver triflate (2ml, 0.1M, 0.2mmol) was added and the reaction was stirred. 2-(1,1,2,2,3,3-hexamethyl-2,3-dihydro-1H-inden-5-yl)pyridine (0.069g, 0.247mmol) was added and the reaction was heated under reflux for 18 hours. Dilute HCl (2M, 5ml) was added and the mixture was then filtered through celite with DCM. The filtrate was then evaporated to dryness under reduced vacuum. The solid was then purified using column chromatography (fine silica, DCM/MeOH, 20:1). The relevant fractions were collected and solvent removed under reduced pressure, the resulting orange solid was filtered. Yield (0.010g, 6%). ^{1}H NMR (400MHz, $CDCl_3$, ppm), δ 10.06 (d, *J*= 5.2Hz, 1H), 8.01 (d, *J*= 8.2Hz, 1H), 7.91-7.78 (m, 6H), 7.68 (d, *J*= 5Hz, 2H), 7.52 (t, *J*= 7.2Hz, 2H), 7.43 (t, *J*= 6.6Hz, 1H), 6.77 (t, *J*=6.7Hz, 2H), 5.45 (s, 1H), 1.51 (s, 9H), 1.03 (s, 6H), 0.66 (s, 6H), 0.61 (s, 6H).

CHAPTER 3

Employing Di-anionic Asymmetrical O^N^C Auxiliary Ligands in Mono-iridium (III) Complexes.

3. Employing Di-anionic Asymmetrical O^N^C Auxiliary Ligands in Mono-iridium (III) Complexes.

In this chapter we discuss chlorine free systems that employ dianionic terdentate ligands of O^N^C coordination type. Monodentate chloride ligands are probably the weakest point in the complexes and by removing the chloride ligands, the operational lifetime of the OLED device is predicted to increase. Further benefits of a tridentate coordination type is that this increases the rigidity of the complex and may be beneficial to the photophysical properties. Di-anionic complexes with O^N^C coordination have scarcely been described in the literature. One relevant example is the complex reported by Williams *et al* where picolinate based ligands were described, as shown in Figure 75.[13] The study showed that the picolinate complex described had a peak QE value of ϕ= 0.04. This relatively low efficiency was attributed to the photo cleavage of the Ir-O bond in the excited state.[13]

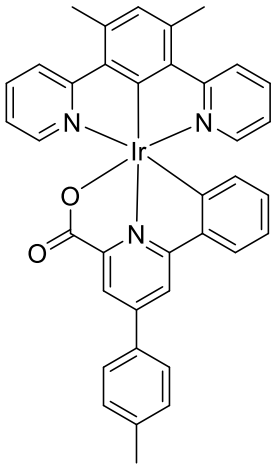

3.0.1
Williams *et al*, 2006
ϕ= 0.04

Figure 75 - The structure of the picolinate cyclometalated complex described by Williams *et al* in 2006.[13]

The key part of this chapter is a series of O^N^C coordinated complexes in which phenolic oxygen is used as the O-coordinating part of the ligand, instead of the carboxylic group in Williams' complex. Similar O^N^C dianionic coordination was reported by Acharrya *et al*

were 2-(arylazo)phenol which was used as a ligand, shown in Figure 76. Whilst the study outlined a successful method for the coordination of some phenolate type ligands these complexes were not luminescent.[177]

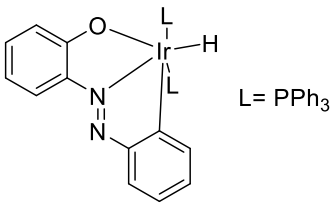

3.0.2
Acharrya *et al*, 2006

Figure 76 - The Ir(III) complex described by Acharrya *et al* that utilises a phenolate type ligand.[177]

As the synthesis of bimetallic systems is more challenging than the corresponding monometallic analogues, the synthetic methodology was first tested and optimised he first on monometallic assemblies and only then attempted using bimetallic analogues.

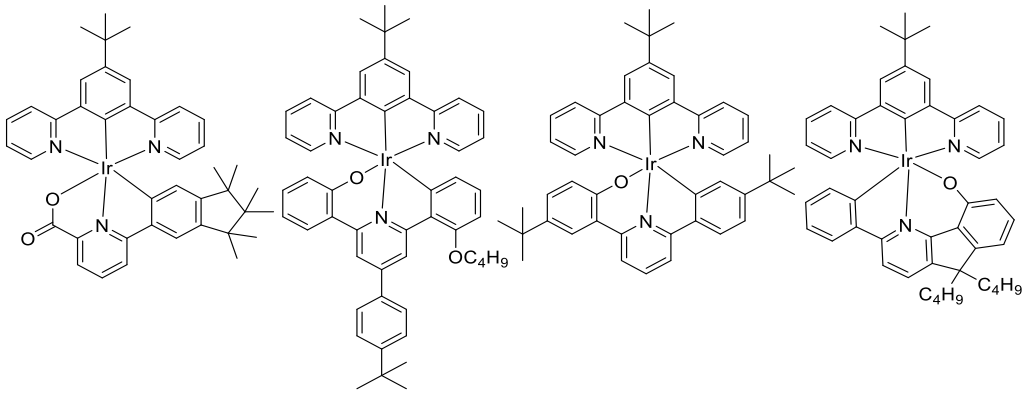

3.1.4 **3.2.15** **3.2.16** **3.2.17**

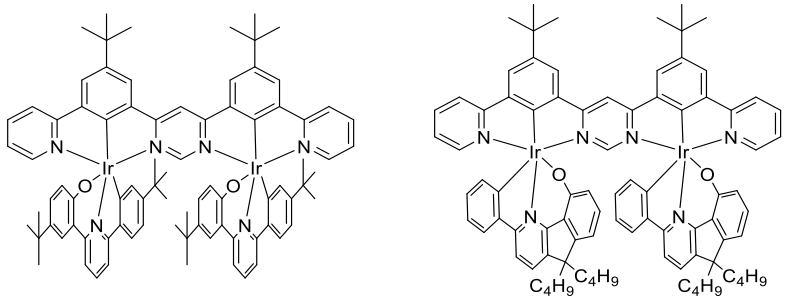

3.4.1 **3.4.3**

Figure 77 - The structures of the complexes described in this chapter.

3.1. Synthesis of the Picolinate based Ligand and Complex

The monometallic complexes with carboxylate O^N^C auxiliary ligands were previously described in literature and the literature procedures were adapted to obtain **3.1.4**.[13] Using the building block provided by Merck, 2-(1,1,2,2,3,3-hexamethyl-2,3-dihydro-1H-inden-5-yl)-4,4,5,5-tetramethyl-1,3,2-dioxaborolane (**Merck1/M1**), an intermediate of **3.1.3** was synthesised through a Suzuki cross coupling with ethyl 6-bromopyridine-2-carboxylate. The yield of this reaction was consistently low over multiple repeats (<~20%). This is considerably lower than the average yield of a typical Suzuki cross coupling (>50%).[175, 178-179] The ethyl ester (**3.1.2**) was deprotected, this was done by heating under reflux with sodium hydroxide in an ethanol and water mixture. After acidification with HCl, **3.1.3** was obtained in high yields (83%). The complete synthetic route to **3.1.3** is shown in Scheme 14. The general mechanism for a Suzuki cross coupling is shown in Scheme 15.

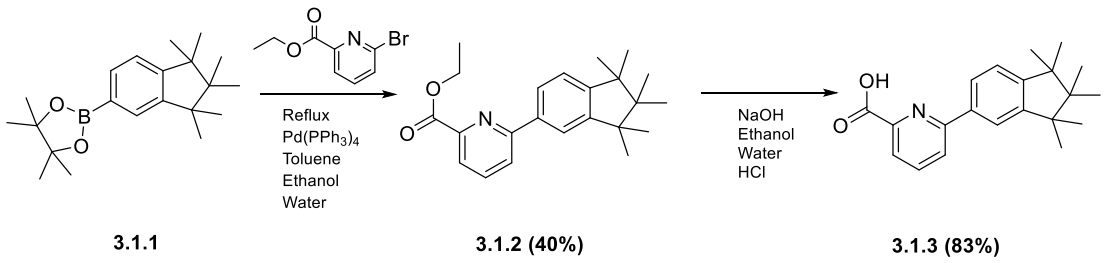

Scheme 14 - The complete reaction scheme showing the formation of **3.1.3**, the protected intermediate **3.1.2** is shown.

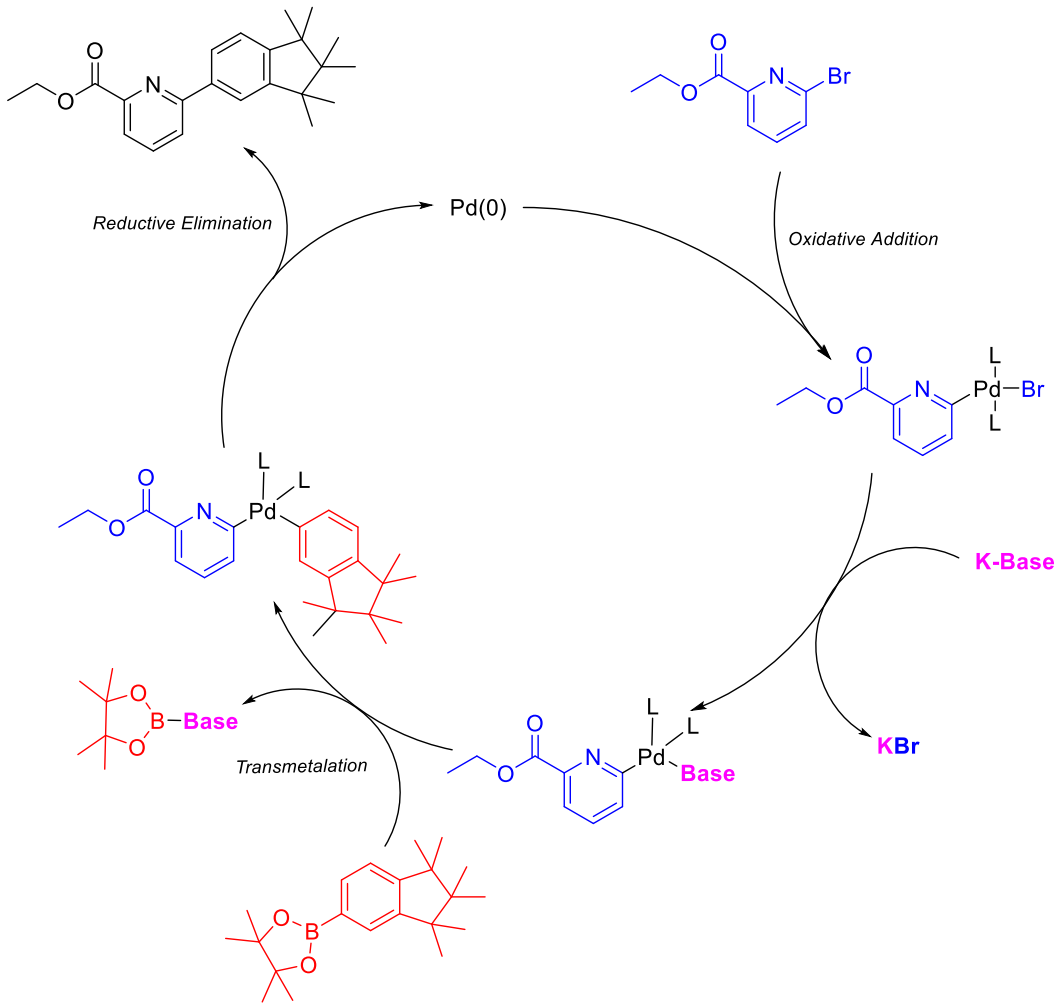

Scheme 15 - The general mechanism for the Suzuki cross coupling. The mechanism uses the synthesis of **3.1.2** as an example with the brominated starting material shown in blue, the required base in purple and the boronic acid building block in red. The individual reaction processes are shown next to the associated step.

The synthesis of the mono-iridium complex, **3.1.4** was carried out using methodologies described by Williams and co-workers.[6, 12-13] The iridium dimer used was synthesised using the N^C^N ligand isolated during the Stille cross coupling in the preparation of the ditopic outer ligand (outlined in Scheme 9). The iridium chloride was reacted with the N^C^N ligand in 2-ethoxyethanol and water, to give **2.2.13** in high yields (>75%).[6, 103] The complex, **3.1.4**, was synthesised by dissolving **2.2.13** (dimer) in toluene and heating with silver triflate (AgOTf, used as a chloride scavenger). Upon heating under reflux with the ligand **3.1.3**, an orange solution formed. The resulting mixture was filtered through celite to remove the excess of silver triflate. Thin layer chromatography identified the most ideal eluent system for the

removal of impurities (DCM/EtOAc/MeOH, 5:1:1), the complex was easily identifiable by an intense yellow spot (R_f= 0.62). The complex was isolated by column chromatography in good yields (~74%). The synthetic route is shown in Scheme 16. The ^{1}H NMR for **3.1.4** is shown in Figure 78.

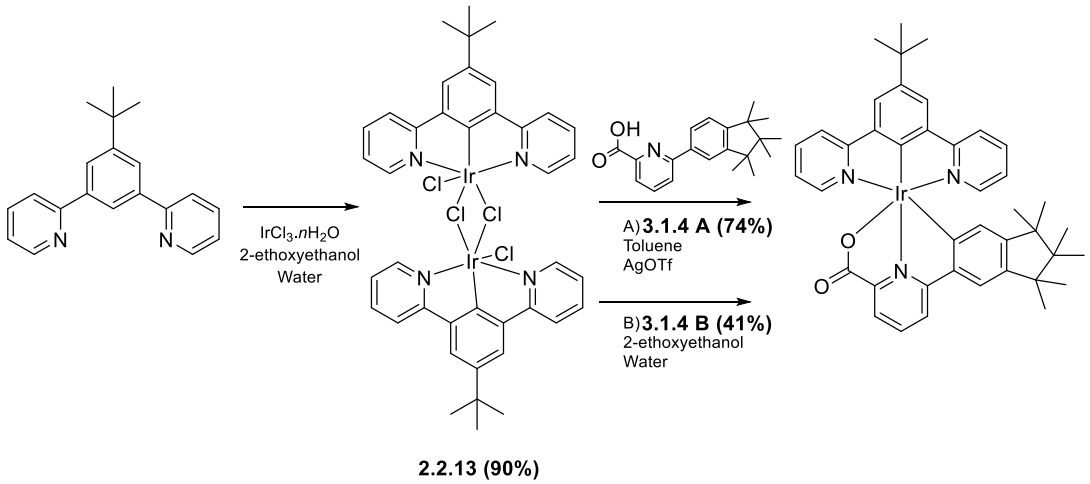

Scheme 16 - The synthesis of **3.1.4** by the methods A and B.

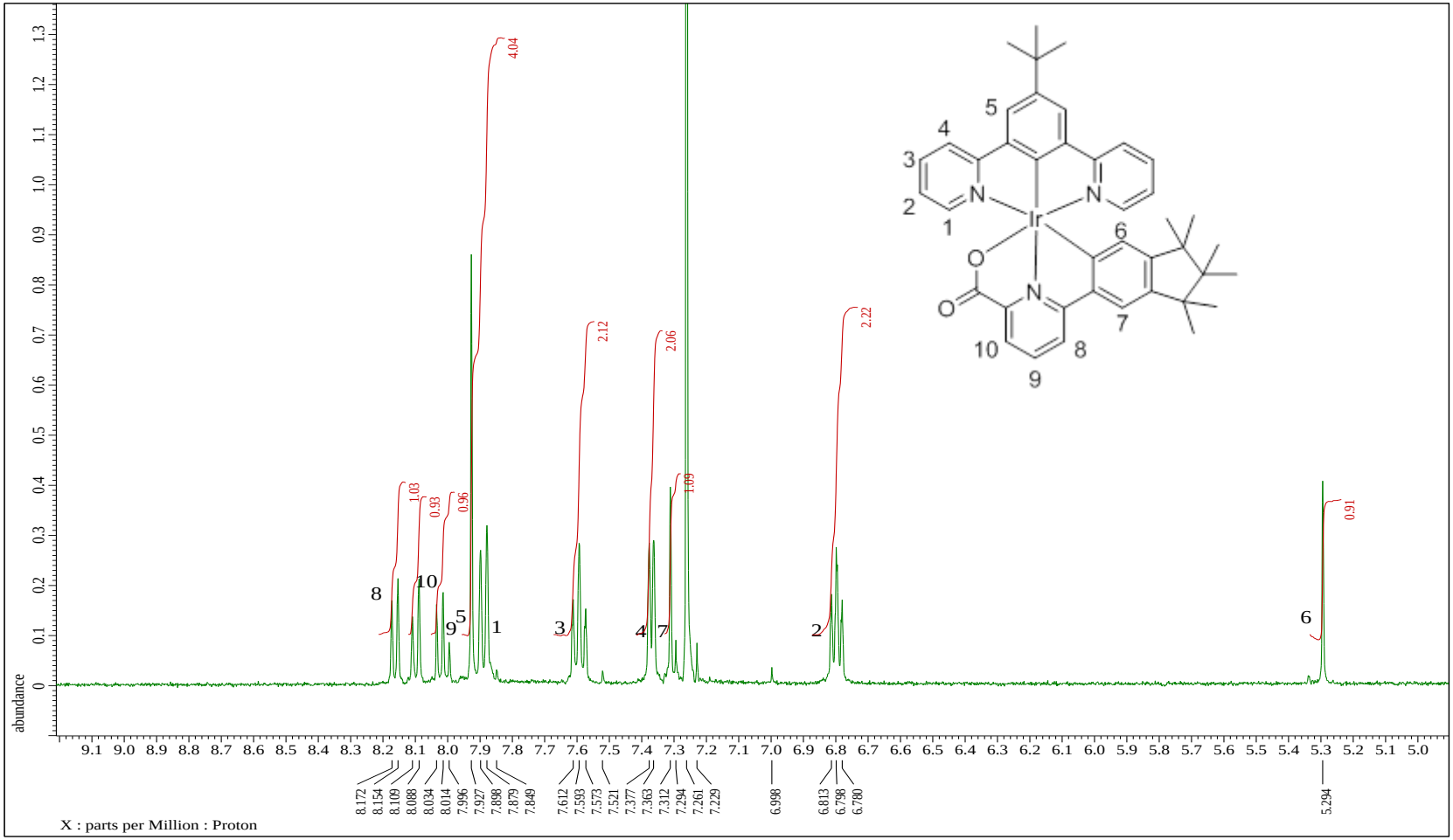

Figure 78 - The aromatic region of the ^{1}H NMR and structure of the complex **3.1.4** (in $CDCl_3$). The spectrum shows the tertiary butyl peak as a singlet at δ 1.55ppm, the methyl groups are shown in the aliphatic region as singlets at δ 1.08, 0.70 and 0.65ppm.

The second method involved heating the dichloro-bridged dimer and auxiliary ligand in 2-ethoxyethanol under reflux in basic conditions (for example, K_2CO_3). A method previously documented to coordinate O^N^C, phenolic type ligands using alcohol/basic conditions.[177] The use of this method was successful but resulted in lower yields of the reaction in comparison to the above toluene/AgOTf methodology (<50%).

The photophysical properties of **3.1.4** followed literature trends by displaying a very low quantum yield (ϕ= 0.04), a property previously displayed by picolinate based complexes.[13] The study by Williams *et al* described that the coordinating oxygen (Ir-O) bond provides a weak ligand field and the picolinate Ir-O bond is cleaved in the excited state as a result of a strong *trans* effect from the cyclometalating carbon. These characteristics result in a large amount of non-radiative decay.

3.2. Synthesis of phenolic type O^N^C proligands and their Ir(III) complexes

3.2.1. The Synthesis of Phenolic O^N^C Auxiliary Ligands

As the use of the picolinate group was unsuitable, the carboxylate group was changed to phenolate. The ligand (**3.2.2**) was prepared by the alkylation of **3.2.1** which was available in the lab. Although the reaction gave a mixture of products, the major product was **3.2.2** and was easily separated by column chromatography (silica gel, PE/EtOAc, 5:1).

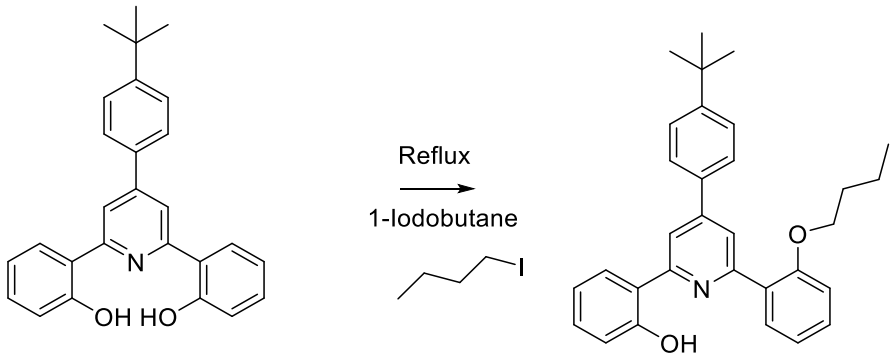

3.2.1 **3.2.2 (25%)**

Scheme 17- The synthetic pathway followed to develop the proligand, **3.2.2**, which is used for the first mono-nuclear complex phenolic O^N^C complex in the study.

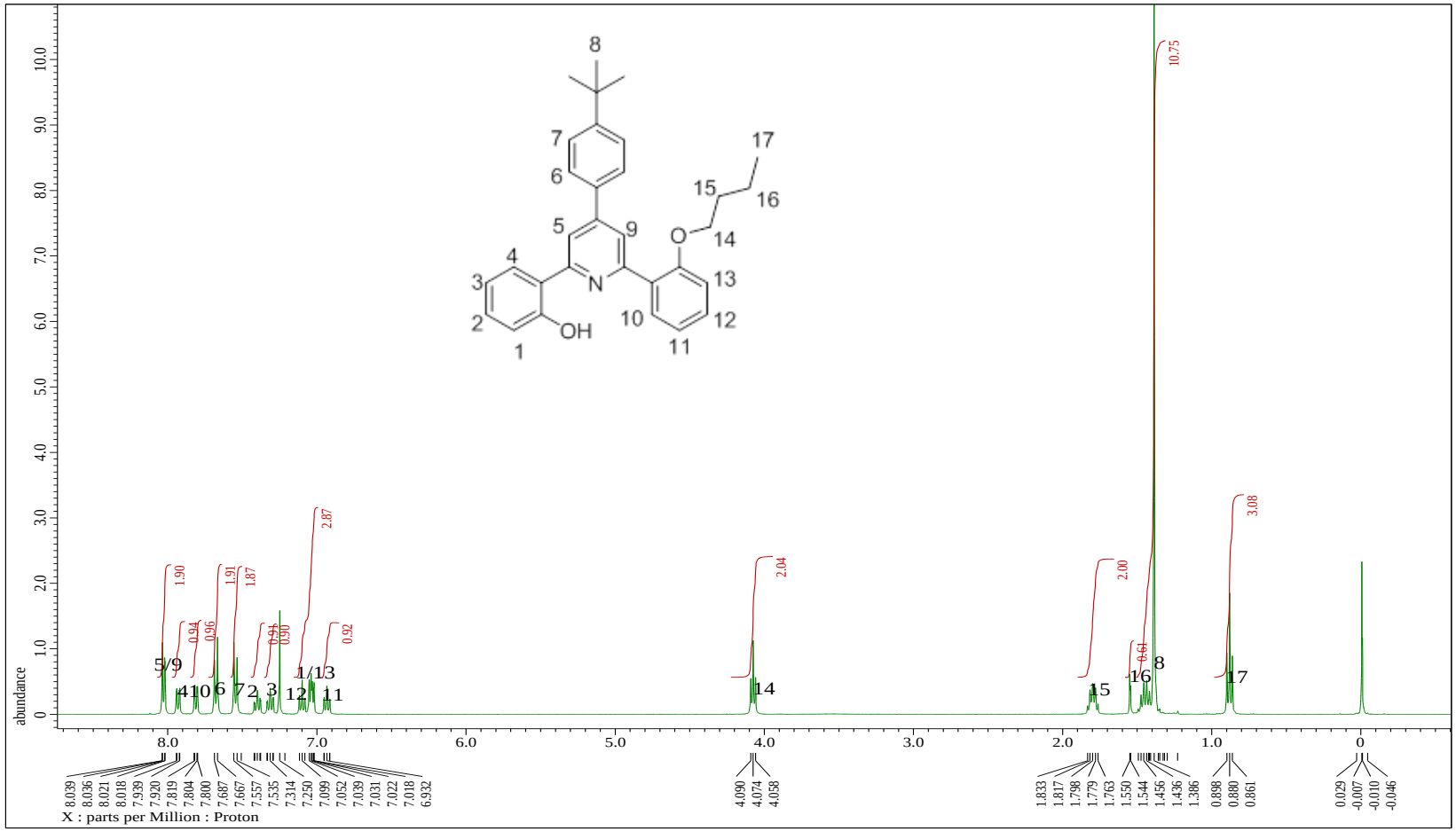

Figure 79 - The complete ^{1}H NMR of the phenolic ligand **3.2.2**, with the overlaid structure. The proton NMR of the resulting solid showed the presence of a triplet peak at δ4.06ppm, characteristic of the -OCH_2-R group. The overall yield of the reaction was low (~25%), and a small amount of product was likely lost due to alkylation of both phenolate groups.

The use of alkoxy groups in OLED devices is not desirable and ideally should be avoided as solubilising groups. Additionally, the presence of the bulky substituent on the pyridine moiety of the auxiliary ligand may cause steric hindrance during the synthesis of bimetallic complexes preventing the synthesis. To remove the detrimental groups, the alkoxy chain was substituted for tertiary butyl groups which would provide the same solubilising effect on the overall ligand. The addition of the tertiary butyl also blocks any possible competitive cyclometalation at other points across the auxiliary ligand, an issue previously discussed. In response to the issues, the auxiliary ligand **3.2.6** and corresponding complex, **3.2.16** were prepared.

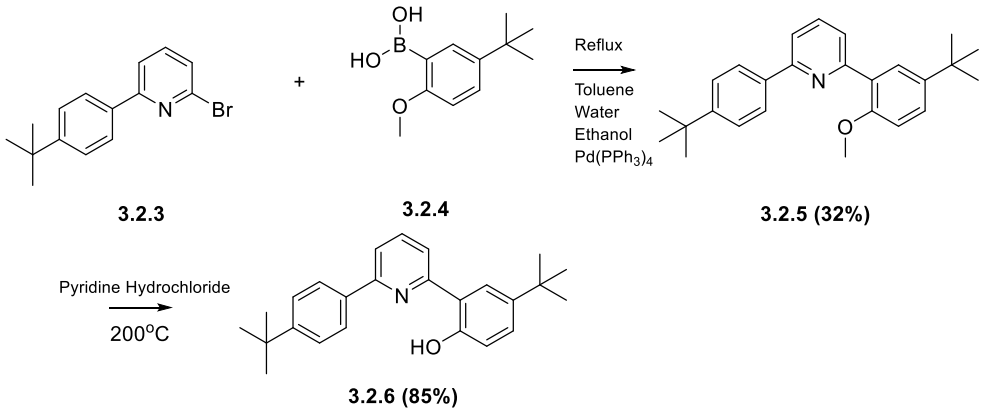

Scheme 18 - The reaction scheme showing the formation of the phenolate auxiliary ligand (**3.2.6**).

The intermediate **3.2.5** was synthesised using a Suzuki cross coupling from **3.2.3** (readily available in the lab) and (5-tert-butyl-2-methoxyphenyl)boronic acid in poor to average yields (32%). **3.2.5** was purified by column chromatography (PE/EtOAc, 10:1) and this resulted in a white crystalline solid. Deprotection of the methyl ether group was carried out through heating with pyridine hydrochloride at 200°C. Upon the addition of water, a white solid formed which was recovered in high yields (85%).

The structure of the auxiliary ligand was altered further by increasing the rigidity and the substituting additional alkyl chains to act as solubilising groups. This was achieved using chemistry previously described by Che *et al*.[180]

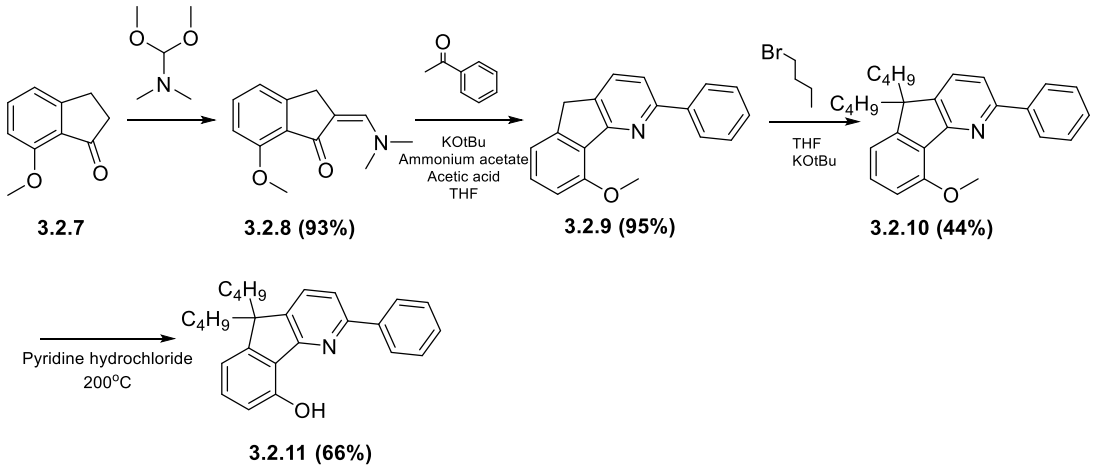

Scheme 19 - The complete reaction pathway for the synthesis of **3.2.11** and the iridium complex **3.2.17**. The synthetic route is relatively high yielding with the limiting step being the alkylation of the alkyl bridge.

The chemistry detailed by Che *et al,* was initially used to design tetradentate ligands for use in Pt(II) complexes.[180] Through changing one of the intermediate building blocks, a mono-phenolic terdentate auxiliary ligand was synthesised in high yields (overall average: ~75%), the limiting steps being the alkylation of the bridging chain and the deprotection of the methyl ether. It can be noted that the starting material in the synthetic route can be synthesised from cheaper and more readily available compounds.[181] The steps required to produce the first building block depicted in Scheme 19 from inexpensive starting materials is depicted below in Scheme 20.

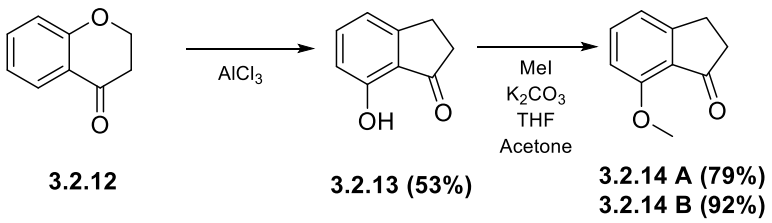

Scheme 20 - The reaction pathway to produce the starting material needed to synthesise **3.2.11**. The process utilises methodologies described by Narine et al.[181]

By using a rearrangement-cycloaddition of 4-chromanone (**3.2.12**) to 7-hydroxy-indan-1-one (**3.2.13**), the cost of the synthetic procedure can be dramatically reduced. The production of the compound involves the use of methyl iodide (MeI) which can be harmful.[182-183] The

protection of the phenolate with methyl iodide, was carried out to prevent interaction in the subsequent steps and this was carried out in high yields (>75%).

3.2.2. Synthesis of Mono-iridium (III) Complexes with O^N^C ligands

The preparation of **3.1.4** showed that the picolinate group was not suitable for the development of efficient luminescent complexes. This led to the development of a new library of complexes using the ligands described in Section 3.2.

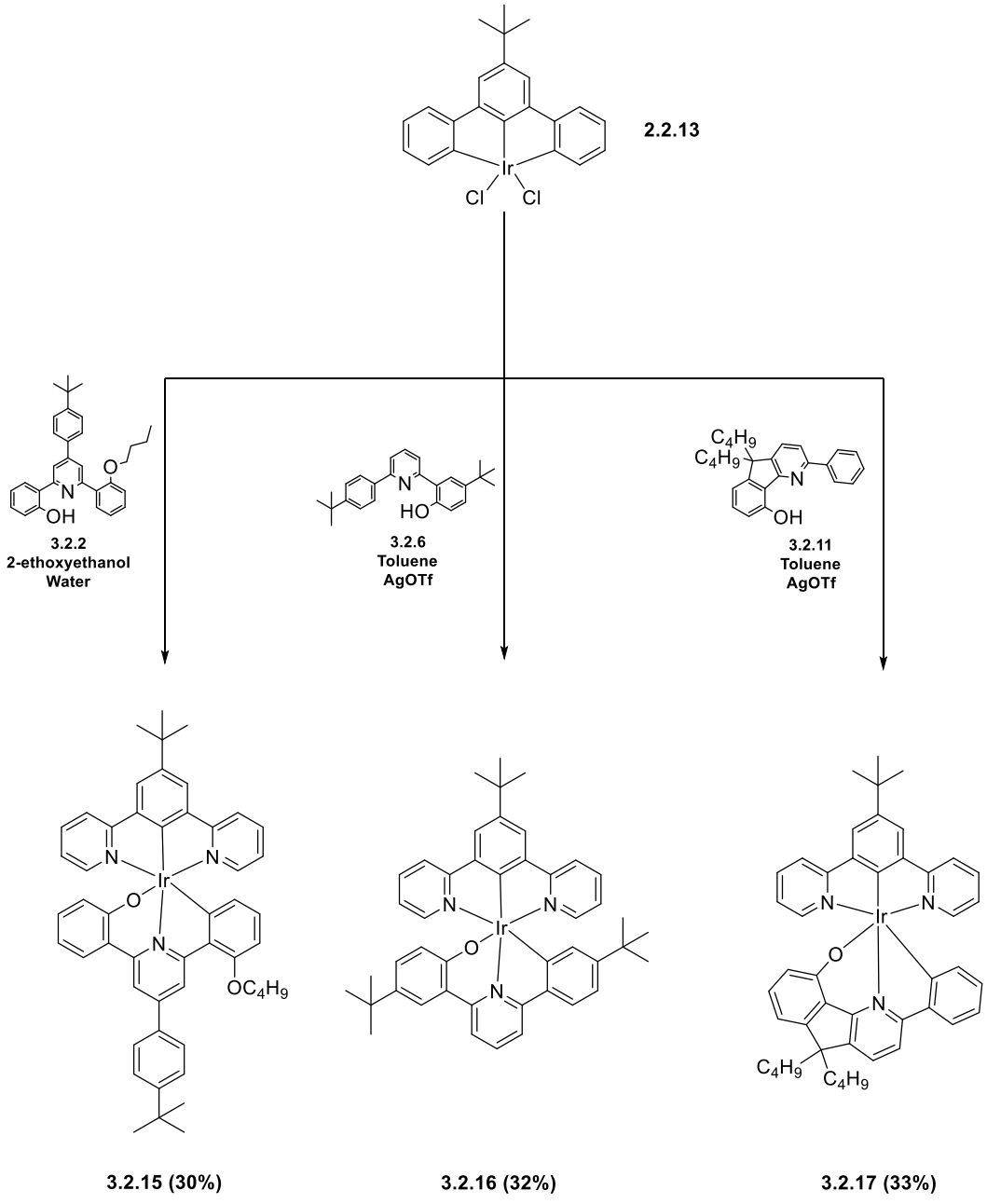

Scheme 21 - The synthetic procedure for the preparation of the mono-iridium phenolate O^N^C complexes.

Following the isolation of the pure auxiliary ligand, **3.2.2**, the preparation of the mono-nuclear complex, **3.2.15** was carried out. Trialling the strategy of heating the dichlorobridged dimer

with the chloride scavenging silver triflate however the yield of the reaction was poor (<5%); multiple trials of condition optimisation resulted in similar results and an alternate strategy was attempted. Heating the dichlorobridged dimer in 2-ethoxyethanol with potassium carbonate and the auxiliary ligand led to the synthesis of the complex in average yields (30%). The success of the reaction can be attributed to the activation of the phenolate group, as described by Achrayya *et al*.[177]

The other mono-nuclear phenolic complexes were prepared under similar conditions. The reactions involved heating the dichlorobridged intermediate **2.2.13** with a 1.2 equivalence of silver triflate. The reactions were typically heated under reflux for 18 hours. The mono-nuclear complexes are highly soluble in organic solvents and are easily purified by column chromatography with yields in the range of 30%. For **3.2.17**, both cyclometalation strategies were tested however heating in toluene with AgOTf was a more effective technique in comparison to the synthesis described by Acharrya *et al*. [177]. The NMR spectrum for **3.2.17** is shown in Figure 80.

.

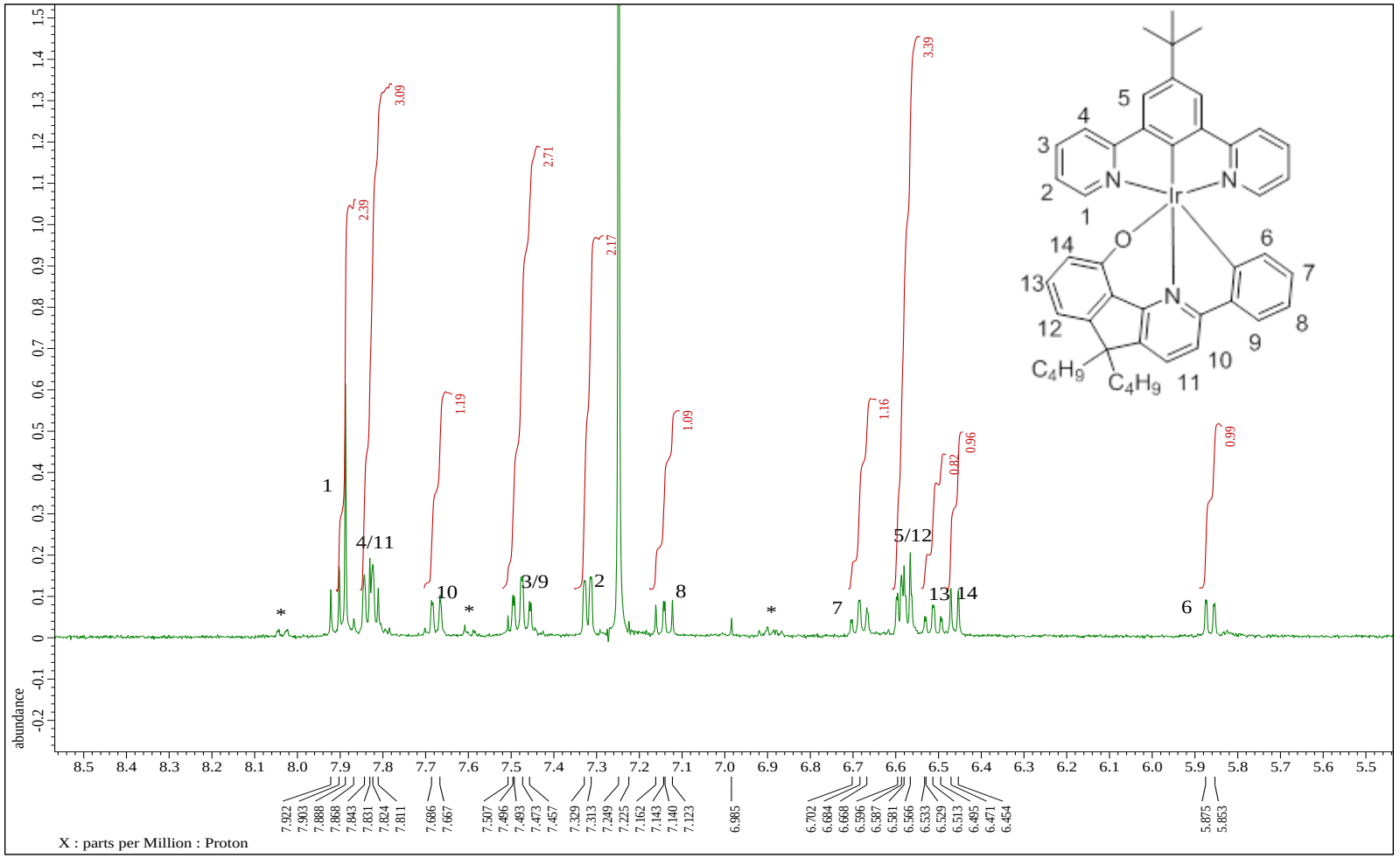

Figure 80- The aromatic region of the 1H NMR spectra for **3.2.17** (in $CDCl_3$). The residual impurities are indicated (*). The structure of the complex is overlaid. The peaks of the aliphatic chains are not shown above.

3.3. Photophysical Properties of the Mono-nuclear Metal Complexes

The compounds synthesised as a series of phenolic O^N^C complexes and the photophysical properties were tested by Merck KGaA. As no previous publications have studied or described photophysical data of phenolic type O^N^C complexes, there were no current literature trends for comparison. As a result, the synthesis of **3.1.4** and the documentation of picolinate based complexes provided a point of comparison. The photophysical properties of the described complexes are described in Table 8.

Table 8 - The photophysical properties of the di-anionic complexes described in this chapter, the emission wavelength (λ_{max}), photoluminescent quantum efficiency (PLQE) and triplet state decay time (µs) are described. The samples are arranged in the order of synthesis from earliest to latest.

Complex	**λ_{max} (Toluene) [nm]**	**PL-QE (Toluene)**	**T1-decay time [µs]**
3.1.4	542	0.04	0.16
3.2.15	558	0.16	0.48
3.2.16	564	0.16	0.56
3.2.17	539	0.19	0.48

In comparison to the picolinate based complex **3.1.4**, the phenolate coordinating complexes, **3.2.15**, **3.2.16** and **3.2.17** showed an instant improvement in quantum yield and triplet state decay time. The initial complex synthesised, **3.2.15**, utilised additional solubilising groups (butoxyl chains and a tertbutyl-phenyl group). The peak emission of **3.2.15** was red shifted (~16nm) to λ_{max} 558nm in comparison to **3.1.4**, possibly due to the electron-donating nature of the phenolate unit. The most interesting result was a significant increase in quantum yield when comparing **3.1.4** and **3.2.15**, ϕ= 0.04 and ϕ= 0.16 respectively. The triplet state decay time also tripled upon the change in coordination mode to phenolate. This indicated a significant decrease in the non-radiative decay when compared to **3.1.4**, which would likely release energy through vibrations.[13] This highlights that the presence of the mono-phenolic

coordination is particularly beneficial to the luminescent properties, rather than the carboxylate group of **3.1.4**.

As the presence of alkoxy groups in OLED devices is not preferable due to their detrimental impact on device efficiency. In **3.2.16**, the alkoxy chain was removed and the desired level of solubility was achieved by introducing *tert*-butyl groups. Such changes did not result in any change in the overall quantum yield of the complex in comparison to **3.2.15**, yet still maintaining a significant increase over **3.1.4**. The peak emission wavelength of the complex was red shifted in comparison to both **3.1.4** and **3.2.15**, by an order of ~22nm and ~6nm respectively. Whilst there was no change in the PLQY of the complex compared to **3.2.15**, the luminescence lifetime increased slightly, which indicates a slight increase in the rate of radiative decay (or decrease in the k_{nr}) in relation to **3.2.15** and **3.1.4**.

The O^N^C ligand **3.2.11** was prepared using chemistry described by Che *et al*, in order to increase the quantum yield by providing a more rigid structure.[150]. The resulting complex, **3.2.17** was tested and showed similar properties to the predecessors **3.2.15** and **3.2.16**. The peak emission wavelength showed a slight blue shift to λ_{max}= 539nm in relation to the whole series. The PLQY was slightly increased and this can be attributed to the increase of rigidity and consequentially the stability of the structure through the incorporation of an alkyl bridge. Despite this, the PLQY is only increased by 0.03 (3%) when compared to **3.2.15**/**3.2.16**, the increase was still significantly higher than the picolinate complex, **3.1.4**. It should be mentioned that **3.2.17** does contain minor impurity that might reduce quantum yield. The impurity is likely to consist of another complex species such as a C^N species or unreacted auxiliary ligand. More accurate data will be obtained in due course after preparation of a pure sample of this compound.

3.4. The Preparation of Di-iridium (III) O^N^C Complexes

The promising photophysical properties displayed by the ONC monometallic metal complexes, resulted in the adaptation of these ligands for the synthesis of di-iridium systems using di-iridium dichloro-bridged intermediate, **2.2.14**. Unfortunately, all attempts to derive bimetallic systems using auxiliary ligands **3.2.6** and **3.2.11**, under conditions optimised for monometallic analogues were unsuccessful. When synthesising the di-iridium analogue for the ligand **3.2.6**, the traditional toluene and AgOTf conditions were employed, however despite the formation of luminescent material, registered under UV light, the complex could not be verified by proton NMR. Alterations to the conditions (duration, stoichiometry and temperature) did not affect the outcome of the reaction. In addition, the reaction time was both increased and decreased. The equivalence (dimer: ligand) was altered slightly from 1:2 to 1:2.5 however these changes did not result in any product. The first attempt of the reaction was not successful, coordination under different conditions was attempted. The conditions tested, utilised 2-ethoxyethanol as a solvent and K_2CO_3 as a base. However these reaction conditions did not yield product. The crude proton NMR of the di-iridium analogues, **3.4.1** and **3.4.3** are shown in Figure 81 and Figure 82 respectively.

Table 9 - The reaction conditions tested in the preparation of the di-iridium O^N^C complexes. The conditions used are outlined in bold.

Complex	**Dimer (mmol)**	**Silver triflate (mmol)**	**O^N^C (mmol)**	**Reaction Time (h)**	**Toluene (mL)**
3.4.1	0.049	**0.039**/0.192/0.215	0.098/**0.101**	6/12/**24**	25/**30**
3.4.2	0.049	0.215	0.120	**6**/12	25
3.4.3	0.049	0.108/**0.215**	**0.098**/0.101	12/**18**/24	25/**30**/40

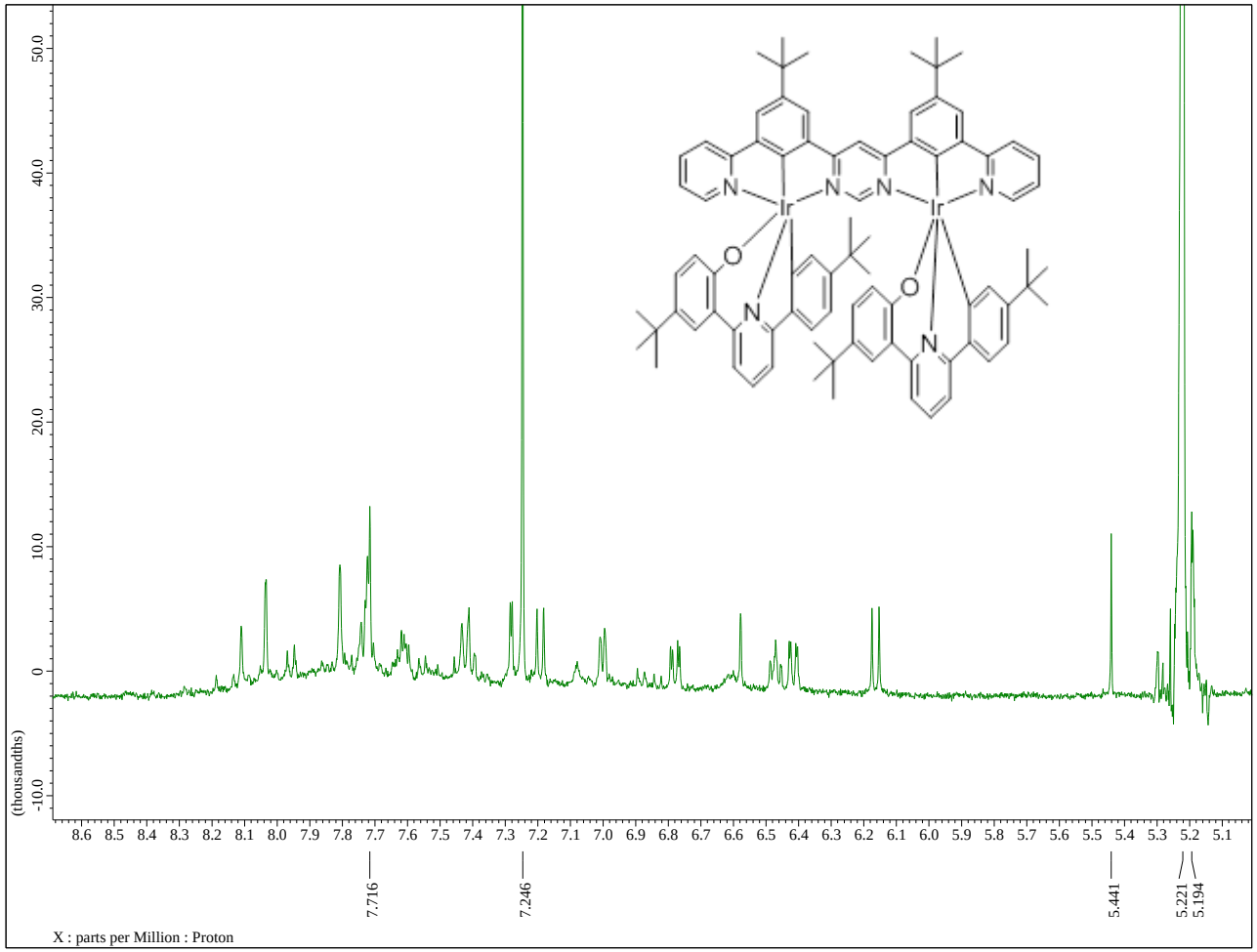

Figure 81 - The aromatic zoom of the proton NMR of **3.4.1**, the di-iridium analogue of **3.2.16**. The NMR highlights the promising presence of aromatic peaks which suggest the presence of product, however this is not conclusive and cannot be considered reliable evidence.

The formation of the di-iridium analogue for **3.2.17** was attempted using the same methods however, the NMR proved to be inconclusive when identifying the product. Once again, different methods were attempted in the synthesis of the complex. Initially dissolving the di-iridium dimer in toluene and stirring with silver triflate, did not result in the formation of a complex. Conditions of the reaction were changed and adapted, with the dimer being stirred in the presence of silver triflate for longer, the reaction time and the temperature being increased. The changes to the conditions of the reaction did not yield a product, the majority of the resulting mixture was starting material, a mix of auxiliary ligand and dimer.

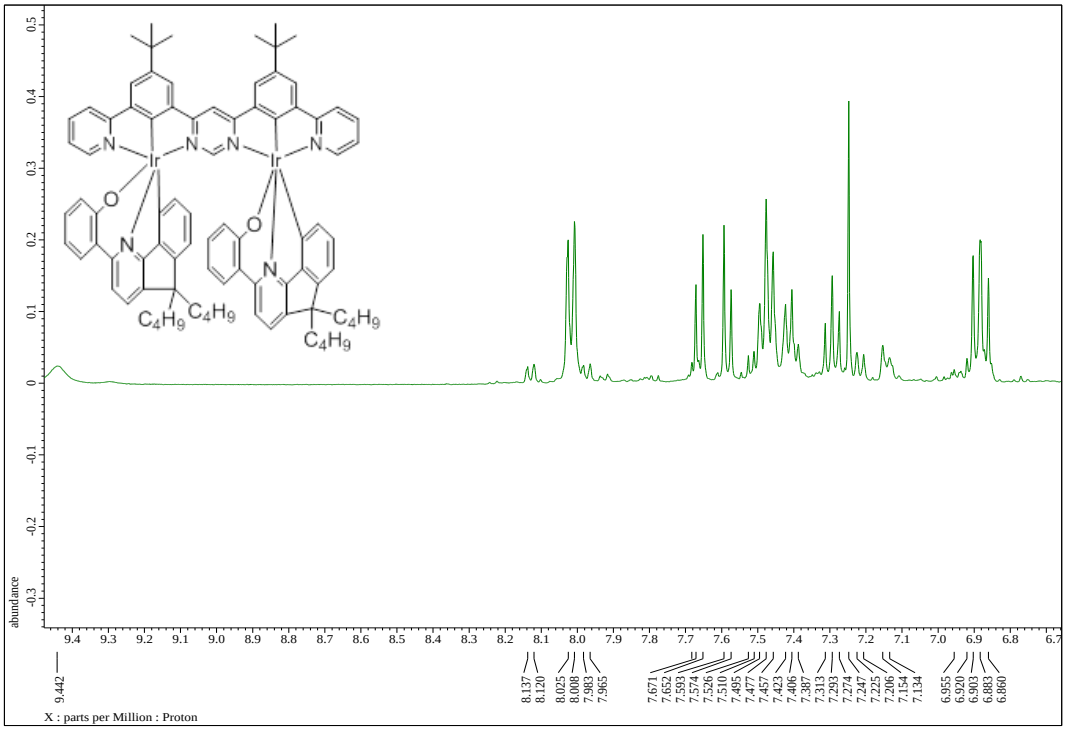

Figure 82 - The aromatic zoom of the ^{1}H NMR for **3.4.3**, the di-iridium analogue of **3.2.17**. This NMR spectrum shows distinct peaks which can be associated with the peaks of the auxiliary ligand. The peak at δ9.46ppm is often typical of the phenolic -OH group present on the uncoordinated auxiliary ligand.

It is very difficult to answer why bimetallic complexes do not form as readily as monometallic ones. This is potentially due to the sterical hindrances induced by the coordination angle of the auxiliary ligands.

3.5. Conclusions

The investigation into the use of phenolic coordination showed that the use of O^N^C ligands have increasing promise in mono-iridium complexes. Alterations and substitutions to the structures of the auxiliary ligands has very little effect on the photophysical properties of the final complex. It should be noted that, while mononuclear carboxylate systems (e.g. **3.1.4**) are known, the phenolate analogues are the first examples of their kind. The use of the O^N^C phenolate coordination showed PLQY of ϕ= 0.19, an almost 5-fold increase in comparison to the carboxylate O^N^C complex **3.1.4**, highlighting the benefit of utilising phenolate based ligands. The rigidifying of the phenolic O^N^C ligand did not lead to major changes in the photophysical properties, as shown by the series, PLQY values were in the range ϕ= 0.16-0.19, regardless of structural changes.

The most discouraging result, however, was that the adaptation of chemistry from mono-metallic to bi-metallic complexes did not work. Despite multiple attempts under different conditions, a pure sample of a bimetallic phenolate complex could not be isolated. Analysis of the ^{1}H NMR spectrum of crude samples suggested the formation of the bimetallic complexes. Further optimisation of ligands and reaction conditions will be carried out in due course.

3.6. Experimental

3.6.1. Di-anionic O^N^C Auxiliary Ligands

3.6.1.1. Synthesis of **3.1.2**

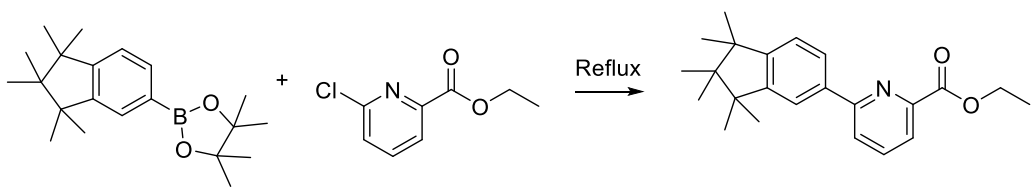

A solution of K_2CO_3 (1.66g, 12mmol, 2M) in water (6ml) was added to toluene (20ml) and ethanol (5ml) then degassed. 2-(1,1,2,2,3,3-hexamethyl-2,3-dihydro-1H-indan-5-yl)-4,4,5,5-tetramethyl-1,3,2-dioxaborolane (1.00g, 3.04mmol) and ethyl 6-chloropyridine-2-carboxylate

(0.56g, 3.04mmol) were added and the reaction was degassed further. $Pd(PPh_3)_4$ (0.10, 0.10mmol) was added and the mixture was heated under reflux for 66 hours. The phases were separated with brine (15ml) and extracted into ethyl acetate (3 x 10ml). The organic layer was dried over $MgSO_4$ and filtered. The solvent was removed under reduced pressure, forming a white solid. The solid was then purified by column chromatography (fine silica, Hexane/EtOAc, 3:1). The fractions containing product were evaporated *in vacuo* yielding in a white solid. (0.42g, 39%). ^1H NMR (400MHz, $CDCl_3$, ppm), δ 8.02 (dd, 1H, *J*= 8.0Hz, 2Hz), 7.89 (s, 1H), 7.87 (s, 1H), 7.77 (s, 1H), 7.23 (d, *J*= 8Hz, 1H), 4.48 (q, 2H), 1.47 (t, 3H), 1.34 (s, 6H), 1.27 (s, 6H), 1.22 (s, 6H).

3.6.1.2. Synthesis of **3.1.3**

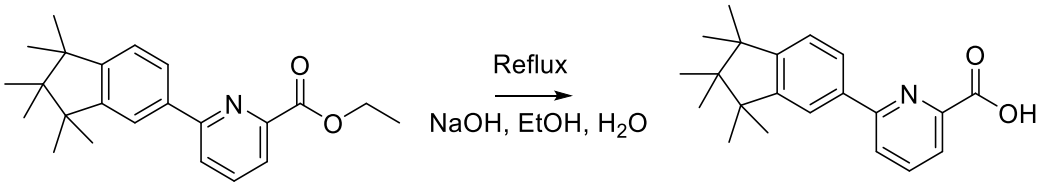

A mixture of ethyl 3-(1,1,2,2,3,3-hexamethyl-2,3-dihydro-1H-inden-5-yl)benzoate (0.32g, 0.91mmol), NaOH (2.32g, 58mmol) in ethanol (30ml) and water (10ml) was heated under reflux for 6 hours in an argon atmosphere. The solution was cooled to room temperature overnight and then acidified with dilute HCl (2M, ~20ml) to pH3. The solution was washed with water and filtered, yielding an off white solid. (0.243g, 83%). ^{1}H NMR (400MHz, DMSO-d6, ppm), δ 8.15 (d, *J*= 7.2Hz, 1H), 8.02 (t, *J*= 8Hz, 1H), 7.96 (s, 3H), 7.31 (d, *J*= 8Hz, 1H), 2.51 (s, 1H), 1.29 (s, 6H), 1.21 (s, 6H), 0.88 (s, 6H). HRMS (ESI) calculated for $C_{21}H_{25}NO_2$ ($[M+H]^+$)= 324.19581. Found m/z= 324.19543.

3.6.1.3. Synthesis of **3.2.2**

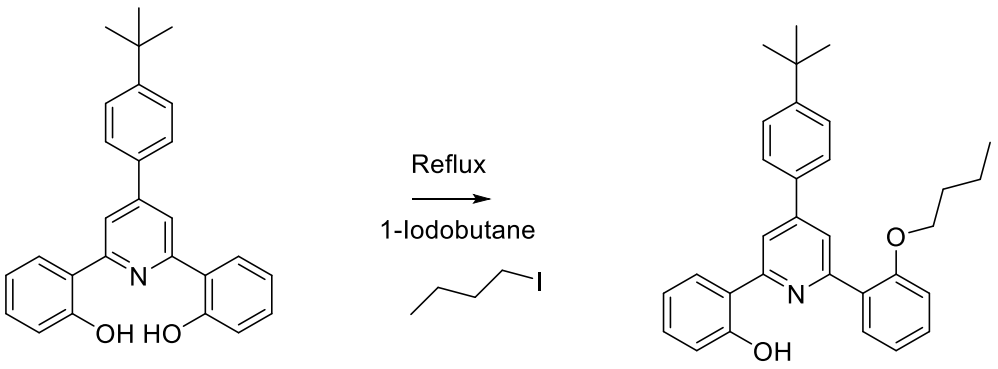

To solid diphenol, **3.2.1** (0.50g, 1.26mmol), DMF was added (20ml) and heated until dissolved. Potassium carbonate (0.75g, 5.4mmol) and 1-iodobutane (0.14ml, 1.26mmol) were added and stirred at 100°C for 14hours. The resulting mixture was then purified by column chromatography (fine silica, PE/EtOAc, 5:1) and the product was obtained. A second chromatographic column was required to remove impurities. Following the second column the fractions were collected and evaporated under reduced pressure. A white crystalline solid was obtained. Yield (0.276g, 24%). ^{1}H NMR (400MHz, $CDCl_3$, ppm), δ 8.12 (s, 1H), 8.03 (d,

J= 6.0Hz, 2H), 7.93 (d, *J*= 6.9Hz, 1H), 7.81 (d, *J*= 7.6Hz, 1H), 7.67 (d, *J*= 8.0Hz, 2H), 7.54 (d, *J*= 8.8Hz, 2H), 7.40 (t, *J*= 7.6Hz, 1H), 7.31 (t, *J*= 7.6Hz, 1H), 7.10 (t, *J*= 7.4Hz, 1H), 7.02 (m, 2H), 6.94 (t, *J*= 7.6Hz, 1H), 4.07 (t, *J*= 6.4Hz, 2H), 1.80 (quin, *J*= 7.0Hz, 2H), 1.55 (s, 1H), 1.43 (m, 2H), 0.88 (t, *J*= 7.4Hz, 3H).

3.6.1.4. Synthesis of **3.2.5**

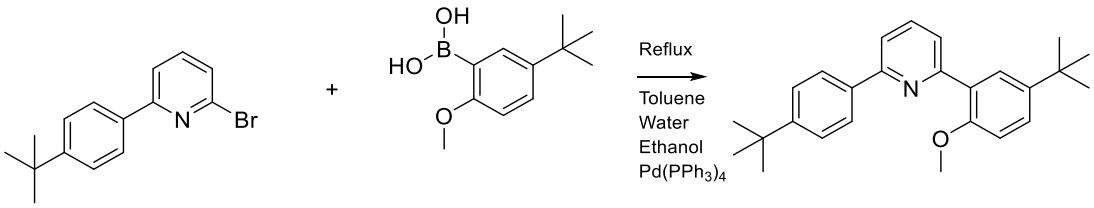

A solution of K_2CO_3 (1.75g, 12.66mmol) in water (10ml) was added to a flask and degassed, whilst being stirred under an Argon atmosphere. Toluene (20ml) and ethanol (10ml) were added and the mixture was degassed for a further 5 minutes. **3.2.3** (0.63g, 2.18mmol) and 5-tertbutyl-2-methoxyphenylboronic acid (0.50g, 2.39mmol) was added and the mixture was degassed for a further 15minutes. The catalyst, $Pd(PPh_3)_4$ (0.18g, 0.176mmol) was added and the reaction was heated under reflux for 18hours. The reaction mixture was separated using brine (15ml) and extracted into EtOAc (3 x 10ml). The organic layers were collected and dried over $MgSO_4$. The resulting solution was filtered and solvent was removed under reduced pressure. The resulting solid was purified by column chromatography (fine silica, petroleum ether/EtOAc, 10:1). The solvent was removed under reduced pressure to give a white crystalline solid. Yield (0.67g, 52%). ^{1}H NMR (400MHz, $CDCl_3$, ppm), δ 8.20 (m, 3H), 7.79 (m, 2H), 7.72 (d, *J*= 6.9Hz, 1H), 7.61 (d, *J*= 7.8Hz, 2H), 7.48 (d, *J*= 5.5Hz, 2H), 6.93 (d, *J*= 8.7Hz, 1H), 3.85 (s, 3H), 2.16 (s, 9H), 1.36 (s, 9H).

3.6.1.5. Synthesis of **3.2.6**

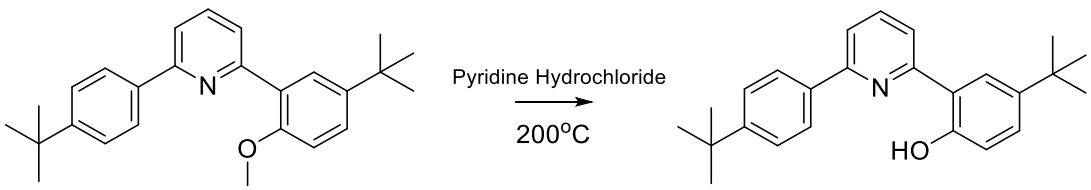

A sample of 2-(5-tert-butyl-2-methoxyphenyl)-6-(4-tert-butylphenyl)pyridine (0.249g, 0.692mmol) was added to a flask with excess pyridine hydrochloride (2.0g, 17.3mmol). The flask was heated to 200°C and stirred for 2 hours. Upon the removal of heat, water (20ml) was added, forming a white precipitate. The solid was filtered and washed with water to give a white solid. Yield (0.204g, 85%). ^{1}H NMR (400MHz, $CDCl_3$, ppm), δ 7.88 (m, 6H), 7.63 (dd, *J*= 7.3, 1.4 Hz, 1H), 7.54 (d, *J*= 6.4 Hz, 2H), 7.39 (d, *J*= 8.7Hz, 1H), 7.01 (d, *J*=8.7 Hz, 1H), 1.36 (s, 18H). ^{13}C NMR (100MHz, $CDCl_3$), δ 158.1, 157.8, 154.8, 152.9, 141.3, 138.6, 135.8, 129.0, 126.7, 126.1, 122.8, 118.4, 118.0, 117.2, 34.9, 34.3, 31.7, 31.3.

3.6.1.6. Synthesis of **3.2.8**

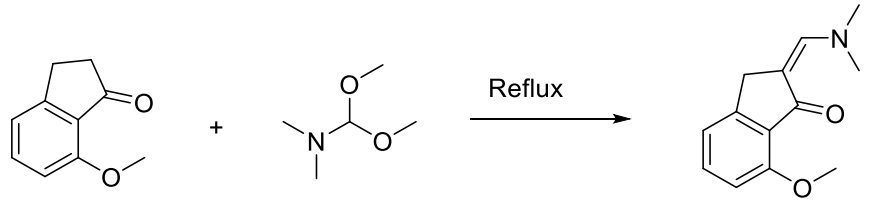

7-methoxy-2,3-dihydro-1H-inden-1-one (5.00g, 30.83mmol) was added to a RBF with *n,n*-dimethylformamide dimethyl acetal (18.36g, 154.51mmol) and heated to reflux for 12 hours under argon atmosphere. Petroleum ether was added to the resulting solid and the crystals were then filtered and weighed. The product was then submitted for NMR. (6.26g, 93%). ^{1}H NMR (400MHz, $CDCl_3$, ppm), δ 7.39 (m, 2H), 6.98 (d, *J*= 8Hz, 1H), 6.78 (d, *J*= 8.4Hz, 1H), 6.78 (d, *J*=8Hz, 1H), 3.93 (s, 3H), 3.83 (s, 2H), 3.13 (s, 6H). ^{13}C NMR (100MHz, $CDCl_3$, ppm), δ 191.5, 159.0, 151.1, 146.2, 133.2, 128.2, 117.5, 109.1, 104.3, 55.8, 31.3.

3.6.1.7. Synthesis of **3.2.9**

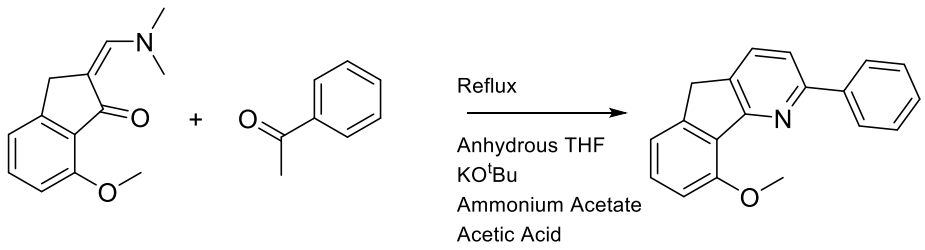

Anhydrous THF (100ml) was added to a dry RBF with KO^{t}Bu (1.86g, 16.56mmol) and stirred under an argon atmosphere. A sample of (2Z)-2-[(dimethylamino)methylidene]-7-methoxy-

2,3-dihydro-1H-inden-1-one (3.00g, 13.8mmol) was then added to the flask and stirred. 1-acetophenone (1.99g, 16.57mmol) was added to the mixture and stirred under argon atmosphere for a further 15minutes. Ammonium acetate (52.5g) in acetic acid (75ml) were added to the flask and the reaction was heated under reflux for 18hours. The reaction was separated using water and the product was extracted into dichloromethane (3 x 10ml). The organic layer was dried over $MgSO_4$ and filtered. The filtrate was evaporated to dryness under vacuum. The resulting residue was then purified through column chromatography (fine silica, Hexane/EtOAc, 5:1). The fractions were collected and the solvent was removed under reduced pressure to yield a brown solid. Yield (4.01g, 96%). ^{1}H NMR (400MHz, $CDCl_3$, ppm), δ 8.16 (d, *J*= 7.3Hz, 2H), 7.83 (d, *J*=8.2Hz, 1H), 7.63 (d, *J*= 8.2Hz, 1H), 7.48 (t, *J*= 7.6Hz, 2H), 7.38 (m, 2H), 7.19 (d, *J*= 7.8Hz, 1H), 6.97 (d, *J*= 8.2Hz, 1H), 4.11 (s, 3H), 3.90 (s, 2H).

3.6.1.8. Synthesis of **3.2.10**

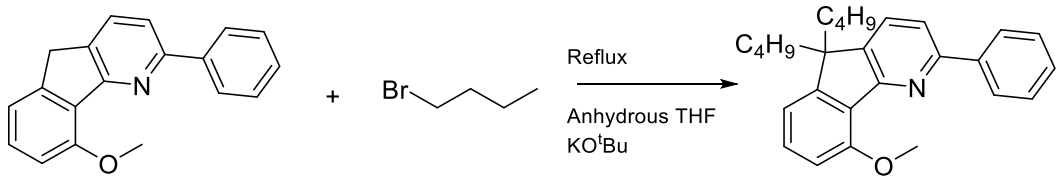

9-methoxy-2-phenyl-5H-indeno[1,2-b]pyridine (2.00g, 7.32mmol) was added to a dry flask flushed with argon. Anhydrous THF (100ml) was added and the reaction was stirred. 1-bromobutane (3.18ml, 18.2mmol) was added to the flask. KO^{t}Bu (2.05g, 18.3mmol) was added to the reaction mixture which was then heated under reflux for 18hours. The reaction was then cooled to room temperature and water was added. The product was then extracted into DCM (3 x 15mL). The organic phase was collected and dried over $MgSO_4$ and the solvent removed under reduced pressure. The resulting brown residue was purified by column chromatography (fine silica, Hexane/EtOAc, 10:1). The desired product was obtained as a brown solid. Yield (1.25g, 44%). ^{1}H NMR (400MHz, $CDCl_3$, ppm), δ 8.18 (d, *J*= 8.2Hz, 1H), 7.64 (s, 1H), 7.47 (t, *J*= 7.6Hz, 2H), 7.38 (t, *J*= 8Hz, 2H), 6.99 (d, *J*= 7.3Hz, 1H), 6.91 (d, *J*= 8.2Hz, 1H), 4.10 (s, 3H), 2.00-1.94 (m, 4H), 1.04 (sex, *J*=7.6Hz, 4H), 0.89-0.79 (m, 4H), 0.637 (t, *J*=7.6Hz, 6H).

3.6.1.9. Synthesis of **3.2.11**

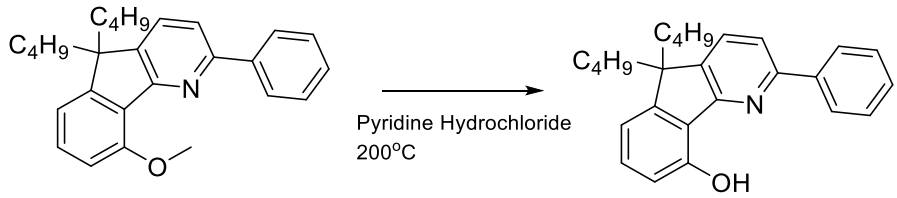

A sample of 5, 5-dibutyl-9-methoxy-2-phenyl-5H-indeno[1,2-b]pyridine (1.00g, 2.59mmol) was added to a flask with excess pyridine hydrochloride (6.0g, 51.9mmol). The flask was then heated to 200°C and stirred for 2 hours. Upon the removal of heat, water (20ml) was added, forming a red precipitate. The precipitate was filtered and washed with water to give a red crystalline solid. Yield (0.640g, 66%). ^{1}H NMR (400MHz, $CDCl_3$, ppm), δ 8.03 (d, *J*= 7.3Hz, 2H), 7.67 (d, *J*= 7.8Hz, 1H), 7.59 (d, *J*= 7.3Hz, 1H), 7.49 (t, *J*= 7.6Hz, 2H), 7.43 (t, *J*=6.9Hz, 1H), 7.31 (t, *J*= 7.8Hz, 1H), 6.90 (t, *J*=8.2Hz, 1H), 2.16 (s, 1H), 2.00-1.94 (m, 4H), 1.09 (sex, *J*=7.6Hz, 4H), 0.75-0.62 (m, 10H). HRMS (ESI) calculated for $C_{26}H_{29}NO$ ($[M+H]^+$)= 372.23219. Found m/z= 372.23129

3.6.1.10. Synthesis of **3.2.13**.[184]

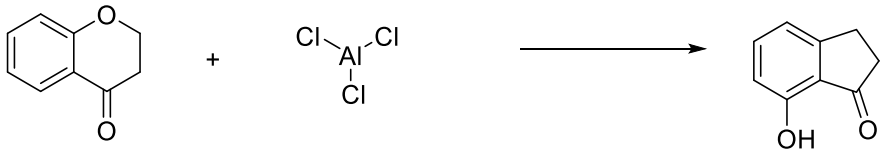

A round bottom flask was loaded with 4-chromanone (5.00g, 37.8 mmol) and anhydrous $AlCl_3$ (10.00g, 97.5 mmol) and was heated at 180 °C for 20 min and then at 200 °C for 30 min. The reaction mixture was cooled down to room temperature and 12M HCl was added. The resulting melt was dissolved in dichloromethane and water. The organic layers were separated and dried over $MgSO_4$. The reaction mixture was purified by column chromatography (fine silica, dichloromethane/EtOAc, 20:1), solvent was removed under reduced pressure and the resulting residue was triturated with diethyl ether. Yield (2.12g, 38%). ^{1}H NMR (400MHz, $CDCl_3$, ppm), δ 9.06 (s, 1H), 7.47 (t, *J* = 8.0Hz, 1H), 6.94 (d, *J* = 7.2Hz, 1H), 6.76 (d, *J* = 8.0Hz, 1H), 3.18–3.05 (m, 2H), 2.77–2.65 (m, 2H). ^{1}H NMR is same as literature values.

3.6.1.11. Synthesis of **3.2.14**.[185]

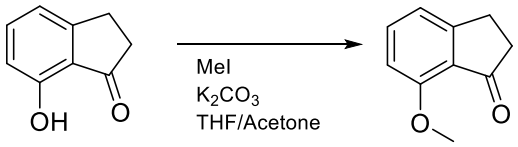

A sample of **3.2.13** (1.00g, 6.82mmol) was added to a flask of K_2CO_3 (1.86g, 13.6mmol) in acetone (50ml) and THF (30ml), the mixture was stirred and heated gradually. Iodomethane (1.16g/ 0.51ml, 8.18mmol) was added and the reaction was heated under reflux for 18 hours. Dichloromethane (50ml) and brine (50ml) were added to the reaction, separating layers. The organic layers were collected and dried over $MgSO_4$. Solvent was removed under reduced pressure and the resulting crystals were triturated with diethyl ether and filtered. Yield (0.88g, 79%). ^{1}H NMR (400MHz, $CDCl_3$, ppm), δ 7.51 (t, *J*= 8Hz, 1H), 7.01 (d, *J*= 7.6Hz, 1H), 6.76 (d, *J*= 8.4Hz, 1H), 3.93 (s, 3H), 3.06-3.04 (m, 2H), 2.67-2.65 (m, 2H).

^{1}H NMR is same as literature values.

3.6.2. Di-anionic O^N^C Complexes

3.6.2.1. Synthesis of **3.1.4** (method A).

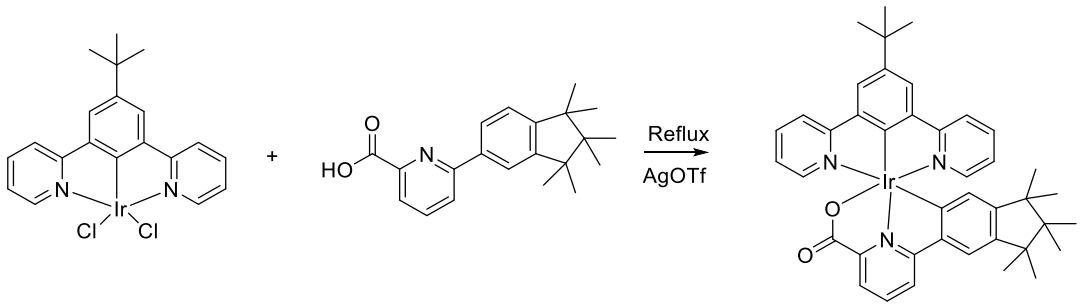

2.2.13 (0.10g, 0.181mmol) and 3-(1,1,2,2,3,3-hexamethyl-2,3-dihydro-1H-inden-5-yl)benzoic acid (0.07g, 0.212mmol) were added to toluene (30ml) and stirred. Silver triflate (0.10g, 0.398mmol) was added and the reaction was heated under reflux for 12 hours. The resulting solution was filtered through celite and the yellow filtrate was purified by column chromatography (fine silica, DCM/EtOAc/MeOH, 5:1:1). The product was collected and solvent removed under reduced pressure. The resulting orange solid was washed with diethyl ether and filtered. Yield (0.108g, 74%). ^{1}H NMR (400MHz, $CDCl_3$, ppm), δ 8.16 (d, *J*= 7.2Hz,

1H), 8.10 (d, *J*= 8Hz, 1H), 8.01 (t, *J*= 7.6Hz, 1H), 7.93 (s, 2H), 7.88 (d, *J*= 8.4Hz, 2H), 7.59 (t, *J*= 7.6Hz, 2H), 7.36 (d, *J*= 5.2Hz, 2H), 7.31 (s, 1H), 6.79 (t, *J*= 6.4Hz, 2H), 5.2 (s, 1H), 1.52 (s, 9H), 1.04 (s, 6H), 0.66 (s, 6H), 0.61 (s, 6H). HRMS (ESI) calculated for $C_{41}H_{42}IrN_3O_2$ ($[M+H]^+$)= 802.29790. Found m/z= 802.29785

3.6.2.2. Synthesis of **3.1.4** (method B).[177]

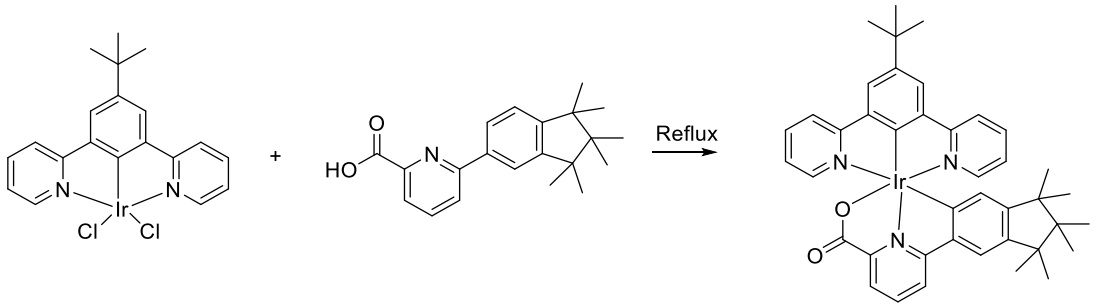

Potassium carbonate (0.175g, 1.267mmol) was added to warm 2-ethoxyethanol (30ml) and stirred. **2.2.13** (0.05g, 0.091mmol) was added to the solution with **3.1.3** (0.035g, 0.1089mmol) and the reaction was heated under reflux for 18hours. Water was added, forming a yellow precipitate. The solid was filtered and purified by column chromatography (fine silica, DCM/EA/MeOH, 5:1:1). The product was collected and solvent was removed under reduced pressure, resulting in an orange solid. Yield (0.03g, 41%). ^{1}H NMR (400MHz, $CDCl_3$, ppm), δ 8.16 (d, *J*= 7.2Hz, 1H), 8.10 (d, *J*= 8Hz, 1H), 8.01 (t, *J*= 7.6Hz, 1H), 7.93 (s, 2H), 7.88 (d, *J*= 8.4Hz, 2H), 7.59 (t, *J*= 7.6Hz, 2H), 7.36 (d, *J*= 5.2Hz, 2H), 7.31 (s, 1H), 6.79 (t, *J*= 6.4Hz, 2H), 5.2 (s, 1H), 1.52 (s, 9H), 1.04 (s, 6H), 0.66 (s, 6H), 0.61 (s, 6H).

3.6.2.3. Synthesis of **3.2.15**

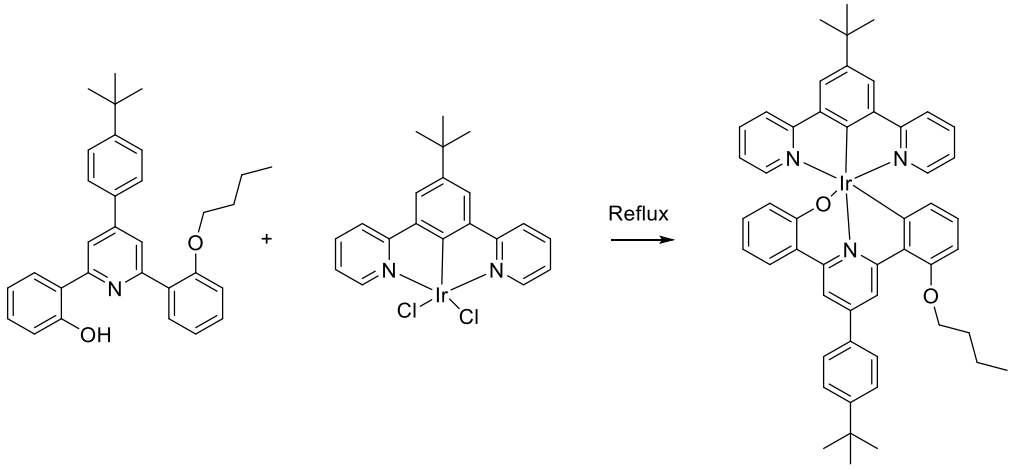

A mixture of **3.2.2** (0.145g, 0.321mmol) and **2.2.13** (0.147g, 0.267mmol) were added to toluene (30ml) and stirred. Silver triflate (4ml, 0.1M, 0.4mmol) was added and the reaction was heated under reflux for 18 hours. Solvent was removed and the resulting solid was purified by column chromatography (fine silica, DCM/EtOAc, 5:1). Solvent was removed under reduced pressure, the resulting solid was triturated with petroleum ether. Yield (0.075g, 30%). ^{1}H NMR (400MHz, $CDCl_3$, ppm), δ 9.23 (s, 1H), 8.24 (s, 1H), 7.92 (d, *J*=8.2Hz, 2H), 7.86 (s, 1H), 7.83 (d, *J*=7.3Hz, 1H), 7.63 (d, *J*=8.2Hz, 2H), 7.48 (t, *J*= 6.8Hz, 2H), 7.32 (d, *J*= 5.5Hz, 1H), 6.94 (t, *J*= 7.4Hz, 1H), 6.62 (t, *J*=6.4Hz, 2H), 6.57-6.41 (m, 3H), 6.26 (d, *J*=8.2Hz, 1H), 5.52 (d, *J*=7.3Hz, 1H), 4.03 (t, *J*= 6.0Hz, 2H), 1.67 (quin, *J*=7.6Hz, 2H), 1.54 (s, 9H), 1.44 (s, 9H), 1.05 (t, *J*=7.2Hz, 3H), 0.88 (m, 2H). HRMS (ESI) calculated for $C_{51}H_{50}IrN_3O_2$ = 930.36050. Found m/z= 930.36090.

3.6.2.4. Synthesis of **3.2.16**

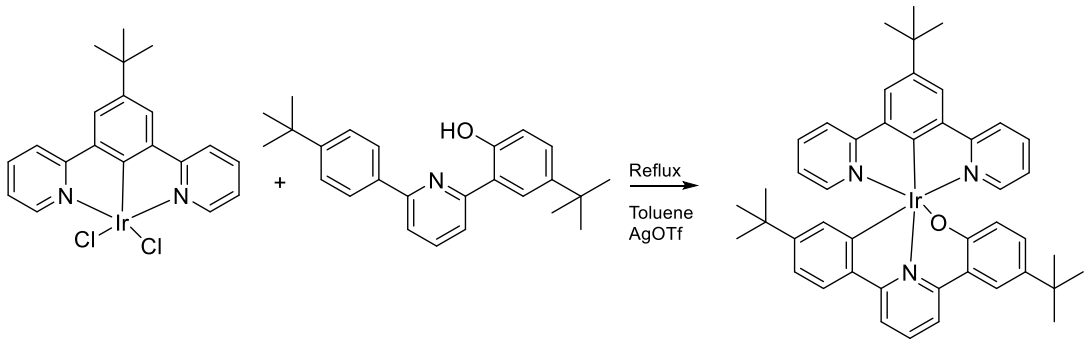

A mixture of **2.2.13** (0.10g, 0.183mmol) and **3.2.6** (0.070g, 0.201mmol) were added to toluene (30ml) and stirred. Silver triflate (2ml, 0.1M, 0.2mmol) in toluene was added and the reaction was heated under reflux for 18 hours. Solvent was removed under reduced pressure and the resulting residue was purified by column chromatography (fine silica, DCM/EtOAc, 5:1). The solvent was removed and the solid was triturated with petroleum ether and filtered. Yield (0.05g, 32%). ^{1}H NMR (400MHz, $CDCl_3$, ppm), δ 7.88 (m, 6H), 7.63 (dd, 1H, *J*= 7.3, 1.4 Hz), 7.54 (d, 2H, *J*= 6.4 Hz), 7.39 (d, 1H, *J*= 8.7, 2.3 Hz), 7.01 (d, 1H, *J*=8.7 Hz), 1.36 (s, 18H).

3.6.2.5. Synthesis of **3.2.17**

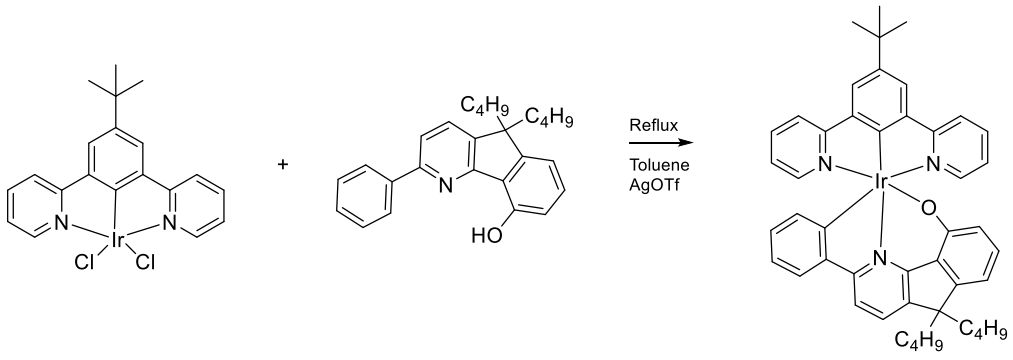

2.2.13 (0.10g, 0.181mmol) was added to toluene (30ml) and stirred. Silver triflate (0.098g, 0.380mmol) was added and the mixture was stirred further. The ligand, 5,5-dibutyl-2-phenyl-5H-indeno[1,2-b]pyridin-9-ol (0.081g, 0.217mmol) was added and the reaction was heated under reflux for 18 hours. The mixture was filtered through celite and the resulting yellow solution was evaporated to dryness under reduced pressure. The resulting orange residue was purified by column chromatography (fine silica, DCM/EtOAc, 10:1). The solvent was removed under reduced pressure. The resulting orange solid was filtered. Yield (0.055g, 33%). ^{1}H NMR (400MHz, $CDCl_3$, ppm), δ 7.88 (s, 3H), 7.82 (t, *J*= 6.4Hz, 3H), 7.67 (d, *J*= 7.8Hz, 1H), 7.47 (ddd, *J*= 7.4, 1.4Hz, 2H), 7.32 (d, *J*= 6.4Hz, 2H), 7.14 (t, *J*= 7.7Hz, 1H), 6.68 (t, *J*= 6.9Hz, 1H), 6.58 (m, 2H), 6.51 (ddd, *J*= 7.2, 1.4Hz, 1H), 6.47 (d, *J*= 6.9Hz, 2H), 5.86 (dd, *J*= 8.7, 1.2Hz, 1H), 2.16-2.038 (m, 4H), 1.54 (s, 9H), 1.19 (q, *J*= 7.4Hz, 4H), 0.87-0.84 (m, 4H), 0.76 (t, *J*= 7.3Hz, 6H). ^{13}C NMR (100MHz, $CDCl_3$, ppm), δ 170.9, 153.6, 151.0, 145.2, 143.8, 142.1, 141.0, 137.5, 135.9, 132.4, 128.0, 127.2, 125.6, 123.1, 122.0, 120.8, 119.7, 113.6, 106.1, 54.5, 40.3, 35.4, 32.2, 26.4, 23.7, 14.3. HRMS (ESI): calculated for $C_{46}H_{46}IrN_3O$ ($[M+H]^+$)= 850.33429. Found m/z= 850.33276.

3.6.2.6. Attempted preparation of **3.4.1**

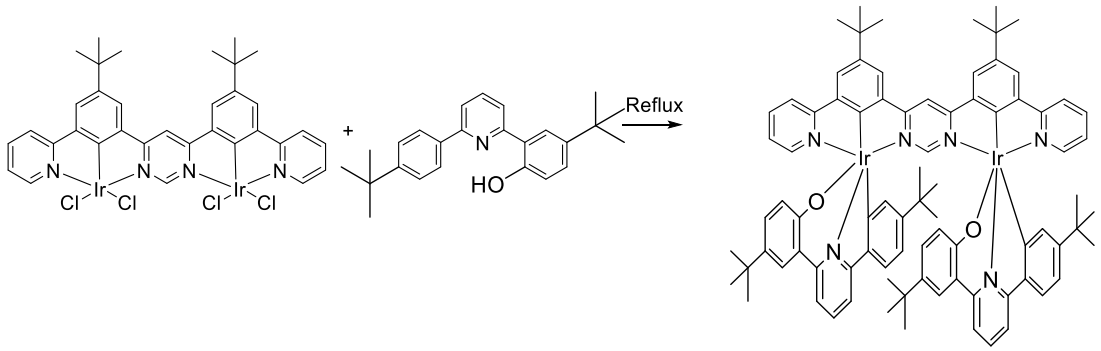

A sample of **2.2.14** (0.05g, 0.048mmol) and **3.2.6** (0.035g, 0.101mmol) were added to toluene (30ml) and stirred before the addition of AgOTf (0.01g, 0.039mmol) and the mixture was put on reflux for 24 hours. The resulting solution was then filtered through celite and purified by column chromatography (SiO_2, DCM/EA, 5:1). Relevant fractions were then submitted for NMR. ^{*1}H NMR unsuccessful due to inseparable mixture of isomers.

3.6.2.7. Attempted preparation of **3.4.2**

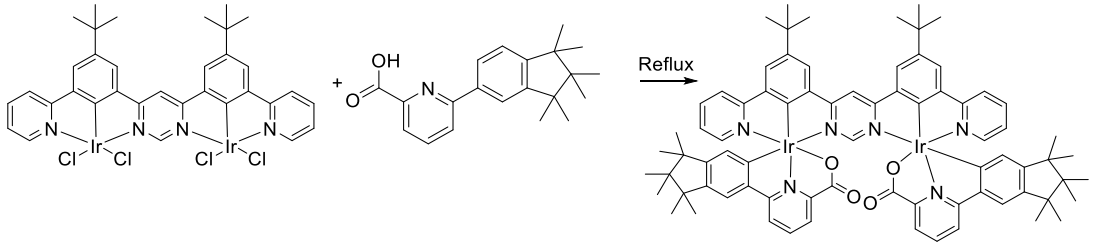

A mixture of **2.2.14** (0.05g, 0.049mmol), 3-(1, 1, 2, 2, 3, 3-hexamethyl-2, 3-dihydro-1H-inden-5-yl)benzoic acid (0.038g, 0.12mmol), silver triflate (0.0553g, 0.215mmol) and Toluene (25ml). The mixture was placed on reflux for 6 hours, resulting in a red precipitate. This was filtered through celite and the solvent was removed under reduced pressure. The resulting solid was purified using column chromatography (SiO_2, DCM/EA/MeOH, 10:2:1). The fractions containing product were evaporated using a rotary evaporator and the resulting solid **3.4.2** (0.0285, 38%). *Inseparable mixture of isomers and therefore an accurate NMR could not be obtained.

3.6.2.8. Attempted preparation of **3.4.3**

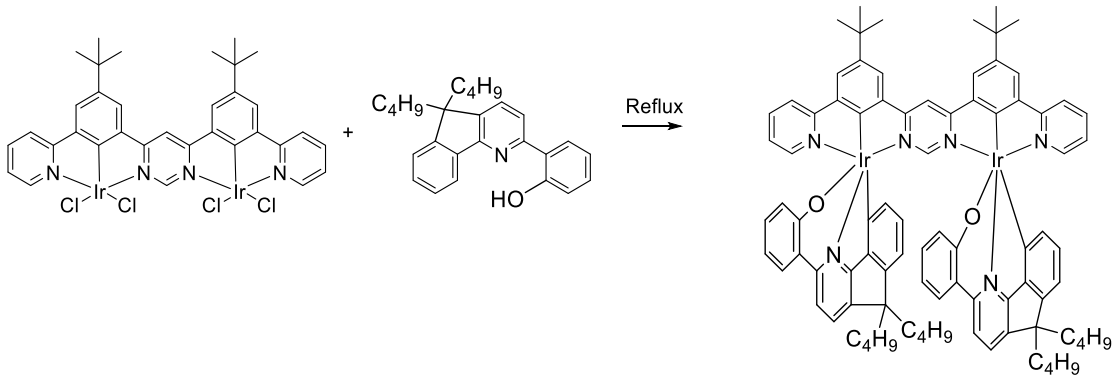

2.2.14 (0.05g, 0.049mmol) was added to toluene (30ml) and stirred with **3.2.11** (0.036g, 0.098mmol). Silver triflate (0.055g, 0.215mmol) was added and the reaction was heated under reflux for 18hours. The resulting orange solution was filtered through celite and the solvent was removed under reduced pressure. The orange solid was purified by column chromatography (fine silica, DCM/EtOAc, 5:1). The solvent was removed from the fractions under reduced pressure to give a brown solid. NMR showed an inseparable mixture of starting materials.

CHAPTER 4

The Use of Symmetrical Di-anionic Auxiliary Ligands in Iridium (III) Complexes

4. Symmetrical Di-anionic Auxiliary Ligands in Ir(III) Complexes

This chapter will describe a series of mono-iridium and di-iridium complexes that incorporate symmetrical di-anionic auxiliary ligands.

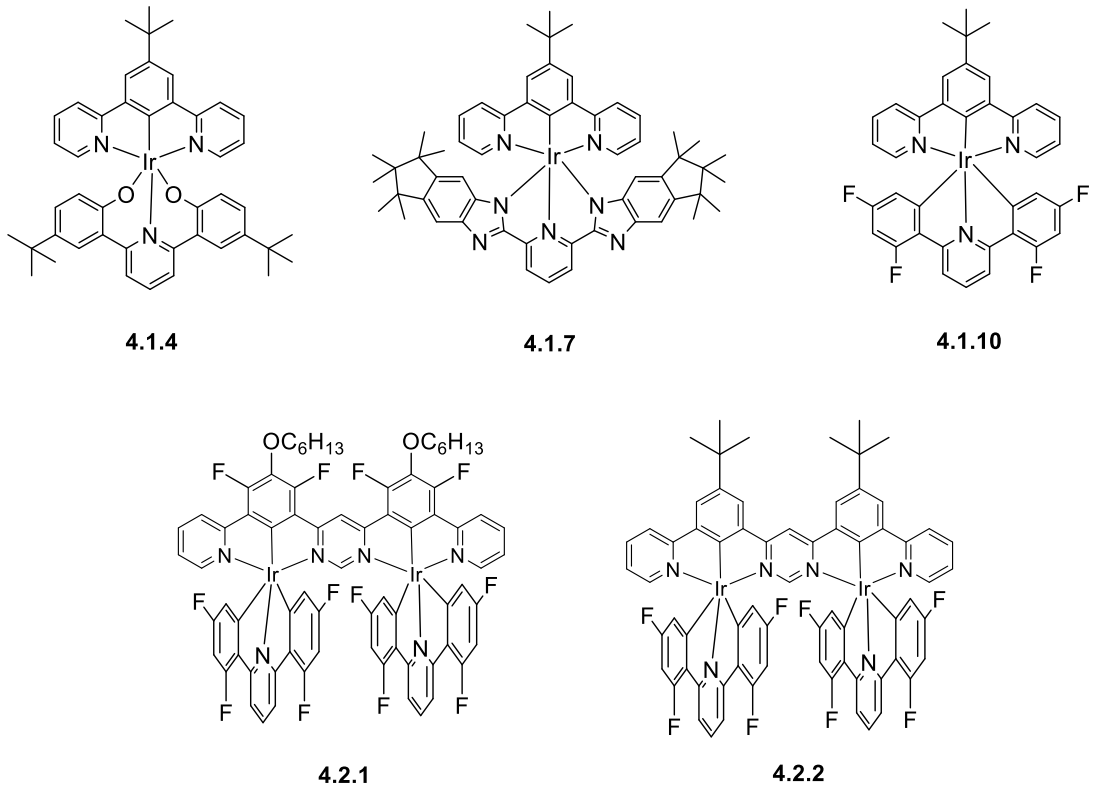

Figure 83 - The series of mono-iridium and di-iridium complexes developed using symmetrical dianionic auxiliary ligands.

As described previously, the use of symmetrical ligands is more beneficial when compared to the asymmetrical equivalents. The development of symmetrical structures prevents the formation of diastereomers and leads to the formation of a single isomer when preparing a di-nuclear complex.

Mononuclear complexes that utilise C^N^C cyclometalating ligands were described by Williams *et al*.[12-13] Complexes of this type show promising luminescent properties (ϕ_{lum}= 0.41) however the yields of the synthetic methods were low (~15-20%).[12-13]

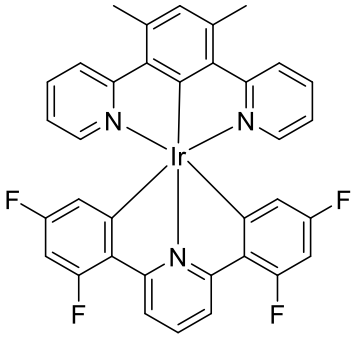

4.0.1
Wilkinson *et al*, 2006
ϕ_{lum}= 0.41

Figure 84 - The structure of the C^N^C complex described by Wilkinson *et al* which showed a quantum efficiency of ϕ= 0.41.

The difficult cyclometalation of the ligand to the central metal ion arises from the strong trans effect induced by the cyclometalating carbon atoms on the auxiliary ligand. This effect can result in the bond being unable to form. This results in a consequential C^N coordination of the terdentate ligand.

4.1. Synthesis of Symmetrical Di-anionic Complexes

The benefits presented by symmetrical auxiliary ligands prompted the development of a library of auxiliary ligands and complexes. Three types (O^N^O, N^N^N and C^N^C) of di-anionic terdentate auxiliary ligands were investigated.

4.1.1. Synthesis of the Bis-phenolate O^N^O Ligand and Complex

Following the successful synthesis of O^N^C cyclometalating ligands, a literature search showed that there was distinct absence of ligands and complexes that utilised bis-phenolate coordination. The inclusion of two phenolate moieties would produce a significant red shift effect due to strong electron donating properties. Utilising 4-tert-butyl-2-[6-(4-tert-butylphenyl)pyridin-2-yl]phenol as a template for the new O^N^O ligand, the structure was altered to possess two units of 5-tertbutyl(2-methoxyphenyl) boronic acid. As the boronic acid is commercially available, the synthesis of the ligand required two steps to yield the final

auxiliary ligand. The boronic acid building block was added to 2,6-dibromopyridine in a Suzuki cross coupling to generate **4.1.2** in good yield (82%).

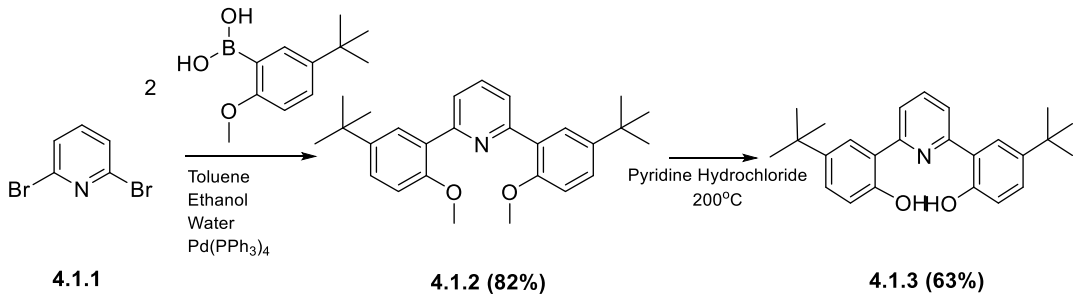

Figure 85 - The synthesis of **3.2.6** using Suzuki cross coupling and demethylation of methoxy functional groups.

The demethylation of the methyl ether groups was carried out by heating at 200°C in a melt of pyridinium chloride. The product crystallised upon the addition of water to the reaction mixture to give the product in high yields (63%). The ^{1}H NMR spectrum of **4.1.3** is shown in Figure 86 and is fully consistent with the structure.

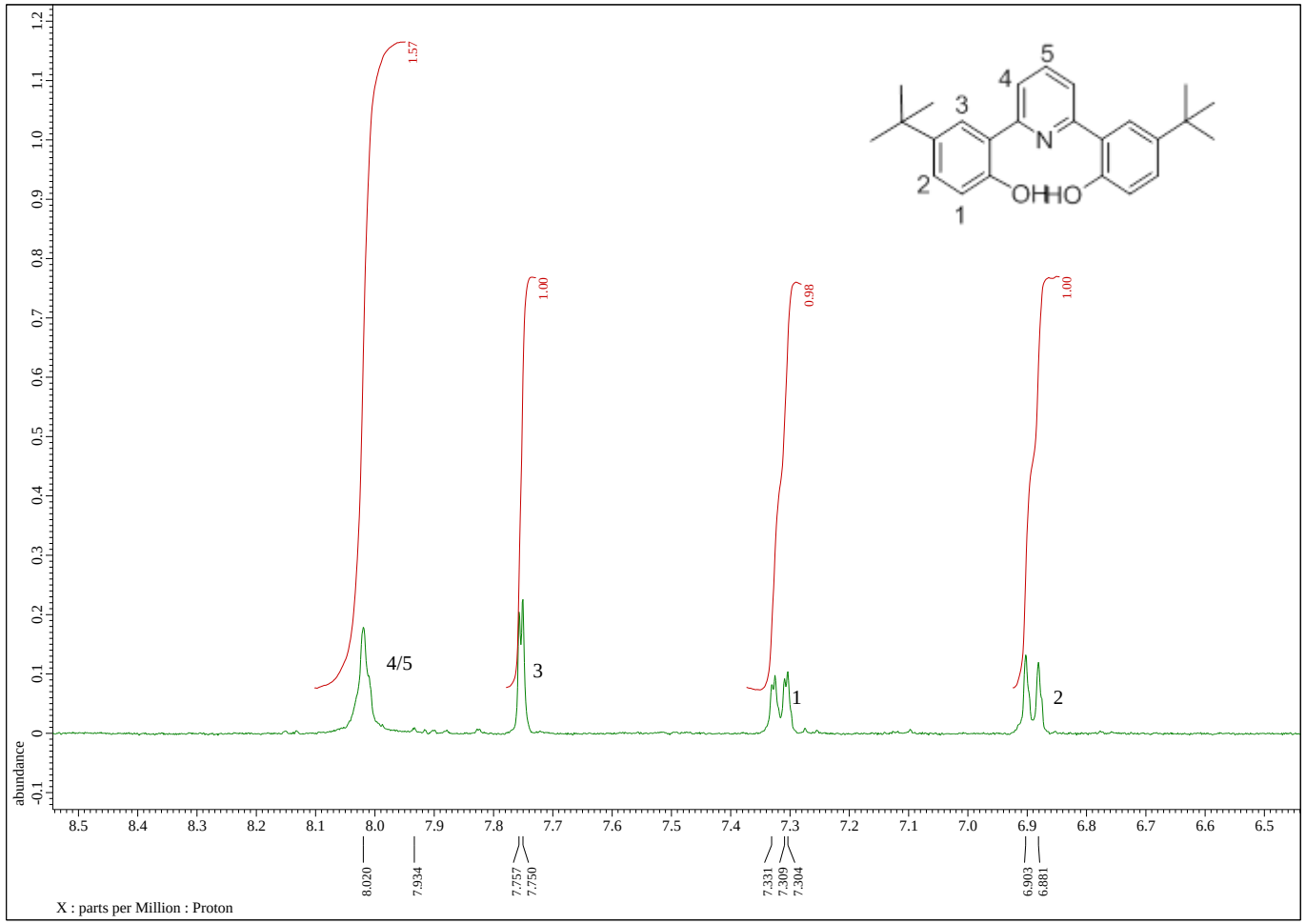

Figure 86- The aromatic region of the ^{1}H NMR spectrum of **4.1.3** in DMSO-d6. The numbered structure of the ligand is overlaid. The *tert*-butyl groups show a singlet at δ1.25ppm.

The synthesis of the O^N^O complex **4.1.4** was first carried out under conditions previously described. The dichlorobridged dimer, **2.2.13**, was added to toluene and heated with silver triflate prior to the addition of the auxiliary ligand. However this method did not yield sufficient amounts of product (~5% yield). The low yield prompted the use of alternative conditions. An equimolar mixture of the O^N^O ligand, **4.1.2**, and the dichlorobridged intermediate was heated under reflux in 2-ethoxyethanol with potassium carbonate. The crude product was precipitated by the addition of water and filtered. The product was purified by column chromatography (DCM/EtOAc/MeOH, 20:2:1). This procedure gave the complex in a yield of 47%.

This indicates that deprotonation of the phenolic groups is required prior to complexation with the central iridium ion.

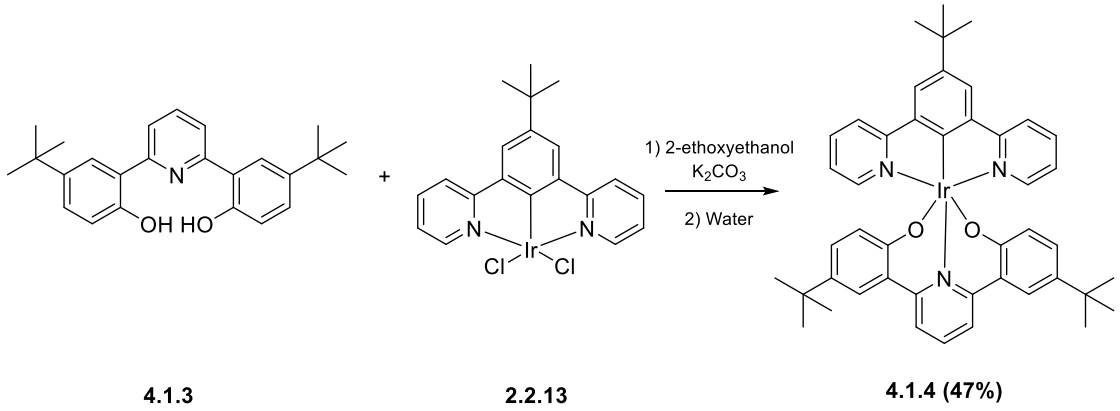

4.1.3 **2.2.13** **4.1.4 (47%)**

Figure 87 - The synthetic procedure used to prepare **4.1.4**.

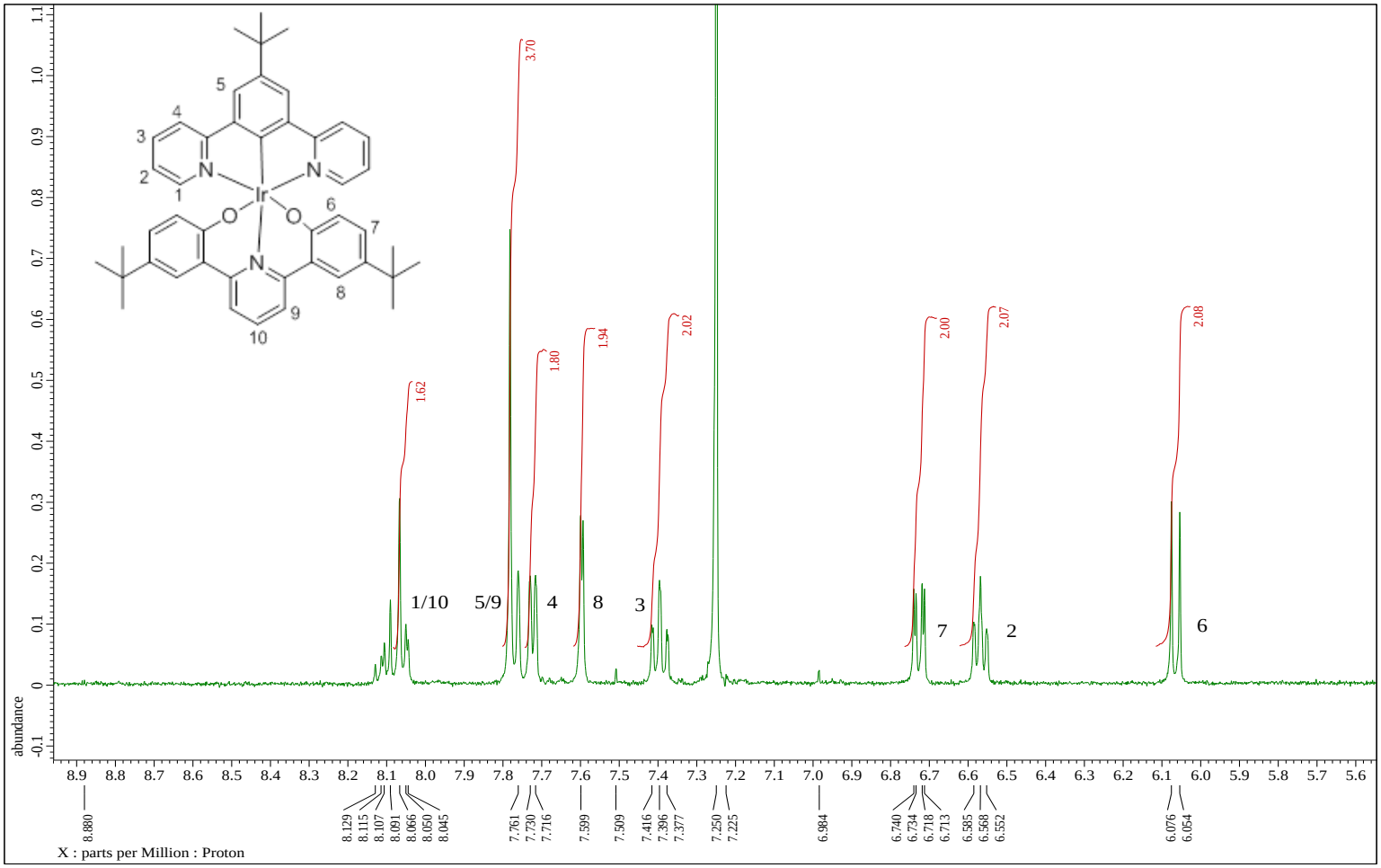

Figure 88- The aromatic region of the ^{1}H NMR of **4.1.4** in $CDCl_3$, characteristic peaks at δ1.47ppm and δ1.25ppm of 9H and 18H respectively show the presence of the tertiary butyl substituents on both the N^C^N ligand and the O^N^O auxiliary ligand.

4.1.2. Synthesis of the N^N^N coordinating Complex

A study by Williams and co-workers in 2006 showed different coordination modes of auxiliary ligands. One of the possible types of coordination, N^N^N, was shown to be a possible coordination type, where terpyridine (tpy) was used as an N^N^N ligand. As tpy is a neutral ligand, the resulting complex had an overall charge of 2+.

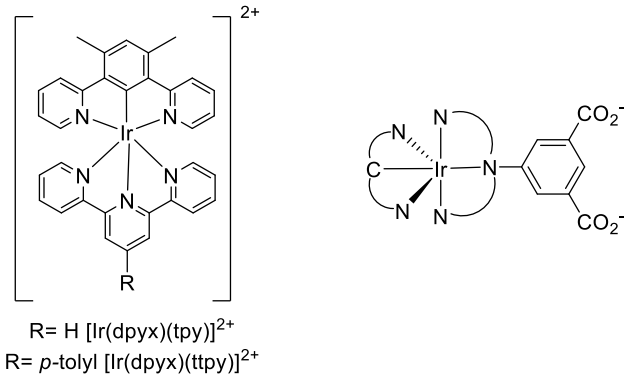

Figure 89 – The structure of the dicationic N^N^N coordinated complexes described by Williams *et al* in 2006. (left). The depiction of the counterbalancing group that provides the charge neutrality as depicted by Wilkinson *et al*. (right). The study concluded that there was not a viable strategy for the developing charge neutral emissive complexes using this method.

4.1.6 was used in place of tpy to prepare the complex **4.1.7**. The ligand contains two imidazole rings that deprotonate during the coordination to give a charge neutral complex.

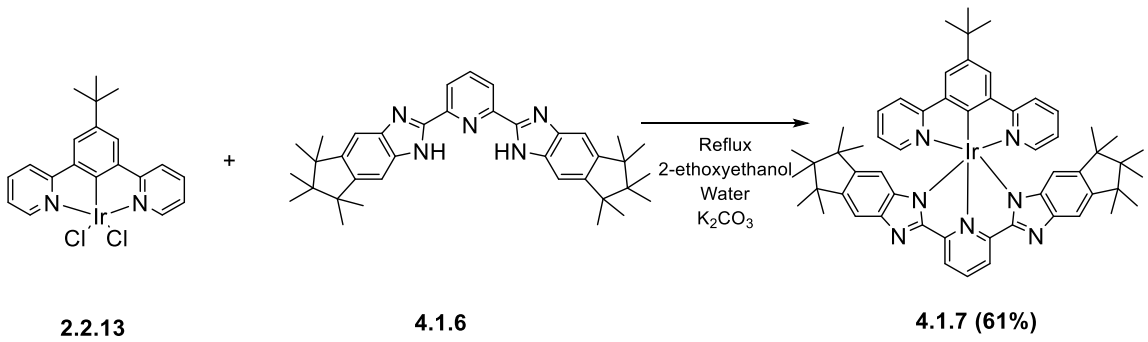

Scheme 22 - The reaction scheme for the formation of **4.1.7**, the synthesis of the complex was carried out using the methodology described by Acharrya et al.[177]

After heating under reflux in 2-ethoxyethanol overnight, the reaction was cooled. Upon cooling, the addition of water to the solution resulted in the formation of a bright yellow

precipitate. The precipitate was filtered prior to purification by column chromatography (dichloromethane/EtOAc, 5:1). This resulted in a bright yellow solid in a good yield (~62%). The solid was triturated with petroleum ether and filtered. The photophysical properties of **4.1.7** were decreased in comparison to previously synthesised complexes. The terpyridyl based coordination is typically poorly luminescent and was likely due to the emissive state being predominantly intraligand transitions of energy of a LLCT nature; an observation which was described by Wilkinson *et al*.[13] The diimidazole analogue prepared, **4.1.7**, was also a poorly emissive species.

4.1.3. Synthesis of Cyclometalating C^N^C Ligands and Complexes

The ligand, **4.1.9** was prepared by Suzuki cross coupling from 2,6-dibromopyridine and 2,4-difluorophenylboronic acid. Following the reaction, the reaction mixture was separated with brine and the product was extracted into ethyl acetate. The organic layer was recovered and dried over $MgSO_4$, the solvent was removed and this resulted in an off white solid. This is often a high yielding reaction and the synthesis of **4.1.9** supported this with high yields (~85%). In literature, the purification of the compound was carried out via column chromatography. It was found that the simple addition of petroleum ether, followed by filtration gave pure product in high yield (~94%). The ^{1}H NMR is shown in Figure 90.

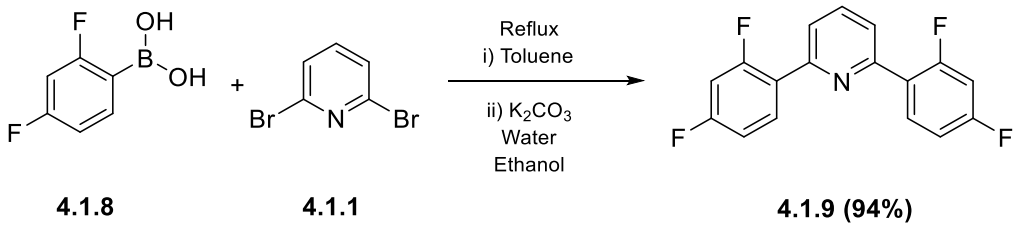

4.1.8 **4.1.1** **4.1.9 (94%)**

Scheme 23- The synthesis of the auxiliary ligand as described by Williams et al. The ligand was purified through trituration rather than column chromatography.[13]

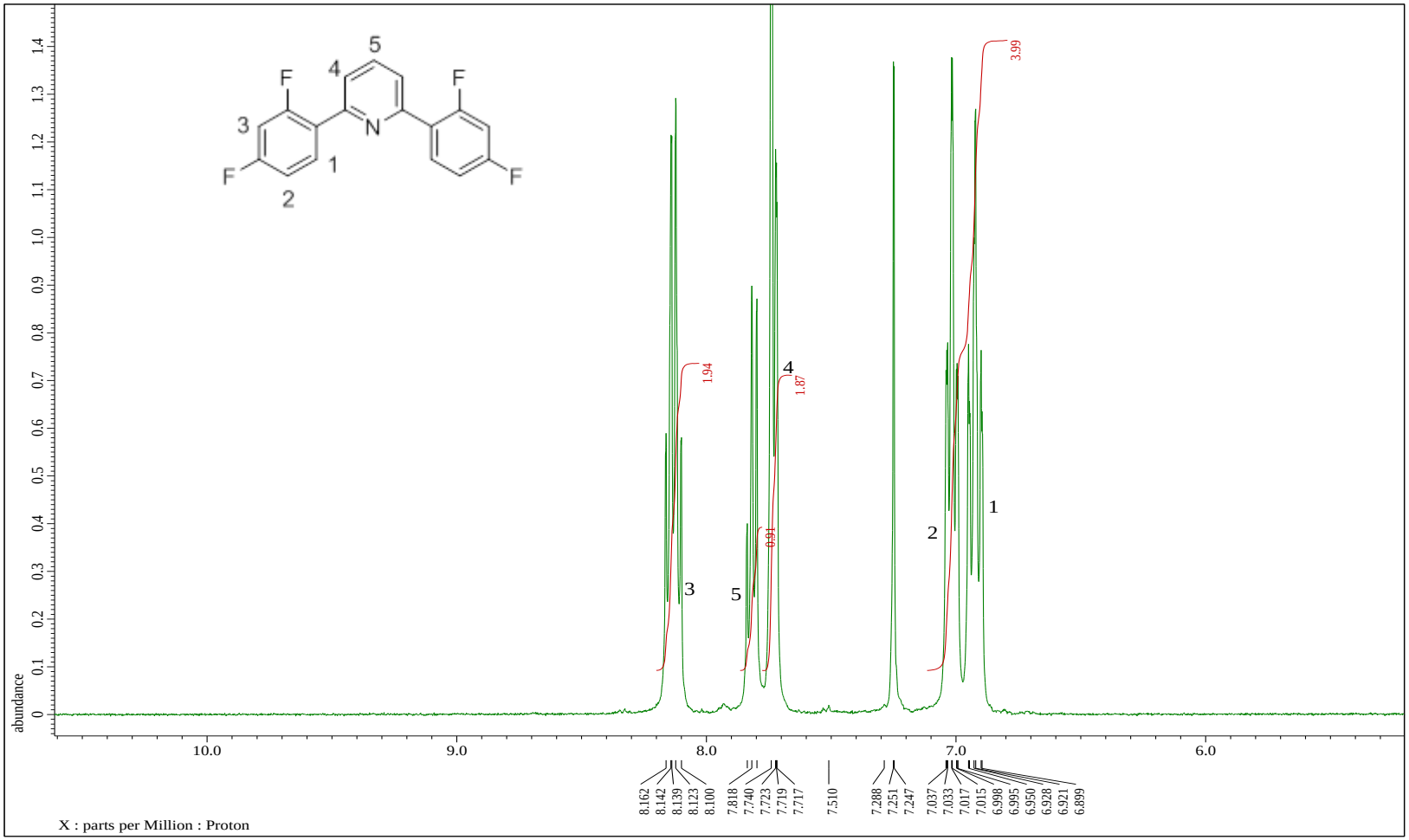

Figure 90 - The aromatic zoom of the ^{1}H NMR of **4.1.9** in $CDCl_3$. The bis(4,6-difluorophenyl)pyridine auxiliary ligand was first synthesised by Williams *et al* and the NMR spectrum matches the peaks described in literature.[13]

The model mono-iridium complex, **4.1.10**, was prepared by the method used by Wilkinson *et al*.[12-13] The synthesis was performed in a melt of the C^N^C ligand at 110°C in the presence of AgOTf. It must be noted that the reaction is carried in the melt and requires a large excess of auxiliary ligand (20 equivalence to the iridium dimer). The complex was purified by column chromatography (petrol ether/Et_2O, 100:1). **4.1.10** was synthesised in average yields (34%), which was similar to the literature values. Following this success, the scale of the reaction was altered with the amounts of starting material being increased from 50mg up to 150mg scale whilst maintaining the stoichiometry. However this increase did not result in an improvement of the reaction yield.

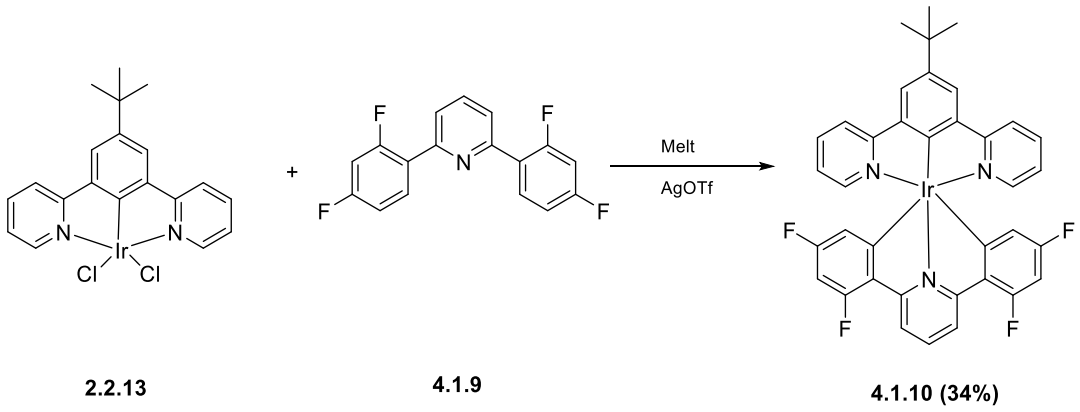

Scheme 24 - The reaction scheme of **4.1.10** showing the successful reaction conditions to form the C^N^C complex. The absence of solvent is paramount to the success of the reaction.

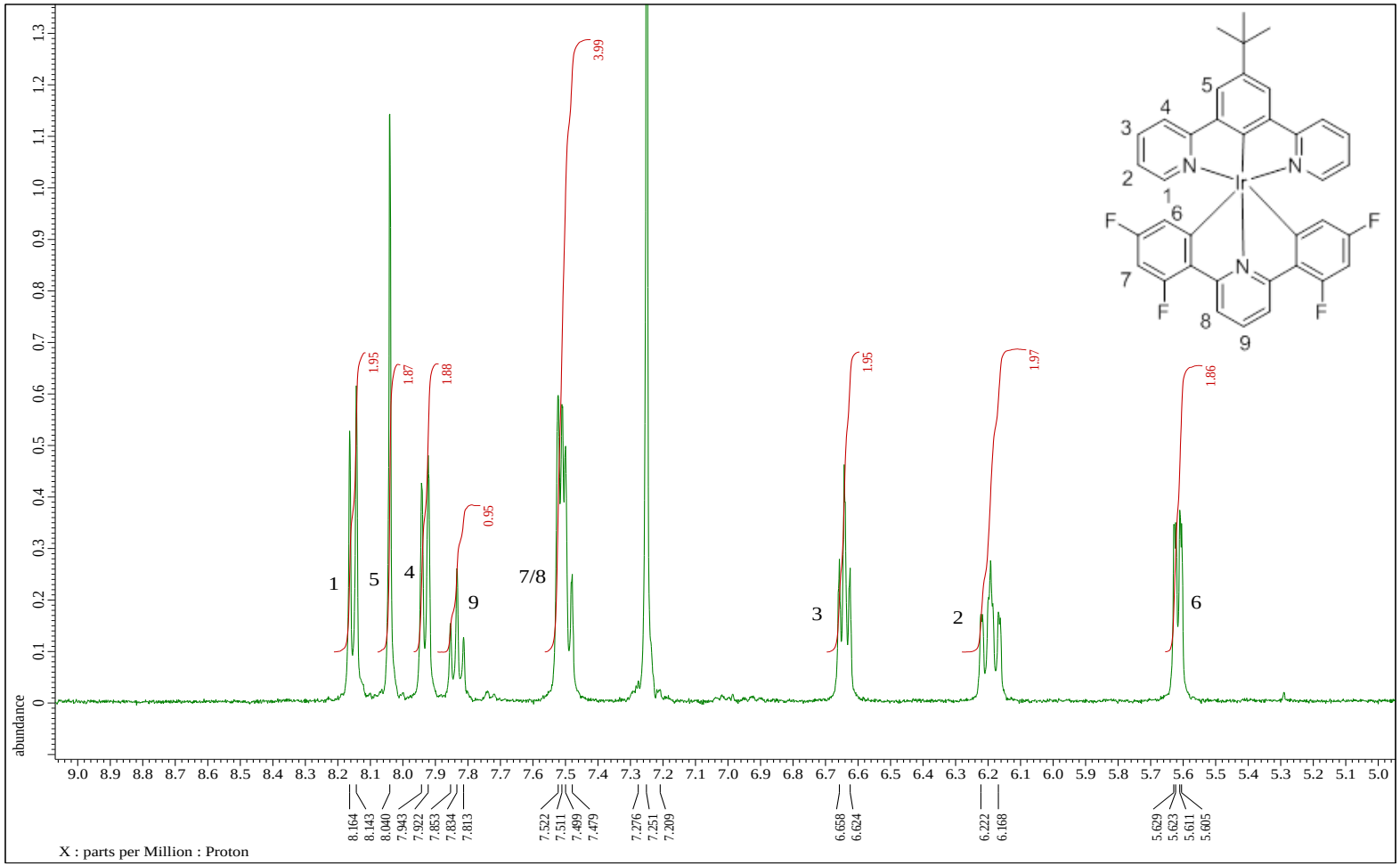

Figure 91 - The aromatic region of the ^{1}H NMR spectrum for **4.1.10** in $CDCl_3$. The tertiary butyl group is signified by a singlet at δ1.59ppm. The numbered structure is overlaid on the spectrum.

It is known that coordinating the C^N^C auxiliary ligand to the dichlorobridged dimer is problematic due to the trans effect, which is exhibited by the cyclometalating carbon atoms in the opposing para-position. This often results in one of the bonds not being formed due to an increased electron density and the ligand coordinating by a C^N binding method. Typically, electron withdrawing groups are used to minimise this problem. However as previously discussed, fluorine groups are not desirable and as a result, the synthesis of **4.1.12** was attempted.

Instead of the fluorine groups, tertiary butyl groups were used in the positions *para* to the central pyridine ring. The use of **3.2.3** was chosen due to the availability in the lab from previous work.[5, 105] Using the previously outlined methods of a solid melt reaction using AgOTf in the absence of solvent, the reaction did not take place. The resulting solid consisted of starting material and iridium dimer. Due to the failure of the reaction, alternative conditions were tested, including the toluene/silver triflate and 2-ethoxyethanol/K_2CO_3 conditions. When using the alternative conditions, the reaction once again failed to synthesise product. The study carried out by Williams and co-workers highlighted that due to the potential instability of the C^N^C complexes, only certain conditions are successful. Changes to these conditions often lead to degradation of the complex or a drastic reduction in reaction yield.[12-13]

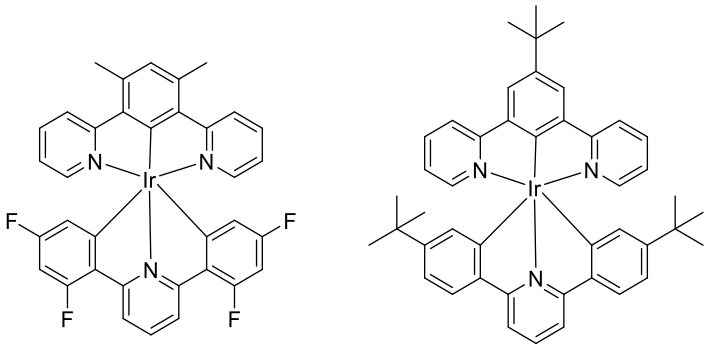

4.1.11
Ir(dpyx)(F_4dppy)
Williams *et al*, 2006

4.1.12

Figure 92 – The structure of the C^N^C complex described by Williams *et al* (left). The changes made to the complex are depicted in **4.1.12** (right). The structure shows the substitution of the four fluorine groups for the *para*-positioned *tert*-butyl solubilising groups. The complex also shows substitution of the methyl groups for a *tert*-butyl group.

The presence of electron withdrawing groups on the auxiliary ligand benefits the cyclometalation. The withdrawal of the electron density from the Ir-C bonds is likely a reason for the successful bonding to the central metal ion. Furthermore, the presence of the fluorine groups is detrimental to OLED device lifetime and therefore require removal. This can be done by introducing different EWG such as pyridine, pyrimidine or nitrile substituents.

In place of the fluorine groups, other assemblies were tested as an attempt to design a fluorine free C^N^C coordinating auxiliary ligand. The development of the first fluorine free C^N^C complex was instigated through the use of the readily available **3.2.3**, synthesised in previous research projects by Kozhevnikov and co-workers.

The formation of this complex was likely hindered due to the large amount of electron density that was produced by the electron donating *tert*-butyl groups on the auxiliary ligand. As a result, changes to the auxiliary ligand aimed to introduce an increased level of electron accepting substituents. The changes resulted in the use of **4.1.13**, this included pyridine rings in place of the phenyl rings in **4.1.9**. The structure of the ligand is depicted in Figure 93.

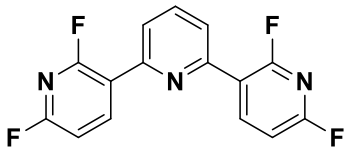

4.1.13

Figure 93 - The structure of the auxiliary ligand **4.1.13**, the substitution of the pyridine group aimed to blue shift the emission and provide an increased level of electron acceptance across the auxiliary ligand.

The conditions are of crucial importance to the success of the reaction, the method used was outlined by Williams *et al.*[13] The ligand and dichlorobridged dimer were ground together and heated at 110°C overnight. The **4.1.13** did not melt and therefore did not yield any product. Following melting point testing, the ligand, **4.1.13** melts at ~198°C, this prompted a repeat of the reaction at this temperature despite the potential detriment to the reaction yield. However this did not result in any improvement to the outcome of the reaction, instead producing an inseparable mix of dimer and auxiliary ligand.

Rather than the use of pyridyl based groups as displayed in **4.1.13**, a pyrimidine based auxiliary ligand was used.

The synthesis started with the development of a (2,6-trimethylstannyl)pyridine central group. This was achieved by substituting trimethyltin chloride with 2,6-dichloropyridine in the presence of sodium metal. The central group was then coupled with 5-bromo-2-tertbutylpyrimidine via Stille cross coupling.

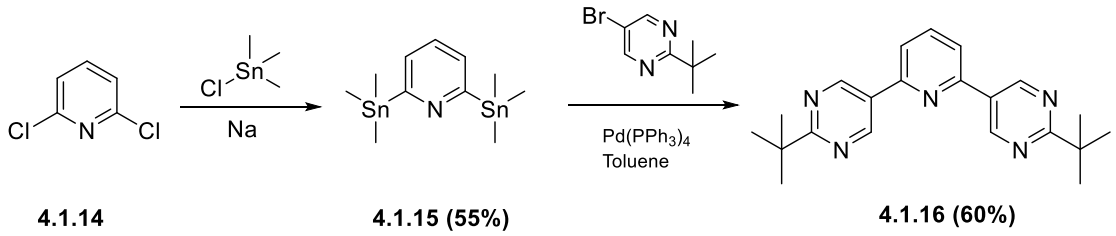

4.1.14 **4.1.15 (55%)** **4.1.16 (60%)**

Figure 94- The reaction pathway followed to develop the novel pyrimidine based C^N^C auxiliary ligand. The average yielding trimethyltin intermediate synthesis was low yielding as some product was likely lost in the washing of the solid filter cake.

The isolation of the ligand **4.1.16** was achieved through column chromatography purification (PE/EtOAc, 4:1). This resulted in a crystalline white solid in a good yield (~60%). The melting point of the ligand was tested to ensure that formation of a novel C^N^C mono-iridium complex would not be affected. The melting point was found to be ~230°C, which indicates that this auxiliary ligand was unsuitable for the formation of C^N^C ligands. The formation of the complex was attempted despite the undesirable high melting point, using the same conditions described previously. The temperature was gradually increased over time in order to observe any changes that took place during the reaction. The high melting point of the auxiliary ligand proved to be detrimental to the outcome of the reaction and rendered the reaction unsuccessful. The synthetic route from the mono-iridium dimer is shown below.

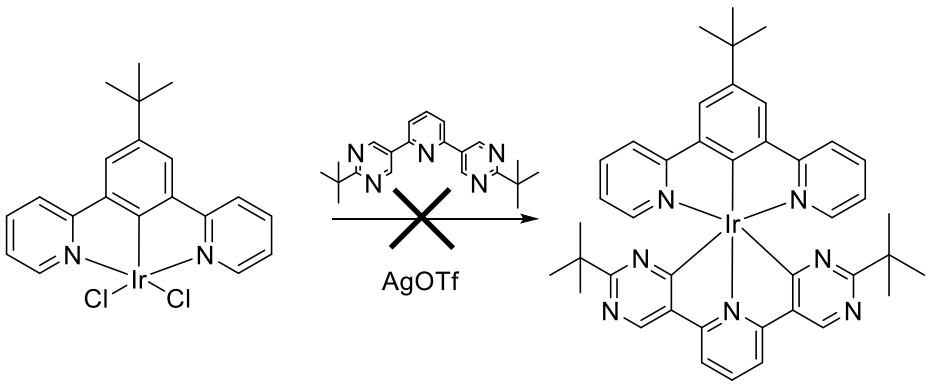

Scheme 25 - The proposed reaction scheme for the formation of the pyrimidine based C^N^C complex. The melting point of the auxiliary ligand was too high and this meant the reaction did not yield the product.

4.2. Synthesis of Di-iridium (III) Complexes using Symmetrical C^N^C Auxiliary Ligands

Following the promising photophysical properties of **4.1.10**, the complex was adapted and developed into a di-iridium assembly. The dimer used in this synthesis was the dichlorobridged compound synthesised by Kozhevnikov *et al* (**2.1.3**). Using the same synthetic method from **4.1.10**, **4.2.1** was synthesised in very low yields (10%). The sample was tested and showed that a bi-metallic analogue of **4.1.10** could display extremely promising photophysical results.

The reaction was optimised and scaled up for OLED device fabrication. In order to increase the yield of the reaction, many conditions were tested. The reaction time was reduced from 18 hours to 4.5 hours, this reduction was crucial as the reaction yield decreases if the mixture is heated longer than 4.5 hours. Reaction times over 12 hours reduced the yield of the complex. The equivalence of auxiliary ligand to iridium dimer was reduced from 20:1 equivalence to 15:1 equivalence. The equivalence of silver triflate and the temperature of the reaction were unaltered. This resulted in an increase in the overall yield of the reaction from 10% to 44% and the successful synthesis of **4.2.1** at a half gram scale, a scale not previously achieved for C^N^C cyclometalating complexes. The ^{1}H NMR is shown in Figure 95.

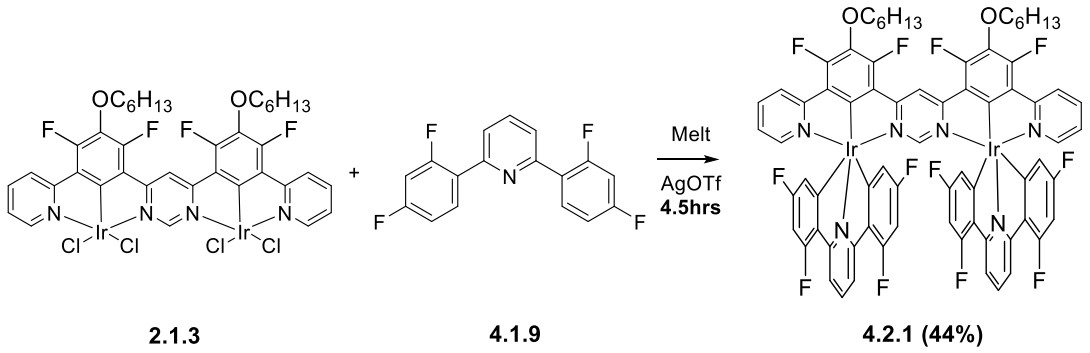

2.1.3 **4.1.9** **4.2.1 (44%)**

Scheme 26 - The reaction conditions developed to synthesise **4.2.1** following the optimisation of the synthetic procedure.

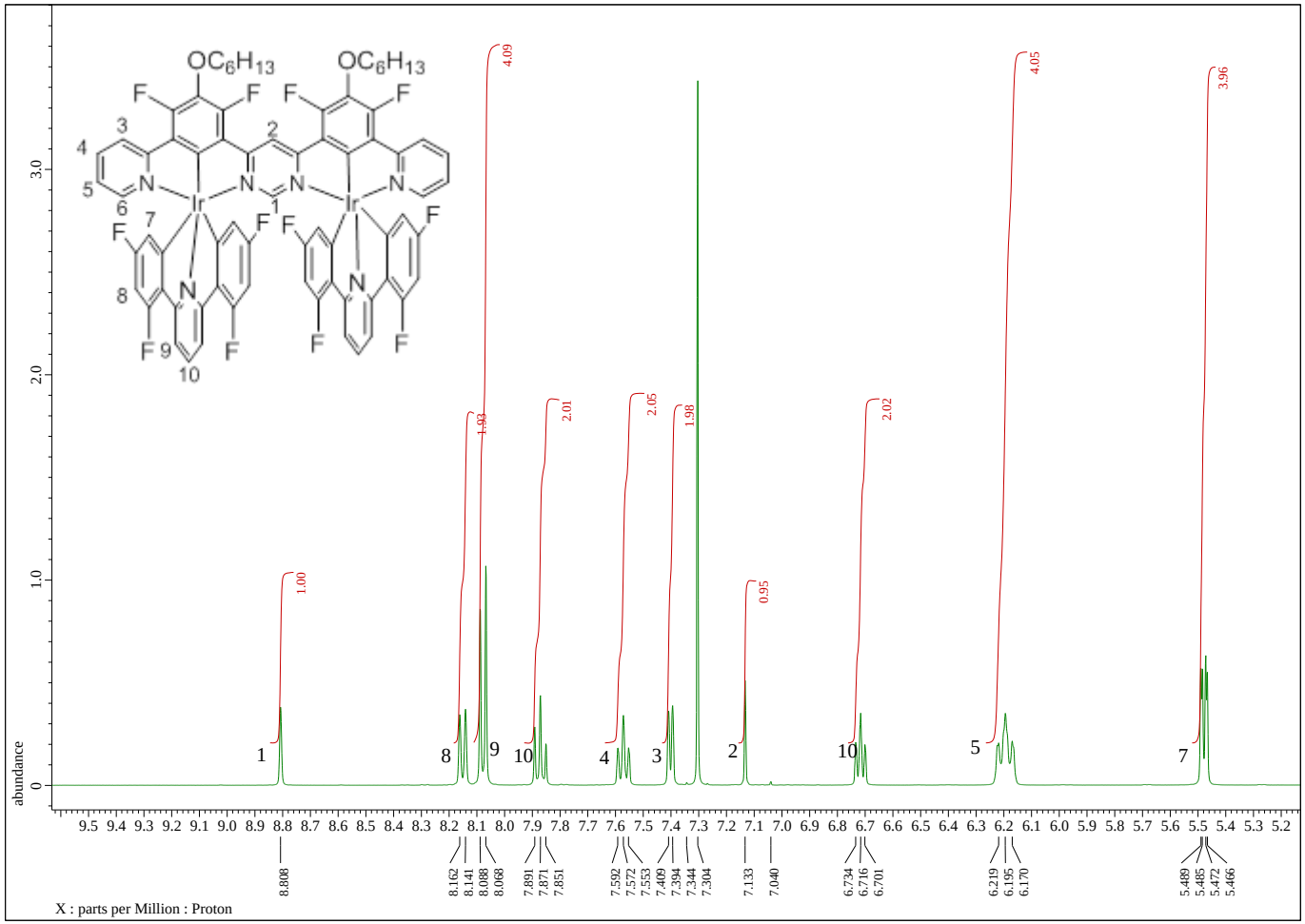

Figure 95 - The aromatic region of the ^{1}H NMR of **4.2.1**. The numbered overlaid structure is shown. The aliphatic region displays the peaks of the alkoxy chain.

The formation of this symmetrical complex removes the possibility of chirality around the metal centres. Following the scale up of this reaction and the highly promising photophysical results, the complex was altered and the fluorine groups were removed from the bridging ligand. The reaction was adapted and the solubilising groups were changed. In order to reduce the amount of fluorine present in the structure, the bridging ligand was changed. This was done by changing the alkoxy chain and the fluorine groups in the *ortho* positions. These groups were replaced with tertiary butyls group at position *4* of the central phenyl rings through use of different starting materials (1,3-dibromo-5-(*tert*-butyl)benzene). The auxiliary ligand remained unchanged and the complex, **4.2.2** was synthesised in average yields (21%). The dimer was heated with AgOTf and the auxiliary ligand at 110°C for 18 hours. Following the reaction, the solid was washed with petrol ether and dissolved in DCM, as previously done for **4.2.1**. The solid was filtered through celite and purified by column chromatography (PE/Et_2O, 50:1). The solvent was removed under reduced pressure and the resulting red solid was isolated. Using the optimised conditions for **4.2.1**, this showed that the conditions are not universal and must be tuned for each complex. The complex was tested which allowed for a comparison between **4.2.2** and **4.2.1** to be established. The ^{1}H NMR for **4.2.2** is shown in Figure 96.

Even though the structure of the complex **4.2.2** still contains fluoro groups on the auxiliary ligand; the alkoxy group and *ortho* fluorine groups on the outer ligand have been removed which in theory should increase the efficiency of possible OLED devices. The two C^N^C compounds, **4.2.1** and **4.2.2** display new avenues for the development of highly luminescent, symmetrical bis-terdentate di-iridium complexes. The use of these charge neutral complexes shows significant potential for use in OLED devices, as described in the photophysical properties.

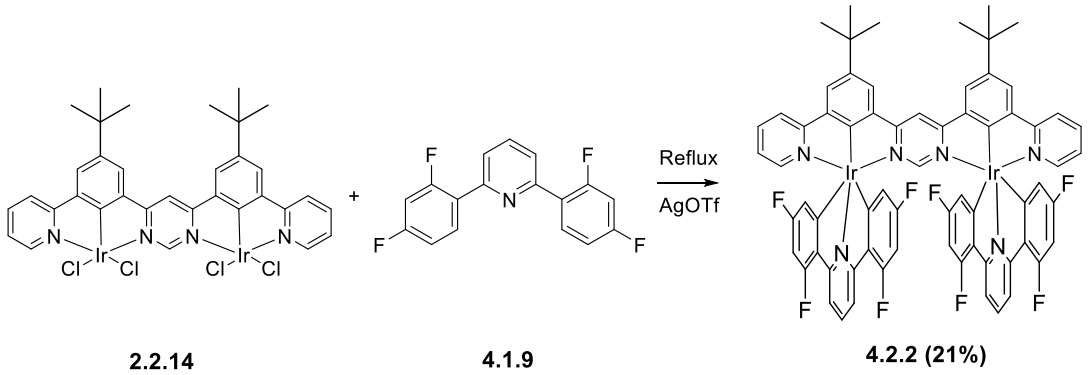

Scheme 27 - The reaction conditions used to prepare **4.2.2**. The optimised conditions for **4.2.1** were not transferable and the conditions described by Wilkinson *et al* resulted in the highest reaction yield.

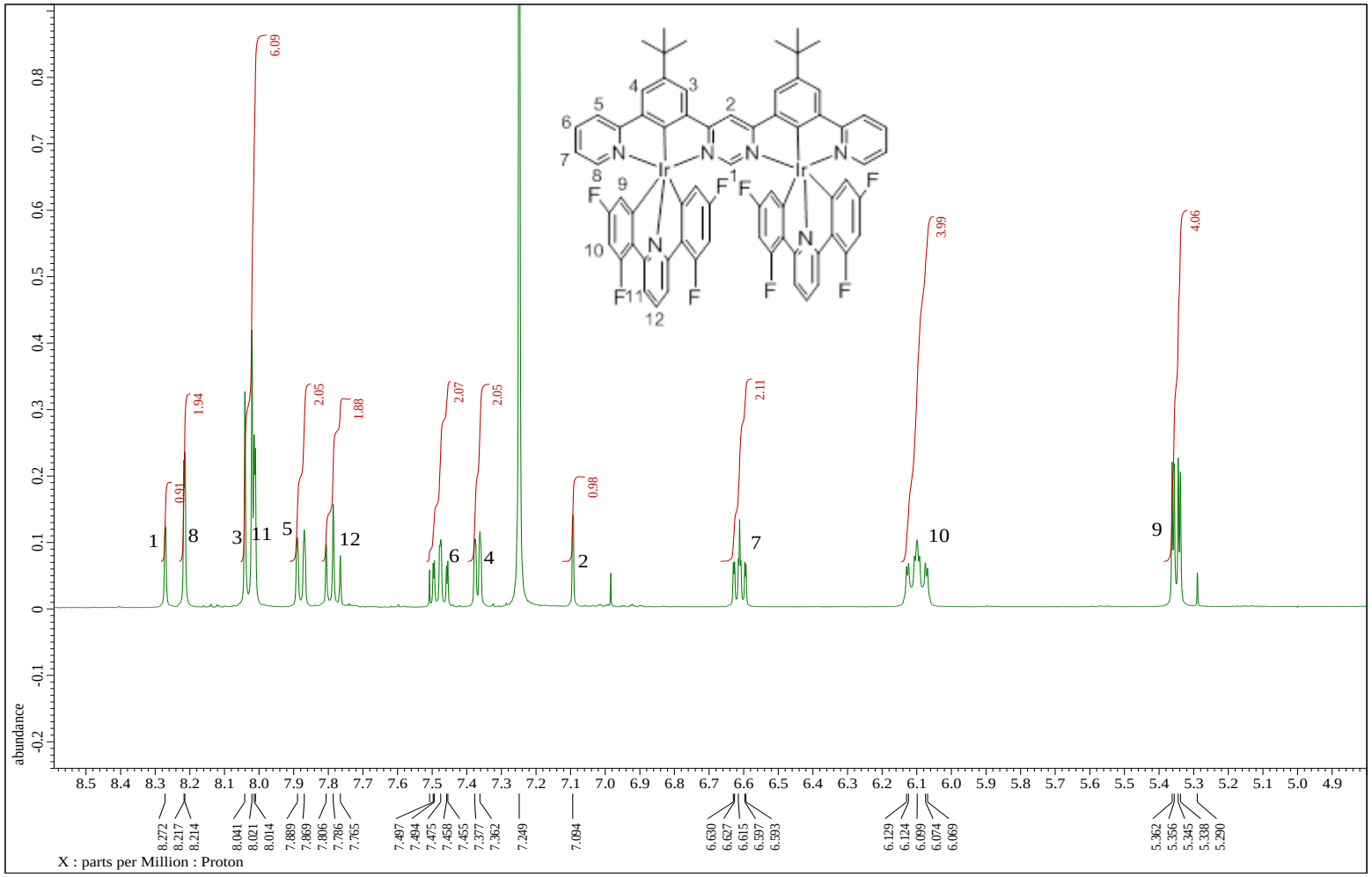

Figure 96 - The aromatic region of the ^{1}H NMR of **4.2.2** $CDCl_3$. The numbered structure is overlaid. The tertiary butyl group is present as a singlet at δ1.62ppm.

4.3. Photophysical Properties

The complexes were tested and only **4.1.10** improved photophysical properties compared to the O^N^C coordinating auxiliary ligands. Despite the presence of the detrimental fluorine groups as part of the auxiliary ligand, **4.1.10** showed a good PLQE value with a long triplet state decay time. The data is shown below in comparison to **3.2.16**, which coordinated via O^N^C binding.

Table 10- The photophysical properties of the symmetrical di-anionic complexes, in comparison to **3.2.16**, the O^N^C complex from the previous section. The complexes are organised in order of PLQE values from lowest to highest quantum efficiencies.

Sample	**λ_{max} (nm)**	**PL-QE (toluene)**	**T-1 Decay time (µs)**
4.1.4 (O^N^O)	562	0.01	N/A
4.1.7 (N^N^N)	606	<0.02	N/A
3.2.16 (O^N^C)	564	0.16	0.57
4.1.10 (C^N^C)	560	0.24	2.90

The data for **4.1.10** shows an improvement in contrast to **3.2.16** and the other ligands in the series, the quantum yield has increased by 8%, with a significant increase in triplet decay time from 0.57 to 2.90 µs. The inclusion of fluorine groups on the auxiliary ligand was expected to show a slight blue shift in emission wavelength due to their electron withdrawing nature. However whilst this is displayed, the blue shift was minimal (4nm).

The other complexes produced did not show the same level of promise in comparison, the bis-phenolate auxiliary ligand in **4.1.4** exhibited a peak emission wavelength of λ_{max}= 562nm, similar to **3.2.16** however the quantum efficiency was dramatically reduced from 0.16 to 0.01 and no recorded triplet state lifetime, which indicates that the complex emitted energy through non-radiative processes.

The coordination modes described by Williams *et al* outlined the use of terpyridyl coordination to the central metal ion, however the distinct presence of counterbalancing

substituents is required to produce the charge neutral complex. The quantum yield was considerably worse than **3.2.16** and only slightly improved when compared with **4.1.4**, once again the triplet state lifetime was not recorded, also indicating that the emission was non-radiative.

The complex, **4.1.10**, was carried forward for use in the development of a di-nuclear complex. The initial complex developed was using the dimer described by Kozhevnikov *et al* and provided important insight into the synthetic procedure required to develop di-iridium analogues of previously studied molecules, resulting in a novel structure. Whilst this insight is important, the photophysical properties followed the expected trends described by Kozhevnikov *et al.*[105]

Table 11 - The photophysical properties of **4.2.1**, accompanied by the photophysical data of the mononuclear analogue, **4.1.10** and the C^N di-iridium complex, **2.2.2**.

Sample	**λ_{max} (nm)**	**PL-QE (toluene)**	**T-1 Decay time (µs)**
4.1.10	560	0.24	2.90
4.2.1	637	0.89	1.33
2.2.2	631	0.87	0.53

The photophysical data shows that the adaptation to a bi-metallic complex shows the expected trend, a large red shift in emission (by an order of ~100nm), the red shift between **4.1.10** and **4.2.1** is approximately 80nm which follows the observations in literature.[105] The PLQE of **4.2.1** has quadrupled following the addition of the secondary metal centre, which also supports the findings of the study carried out by Kozhevnikov *et al*.[105] When comparing the data for both **4.2.1** and **2.2.2**, there was a small improvement of PL-QE (~2%) which indicates that the presence of the mono-dentate chloride ligands has little effect on the quantum efficiency. however it is shown that there is a detrimental effect on the triplet state lifetime when chloride ligands are present in the structure. The use of the terdentate cyclometalating ligand also showed a small increase in the peak emission wavelength. This increase can be attributed to

the increase in π-conjugation of the entire system due to the presence of an additional phenyl ring in the auxiliary ligand.

The highly promising PLQY value and triplet state decay time exhibited by **4.2.1** showed that the fabrication of an OLED device was the next logical step. The OLED device was fabricated using **4.2.1** and showed an improvement over the device which utilised **2.2.2,** described in Section 2.2. The device using **4.2.1** as an emitter showed a significantly larger external quantum efficiency (3 times larger) than **2.2.2**. However, **4.2.1** had a poor lifetime which could be attributed to the presence of the fluorine groups. **4.2.1** was compared against a different previously fabricated OLED devices which used complex **4.2.3** (shown in Figure 98). Despite the maximum quantum efficiencies being similar, the device fabricated with **4.2.1** rapidly decreased below sufficient standards. This can possibly be explained because of the level of tailing present in the emission spectra for **4.2.1.** The amount of tailing present in the emission profile has increased with a longer luminescent lifetime and due to this some of the luminescence can be quenched through triplet-triplet annihilation. The lifetime of the **4.2.1** device showed a marginal increase in lifetime over **4.2.3** but this can also be attributed to the reduction in the amount of fluorine groups. The photophysical data is shown in Table 12.

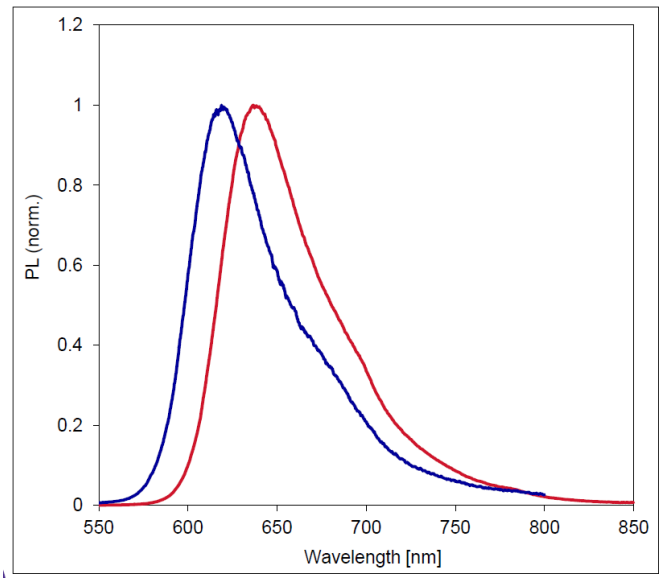

Figure 97 - The emission spectra of **4.2.1** (red) compared with the emission spectra of **4.2.3** (blue). The graph shows the photoluminescence vs the emission wavelength and highlights the effect of terdentate auxiliary ligands.

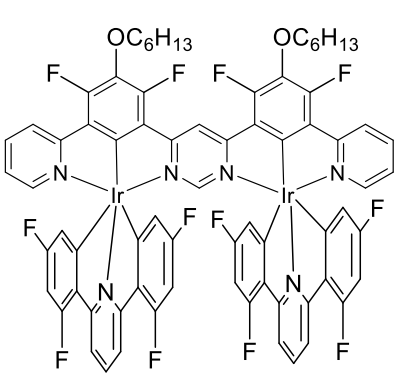

4.2.1

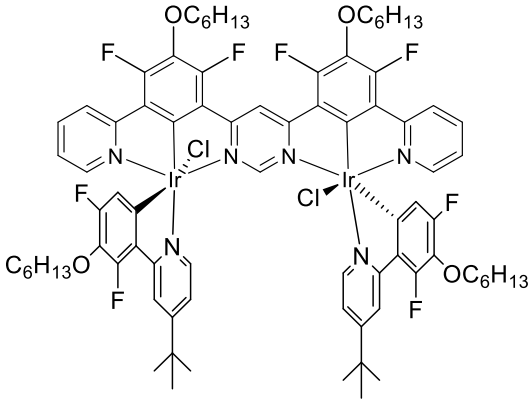

4.2.3

Figure 98 - The structures of the complexes **4.2.1** and **4.2.3** detailed in Figure 97.

The comparison between the complexes **4.2.1** and **4.2.3** stems from the use of the same bridging ligand. The use of the terdentate symmetrical ligand, **4.1.9**, removes the chirality from these bi-metallic complexes. The use of this terdentate ligand has also shown a distinct red shift in emission. This can be attributed to the increase in the π-system and the additional point of cyclometalation. Whilst the red shift is only by ~20nm, the PLQE values are in fact similar. There was a decrease in PLQY between the two complexes from **4.2.3** to **4.2.1**, with values of ϕ= 0.96 and ϕ= 0.89 respectively.

Table 12 - The photophysical data for **4.2.1** and **4.2.3**. The table describes the emission wavelength (λ_{max}), the full width half maximum (FWHM) indicating the peak shape, the PLQE and the triplet state lifetime.

Sample	**λ_{max} (nm)**	**FWHM (eV)**	**PLQE (%)**	**T-1 Decay time (µs)**
4.2.1	637	0.191	0.89	1.33
4.2.3	619	0.188	0.96	0.57

In addition, the short lifetime of **4.2.3** (0.57µs) can be associated with the presence of fluorine, alkoxy and monodentate chloride ligands. Upon the removal of these groups, **4.2.1** (1.33µs) showed a distinct increase in triplet state decay time. An increase in triplet state lifetime can

result in quenched emission through triplet-triplet annihilation, however the longer lifetime does not appear to have affected the results.

The fabrication of the OLED device using **4.2.1** was compared to a previous device which utilised **4.2.3** as an emitter. The device of **4.2.1** showed promising results however did not produce an improved efficiency when compared to the device of **4.2.3**. The peak EQE of the device using **4.2.1** was η_{ext}=19.7% at a current density of 0.1 mA cm^{-1}, however whilst this is similar to the η_{ext}=22.0% of **4.2.3**, the lifetime of the device using **4.2.1** (7hours) is over half that of **4.2.3** (15hours).

The best combination developed using **4.2.1** as an emitter showed an EQE of η_{ext}=18.9%. Whilst this is lower in efficiency, the overall half-life (LT_{50}) is increased to 26 hours, an increase compared to every configuration of the devices of **4.2.1**. Despite the similar efficiencies between the two devices, the current density of the device using **4.2.1** quickly drops to below meaningful values and therefore becomes unsuitable. The data for the OLED device fabrication is shown in the appendix, section 8.3.

4.2.1 is the first example of a di-iridium C^N^C complex to be evaluated in an OLED device. The promising results highlight that through development, highly luminescent and efficient emitters are achievable using C^N^C complexes. The device fabricated using **4.2.1** displayed a high efficiency but short lifetime and a strong roll off in the emission profile, however the decreased efficiency of the device can be attributed to the presence of the fluorine groups.

The promising photophysical properties of the OLED device fabricated using **4.2.1** could be improved by removing the fluorine groups. As a result, **4.2.2** was synthesised and tested. Constructing the di-nuclear analogue of **4.1.10** introduced a secondary metal centre which presented the predicted red shift in emission of ~100nm, from 560nm to 655nm.[105] As the complex is further red shifted, the emission is closer to the near-IR region of the visible spectrum which is not ideal for OLED devices. The benefit of the secondary metal centre is also supported by a three-fold increase in PLQE to 75%. The triplet decay time has also been

reduced by over half to 1.30µs which shows promise, as the rate of radiative decay has increased and is in line with optimal values (~1µs).

When comparing **4.2.2** with **4.2.1**, the removal of the fluorine groups has resulted in a red shift of the emission from 637nm to 655nm, this can be attributed to the change of an electron withdrawing group to a tertiary butyl group which is slightly electron donating in nature. The removal of the fluorine and alkoxy group led to a significant decrease in PLQE, which is likely due to the red shift, as the PLQE is known to decrease when the emission is approximately in the near IR region.[15, 186] Despite the changes to the structure of the complex and the changes to the solubilising groups there is a very minor change to the triplet state decay time, which indicates that the changes to the structure has very little effect on the length of the excited triplet state. The graph below shows the different emission of each di-iridium complex with the accompanying mono-iridium analogues of **2.2.2** and **4.2.2**.

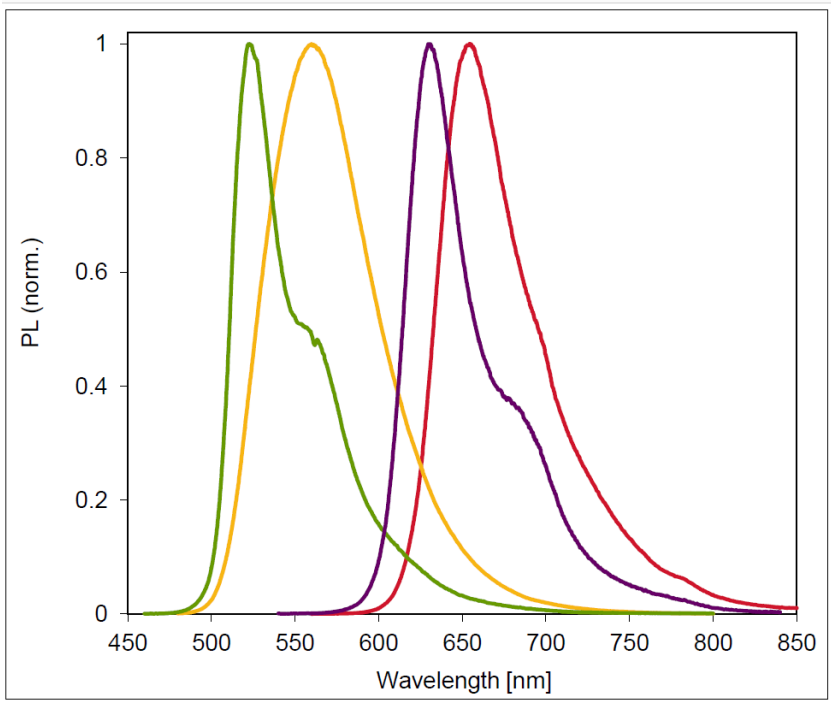

Figure 99 - The photoluminescence spectra for **2.2.2** (purple) and **4.2.2** (red), the mono-iridium analogues **2.2.1** (green) and **4.1.10** (yellow) are shown, which highlights the red shift induced by the addition of the second metal centre.

Table 13- The photophysical data for the C^N complexes, **2.2.1** and **2.2.2**, the comparative data is the terdentate C^N^C complexes, **4.1.10** and **4.2.2**. The table details the emission wavelength (λ_{max}), the full-width half maximum (FWHM), photoluminescent quantum efficiency (PLQE) and the triplet state decay time (T-1 decay time).

Sample	**Composition (complex/ligand)**	**λ_{max} (nm)**	**FWHM (eV)**	**PLQE (%)**	**T-1 Decay time (µs)**
2.2.1	Mono-nuclear/bidentate 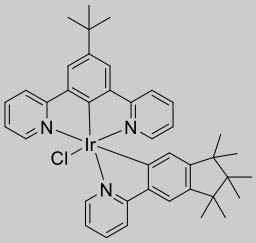	523	0.205	**0.37**	0.94
2.2.2	Di-nuclear/bidentate 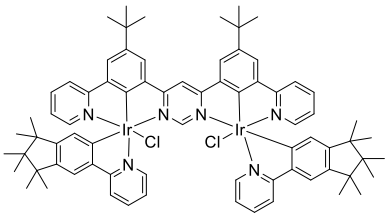	631	0.135	**0.87**	0.53
4.1.10	Mono-nuclear/terdentate 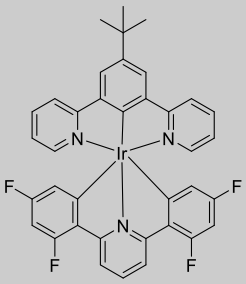	560	0.294	**0.24**	2.9
4.2.2	Di-nuclear/terdentate 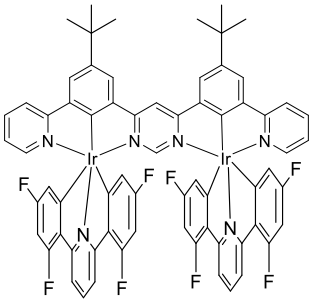	655	0.177	**0.74**	1.30

The table and spectra show that the inclusion of the secondary metal centre results in the expected red shift of the emission wavelength, but also in the large increase in the PLQE. The introduction of the second metal centre also results in a reduction in the triplet state lifetime, shown in both the C^N complexes and the C^N^C complexes, however the terdentate arrangements display much more desirable lifetimes. The removal of the mono-dentate chloride ligand results in a broader emission spectrum however a more preferable 'Gaussian' shaped emission profile.

The synthesis of **4.2.1** and **4.2.2** highlighted the effect of ligand substituents on the photophysical properties of a complex. In addition, the removal of the chloride ligand from the complex had significant benefits to the overall efficiency and the lifetime of devices fabricated.

A comparison of the results highlighted the main effects of changing the auxiliary ligand coordination type. The comparison of the di-iridium complex series is depicted in Figure 100, the figure includes data of the C^N mono-nuclear and di-iridium complexes, **2.2.1** and **2.2.2** with both mono-iridium and di-iridium terdentate C^N^C complexes, **4.1.10**, **4.2.2** and **4.2.1**.

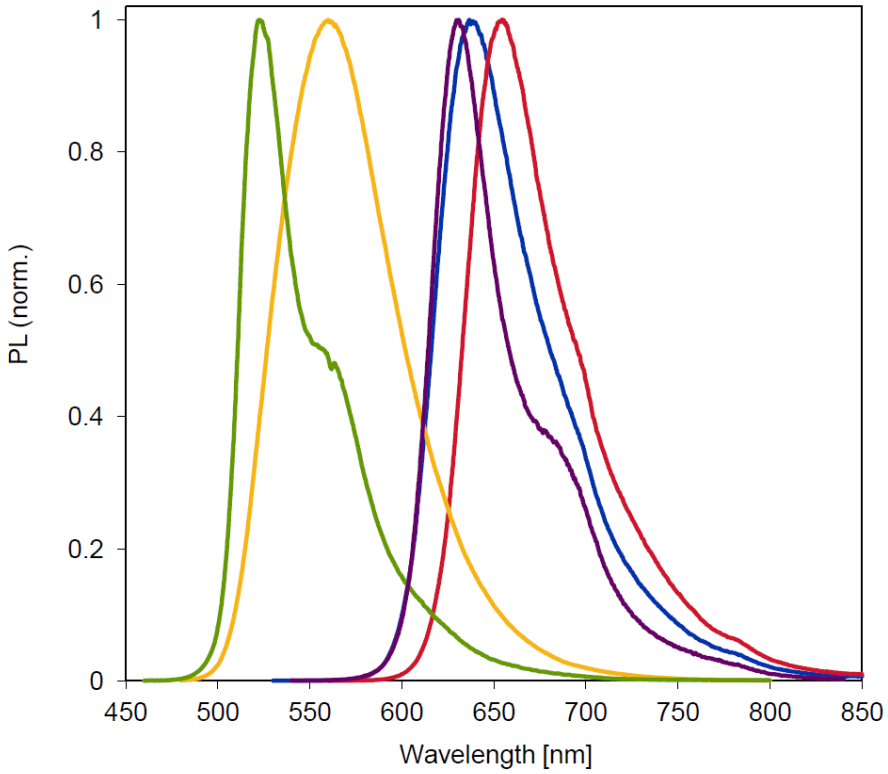

Figure 100 - The emission spectra of the complexes, **2.2.1** (green), **4.1.10** (yellow), **2.2.2** (purple), **4.2.1** (blue) and **4.2.2** (red). This highlights the effect that the use of terdentate complexes has on the overall emission of the di-iridium complexes.

Table 14 - The photophysical properties of the complexes shown in figure 74. The data highlights the effect of the secondary metal centre and the inclusion of the cyclometalating C^N^C auxiliary ligand.

Sample	**λ_{max} (nm)**	**FWHM (eV)**	**PLQE (%)**	**T-1 Decay time (µs)**
2.2.1	523	0.205	0.37	0.94
2.2.2	631	0.135	0.87	0.53
4.1.10	560	0.294	0.24	2.9
4.2.1	637	0.191	0.89	1.33
4.2.2	655	0.177	0.74	1.30

The spectrum and table highlights data for the most promising bimetallic complexes including those with C^N coordinating ligands. This would suggest that the presence of the monodentate Cl ligand has a considerable effect on the emission of the complex and the removal of this group results in a more stable complex. Whilst the C^N di-iridium complex, **2.2.2** shows a high quantum yield (ϕ= 0.87), the triplet state lifetime is considerably lower than the terdentate complexes, indicating a more rapid rate of radiative decay. The amount of fluorine groups between **4.2.1** and **4.2.2** was reduced by half. This removal of fluorine led to a decrease from 1.33µs to 1.30µs, and a red shift of peak emission from 637nm to 655nm. The decrease can be attributed to the removal of the electron withdrawing fluorine and the inclusion of the electron donating tertiary butyl substituent.

4.4. Conclusions

The development of terdentate C^N^C complexes was the most promising of the symmetrical coordination types tested. However the formation of these complexes displayed the highest level of synthetic difficulty. The procedures for each complex required optimisation for the individual compounds when adapting the chemistry from mono-iridium to di-iridium structures. Currently the only successful mono-nuclear C^N^C complex was **4.1.10**, adaptations to the structure in the removal of fluorine or introduction of electron accepting

groups were unsuccessful. This is likely due to high melting points of the auxiliary ligands preventing the cyclometalation. Future developments will require ligands with a melting point ~110°C; this could be achieved by substituting the existing fluorine groups with a group that is a better electron acceptor. The temperature ceiling of the reaction is a limiting factor to the production of C^N^C cyclometalating complexes, with the use of auxiliary ligands melting above 110°C often resulting in an unsuccessful reaction. The failed nature of the reaction likely arises due to the auxiliary ligand remaining in a solid state and therefore not dissolving the dichlorobridged dimer and silver triflate. A different explanation could be the possible thermal degradation of the dimer at high temperatures however the high melting point of the auxiliary ligands is more probable. Despite the complications encountered, the development of the complexes could be improved and facilitated through ligand optimisation.

The development of di-iridium analogues such as **4.2.2** and **4.2.1** was carried out following the promising photophysical properties of **4.1.10** (λ_{max}= 560nm, τ = 2.90µs, ϕ= 0.24). The initial synthesis of **4.2.1** used the exact conditions tested with **4.1.10** and this resulted in the successful synthesis, however this was in poor yield. This showed that the process requires additional optimisation for adaptation to di-nuclear structures. The optimisation of the conditions led to a significant increase of the overall reaction yield (10% to 44%), however when the synthesis of the tert-butylated analogue was carried out, the new optimised conditions did not result in an increase in the reaction yield. Further changes to the conditions still did not result in any improvements.

The application of **4.2.1** to an OLED device showed that the use of C^N^C complexes have encouraging and promising futures as red emitters in devices. The OLED device fabricated showed a peak external quantum efficiency of η_{ext}= 19.7%. In order to develop efficient OLED devices with cyclometalated C^N^C ligands, the structure will require changes and the removal of the detrimental fluorine and alkoxy chains. The presence of these groups were to prevent competitive cyclometalation and to induce a blue shift of emission. Therefore a library

of substituents could be used to develop a series of analogues complexes that do not possess the detrimental groups such as -C≡N, -COOR or –COR.

Prior to future iterations, melting point tests before cyclometalation can identify auxiliary ligands that are not suitable for the use in a solid melt reaction, the melting point is required to be below 110°C. Any increments to this result in a decrease of reaction yield. Other conditions could also be tested such as using small amounts of benzoic acid to homogenise the reaction mixture completely following the solid material being ground together.[163] The formation of devices using these C^N^C complexes do not possess long lifetimes.

Regardless of the complications outlined, the work described in this chapter has resulted in the synthesis of two novel bis-terdentate di-iridium C^N^C complexes. Both displayed high levels of efficiency and intense luminescence. Through additional studies, highly efficient optoelectronic devices could be a realistic possibility.

4.5. Experimental

4.5.1. Symmetrical Di-Anionic Auxiliary Ligands

4.5.1.1. Synthesis of **4.1.2**

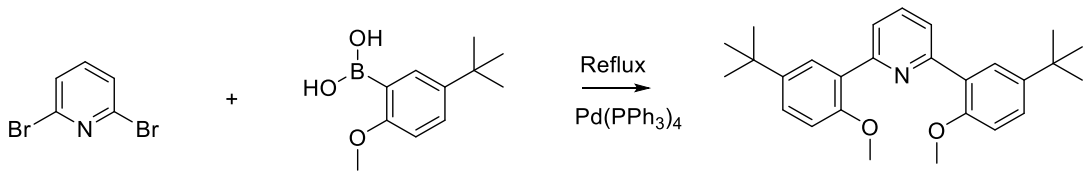

A mixture of K_2CO_3 (2.79g, 2M, 20.30mmol) and water (10ml) were added to a flask and degassed by bubbling argon through the mixture for 5 minutes. Toluene (30ml) and ethanol (5ml) were added and the mixture was deoxygenated for a further 5 minutes. A sample of 5-tertbutyl-2-methoxybenzene boronic acid (1.00g, 4.81mmol) and 2, 6-dibromopyridine (0.52g, 2.19mmol) were added and deoxygenated for 10minutes. The catalyst, $Pd(PPh_3)_4$ (0.21g, 0.20mmol), was added and the reaction was heated under reflux for 12hours. Brine (20ml) was added and the reaction mixture was separated. The aqueous layer was washed with EtOAc (3 x 10ml). The combined organic layer was dried over $MgSO_4$ and filtered. The

solvent was removed under reduced pressure and the resulting residue was purified by column chromatography (SiO_2, Hexane/EA, 4:1), yielding an off white solid (0.72g, 82%). ^{1}H NMR (400MHz, $CDCl_3$, ppm), δ 8.08 (d, *J*= 2.0Hz, 2H), 7.81 (d, *J*= 8.0Hz, 2H), 7.71 (ddd, *J*= 7.0, 2.0Hz, 1H), 7.39 (dd, *J*= 7.0, 2.0Hz, 2H), 6.92 (d, *J*= 8.7Hz, 2H), 3.85 (s, 6H), 1.36 (s, 18H).

4.5.1.2. Synthesis of **4.1.3**

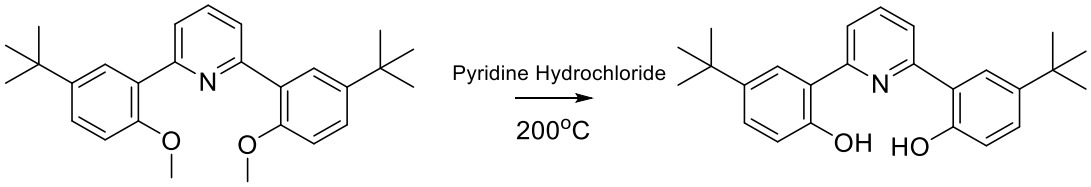

A sample of 2,6-bis(5-tert-butyl-2-methoxyphenyl)pyridine (0.900g, 2.23mmol) was added to a flask containing excess pyridine hydrochloride (5.00g, 43.3mmol) under an Argon atmosphere. The flask was heated to 200°C and stirred for 2 hours. The reaction was cooled to room temperature, water (20ml) was added, forming a solid. The solid was filtered and washed with water to obtain a white solid. (0.53g, 63%). ^{1}H NMR (400MHz, DMSO, ppm), δ 8.07 (s, 2H), 7.81 (d, *J*= 3.0Hz, 1H), 7.37 (dd, *J*= 8.0, 2.0Hz, 1H), 6.95 (d, *J*= 8.0Hz, 1H), 1.28 (s, 9H). HRMS (ESI) calculated for $C_{25}H_{29}NO_2$ ($[M+H]^+$) = 376.22710. Found m/z = 376.22614.

4.5.1.3. Synthesis of **4.1.9**.[13]

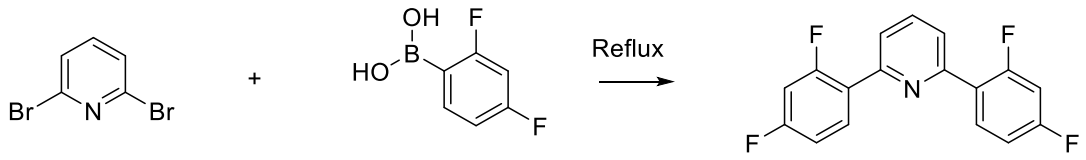

A potassium carbonate (5.00g, 36.20mmol) and toluene (150ml) mixture was degassed for 5minutes. Water (50ml) and ethanol (50ml) were added and degassed under argon. 2,6-dibromopyridine (10.43g, 43.1mmol) and 2,4-difluorobenzeneboronic acid (15.0g, 94.5mmol) were then added and the mixture degassed further. The catalyst, $Pd(PPh_3)_4$ (2.49g, 2.16mmol), was added and the reaction was heated under reflux for 18 hours. The mixture was then mixed with brine (30ml) and extracted into ethyl acetate. The organic layer was collected, dried over $MgSO_4$ and then evaporated to dryness *in vacuo*. Petroleum ether was added to the resulting residue, white crystals formed upon cooling (12.24g, 94%). Literature melting point: 83-84°C. Observed melting point: 82-83°C. ^{1}H NMR (400MHz, $CDCl_3$, ppm), δ 8.17 (q, *J*= 7.8Hz, 2H), 7.82 (t, *J*=7.8 Hz, 1H), 7.74 (dd, *J*= 7.3, 2.3 Hz, 2H), 7.02 (t, *J*= 8.2, 5.5, 2.8 Hz, 2H), 6.93 (t, *J*= 8.7, 5.0, 2.3 Hz, 2H). ^{19}F NMR (376MHz, $CDCl_3$), δ -109.04 (s, 2F), -112.33 (s, 2F). ^{13}C NMR (100MHz, $CDCl_3$), δ 162.8, 161.2, 152.3, 137.2, 132.4, 126.5, 122.9, 112.1, 104.5. *NMR similar to literature values.

4.5.1.4. Synthesis of **4.1.15**

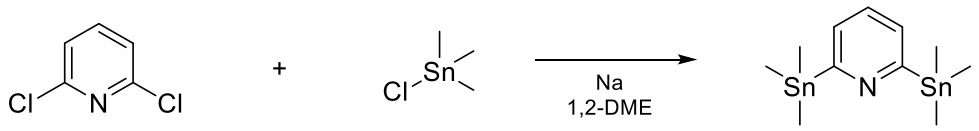

Sodium (5.7g, 0.248mol) was pressed into Na wire and cut with scissors (1cm pieces) and kept under a layer of petroleum ether. The sodium was added to a flask of 1,2-dimethoxyethane (60ml) and the the flask was capped with a septum. An argon atmosphere was added and the suspension was cooled to -20°C (ice/salt/ethanol bath). Trimethyltin chloride (10g, 0.05mol) in 1,2-DME (20ml) was added dropwise by syringe and the mixture was stirred at -20°C for 3 hours. The reaction was filtered through a Hirsch funnel (must be done as quickly as possible) to remove sodium pieces. The filtrate was transferred to a 250ml flask and cooled to -20°C. Dichloropyridine (2.86g, 0.019mol) in 1,2-DME (20ml) was added to the cold mixture dropwise and left to stir overnight. The solvent was removed under reduced pressure and petroleum ether was added (50-100ml) resulting in the formation of solid. The filter cake formed was dissolved in a mixture of water (50ml) and petroleum ether (50ml) and separated. The organic phase was isolated and dried over $MgSO_4$. Yield (4g, 52%). ^{1}H NMR (400MHz, $CDCl_3$, ppm), δ 7.36-7.26 (m, 3H), 0.30 (s, 18H).

4.5.1.5. Synthesis of **4.1.16**

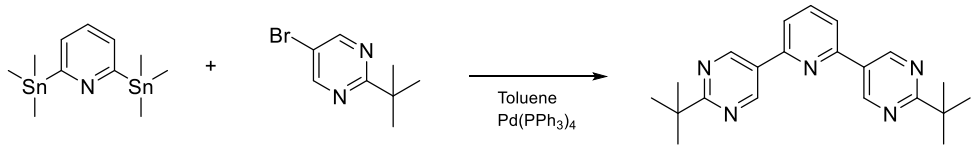

A mixture of 2,6-bistributyltinpyridine (0.54g, 1.32 mmol), 5-bromo-2-tert-butylpyrimidine (0.57g, 2.65 mmol), palladium tetrakistriphenylphosphine (90 mg) and toluene (15 mL) was deairated by bubling argon through the mixture for 5 minutes. The mixture was then heated under reflux for 19 hours. The product was purified by column chromatography (did not evaporate toluene, but added straight from flask, silica gel, (PE/EtOAc 4/1, Rf 0.4, product).

Yield (275 mg, 60%). ^{1}H NMR (400MHz, $CDCl_3$, ppm), δ 9.35 (s, 4H), 7.94 (t, *J*= 8.24Hz, 1H), 7.74 (d, *J*= 8.24Hz, 2H), 1.47 (s, 18H). Melting point = 220-224°C.

4.5.2. Symmetrical Di-anionic Complexes

4.5.2.1. Synthesis of **4.1.4**

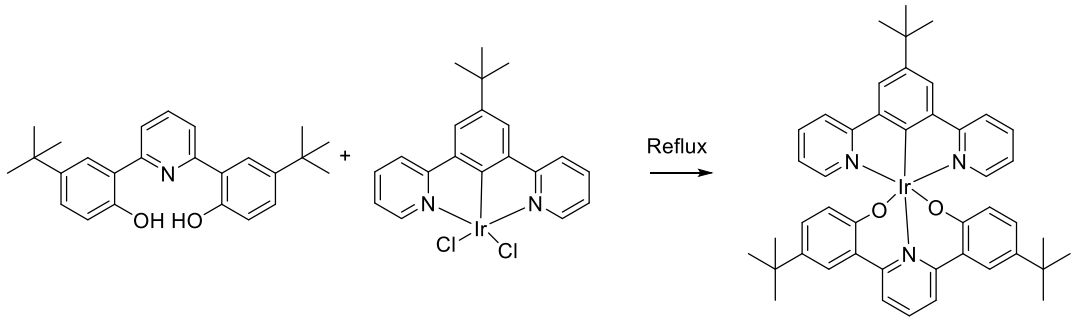

A mixture of K_2CO_3 (0.175g, 1.27mmol), **2.2.13** (0.05g, 0.091mmol) and **3.1.3** (0.041g, 0.109mmol) in 2-ethoxyethanol (30ml) was heated under reflux for 12 hours. Water was added and a red precipitate formed. The complex was purified by column chromatography (fine silica, DCM/EA/MeOH, 20:2:1). The relevant fractions were evaporated to dryness under reduced pressure resulting in an intense red solid. Yield (0.036g, 47%). ^{1}H NMR (400MHz, $CDCl_3$, ppm), δ 8.14-7.95 (m, 3H), 7.78 (s, 4H), 7.73 (t, *J*= 6.8Hz, 2H), 7.60 (d, *J*= 2.3Hz, 2H), 7.41 (t, *J*= 7.8Hz, 2H), 6.72 (dd, *J*= 6.4, 2.3 Hz, 2H), 6.57 (t, *J*=6.6Hz, 2H), 6.06 (d, *J*= 8.7Hz, 2H), 1.47 (s, 9H), 1.25 (s, 18H). HRMS (ESI) calculated for $C_{45}H_{46}IrN_3O_2$ $([M+H])^+$= 854.32920. Found m/z = 854.32898.

4.5.2.2. Synthesis of **4.1.7**

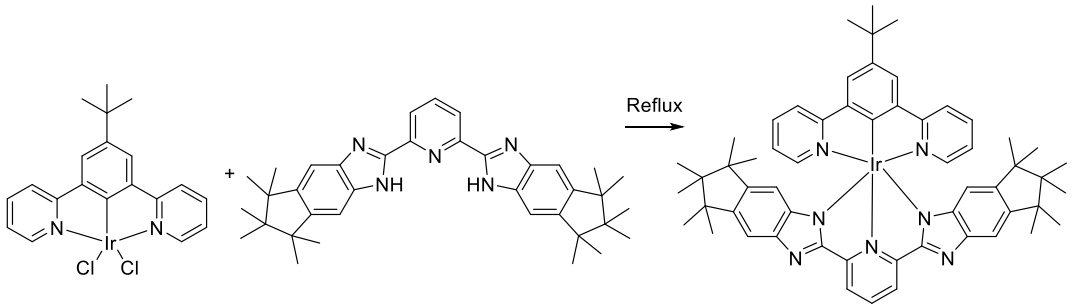

2-ethoxyethanol (20ml) was stirred and heated gradually with potassium carbonate (0.2g, 1.447mmol). **2.2.13** (0.100g, 0.181mmol) was added to the solution and stirred. The ligand, **4.1.6** (0.121g, 0.217mmol) was added to the mixture and the reaction was heated under reflux for 16 hours. Water (10ml) was added and the yellow precipitate was filtered off. The solid was purified by column chromatography (fine silica, DCM/EA/MeOH, 5:1:1). The relevant fractions were evaporated to dryness under reduced pressure, resulting in an orange solid. Yield (0.115g, 61%). ^{1}H NMR (400MHz, $CDCl_3$, ppm), δ 8.31 (d, *J*= 7.6Hz, 2H), 8.16 (s, 4H), 7.89 (d, *J*= 7.8Hz, 2H), 7.48 (t, *J*= 7.8Hz, 2H), 6.72 (t, *J*= 6.4Hz, 2H), 5.62 (s, 2H), 1.68 (s, 12H), 1.09 (s, 12H), 0.83 (s, 12H), 0.70 (s, 12H). HRMS (ESI) calculated for $C_{57}H_{62}IrN_7$ $([M+H])^+$ = 1038.47687. Found m/z= 1038.46924.

4.5.2.3. Synthesis of **4.1.10**

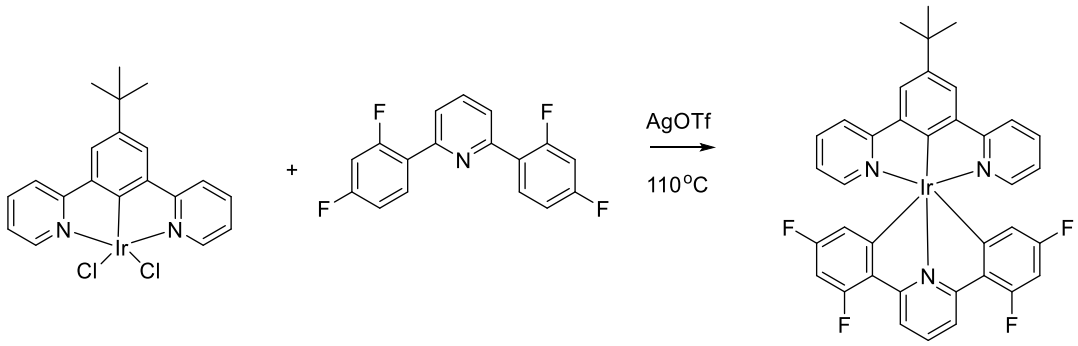

2.2.13 (0.068g, 0.124mmol), bis(2,4-difluorophenyl)pyridine (0.376g, 1.24mmol) and AgOTf (0.068g, 0.264mmol) were ground together in a porcelain mortar. The resulting powder was then heated at 110°C for 24hours. Fine needles of bis(2,4-difluorophenyl)pyridine had sublimed and removed. The remaining solid was washed with petrol ether and filtered prior to purification by column chromatography (fine silica, PE/Et_2O, 50:1). The solvent was removed under reduced pressure and the resulting orange solid was filtered. Yield (0.033g, 34%). ^{1}H NMR (400MHz, $CDCl_3$, ppm), δ 8.15 (d, *J*= 8.2Hz, 2H), 8.04 (s, 2H), 7.93 (d, *J*= 8.2Hz, 2H), 7.83 (t, *J*= 8.0Hz, 1H), 7.51 (m, 4H), 6.64 (t, *J*= 6.7Hz, 2H), 6.19 (t, *J*= 9.8Hz, 2H), 5.62 (dd, *J*=5.0, 2.3Hz, 2H), 1.61 (s, 9H). HRMS (ESI) calculated for $C_{37}H_{26}F_4IrN_3$= 782.17649. Found m/z= 782.17279

4.5.2.4. Attempted preparation of **4.1.12**

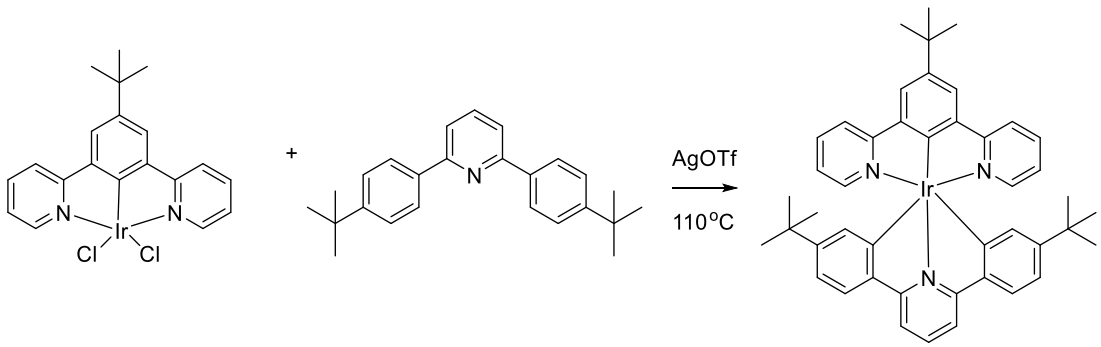

2.2.13 (0.100g, 0.181mmol), **3.2.3** (0.075g, 0.217mmol) and AgOTf (0.102g, 0.400mmol) were ground together in a porcelain mortar. The resulting ground powder was heated to 110°C for 24 hours. Upon the removal of heat, it was noticed the reaction had not occurred. The heat

was applied for a further 24 hours, however the reaction was unsuccessful. The orange powder was dichlorobridged dimer starting material.

4.5.2.5. Attempted preparation of **4.1.17**

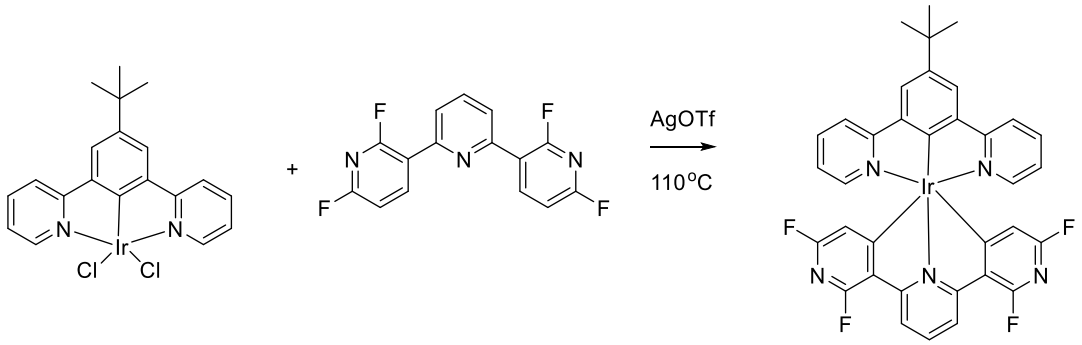

A sample of **2.2.13** (0.05g, 0.091mmol), **4.1.13** (0.277g, 0.91mmol) and AgOTf (0.03g, 0.117mmol) were added to a porcelain mortar and ground together. The resulting orange powder was added to a round bottom flask and heated to 110°C for 24 hours. Upon the removal of heat, it was noticed the reaction had not occurred. The heat was applied for a further 24 hours, however the reaction was unsuccessful. The orange powder was dichlorobridged dimer starting material.

4.5.2.6. Synthesis of **4.2.1**

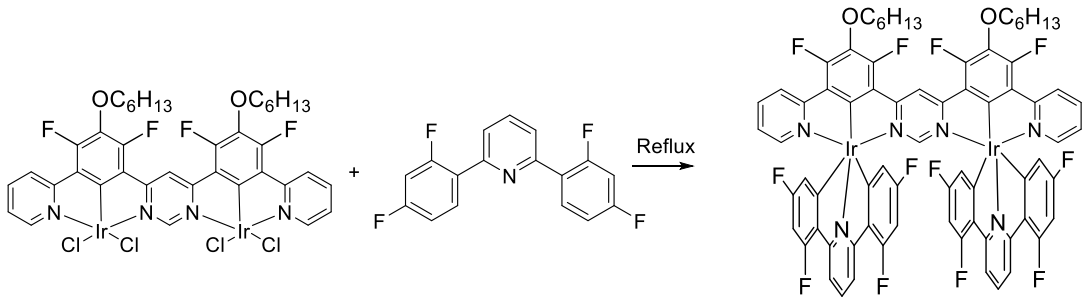

A mixture of **2.1.3** (0.472g, 0.4mmol), bis(2,4-difluorophenyl)pyridine (2.42g, 4mmol) and AgOTf (0.408g, 1.6mmol) were ground thoroughly together in a porcelain mortar. The resulting powder was then heated at 110°C for **4.5**hours. The resulting solid was washed with petrol ether which was decanted before being dissolved in DCM and filtered through celite. The resulting solution was purified by column chromatography (fine silica, DCM). The first intense fraction was collected. Methanol (15ml) was added and the fractions were evaporated

to dryness. The resulting red solid was filtered to give **4.2.1**. (0.288g, 44%). ^{1}H NMR (400MHz, $CDCl_3$, ppm), δ 8.75 (s, 1H), 8.10 (d, *J*= 7.79Hz, 2H), 8.02 (d, *J*= 8.24Hz, 4H), 7.83 (t, *J*= 8Hz, 2H), 7.52 (t, *J*= 7.79Hz, 2H), 7.35 (d, *J*= 5.50Hz, 2H), 7.08 (s, 1H), 6.68 (t, *J*= 7Hz, 2H), 6.17 (t, *J*= 9.52, 4.62Hz, 4H), 5.43 (dd, *J*= 6.89, 2.29Hz, 4H), 4.27 (t, *J*= 6.65Hz, 4H), 2.02 (quin, *J*= 6.87Hz, 4H), 1.70 (br.quin, *J*= 7.33Hz, 4H), 1.50 (m, 8H), 1.05 (t, *J*= 6.87Hz, 6H) . ^{19}F NMR (376MHz, $CDCl_3$), -109.1 (s, *J*= 9.19Hz), -109.3 (s, *J*= 9.19Hz), -121.5 (d, *J*= 16.1Hz), -122.1 (d, *J*=16.1Hz). Elemental Analysis: Calculated values: C 52.61%, H 3.07%, N 5.11% Obtained values: C 52.70%, H 3.30%, N 5.00%. HRMS (ESI): calculated for $C_{72}H_{50}F_{12}Ir_2N_6O_2$ ($[M+H]^+$)= 1645.31349. Found m/z= 1645.30066.

*Due to coupling with fluorides, the ^{13}C NMR was not fully assigned.

4.5.2.7. Synthesis of **4.2.2**

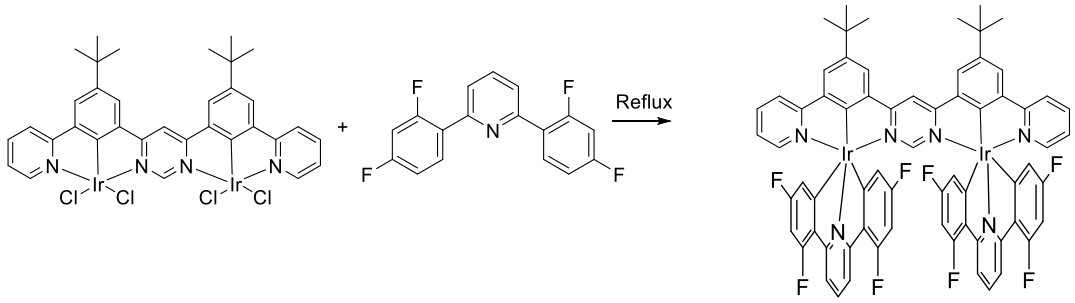

A sample of **2.2.14** (0.050g, 0.048mmol), bis(2,4-difluorophenyl)pyridine (0.296g, 0.977mmol) and AgOTf (0.048g, 0.048mmol) were ground together in a porcelain mortar. The resulting powder was then heated at 110°C for 24hours. Fine needles of bis(2,4-difluorophenyl)pyridine had sublimed and were removed. The remaining solid was washed with petrol ether which was filtered off before being purified by column chromatography (SiO_2, PE/Et_2O, 50:1). The relevant fractions were evaporated and the resulting blue solid was filtered. Yield (0.015g, 21%). ^{1}H NMR (400MHz, $CDCl_3$, ppm), δ 8.27 (s, 1H), 8.22 (d, *J*= 1.2Hz, 2H), 8.03 (d, *J*= 8Hz, 2H), 8.01 (d, *J*= 1.6Hz), 7.88 (d, *J*= 8Hz, 2H), 7.79 (t, *J*= 8.2Hz, 2H), 7.48 (ddd, *J*= 7.6, 1.2Hz, 2H), 7.37 (d, *J*= 6Hz, 2H), 7.09 (s, 1H), 6.62 (dd, *J*= 6, 1.4Hz, 2H), 6.10 (t, *J*= 10, 2Hz, 4H), 5.35 (dd, *J*= 4.4, 2.4Hz, 4H), 1.62 (s, 9H), 1.53 (s, 9H). HRMS (ESI) calculated $C_{68}H_{46}F_8Ir_2N_6$= 1485.29874. Found m/z= 1485.29236.

CHAPTER 5

Alteration to the Linking Heterocycle from Pyrimidine to Thiazolo[5, 4-d]-thiazole

5. Alteration to the Linking Heterocycle from Pyrimidine to Thiazolo-[5, 4-d]-thiazole

All ditopic bis-terdentate bridging ligands and their complexes described so far contained pyrimidine as a central linking heterocycle. In this chapter we present new bridging ligands that employ thiazolo[5,4-d]thiazole (TzTz) as the linking heterocycle as shown in Figure 101. Although TzTz units are commonly applied in organic electronics as robust heterocycles with an extended π-system, there are only a few examples of corresponding metal complexes of which none are luminescent.[187-189] The switch from pyrimidine to thiazolo[5,4-d]thiazole caused considerable change to the geometry of the complexes and eliminate a problem of steric hindrance between auxiliary ligands. It was also expected that this change would affect the photophysical properties by providing an additional tool in tuning photophysical properties of dinuclear complexes.

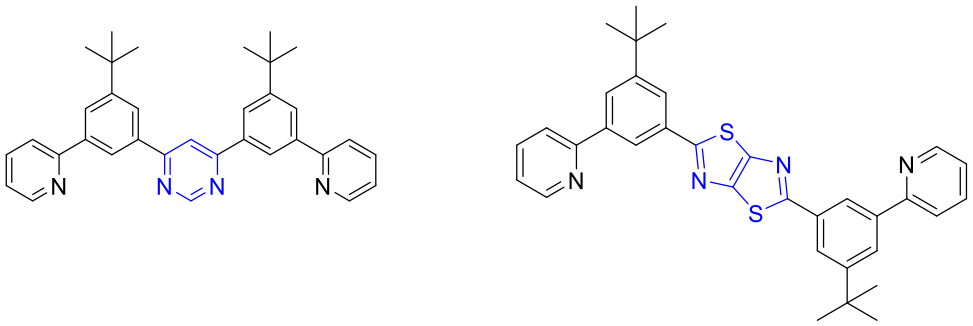

Figure 101 - The difference in bridging ligand brought about by the change in linking heterocycle from pyrimidine to TzTz.

Thiazole is a well-known heterocycle that is capable of replacing pyridine in cyclometalated complexes. For example Lamansky *et al* reported a series of cyclometalating complexes employing benzothiazole.[20] The ligands described often used benzothiazole as a derivative and the resulting heteroleptic complexes showed promising results (λ_{max}= 557nm, ϕ= 0.26, τ = 1.80μs at 298K), these luminescent properties are matched and result in a range of PLQY values between ϕ= 0.16-0.6 dependent on the substituents present.

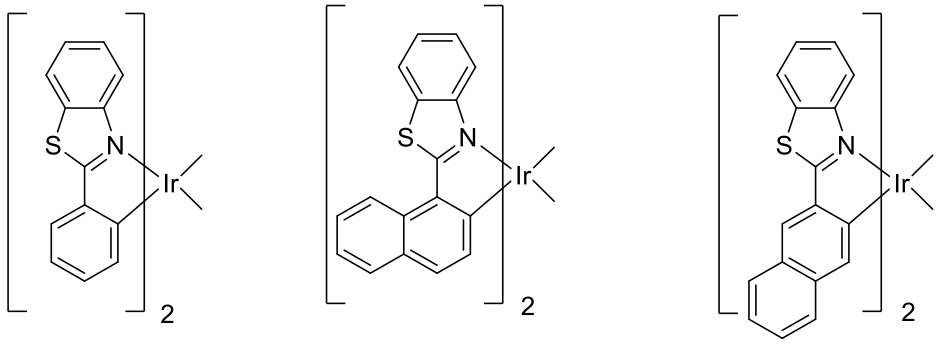

1.2.59
$Ir(bt)_2(acac)$
λ_{max}= 557nm
ϕ = 0.26
τ= 1.80μs

1.2.60 A
$Ir(\alpha bsn)_2(acac)$
λ_{max}= 606nm
ϕ = 0.22
τ= 1.80μs

1.2.60 B
$Ir(\beta bsn)_2(acac)$
λ_{max}= 594nm
ϕ = 0.16
τ= 2.20μs

Figure 102 - The structures of the thiazole based bis-cyclometalated heteroleptic complexes described by Lamansky *et al*. The structural changes show a distinct effect on the photoluminescent properties.[20]

The promising properties of the thiazole group in iridium (III) complexes was further supported by Park *et al* which showed that the strong Ir-C bond provides rigidity and high polarizability from the basicity of the sulphur atom which increases the overall stability.[84] A different study by Gras *et al* investigated the use of thiazole in bipyridine type coordinating ligands with ruthenium (II) as the central atom. The focus of the study was to develop complexes in the formation of anti-cancer drugs. The complexes showed red shifted phosphorescence as described by Park *et al* and were converted to PF_6 salts, a commonly used strategy in charged complexes.[190] Despite describing the red shift in luminescence, no additional photophysical properties were described.

The design of our systems is inspired by dinuclear complexes reported by Steel *et al* who first described the synthesis of dinuclear copper and ruthenium complexes that utilised TzTz as a linking group. The complexes developed in the study formed diastereomers in *meso* and *rac* forms due to the use of $[Ru(bpy)_2Cl_2]$ as a precursor denoted in the study as $\Delta\Delta/\Delta\Lambda$. The photoluminescent properties of the resulting complexes were not tested. However the study provided the successful synthesis of novel dinuclear TzTz linked complexes.[188]

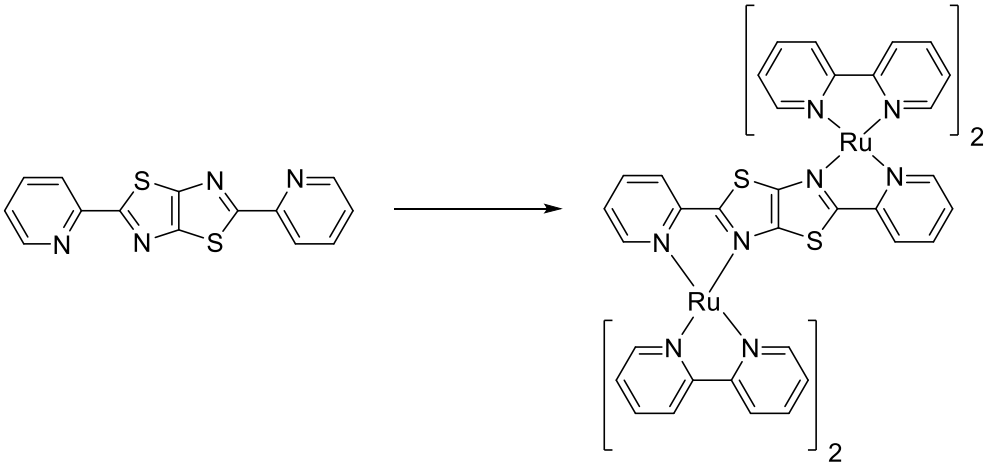

5.0.1 **5.0.2**

Steel *et al*, 2004

Figure 103 - The structure of the TzTz bridging ligand and the derived complex described by Steel *et al*, the photophysical properties of the complexes in the paper were not tested.

A complementary study by Steel and co-workers further investigated the synthesis of TzTz bridging ligands in which the arrangement of the binding sites is described as "stepped-parallel".[188]

To eliminate the problem associated with chirality of bidentate systems, the study outlined the first example of a tridentate coordinating bridging ligand using TzTz as the linking heterocycle. The ligand uses a terpyridine coordination mode and was obtained in a high yield (61%). However the coordination behaviour of the ligand was not investigated and metal complexes were not obtained.[187]

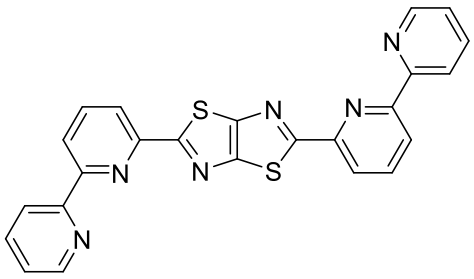

5.0.3
Steel *et al*, 2006

Figure 104 - The structure of the terpyridyl TzTz linked bridging ligand described by Steel *et al*.

An additional investigation into the use of TzTz linking groups was described by Maes *et al* and outlines the encouraging potential for the use of TzTz groups in the development of semiconductors for plastic electronics and OLED devices.[191]

In addition, Beves *et al* described the use of TzTz linkers for the one-pot synthesis of a molecular Solomon link. The ligands described used bis-terpyridyl binding modes and the crossing points within the link was defined by the coordinating metal (examples include zinc (II), copper (II) or cobalt (II)).[189]

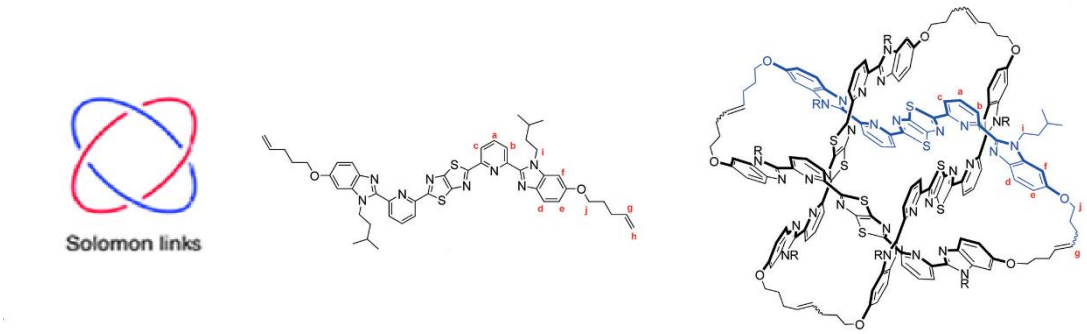

Figure 105 - The documented structure of a Solomon link described by Sauvage and Chambron (left).[192] The structure of the TzTz bridged ligand described by Beves *et al* (centre) is shown next to the synthesised Solomon link structure (right) where the R groups are isopentyl. The structure on the right does not include the coordinated zinc (II) centres.[189]

To the best of our knowledge there are currently no examples of luminescent TzTz bridged dinuclear complexes described in literature. The first example of a cyclometalated luminescent TzTz complex was prepared by the Kozhevnikov group. The complex used the bis-bidentate bridging ligand in complex **5.0.4** (shown in Figure 106) as a means of linking the two metal centres. The intense luminescence shown by **5.0.4** encouraged further investigation into the preparation of TzTz based complexes. The results of the investigation are described in this chapter.

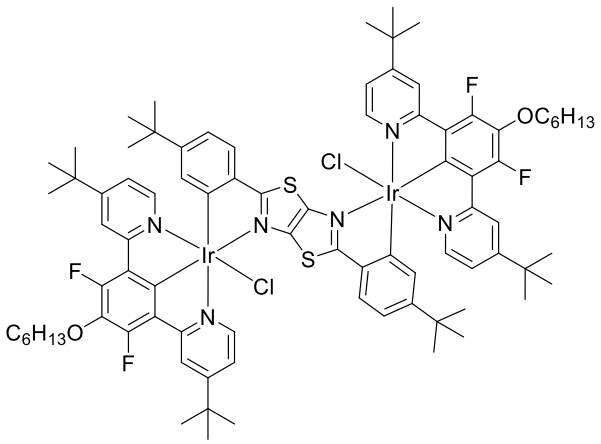

5.0.4

Figure 106 - The structure of the first cyclometalated TzTz linked complex previously prepared by the Kozhevnikov group.

5.1. Synthesis of the TzTz Linking Heterocycle and Di-nuclear Complexes

The main synthetic route to TzTz systems is a condensation of dithiooxamide with aldehyde firstly reported by Ketcham *et al* in 1960. Although other methods have also been developed, the Ketcham method is still most commonly used.[153] The synthesis of the bridging ligand was carried out by using similar route and depicted in Scheme 28. The aldehyde **5.1.1** was prepared by treatment of 1,3-dibromo-5-*tert*-butylbenzene with *n*-BuLi, followed by the addition of DMF. **5.1.1** was reacted with dithiooxamide to give highly insoluble dibromo intermediate **5.1.2** (53%). Despite low solubility, this intermediate was reacted with 2-(tributylstannyl)pyridine in a Stille cross-coupling reaction which produced the final ligand in 58% yield. The purification of **5.1.3** was carried out by recrystallization from DMF. It should be noted that the ligand is not soluble in most solvents (such as MeOH, DCM and diethyl ether).

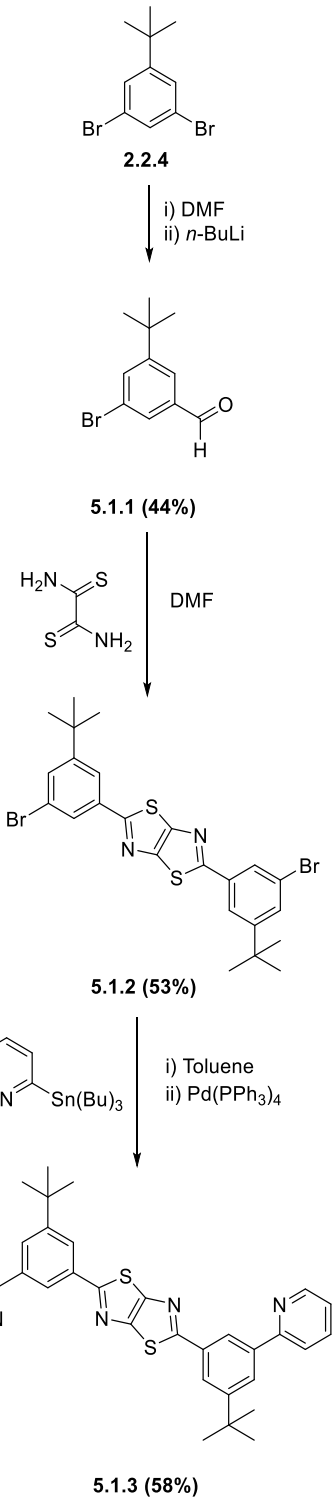

Scheme 28 – Synthesis of novel bridging ligand **5.1.3** containing TzTz linking heterocycle.

The ligand, **5.1.3**, was used in the synthesis of di-iridium complexes. However, this synthesis proved to be very challenging and many initial attempts were unsuccessful. We attributed these difficulties to a very low solubility of the ligand in 2-ethoxyethanol. We found that it is

crucial to dissolve the ligand prior to the addition of iridium chloride. In the successful reaction the ligand was boiled in 2-ethoxyethanol until complete dissolution and only then the iridium chloride hydrate was added. After heating under reflux for 18 hours the deep red solid was isolated in high yield (80~92%). The synthesised dichlorobridged dimer is highly insoluble. This can be explained by the possibility of polymer formation through the chlorine bridges between the iridium centres. In order to prove that cyclometalating took place we used DMSO to cleave the chloride bridge between the iridium atoms and thus destroying polymer structure. The solubility of the corresponding DMSO complex dramatically increased in most solvents (such as dichloromethane, methanol and diethyl ether) and we were able to isolate the product **5.1.5** using column chromatography. The aromatic region of the ^{1}H NMR (in DMSO-d6) of **5.1.5** is depicted in Figure 108 with all signals assigned to the structure.

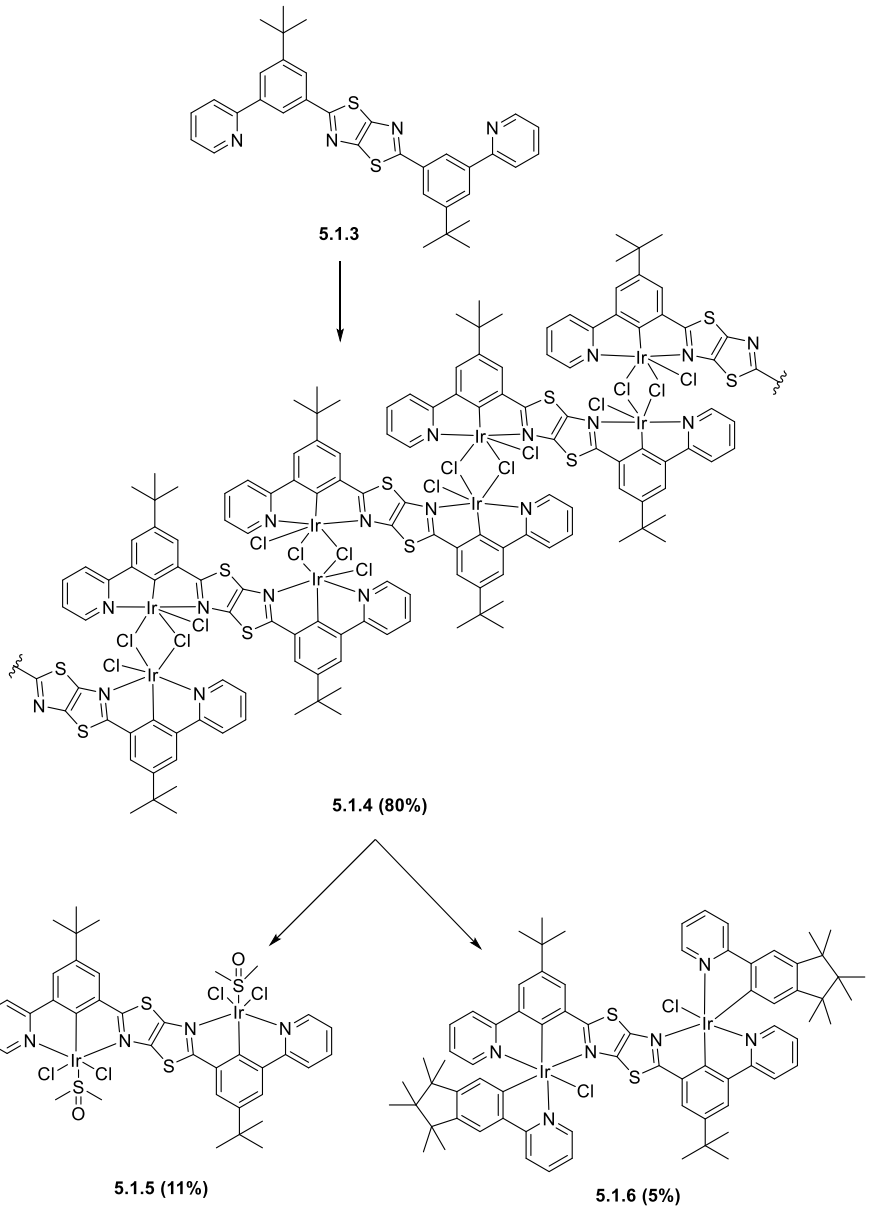

Scheme 29 - The reaction scheme for the preparation of the TzTz complexes, **5.1.5** and **5.1.6**.

Interestingly the DMSO complex, **5.1.5** showed luminescence, which is not typical of DMSO based complexes. The sample of **5.1.5** was tested using the fluorimeter for excitation and emission wavelengths, giving an indication of the region of emission.

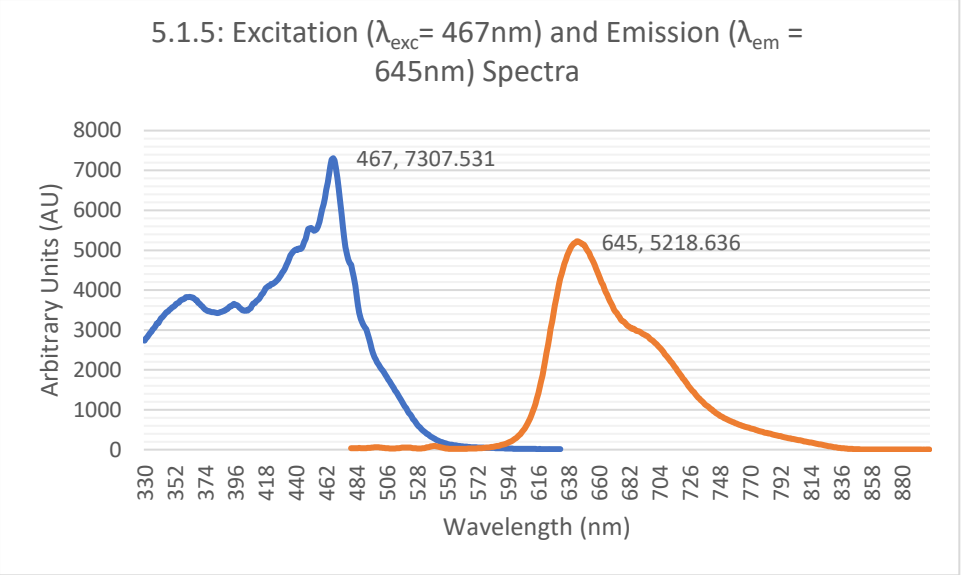

Figure 107 - The excitation (blue) and emission (orange) spectra of **5.1.5** in acetonitrile.

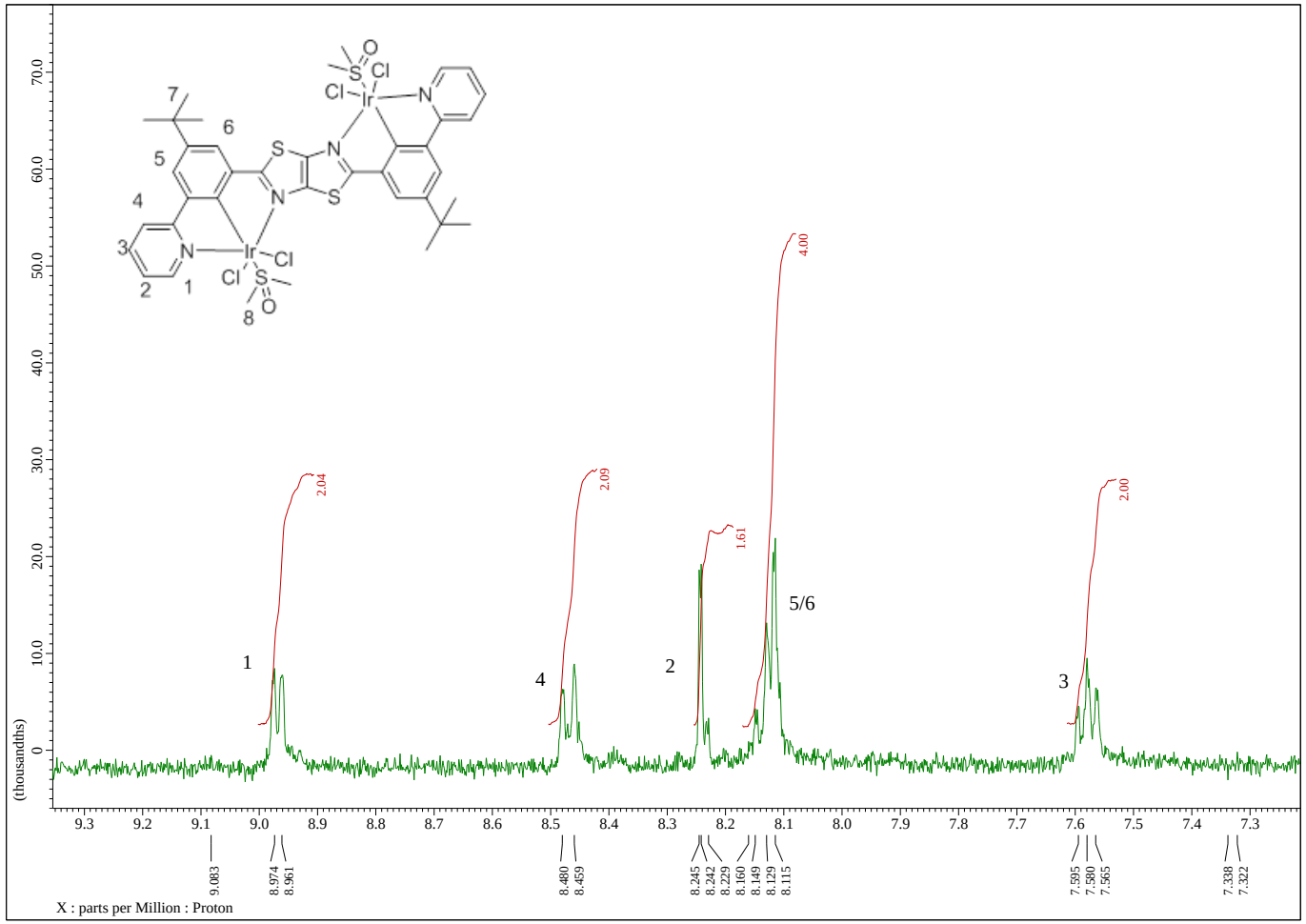

Figure 108 - The aromatic zoom of the ^{1}H NMR for **5.1.5** in DMSO-d6, the structure of the DMSO complex is overlaid and numbered. The peaks of the ^{t}Bu group (7) is present at δ1.45ppm as a singlet. The –CH_3 peak in DMSO (8) is present at δ2.95ppm as a singlet.

Following the synthesis of the DMSO complex, the dichlorobridged dimer was used to synthesise the TzTz analogue of **2.2.2**, the complex **5.1.6**. The cyclometalation was carried out as a follow up to the promising luminescent properties of **5.1.5**. Using previously described conditions, the dichlorobridged dimer was heated in toluene with silver triflate. Following the dissolution of the dimer, the ligand was added and the reaction as heated under reflux for 18 hours. Hydrochloric acid (2M) was added to replace missing chloride atoms, and the aqueous layer was removed. The resulting organic layer was filtered through celite which produced an intense red filtrate. The complex was purified through column chromatography (DCM/MeOH, 10:1). TLC showed a single spot with an R_f value of ~0.8, this product was isolated through column chromatography (DCM/EtOAc, 10:1) in very low yield (5%). The ^{1}H NMR of the product, **5.1.6**, is shown in Figure 109. The spectrum shows the presence of one set of signals of either the *meso* or *rac* isomers. At this point it is difficult to predict the exact configuration. In order to confirm the identity of the isomer, HPLC or the use of chiral columns would be required to separate the *meso* and *rac* forms. An alternative and regularly used strategy for isomer identification is the use of X-ray crystallography which would give the definitive structure of the complex. The proton NMR is shown below with the overlaid numbered structure.

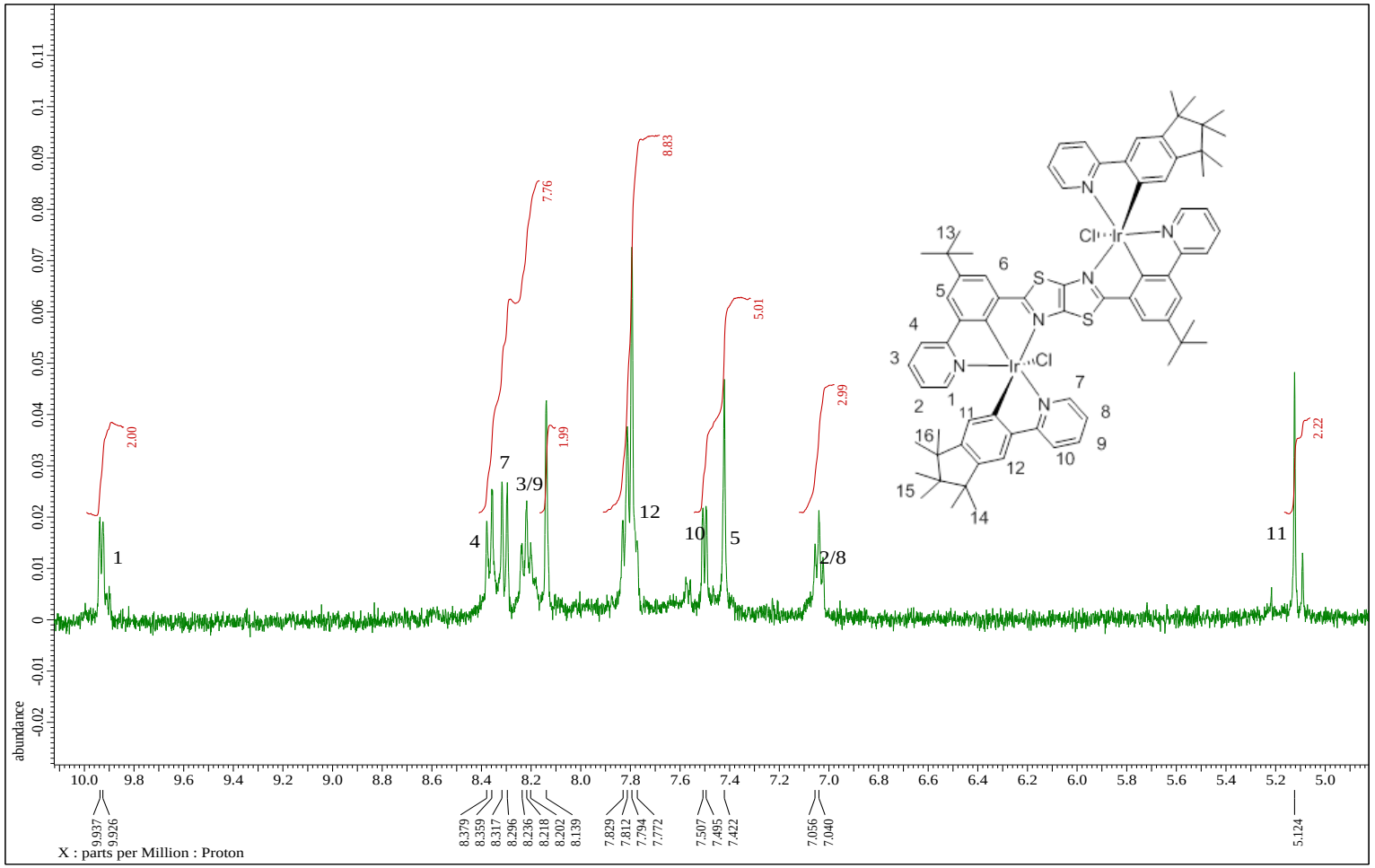

Figure 109- The aromatic zoom of the ^{1}H NMR for **5.1.6** in DMSO-d6, the numbered structure is overlaid and corresponds to the numbered peaks. The methyl groups present on the cyclopentane (14-16) group are shown at δ0.46, 0.83 and 0.92ppm respectively. The ^{t}Bu group on the bridging ligand (13) is present at δ1.46ppm.

No other products of a sufficient purity were isolated following chromatographic purification. The product was confirmed by ^{1}H NMR and exhibited little/no luminescence to the eye under exposure to UV light. The complex was tested further using fluorimetry which will be discussed in section 5.2.

5.2. The influence of the linking TzTz heterocycle on photophysical properties

The change of linking heterocycle from pyrimidine to TzTz was expected to lead to a change in the emission wavelength due to the increased level of conjugation in the structure. This would result in a red shift of the emission, due to the increase in stability and rigidity of the compound. Dinuclear complexes **2.2.2** and **5.1.6** only differ by the linking heterocycle and therefore will provide the clear picture of the influence of the linking unit on photophysical properties. Unfortunately, due to time constraints we only perfomed relatively simple experiments and did not perfomed any computational analysis.

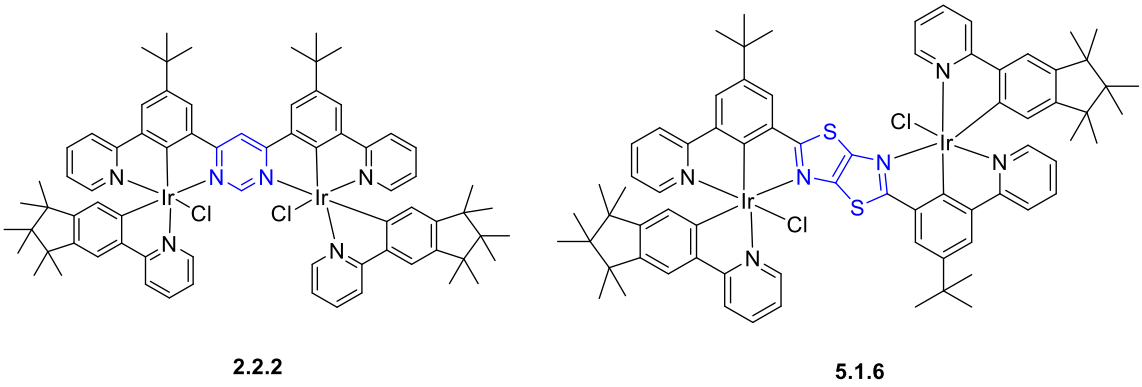

Figure 110 - The structures of both **2.2.2** (pyrimidine linked) and **5.1.6** (TzTz linked).

Both complexes are soluble in toluene and this solvent had been chosen for the photophysical characterisation of two complexes. Figure 112 shows the emission and excitation spectra for pyrimidine-linked **2.2.2** and TzTz-linked **5.1.6**.

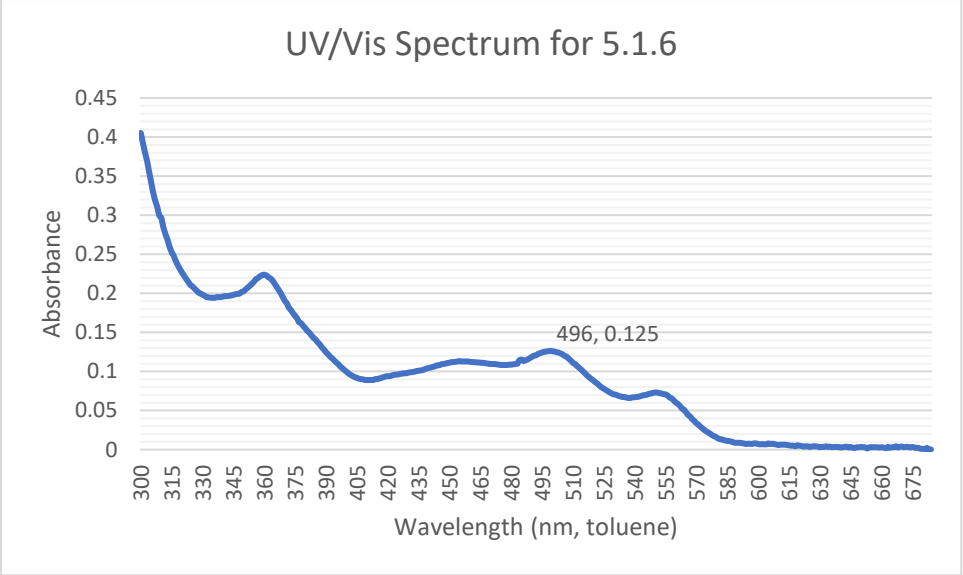

Figure 111 - The UV/Vis spectrum for **5.1.6**, showing that the complex absorbs at λ_{max}= 496nm and the corresponding absorbance (A) in toluene. The extinction coefficient for this sample was ε= 1964588.780 L mol^{-1} cm^{-1} (c= 1 mg ml^{-1}, L=1cm). This molar absorption value is lower than previous samples.

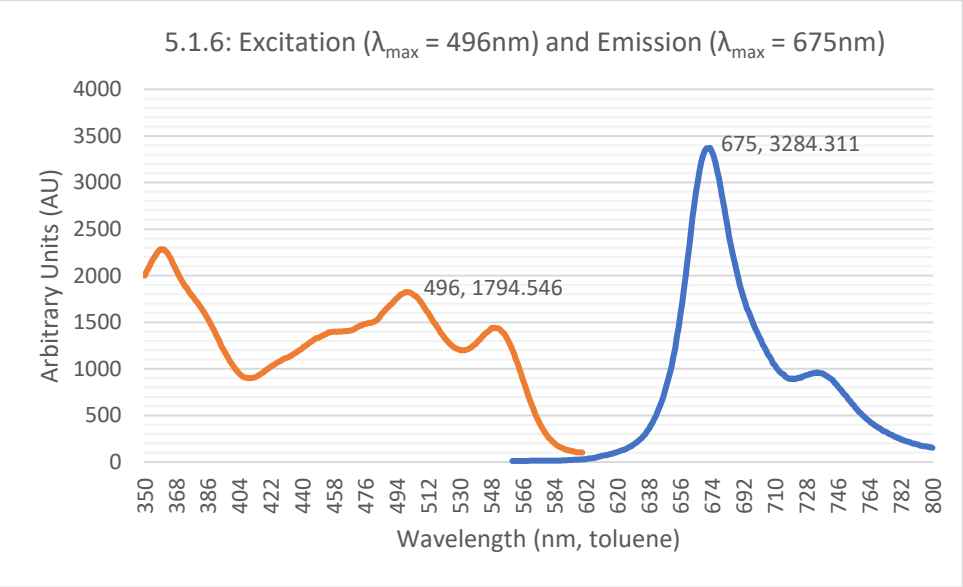

Figure 112 - The excitation (orange) and emission (blue) spectra of **5.1.6** in toluene, the complex was excited at λ_{max} 496nm and showed a significantly red shifted emission at λ_{max} 675nm.

It is immediately apparent that the switch from pyrimidine to TzTz unit caused significant red shift in emission. The emission maximum of **5.1.6** is at λ_{max}= 675nm manifesting a red-shift of emission of about 45nm in comparison to **2.2.2** (λ_{max}= 631nm). The nature of this shift could be attributed to increased π system of TzTz over the pyrimidine. However, more in-depth studies are required in order to obtain a more detailed picture. According to energy-gap law,

the considerable red shift of the emission is likely to result in a substantial reduction in quantum yield. However, many dinuclear systems developed previously showed remarkable resistence to energy-gap law offering quantum yields of nearly unity for red emission. It can be seen that 0-0 emission band has much higher intensity than 0-1 band, which is indicative of a very rigid nature of **5.1.6** and may be beneficial to the quantum yield. The most commonly used standard for quantum yield measurements is $Ru(bpy)_3$, however this was unfortunately not available in the lab, this analysis was limited by time and prevented further analysis. This will be accomplished in the follow-up studies.

In conclusion, we successfully prepared a novel bis-terdentate cyclometallating bridging ligand that incorporates TzTz linking heterocycle. The synthesis of the dinuclear complexes was very challenging, presumably due to the insoluble nature of the ligands and intermediates. The targeted dinuclear iridium complex **5.1.6** was prepared, albeit very low yield. We showed that the switch from pyrimidine to TzTz linking unit caused significant (45nm) red-shift in emission, which is of interest for the development of NIR emitters. More in depth studies are still required to assess the efficiency of these systems as phosphorescent emitters in OLEDs.

5.3. The Use of Alternative Bridging Ligands Based on the TzTz Heterocycle

In previous sections, a single type of ditopic bridging ligand, namely a bis N^C^N system with pyrimidine as a bridging heterocycle was used. Prompted by the successful synthesis of TzTz based bridging ligands, we prepared two unprecedented bridging ligands containing two ONN binding sites. Although, outside the timeline of this project, these ligands can be potentially used in the synthesis of neutral di-iridium complexes by using dianionic auxiliary ligands. An example structure of such complex (**5.3.3**) is given in Figure 113.

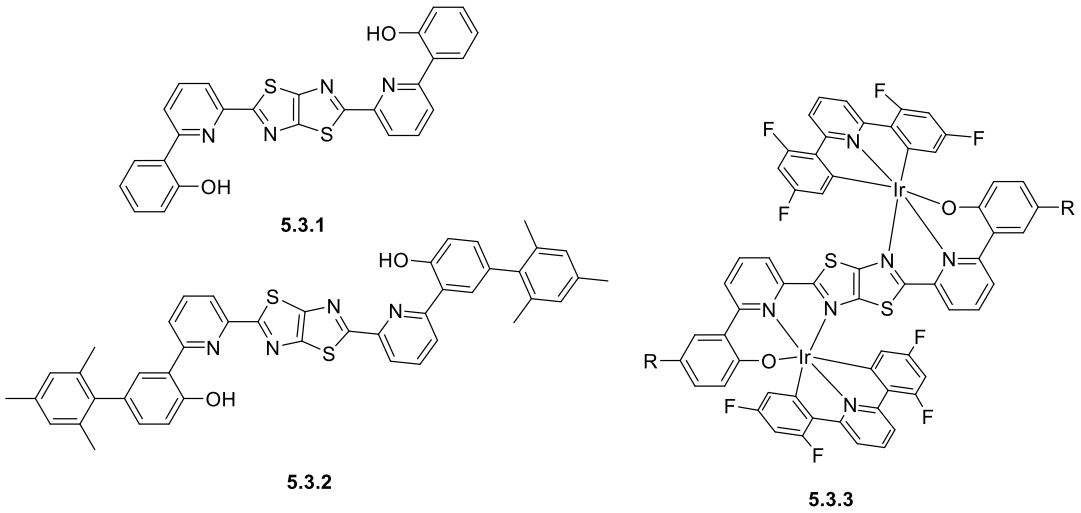

Figure 113 - The model structures of the two novel bridging ligands utilising the TzTz linking heterocycle. (left). The general structure of a potential neutral complex for OLED applications (right).

The synthesis of the initial bridging ligand was prompted by the successful synthesis described above. The synthesis of the bridging ligand **5.3.1** is depicted in Scheme 30. Starting with 6-bromopyridine-2-carbaldehyde, the first intermediate was synthesised through a Suzuki cross coupling with (2-methoxyphenyl)boronic acid. The product was synthesised in average yields and formed a white crystalline solid (52%). The white crystalline solid can be purified through trituration with petroleum ether, the purity level can then be improved further through column chromatography. The aldehyde intermediate was heated in anhydrous DMF with dithiooxamide, resulting in the methyl ether product. The formation of the TzTz linking heterocycle typically drastically reduces the solubility of the compound in many solvents.[193] To deprotect the methyl ether intermediate, two methods were attempted. The first method used was a solid melt with pyridine hydrochloride, a deprotection route previously described to produce a phenolic functional group. This route did not yield product as the methyl protected starting material did not dissolve in the pyridine melt. Another method used, similar in principle, utilised sulfolane with pyridine hydrobromide.[194] The methyl protected intermediate was heated with sulfolane with pyridine hydrobromide at 150°C overnight before being cooled to 80°C. Water was added gradually over a 20 minute period, forming an off white precipitate in good yields (~85%).

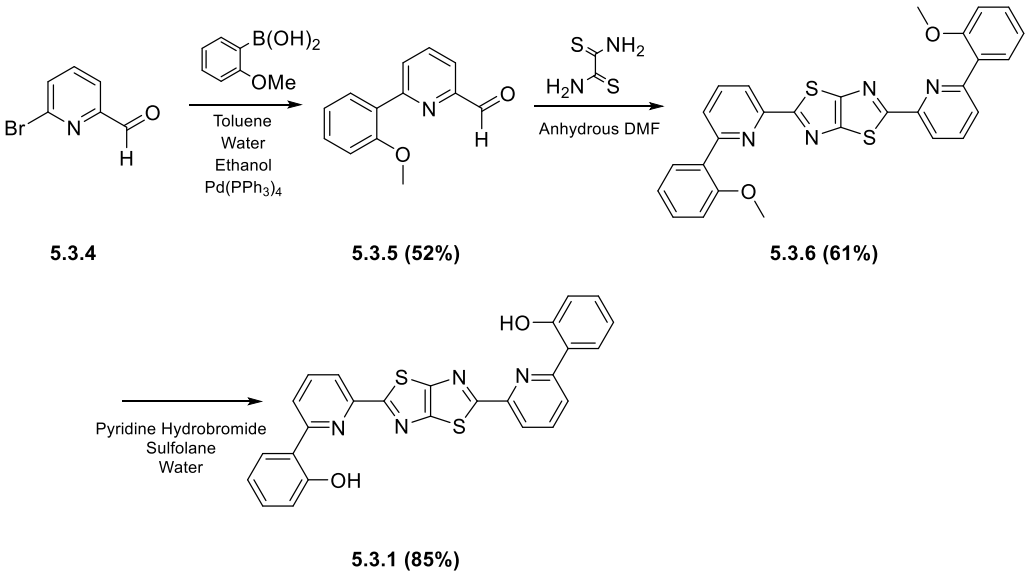

Scheme 30 - The reaction scheme followed to synthesise **5.3.1**.

The deprotection of the bridging ligand resulted in a highly insoluble product, which is problematic for the synthesis of metal complexes.

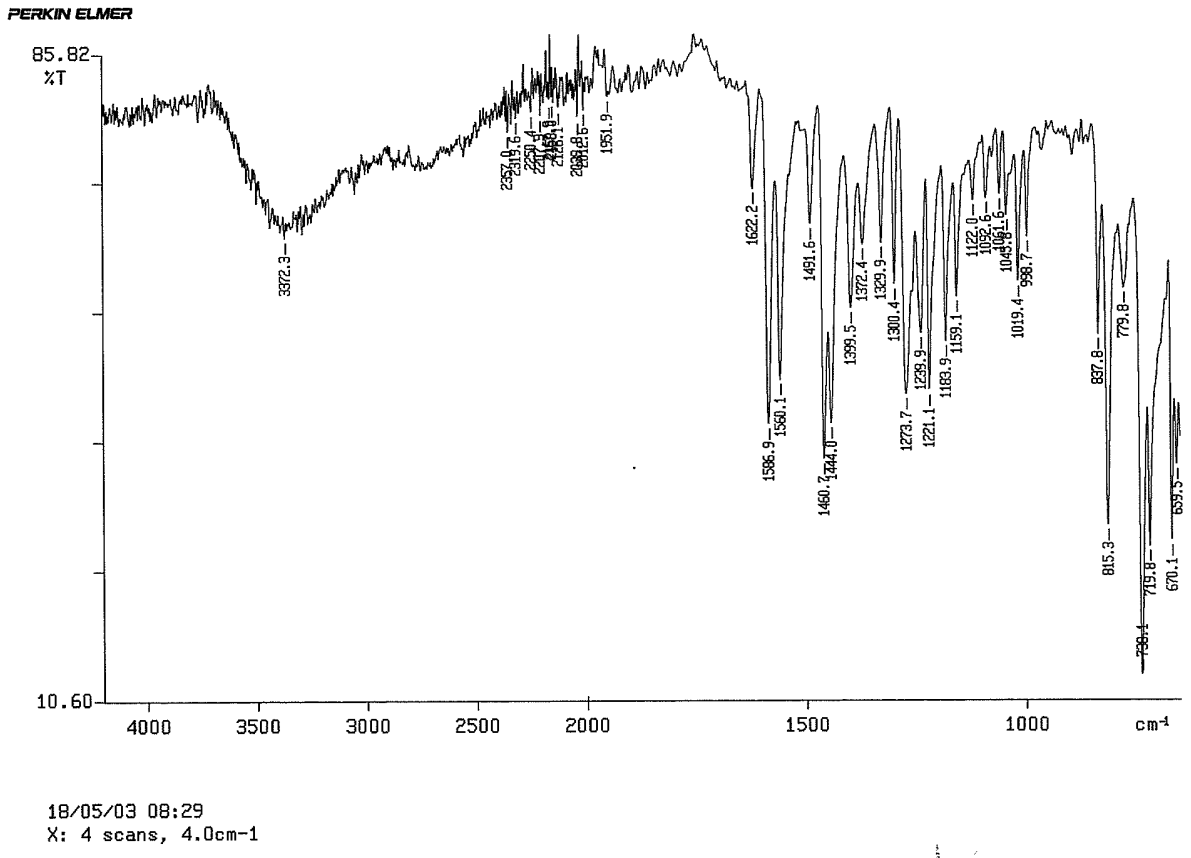

Figure 114 - The infrared spectrum for **5.3.1**, the insolubility of the ligand meant that vital characterisation by ^{13}C NMR or mass spectrometry could not be completed. The phenolate group (-OH) can be seen at 3372cm^{-1}.

In order to increase the solubility of the bridging ligand, additional functional groups were added to the structure in place of the phenyl protons, a mesitylene group was substituted (R= Mes). The addition of the mesitylene group increases the solubility through the prevention of intermolecular interaction. Starting with (5-bromo-2-methoxyphenyl)boronic acid, a Suzuki cross coupling was carried out with 6-bromopyridine-2-carbaldehyde to give a bromo derivative in high yields (90%). This product (**5.3.7**) was crystallised from petroleum ether. The bromo intermediate was used for a secondary Suzuki coupling reaction to add the mesityl group. The addition of the mesityl group resulted in **5.3.8** and was achieved in a lower yield (41%). This crystallised upon the addition of petroleum ether and diethyl ether. The remaining impurities were removed through column chromatography (silica, dichloromethane). Using the previously described method, the intermediate was added to anhydrous DMF and heated with dithiooxamide to produce the TzTz linking heterocycle (75%). Upon the addition of water (10ml) a brown precipitate formed, the brown solid was filtered and purified through column chromatography. The solid showed an increased level of solubility in comparison to **5.3.6**. The deprotection of **5.3.9**, was tested using pyridine hydrochloride, which did not result in a successful deprotection of the methyl ether. As the solid **5.3.9** did not melt in the presence of the pyridine hydrochloride, this is likely the reason for the unsuccessful nature of the reaction. Using the previously described method, the deprotection was carried out using sulfolane and pyridine hydrobromide successfully in a good yield (69%). The resulting brown solid was then purified further by recrystallization from methanol.

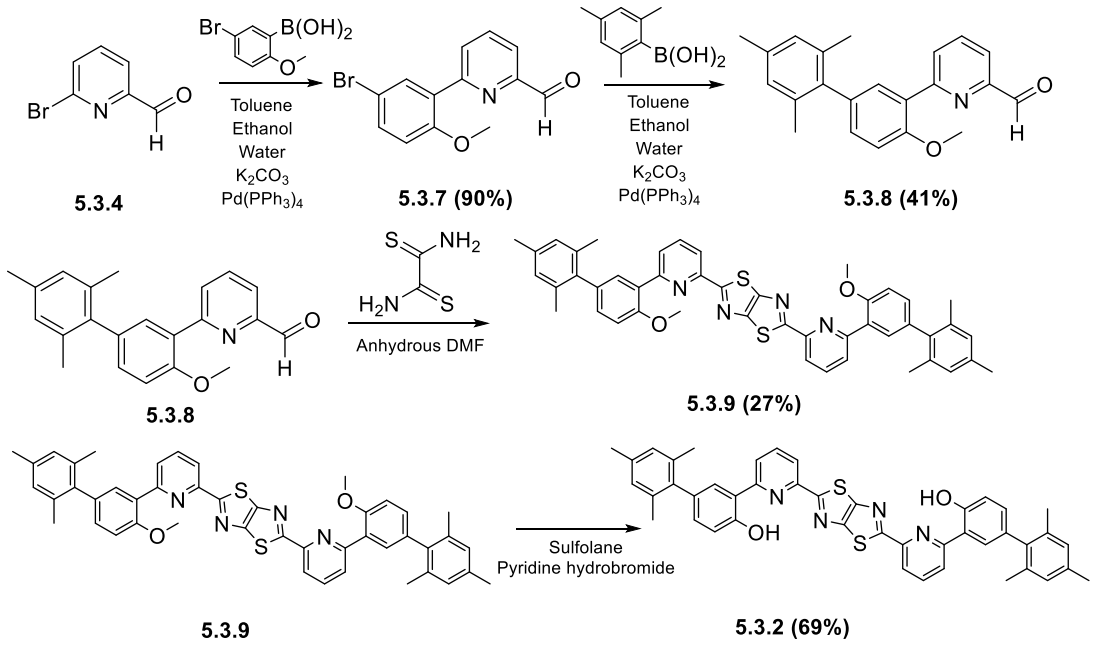

Figure 115 - The synthetic route to develop the novel ligand **5.3.2**, following a similar method to **5.3.1**, the mesitylene group was added prior to the formation of the TzTz linking heterocycle.

The synthetic route to produce **5.3.2**, is a high yielding method with average yields ~70%, the limiting step of the synthesis was the addition of the mesitylene group, some of the product was likely lost during purification and isolation of the product. The optimisation of this step will improve the overall efficiency of the bridging ligand synthesis.

The NNO coordination mode was firstly tested in the synthesis of monometallic complex **5.3.11**. This monocationic complex was successfully prepared by the reaction of di-chlorobridged intermediate **2.2.13** and NNO ligand (**5.3.10**) which was available in the lab.[195] The reaction was carried out in presence of silver triflate (used as a chloride scavenger).

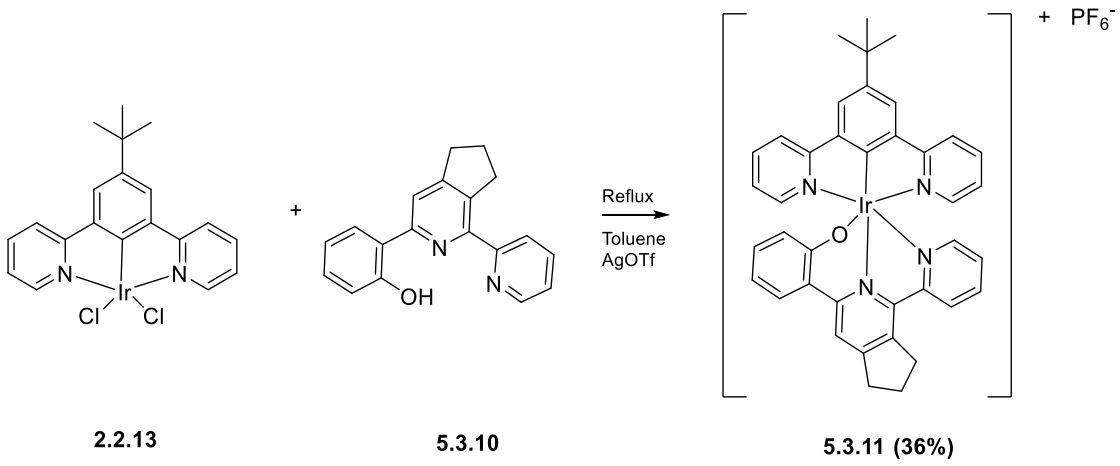

Scheme 31 - The reaction showing the formation of the mono-iridium O^N^N complex **5.3.11**.

Inspired by a successful synthesis of **5.3.11** we used the same reaction conditions in an attempt to prepare corresponding dinuclear complex.

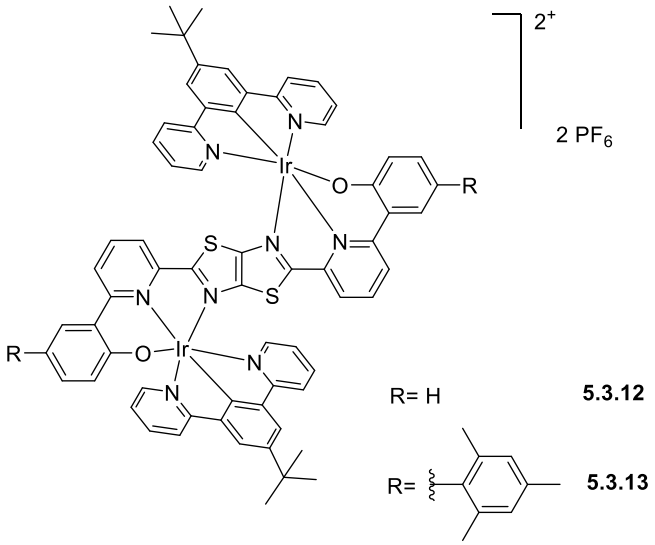

Figure 116 - The general structure of the complexes attempted using the two O^N^N coordinating bridging ligands. Despite multiple conditions tested, the reactions did not yield a product.

As the coordination mode of the bridging ligand is O^N^N, the use of **2.2.13** as a mono-iridium dimer would result in a dicationic complex. The synthesis of the complex was attempted using AgOTf and toluene, a previously outlined method. Unfortunately, however, the reaction was unsuccessful. The failure of the reaction can be attributed to the insolubility of the bridging ligand. The NMR of the product was difficult to acquire due to the high level of insolubility, to verify that the ligand had been successfully deprotected to produce the –OH

group infrared analysis was carried out. The –OH group of the phenolate showed a distinct broad band at ~3100-3300cm^{-1} depicted in Figure 114.

Even the more soluble ligand **5.3.2** did not produce any encouraging results. Using the previously tested conditions of toluene and silver triflate (chloride scavenger). The mono-iridium dimer was stirred in the presence of AgOTf to cleave the monodentate chloride ligands, prior to the addition of the di-topic TzTz linked bridging ligand. The resulting suspension was heated under reflux overnight before being filtered through celite to remove excess silver salts. Upon filtration through celite an orange solution was formed. The solvent was removed and a crude proton NMR was carried out. The ^{1}H NMR showed that there was no distinct peaks to indicate the presence of the desired complex as the spectrum was predominantly comprised of starting materials.

Unfortunately, due to time constrains no further investigation of the coordination behaviour of two novel bridging ligands **5.3.1** and **5.3.2** was carried out. This will be a subject of follow-up research within the group. The development of complexes using a bridged auxiliary ligand could be of huge benefit and the investigation into different coordination modes would open up new avenues into the development of near-IR emitters both of neutral and cationic nature.

5.4. Conclusions

The major achievement of the research described in this chapter is the synthesis of two unprecedented ditopic bisterdentate ligands that contain the TzTz linking heterocycle. The ligands will undoubtedly be of interest for scientific society due to their relatively simple tuning capability. The adaptation of the ligand structures means that a wide range of photophysical and chemical properties can be targeted. However, their coordination behaviour remains largely unexplored and will require further in-depth studies.

5.5. Experimental

5.5.1. TzTz linked Bridging Ligands

5.5.1.1. Synthesis of **5.1.1**.

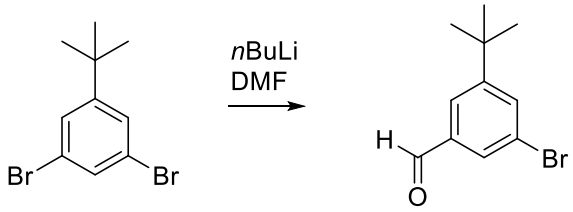

To a flask of 1,3-dibromo-5-(tert-butyl)benzene (5.5g, 19mmol) in dry THF (50ml), *n*Bu-Li (1.6M in hexanes, 10ml, 16mmol) was added and cooled to -78°C under an argon atmosphere. The solution was stirred at -78°C for 1 hour. DMF (2.1g, 28.3mmol) was added slowly and the solution was stirred for 3 hours at -78°C before being warmed to RT and quenched with saturated NH_4Cl (30ml) and extracted with ethyl acetate. The organic layer was washed with brine and dried over sodium sulphate before being filtered. The filtrate was evaporated to dryness under reduced pressure and purified using column chromatography (fine silica, petroleum ether). Solvent was removed under reduced pressure, resulting in a clear oil. Yield (2.02g, 44%). ^{1}H NMR (400MHz, $CDCl_3$, ppm), δ 9.94 (s, 1H), 7.76 (s, 2H), 7.73 (d, *J*= 1.6Hz, 1H), 1.34 (s, 9H).

5.5.1.2. Synthesis of **5.1.2**.[187, 196]

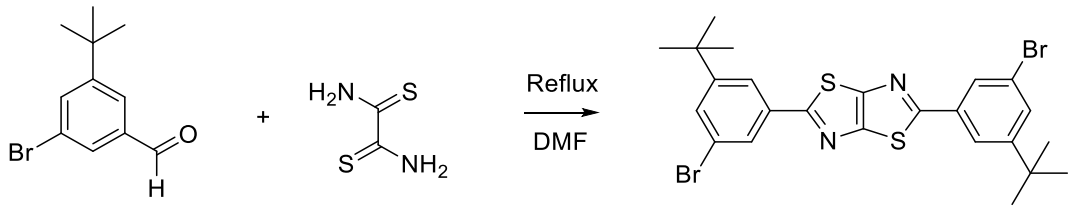

3-bromo-5-tert-butylbenzaldehyde (2.02g, 8.377mmol) and dithiooxamide (0.503g, 4.189mmol) were added to anhydrous DMF (40ml). The reaction mixture was heated under reflux for 24hours. The reaction mixture was cooled in an ice bath. A solid formed upon cooling and was filtered to give a brown solid. The solid was washed with petroleum ether. Yield (1.25g, 53%). ^{1}H NMR (400MHz, $CDCl_3$), δ 7.93 (m, 4H), 7.60 (t, 2H, *J*= 1.8Hz), 1.37

(s, 9H). ^{13}C NMR (100MHz, DMSO), δ 168.2, 154.6, 135.4, 131.1, 126.7, 123.2, 122.3, 58.5, 35.2, 31.2, 18.5.

5.5.1.3. Synthesis of **5.1.3**

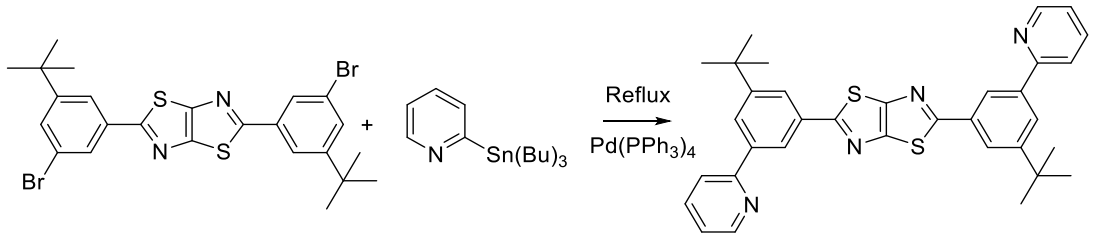

Bis(3-bromo-5-tert-butylphenyl)-[1,3]thiazolo[5,4-d][1,3]thiazole (0.500g, 0.886mmol) was added to degassed toluene (40ml). 2-(tributylstannane)pyridine (0.652g, 1.772mmol) was added and the mixture was degassed for 15minutes. The catalyst, $Pd(PPh_3)_4$ (0.06g, 0.051mmol) was added and the reaction was degassed before being heated under reflux for 18hours. Upon cooling a grey solid formed, which was filtered and dried. The grey solid was recrystallized in DMF. Pure solid formed upon cooling and filtered. Yielding a beige solid. Yield (0.266g, 58%). ^{1}H NMR (400MHz, $CDCl_3$, Me_3Si), δ 8.75 (d, *J*= 4.8Hz, 2H), 8.36 (t, *J*=1.6Hz, 2H), 8.14 (dd, *J*= 8.8, 2.0Hz, 4H), 7.82 (m, 4H), 7.29 (t, *J*=3.2Hz, 2H), 1.47 (s, 18H). HRMS (ESI) calculated for $C_{34}H_{32}N_4S_2$ ([M+H]$^+$)= 561.21411. Found m/z= 561.21448

^{13}C NMR could not be acquired due to poor solubility of the ligand.

5.5.1.4. Synthesis of **5.3.1**.[194]

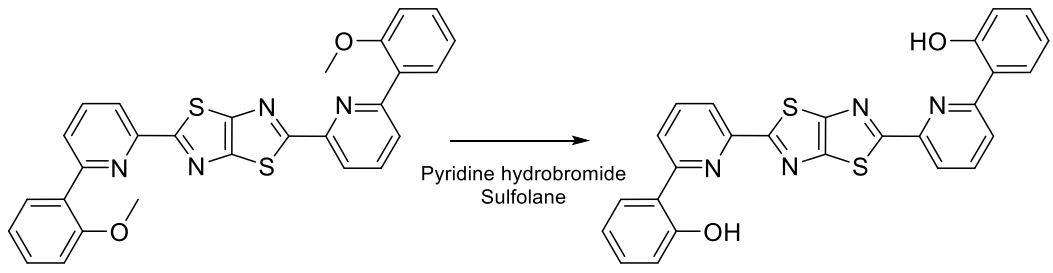

5.3.6 (0.500g, 0.983mmol) was added to a flask with pyridine hydrobromide (0.629g, 3.93mmol) and stirred in sulfolane (10ml). The reaction was heated to 200°C for 18hours. The reaction was cooled to 80°C and stirred for 1 hour resulting in the formation of solid, water (30ml) was added gradually, maintaining a constant temperature, resulting in the formation of

a precipitate. The solid was filtered with a sintered glass funnel and washed with water (10ml) and diethyl ether (20ml). Yield (0.400g, 85%). ^{1}H NMR (400MHz, DMSO-d6, ppm), δ 9.19 (d, *J*= 8.4Hz, 2H), 7.93 (dd, *J*= 7.6, 1.8Hz, 2H), 7.79 (d, *J*= 6.8Hz, 2H), 7.72 (t, *J*= 7.8Hz, 2H), 6.80 (t, *J*= 6.8Hz, 2H), 6.36 (d, *J*= 8Hz, 2H), 6.13 (t, *J*= 7.0Hz, 2H). Infra-red spectroscopy: 3372cm^{-1} (-OH).

5.5.1.5. Synthesis of **5.3.2**.

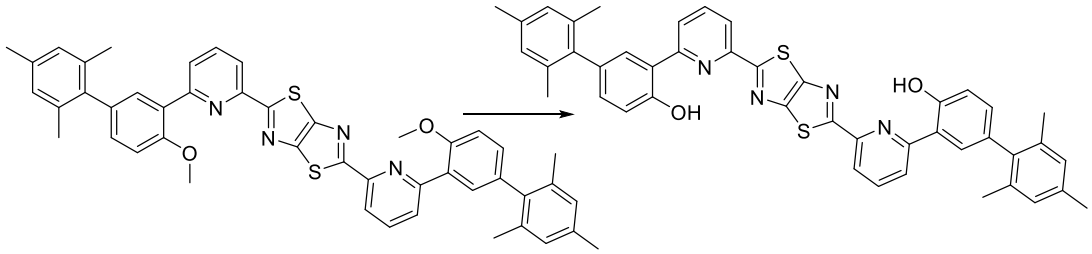

5.3.2 (0.300g, 0.403mmol) was added to a flask with sulfolane (5ml) and stirred. Pyridinium bromide (0.257g, 1.61mmol) was added and the reaction was heated to 200°C for 24 hours. The reaction was cooled to 80°C, water (20ml) was added over 10minutes, maintaining constant temperature. The resulting light brown solid was filtered. Yield (0.200g, 69%). ^{1}H NMR (400MHz, $CDCl_3$, ppm), δ 8.22 (d, *J*= 6.8Hz, 2H), 7.97 (t, *J*= 8.0Hz, 2H), 7.91 (d, *J*= 7.6Hz, 2H), 7.61 (s, 2H), 7.16 (s, 4H), 6.98 (s, 4H), 2.35 (s, 6H), 2.06 (s, 12H). HRMS (ESI) calculated for $C_{44}H_{36}N_4O_2S_2$ ($[M+H]^+$) = 717.23524. Found m/z = 717.23407

5.5.1.6. Synthesis of **5.3.5.** [197]

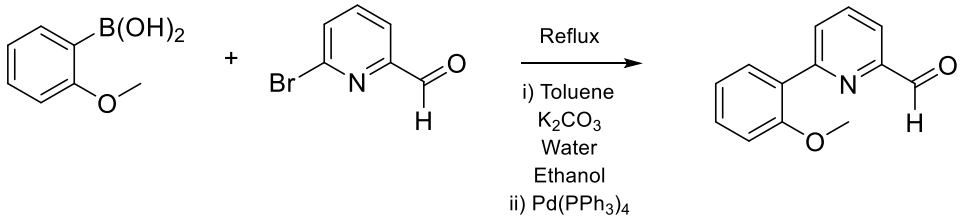

Toluene (100ml) was added to a flask with ethanol (25ml) and water (25ml) and bubbled with argon for 5 minutes. Potassium carbonate (6.56g) was added to the solvent and stirred for a further 5 minutes. Samples of (2-methoxyphenyl)boronic acid (2.73g, 18mmol) and 6-bromopyridine-2-carbaldehyde (3.00g, 15mmol) were added and the reaction was stirred.

$Pd(PPh_3)_4$ was added to the flask and the reaction was heated under reflux for 18hours. The reaction was separated with brine (20ml) and extracted into ethyl acetate (30ml). The organic layers were collected and dried over MgSO4. The solvent was removed under reduced pressure and the resulting residue was triturated with diethyl ether (10ml) and the solid was filtered. Yield (2.00g, 53%). ^{1}H NMR (400MHz, $CDCl_3$, ppm), δ 10.14 (s, 1H), 8.08 (dd, *J*= 6.6, 2 Hz, 1H), 7.90-7.85 (m, 3H), 7.47-7.38 (m, 2H), 7.12 (t, *J*= 7.6Hz, 1H), 7.02 (d, *J*= 8.2Hz, 1H), 3.87 (s, 3H).

5.5.1.7. Synthesis of **5.3.6**.[196]

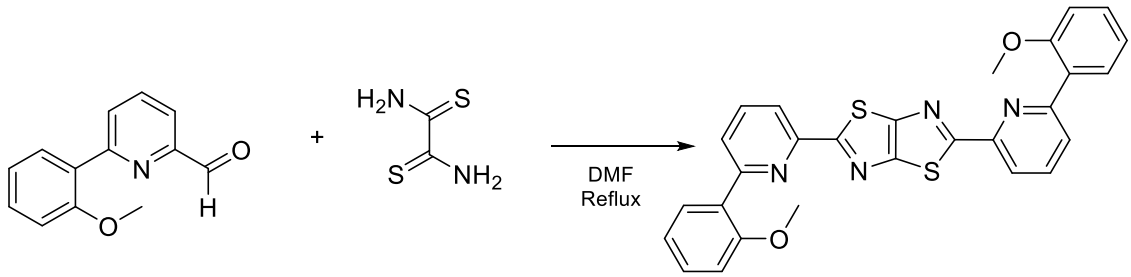

Anhydrous DMF (30ml) was added to a flask and stirred with **5.3.5** (2.00g, 11mmol) under an argon atmosphere. Dithiooxamide (0.781g, 6.5mmol) was added to the flask and heated under reflux for 18hours. The reaction was cooled to room temperature and then cooled further to 0°C. The resulting solid was filtered and washed with water (10ml) and diethyl ether (20ml). Yield (2.00g, 61%). ^{1}H NMR (400MHz, $CDCl_3$, ppm), δ 8.12 (d, *J*= 7.8Hz, 2H), 8.03 (dd, *J*= 7.4, 1.6Hz, 2H), 7.99 (d, *J*= 7.8Hz, 2H), 7.83 (t, *J*= 7.8Hz, 2H), 7.43 (t, *J*= 7.7Hz, 2H), 7.17 (t, *J*= 7.5Hz, 2H), 7.04 (d, *J*= 8.2Hz, 2H), 3.89 (s, 6H).

5.5.1.8. Synthesis of **5.3.7**.

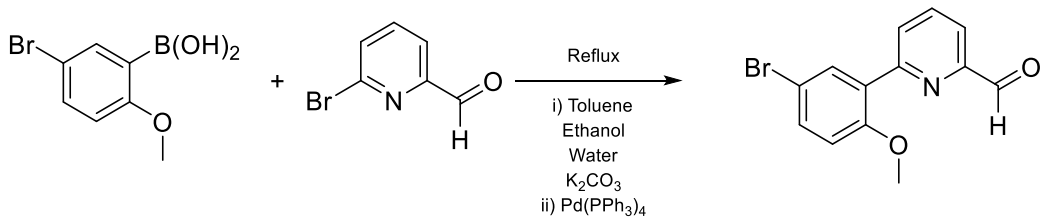

K_2CO_3 (1.75g) was added to a flask of toluene (100ml), ethanol (20ml) and water (20ml) and degassed with argon. Measurements of 6-bromopyridine-2-carbaldehyde (2.65g, 14.2mmol)

and (5-bromo-2-methoxyphenyl)boronic acid (3.00g, 13.0mmol) were added and stirred under an argon atmosphere. The catalyst, $Pd(PPh_3)_4$ (0.73g, 0.632mmol), was added and the reaction was heated under reflux for 18 hours. The reaction was separated with brine and the product was extracted into ethyl acetate (3 x 10ml), the organic layers were collected and dried over $MgSO_4$. The solvent was removed under reduced pressure and the resulting brown oil was triturated with petroleum ether and diethyl ether. The resulting off white solid was filtered. Yield (3.8g, 95%). ^{1}H NMR (400MHz, $CDCl_3$, ppm), δ 10.14 (s, 1H), 8.09 (t, *J*= 6.8Hz, 1H), 7.89 (d, *J*= 8Hz, 1H), 7.47 (dd, *J*= 8.2, 1.6Hz, 1H), 7.35 (s, 1H), 7.15 (d, *J*= 7.2Hz, 1H), 6.90 (d, *J*= 4.8Hz, 1H), 3.86 (s, 3H).

5.5.1.9. Synthesis of **5.3.8**.

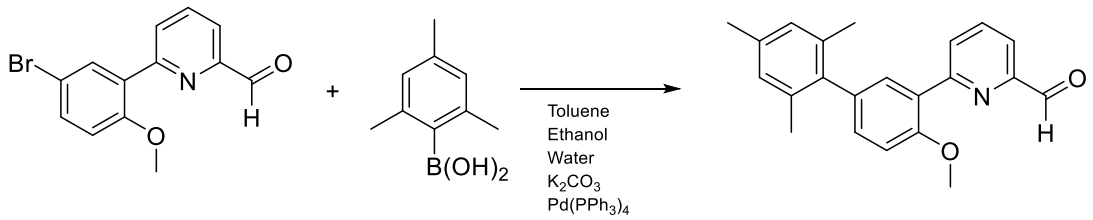

K_2CO_3 (1.75g) was added to a flask of toluene (100ml), ethanol (20ml) and water (20ml) and degassed with argon. Measurements of **5.3.7** (3.5g, 11.43mmol) and 2,4,6-trimethylphenylboronic acid (2.06g, 12.5mmol) were added and stirred under an argon atmosphere. The catalyst, $Pd(PPh_3)_4$ (0.66g, 0.571mmol), was added and the reaction was heated under reflux for 18 hours. The reaction was separated with brine and the product was extracted into ethyl acetate (3 x 10ml). The organic layers were collected and dried over $MgSO_4$. The solvent was removed under reduced pressure and the resulting brown oil was purified by column chromatography (fine silica, DCM). The solvent was removed under reduced pressure and yielding an orange crystalline solid. Yield (1.56g, 41%). ^{1}H NMR (400MHz, $CDCl_3$, ppm), δ 10.07 (s, 1H), 8.18-8.16 (m, 1H), 7.87 (t, *J*= 3Hz, 1H), 7.77 (d, *J*= 2.3Hz, 1H), 7.19 (dd, *J*= 8.7, 2.3Hz, 1H), 7.08 (d, *J*=8.7Hz, 1H), 6.95 (s, 2H), 3.92 (s, 3H), 2.33 (s, 3H), 2.07 (s, 6H).

5.5.1.10. Synthesis of **5.3.9**.

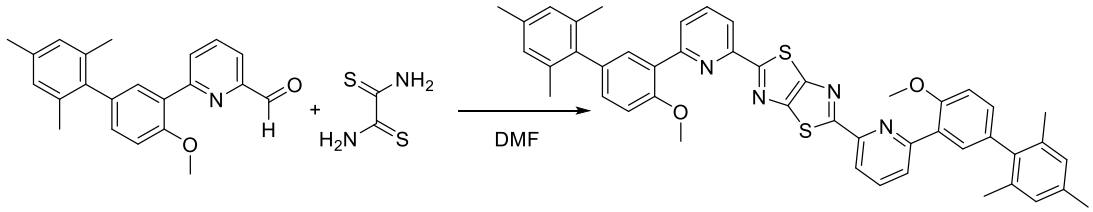

Anhydrous DMF (30ml) was added to a flask and stirred. A sample of **5.3.8** (2.00g, 6.03mmol) was added to the flask and stirred until dissolution. Dithiooxamide (0.363g, 3.02mmol) was added and the reaction was heated under reflux for 18 hours. The heat was removed and water (10ml) was added to the reaction mixture forming a brown solid. The solid was purified column chromatography (fine silica, DCM/EtOAc, 10:1). The solvent was removed under reduced pressure, resulting in a light brown solid. Yield (0.600g, 27%). ^{1}H NMR (400MHz, $CDCl_3$, ppm), δ 8.09 (d, *J*= 7.6Hz, 2H), 8.04 (d, *J*=7.6Hz, 2H), 7.85-7.81 (m, 4H), 7.19 (dd, *J*= 8.4, 2Hz, 2H), 7.07 (d, *J*= 8.8Hz, 2H), 6.99 (s, 4H), 3.95 (s, 6H), 2.35 (s, 6H), 2.15 (s, 12H).

5.5.1.11. Synthesis of **5.3.11.**[195]

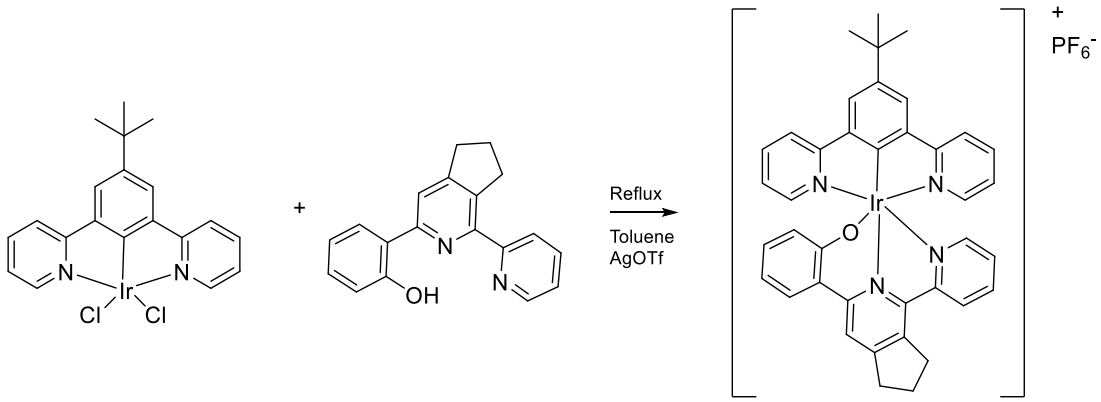

A sample of **2.2.13** (0.100g, 0.182mmol) was added to toluene (30ml) and stirred. AgOTf (0.093g, 0.364mmol) was added to the flask and heated. **5.3.10** (0.063g, 0.218mmol) was added to the mixture and was heated under reflux for 18 hours. The reaction mixture was removed from the heat. 3M aqueous HCl (8 mL) and DCM (15 mL) were added to the warm mixture and the mixture was stirred for 15 min. The reaction mixture was then filtered through

Celite and the organic phase separated. The solvent was evaporated to dryness. The residue was dissolved in a small amount of MeCN and to this solution, excess saturated aqueous KPF_6 solution was added dropwise. The MeCN was evaporated and an orange-brown solid precipitated. The solid was filtered and washed with water to give the crude product (0.100g, 0.130mmol). The solid was dissolved in dichloromethane and purified by column chromatography (fine silica, DCM/EtOAc, 5:1). The solvent was removed under reduced pressure resulting in an orange residue. The residue was triturated with water and filtered. Yield (0.05g, 36%). ^{1}H NMR (400MHz, DMSO-d6, ppm), δ 8.74 (s, 1H), 8.43 (t, *J*= 8.5 Hz, 3H), 8.24 (s, 2H), 8.05 (d, *J*= 8.2 Hz , 1H), 7.86 (m, 3H), 7.37 (d, *J*= 6.0Hz, 1H), 7.26 (t, *J*= 6.4 Hz, 1H), 7.13 (d, *J*= 6.0 Hz, 2H), 7.02 (t, *J*= 6.9 Hz, 2H), 6.87 (t, *J*= 8.2 Hz, 1H), 6.60 (t, *J*= 8.2 Hz, 1H), 6.30 (d, *J*= 8.2 Hz, 1H), 3.74 (t, *J*= 7.1 Hz, 2H), 3.35 (m, 2H), 2.36 (quin, *J*= 7.8 Hz, 2H), 1.56 (s, 9H). ^{13}C NMR (100MHz, DCM-d2, ppm), δ 169.5, 164.2, 159.8, 159.6, 154.3, 152.0, 151.3, 148.6, 147.8, 141.0, 140.3, 139.3, 137.7, 131.1, 130.9, 126.2, 123.7, 123.4, 123.3, 123.1, 121.7, 121.1, 120.5, 116.4, 35.3, 33.7, 33.4, 31.7, 25.2. HRMS (ESI) calculated for $C_{39}H_{34}IrN_4O$ $([M+H])^+$= 768.24346. Found m/z= 768.23810

5.5.1.12. Synthesis of **5.3.14**.

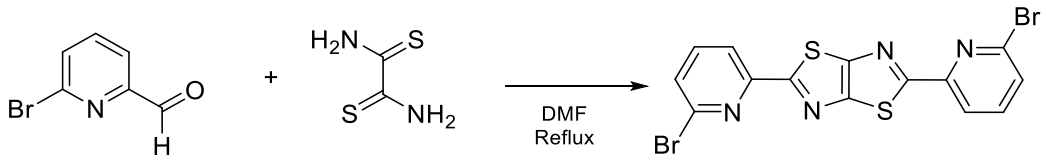

Anhydrous DMF (40ml) was added to a flask and stirred for 15minutes under an argon atmosphere. 6-bromopyridine-2-carbaldehyde (1.86g, 10mmol) and dithiooxamide (0.658, 5mmol) were added to the flask and heated under reflux for 18hours. The reaction was cooled to room temperature and then cooled further in an ice bath. The resulting solid was filtered. Yield (0.985g, 41%). ^{1}H NMR could not be obtained due to the insoluble nature of the product.

5.5.2. TzTz Linked Di-nuclear Complexes

5.5.2.1. Synthesis of **5.1.4**

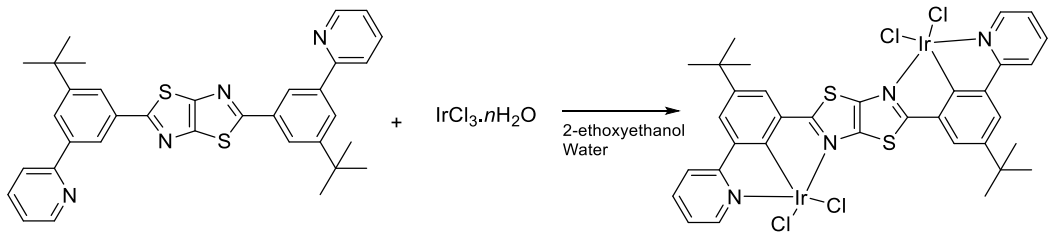

5.1.3 (0.075g, 0.134mmol) to warm 2-ethoxyethanol and heated gradually until boiling. Increments of 5ml of 2-ethoxyethanol were added until the solid dissolved. Water (20ml) was added and the mixture was stirred. Iridium chloride hydrate (0.102g, 0.280mmol) was added and the mixture was heated under reflux for 18hours. The reaction was gradually cooled and water (30ml) was added slowly forming a red precipitate. The solid was filtered and washed with water. Yield (0.130g, 90%). ^{1}H NMR (400MHz, DMSO-d6, ppm), δ 8.95 (m, 2H), 8.46 (d, *J*= 8.2Hz, 2H), 8.24 (d, *J*= 5.0Hz, 2H), 8.09 (m, 4H), 7.57 (q, *J*= 6.4Hz, 2H), 1.45 (s, 18H).

5.5.2.2. Synthesis of **5.1.5**

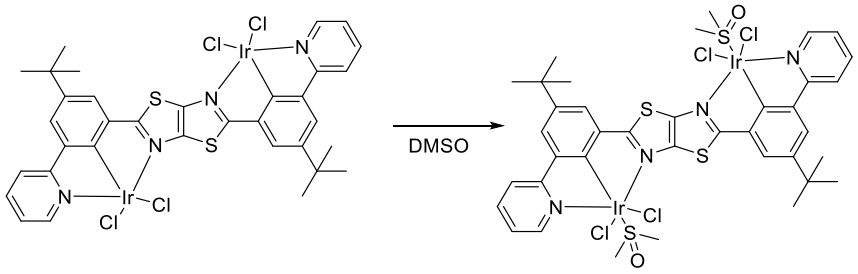

A sample of **5.1.4** (0.04g, 0.036mmol) was added to a test tube with DMSO (1ml) and heated to 180°C for 1 hour. The reaction was cooled and extracted into DCM. The organic layer was dried over $MgSO_4$ and filtered. The resulting orange solution was purified by column chromatography (fine silica, DCM/MeOH, 20:1). The solvent was removed under reduced pressure resulting in an orange residue. Yield (5mg, 11%). ^{1}H NMR (400MHz, DMSO-d6, ppm), δ 8.95 (d, *J*= 8.2 Hz, 2H), 8.46 (d, *J*= 8.8Hz, 2H), 8.24 (s, 2H), 8.12 (d, *J*= 5.6 Hz, 4H), 7.57 (t, *J*=6.8Hz, 2H), 2.53 (s, 12H), 1.45 (s, 18H).

5.5.2.3. Synthesis of **5.1.6**

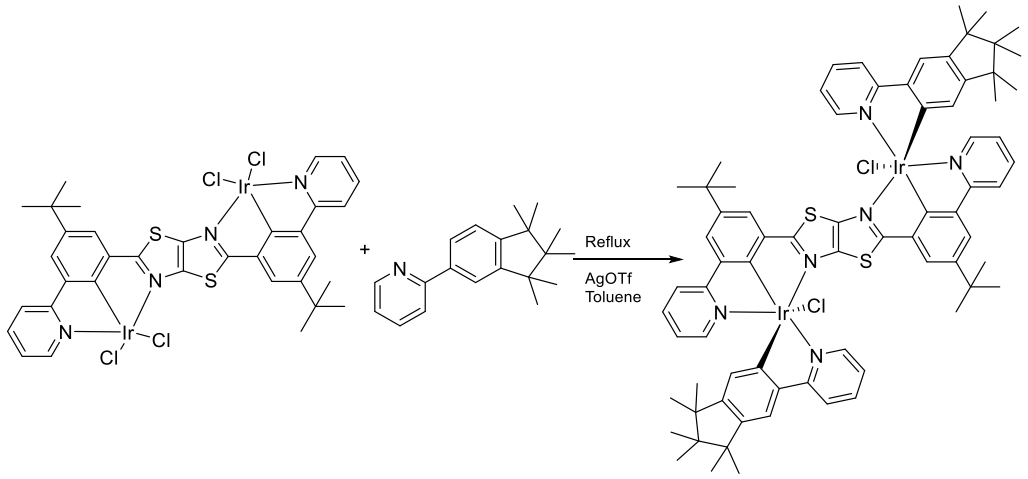

5.1.4 (0.100g, 0.092mmol) was added to toluene (20ml) and stirred. Silver triflate (0.094g, 0.368mmol) was added to the suspension and the reaction was stirred further. The ligand, M2 (0.054g, 0.194mmol), was added to the suspension and the reaction was heated under reflux for 18hours. 3M HCl (10ml) was added to the reaction whilst hot and stirred at 80°C for 20minutes. The warm mixture was filtered through celite and washed with DCM (20ml) and MeOH (20ml). The organic layer was collected and the solvent was removed under reduced pressure. The resulting red residue was purified by column chromatography (fine silica, DCM/MeOH, 25:1). The solvent was removed under reduced pressure resulting in a dark red solid. Yield (5mg, 4%) . ^{1}H NMR (400MHz, DMSO-d6, ppm), δ 9.92 (d, *J*= 4.4Hz, 2H), 8.36 (d, *J*= 8Hz, 2H), 8.30 (d, *J*= 8.4Hz, 2H), 8.22 (t, *J*= 7.6Hz, 2H), 8.14 (s, 2H), 7.81 (m, 8H), 7.50 (d, *J*= 4.8Hz, 2H), 7.42 (s, 2H), 7.04 (t, *J*= 6.8Hz, 2H), 5.12 (s, 2H), 1.46 (s, 18H), 0.94 (s, 8H), 0.83 (s, 8H), 0.56-0.43 (m, 18H). HRMS (ESI): calculated for $C_{74}H_{78}Cl_2Ir_2N_6S_2$ ($[M+H]^+$)= 1571.44376. Found m/z= 1571.43865.

5.5.2.4. Attempted preparation of **5.3.12**

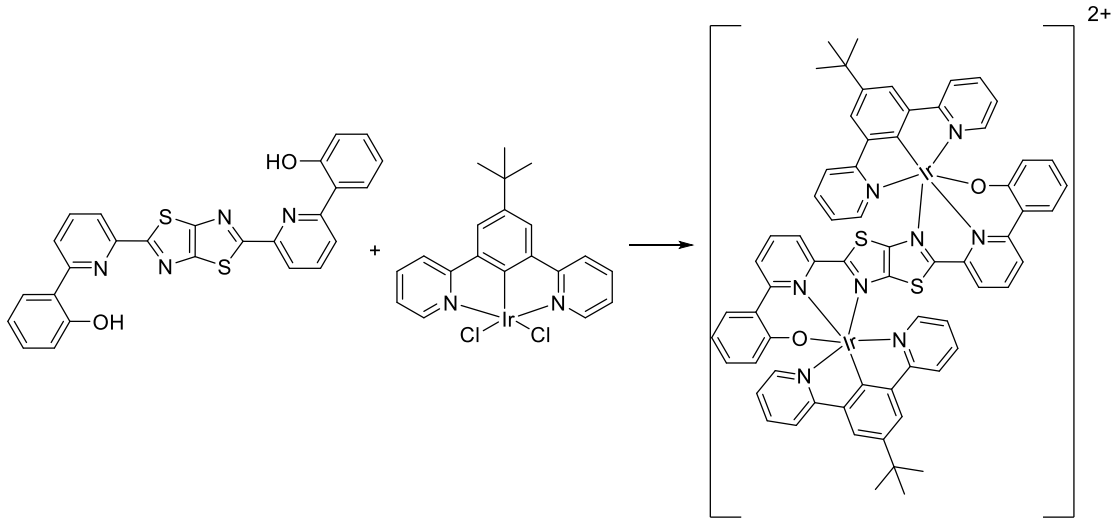

A sample of **2.2.13** (0.050g, 0.091mmol) was added to a flask of toluene (20ml) and stirred. Silver triflate (0.047g, 0.181mmol) was added and the reaction mixture was stirred for 10minutes. **5.3.1** (0.022g, 0.0454mmol) was added to the mixture and the reaction was heated under reflux for 18 hours. Colour change noticed from orange to deep red. 3M HCl (10ml) was added with DCM (10ml) and stirred, the suspension was filtered through celite whilst still hot. The organic layers were separated and evaporated to dryness. The resulting residue was purified by column chromatography (fine silica, DCM/MeOH, 10:1). The fraction was evaporated to dryness under reduced pressure, the resulting yellow/grey solid was filtered. ^{1}H NMR showed the sole presence of starting materials.

5.5.2.5. Attempted preparation of **5.3.13**

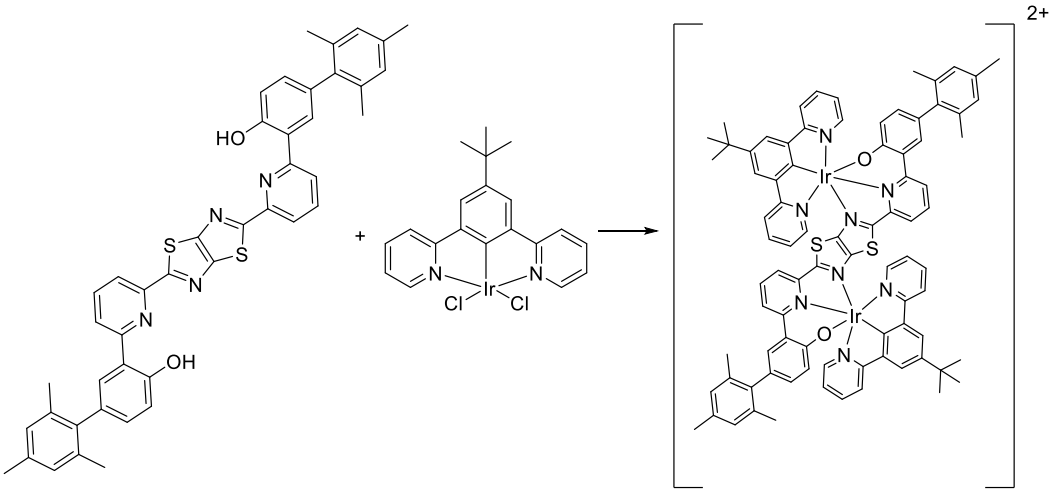

A sample of **2.2.13** (0.050g, 0.091mmol) was added to a flask of toluene (20ml) and stirred. Silver triflate (0.047g, 0.181mmol) was added and the reaction mixture was stirred for 10minutes. Triethylamine (20ml) was added with **5.3.1** (0.022g, 0.0454mmol) to the mixture and the reaction was heated under reflux for 18 hours. Colour change noticed from orange to brown. The reaction mixture was filtered through celite whilst still hot and the filtrate was evaporated to dryness under reduced pressure. The resulting residue was purified by column chromatography (fine silica, DCM/MeOH, 10:1). The fraction was evaporated to dryness under reduced pressure and the resulting brown solid was filtered. ^{1}H NMR showed the sole presence of starting materials.

CHAPTER 6

SALEN-type Tetradentate O^N^N^O

Platinum (II) Complexes

6. SALEN-type Tetradentate Platinum Complexes

This chapter describes the synthesis and development of platinum (II) complexes that utilise tetradentate coordinating ligands. The tetradentate ligands binding to the platinum by O^N^N^O coordination is based on the chemistry of 1, 2, 4-triazines. Synthesis incorporated different cross coupling methods and the inclusion of different functional groups that proved to be influential in the photophysical properties of the Pt (II) complexes.

The use of tetradentate SALEN type O^N^N^O ligands and their analogous Pt(II) complexes are notable in coordination chemistry.[112-114] These metal complexes have a wide range of uses and an example is the application of luminescent Pt(II) complexes as dopants in phosphorescent organic light emitting diodes (PhOLED's).[150] The use of tetradentate ligands benefits the stability and the photophysical properties of the complex whilst also preventing ligand exchange reactions.[198] Typical SALEN type ligands can be easily synthesised through the condensation of salicylic aldehydes and corresponding diamines. Despite the simple synthesis, the resulting C=N bond is susceptible to hydrolysis and other types of degradation.[198] In response to this, the more robust bipyridine bisphenolate (BpyBph) system was developed. These showed strong luminescence in solution and excellent thermal stability. A previous study has shown that complexes using the BpyBph ligands have quantum yields ranging from 5-12%, and therefore require development.[112]

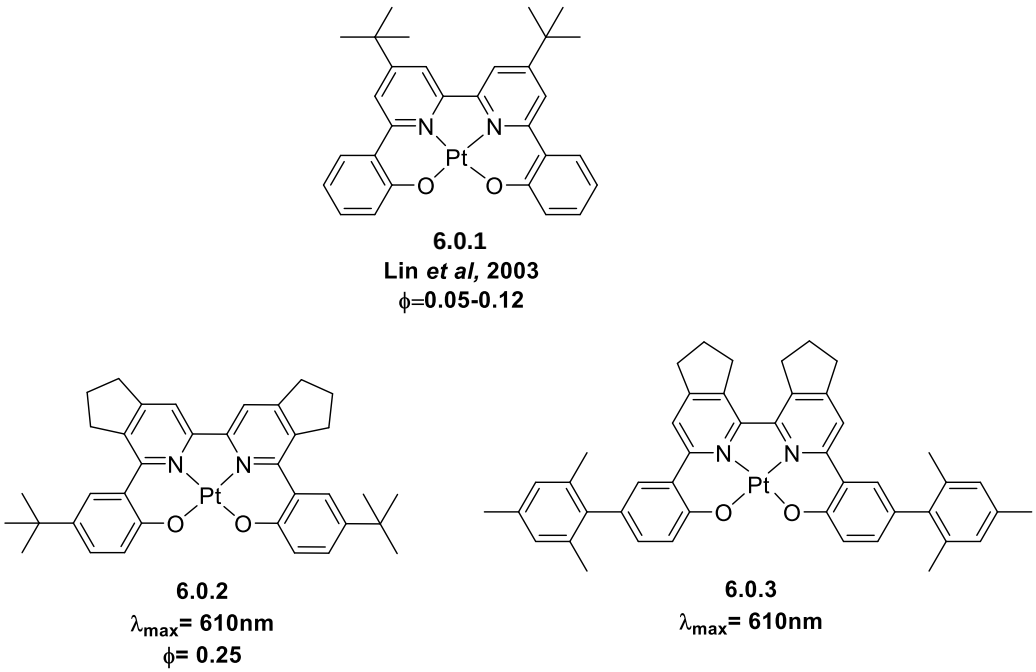

Figure 117 - The structure of the BpyBph complex described by Lin *et al* (**6.0.1**) which serves as a precedent for the novel complexes described and prepared, **6.0.2** and **6.0.3**.

Using the chemistry of 1,2,4-triazines, BpyBph ligands can be synthesised from readily available starting materials. The triazine intermediates are converted to pyridine-based compounds through Boger pyridine synthesis. This method also introduces cyclopentene groups to the resulting pyridine rings (detailed further in section 6.1). The addition of cyclopentene prevented intermolecular interactions between the final complex molecules. Preventing these interactions is important as Pt (II) complexes have been shown to self-quench in the excited state which can be attributed to the stacking of the complex molecules.[43]

The study outlines the development of two novel synthetic routes which were used to produce two novel BpyBph ligands and their analogous complexes. The methodology specifically employed the use of 3,3'- and 5,5'- bis-triazines to develop the tetradentate ligands. This was due to the loss of dinitrogen during the Boger reaction. The addition of the cyclopentene rings played an instrumental part in increasing the solubility of the Pt (II) complexes. This change in the level of solubility was mainly due to the twist effect imparted by the cyclopentene positioning (depicted in Figure 119). Additional solubilising groups such as tertiary butyl and mesitylene were introduced to the phenolate moieties to investigate their effect on the

photophysical properties and solubility's of the complexes. The inclusion of these groups resulted in a slight red shift in the emission wavelength in comparison with previous examples.[113]

The study highlighted that BpyBph ligands can be readily prepared from the 3,3' and 5,5' bistriazine precursors. The study has shown that using this methodology highly luminescent Pt(II) complexes can be prepared, furthermore these complexes can then be successfully used as dopants in solution processable OLED devices. It was highlighted that the introduction and positioning of the cyclopentene rings was beneficial to the overall solubility. In addition, this increase in solubility allowed for the required doping concentration to develop single dopant candle light OLED devices. Previously for devices of this kind, multiple dopants have been required.[199-200]

6.1. Synthesis of the O^N^N^O ligands from 1, 2, 4-triazines

To develop novel O^N^N^O ligands, two synthetic routes were developed using readily available starting materials. The use of the Boger reaction results in the loss of two nitrogen atoms as dinitrogen, and this limits the building blocks to 3,3'- and 5,5'- bis-triazines. The two pathways used different methods to reach the final ligands, one route used desulfative cross coupling followed by a reaction with KCN to form the 5,5'-triazine precursor (route A). Whereas the other method used bis-amidrazone to synthesise the 3,3'-triazine intermediate (route B). Both of the routes utilised chemistry of 1,2,4-triazines to reach the final phenolic ligands, such as inverse Diels-Alder and the deprotection of methyl ethers. The full synthetic routes are displayed below in Scheme 32.

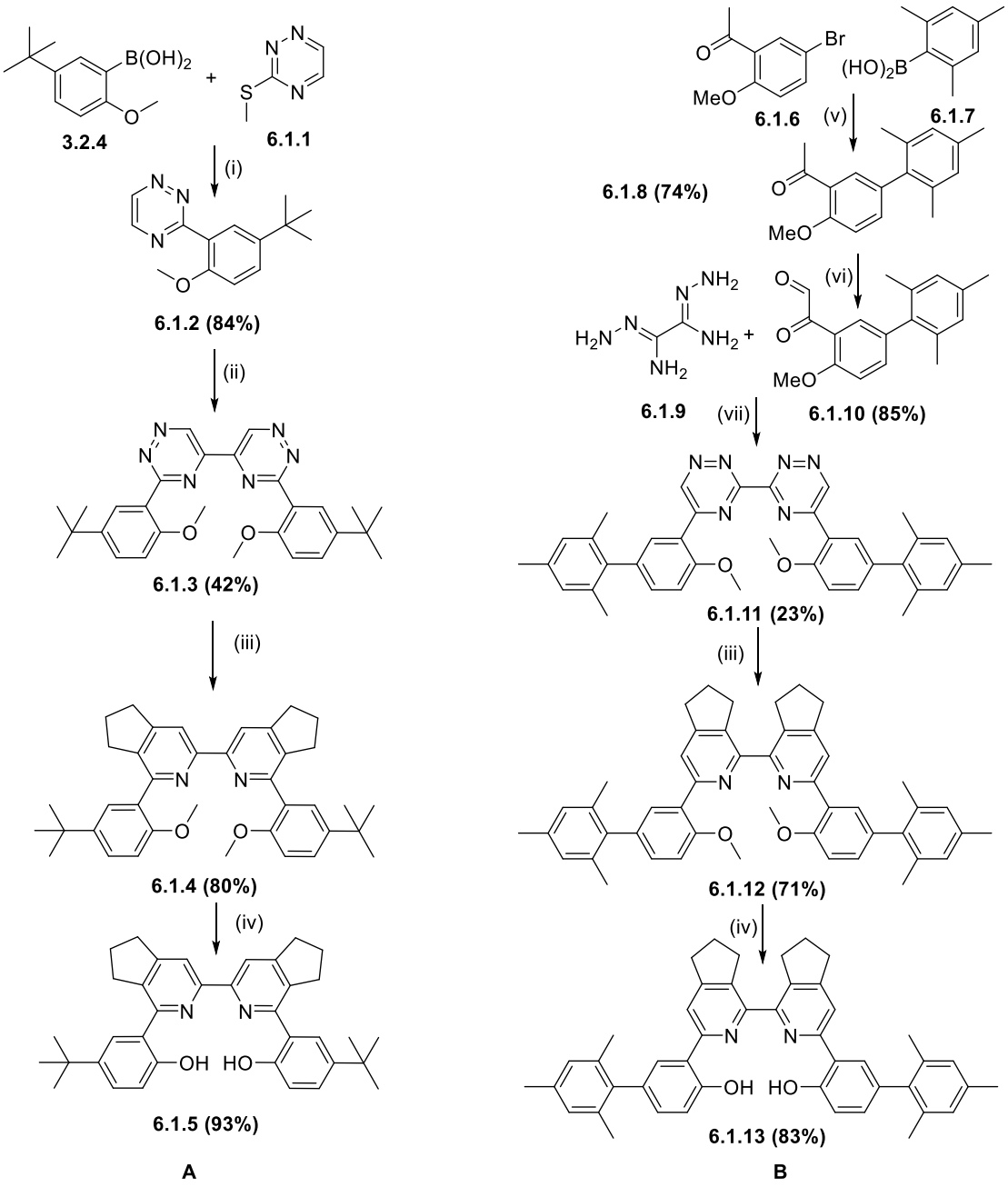

(i) 3-t-butyl-5-methoxyphenyl boronic acid, CuMeSal, Na2CO3, Pd(PPh3)4, THF, reflux; Ethanol, reflux, 4-24 h.
(ii) KCN, 1,4-dioxane/water, RT, 14 h;
(iii) 1-morpholino-1-cyclopentene/ 1-pyrrolidino-1-cyclopentene, 140°C, 1h. Acetic acid, H2O, 30mins.
(iv) Pyridine hydrochloride, 200°C, 2-6 h.
(v) Toluene, Ethanol, Water, K_2CO_3, $Pd(PPh_3)_4$, reflux, 18h
(vi) SeO_2, 1,4-dioxane, Water, reflux, 18h
(vii) Ethanol, reflux, 18h

Scheme 32 - The overall synthetic pathway to generate two of the novel complexes discussed in this section, the yields of each individual step are shown in bold.[198]

The synthesis of the first tetradentate ligand (route A) started with the formation S-Me thiosemicarbazide followed by the desulfative coupling with (5-tert-butyl-2-methoxyphenyl)boronic acid to produce the methyl ether triazine intermediate. This was achieved in a high yield and the product was purified using flash column chromatography (DCM/EtOAc, 2:1). The triazine **6.1.2**, was dimerised using potassium cyanide (KCN), to give **6.1.3** in low yield (42%). The formation of the pyridine ring was achieved through the inverse Diels-Alder reaction (or the Boger pyridine synthesis), using pyrollidino-1-cyclopentene or morpholino-1-cyclopentene.[201]

The methyl ether, **6.1.4** was deprotected to an –OH group by heating in the melt of pyridine hydrochloride at 200°C (93%). This ligand did not require further purification and was heated in acetic acid with K_2PtCl_4, to give the complex, **6.0.2** in low yield (~28%).

To synthesise the 3,3'-triazines, in route B, required the combination of 2,4,6-methylphenylboronic acid and 1-(5-bromo-2-methoxyphenyl)ethan-1-one via Suzuki cross coupling. The acetyl derivative was carried forward and oxidised using selenium dioxide.[202] The glyoxal derivative was reacted with bis-amidrazone to produce the 3,3'-bis-triazine intermediate in low yields (23%). **6.1.11** was significantly more soluble when compared to the tertiary butyl analogue, **6.1.3**. This is probably due to the introduction of the mesityl group, which is known to prevent intramolecular interactions and therefore increase solubility. Incorporation of the cyclopentene groups required use of the Boger reaction, which results in the loss of two nitrogen atoms from the structure. The reaction of **6.1.11** with 1-morpholino-1-cyclopentene gave **6.1.12** in 71% yield. The deprotection of the methoxy unit was achieved successfully in high yields (~80%) by using pyridine hydrochloride. The pyridine hydrochloride acts as the solvent in a "melt" reaction.[203]

The complex was synthesised in 83% yield using the potassium tetrachloroplatinate and acetic acid described previously. The complex was purified using column chromatography (DCM), which resulted in a bright orange solid.

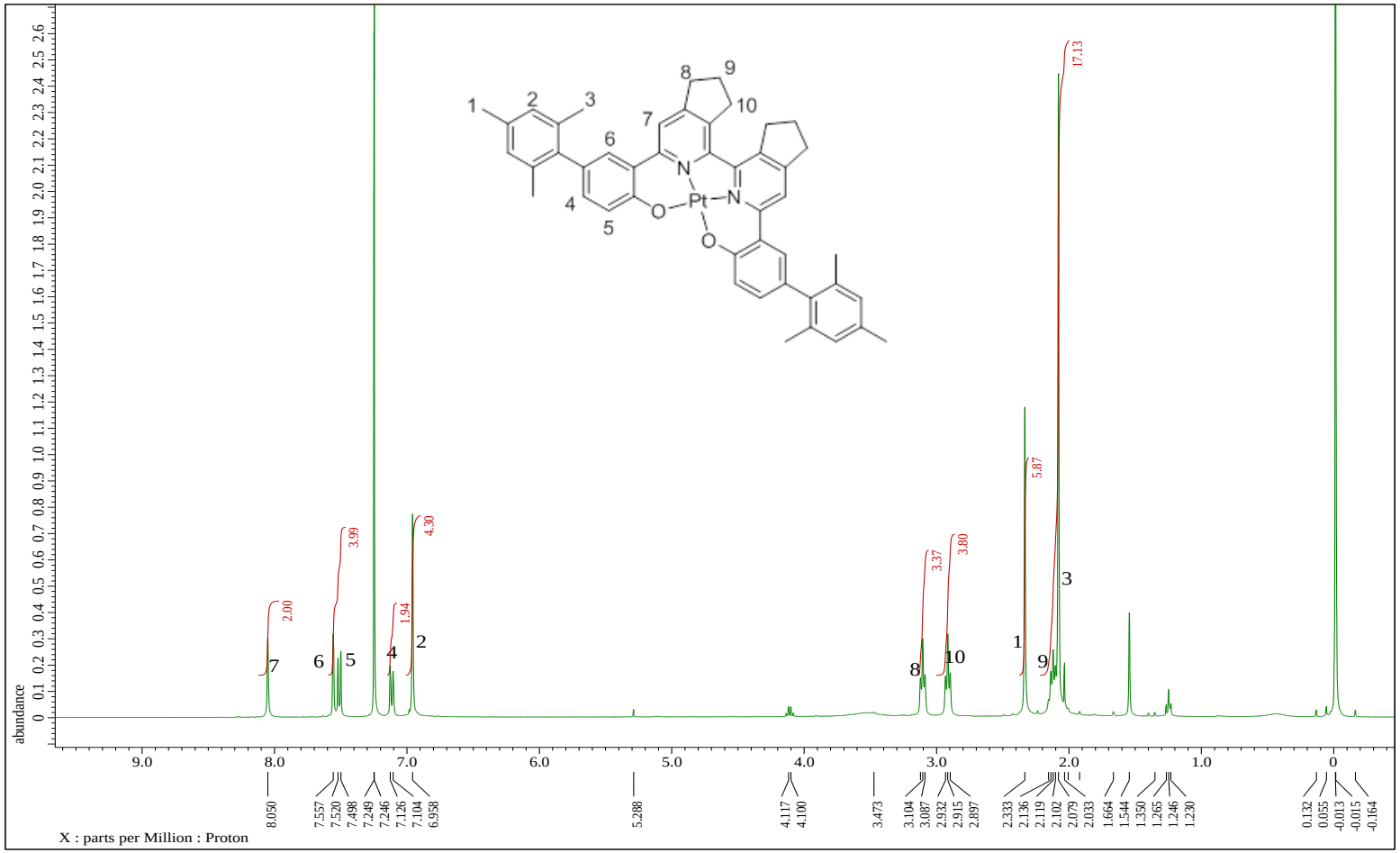

Figure 118- The 1H NMR spectrum for **6.0.3** (in $CDCl_3$) following chromatographic purification. The numbered structure of the complex is overlaid, the numbered peaks associate to the numbered peaks.

The Pt(II) complex **6.0.3** was more soluble than **6.0.2**, this could be explained by the positioning of the cyclopentene rings. The cyclopentene rings induce a slight twist in the resulting pyridine rings which boosts the solubility of the complex. Computational data carried out on the non-*tert*-butylated complexes by Pander *et al* depict this twist.[198]

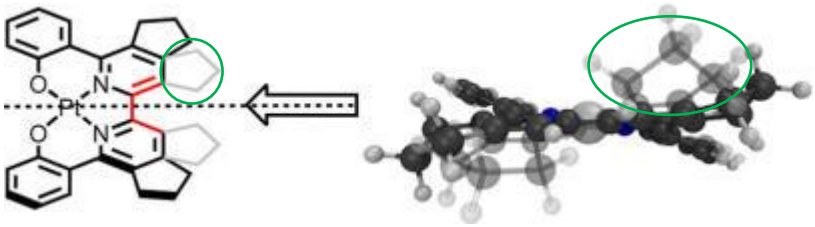

Figure 119 - The depiction of the twist induced on the pyridine rings by the positioning of the cyclopentene rings. The image is taken from the study by Pander *et al*.[198]

The inclusion of the mesitylene group to the phenolate moiety of the ligands improves solubility. There was an improvement in the solubility as the mesityl group would facilitate/augment the effects of this cyclopentene twist due to the

6.2. Photophysical Properties

Testing the photophysical properties of the complexes synthesised in this chapter was carried out at both Durham University and Northumbria University. The complex included in the paper, **6.0.2**, was tested at Durham University by Piotr Pander and Dr Fernando Dias. The mesitylene analogue, **6.0.3** was tested at Northumbria University.

The tert-butyl complex of **6.0.2** showed a peak emission wavelength of λ_{max}= 610 nm at 298 K (λ_{max}= 572nm at 77K), and an emission profile that was similar to the other complexes synthesised (**6.2.1-6.2.3**). The spectrum showed a broad peak and typical Gaussian shape to the curve, however the different vibrational modes of the tert-butyl could be seen in the emission peak when the complexes were placed in Zeonex. This also indicated that the electron donating nature of the tertiary butyl did not have much effect on the emission profile.

Table 15 - The table of photophysical properties of the complexes from the study by Pander *et al*, **6.0.2** is identified by the bold text. The structures of the complexes 6.2.1-6.2.3 and 6.0.2 are shown in Figure 120.

Complex	**Emission**				
	λ_{max}, Toluene, nm	τ, μs	Φ_{PL}	λ_{max}, Zeonex 480, nm	τ, μs
6.2.1	624	1.76	0.24	580	7.6
6.2.2	593	2.98	0.34	564	5.5
6.2.3	646	0.93	0.12	589	5.4
6.0.2	**610**	**1.42**	**0.25**	**572**	**4.8**

The tert-butylated complexes, **6.2.3** and **6.0.2** show red shifted emissions in comparison to the non-alkylated analogues (~20nm) and can be associated to the presence of the tertiary butyl group. However in the case of **6.0.2**, there was a decrease in the quantum yield and lifetime of the triplet state decay in relation to **6.2.2**, this was also observed for the triazine isomers **6.2.1**/**6.2.3**.

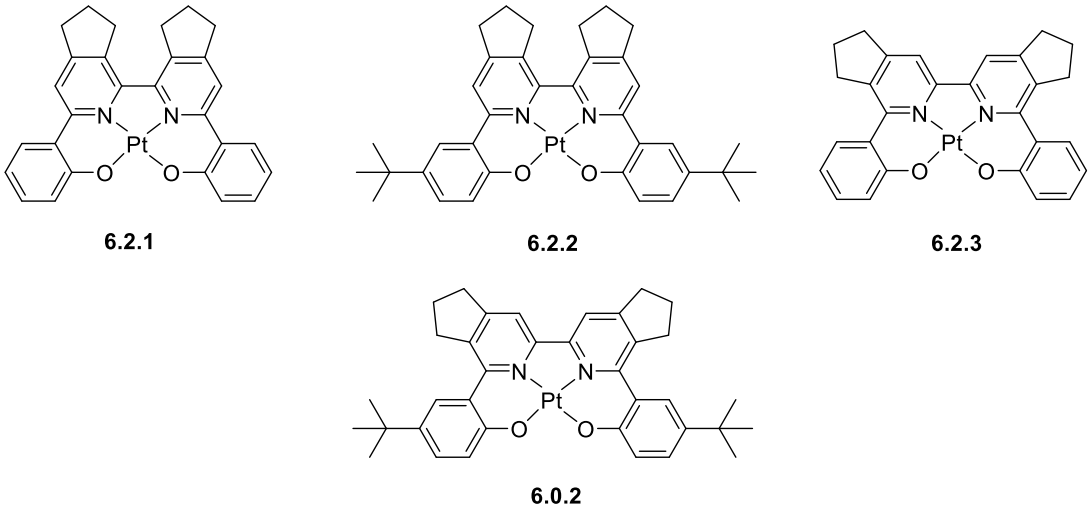

6.2.1 **6.2.2** **6.2.3**

6.0.2

Figure 120 - The structures of the complexes in the study by Pander *et al*. The photophysical data for complexes **6.0.2**, **6.2.1-6.2.3** is shown in Table 15 and Figure 121.

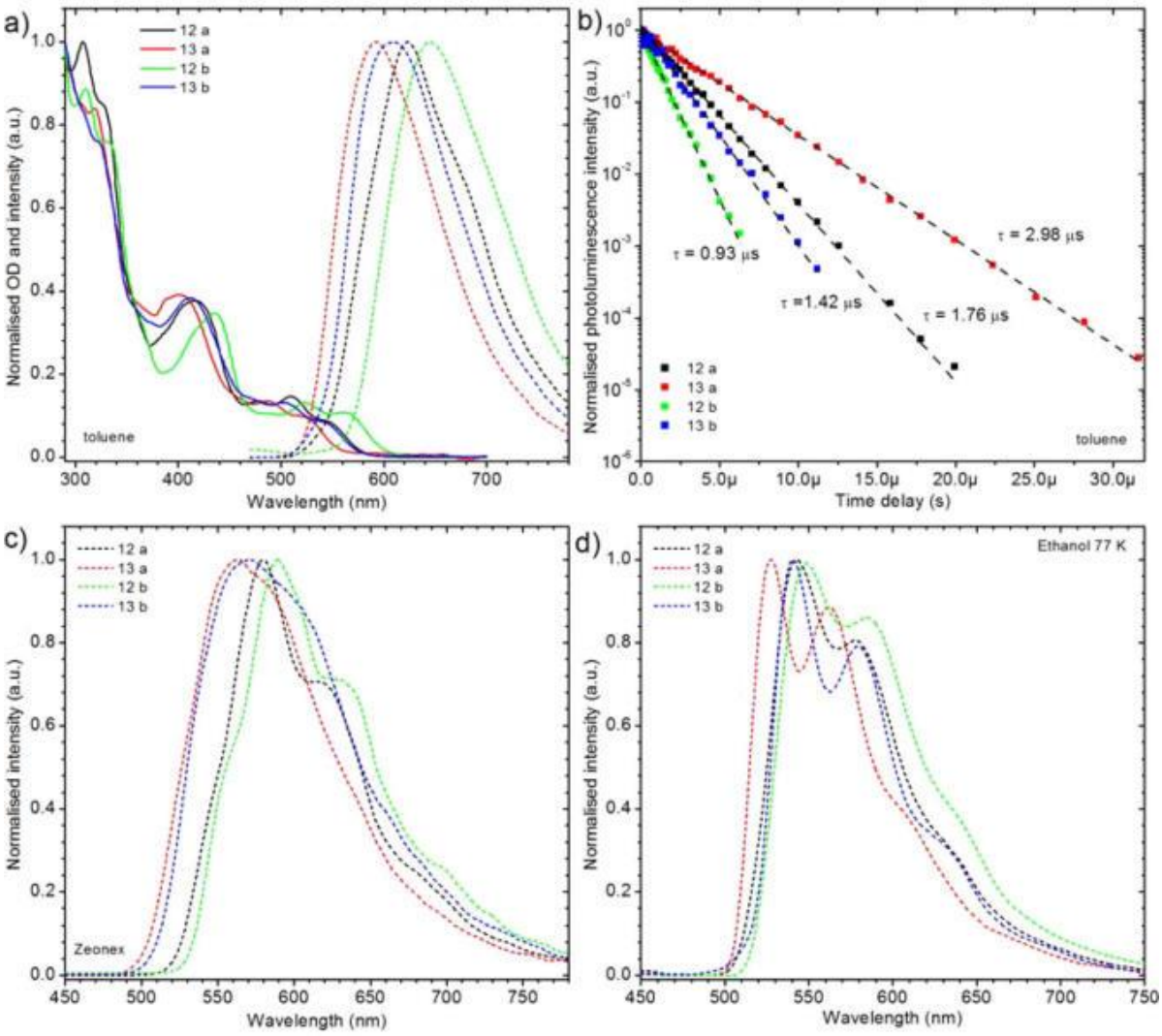

Figure 121 - The photophysical spectra for all of the complexes in the study by Pander *et al*. The complex of interest to the work in this project is **6.0.2** (dark blue). The image was taken from the paper itself.[198] A= The overlaid excitation and emission spectra. B= The decay times of the triplet state at RT. C= The emission spectra of each complex in Zeonex. D= The emission spectra of each complex in ethanol at 77K.

The emission profile of **6.0.2** remains similar from toluene and chlorobenzene to the Zeonex polymer shown by (*a*) and (*c*) in Figure 121. The emission spectra changes at 77K in ethanol where a secondary vibronic peak is more prominent. The complexes all display similar properties with only a slight red shift emission being exhibited by the tert-butylated products.

The emission and excitation of **6.0.3** was carried out in toluene and therefore could be compared to the previously synthesised complexes.

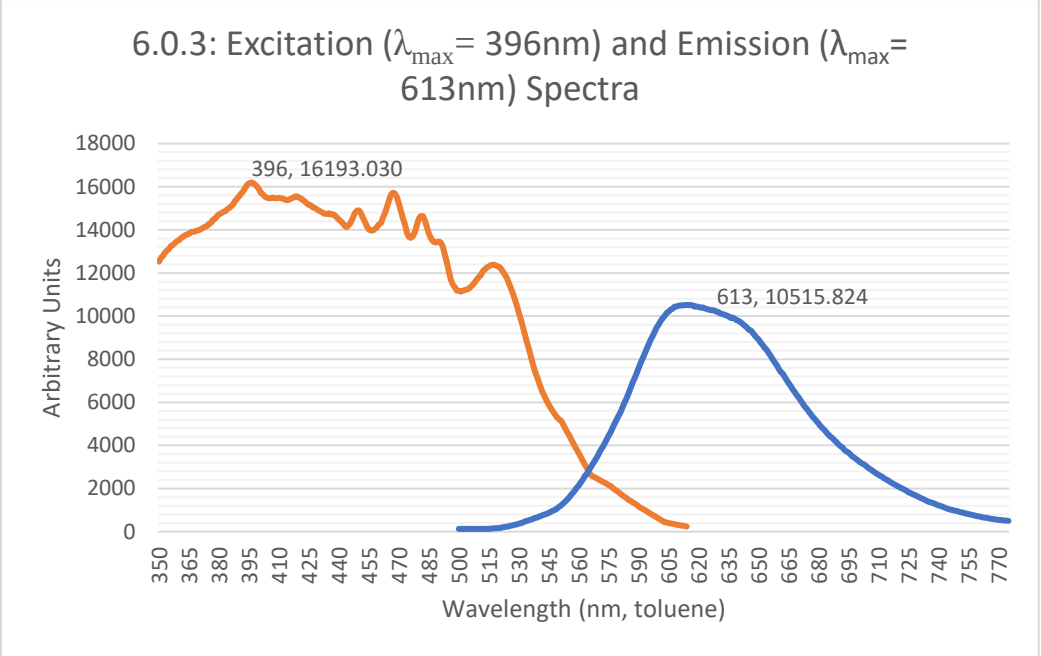

Figure 122 – The excitation and emission spectra of **6.0.3** in toluene showing a peak emission wavelength of λ_{max} 613nm, comparable to the previously described complexes.

Table 16 - The excitation and emission wavelengths of **6.0.2** and **6.0.3**, highlighting the effect of the addition of the mesitylene group to the phenolate moieties.

Complex	**Excitation, nm [toluene]**	**Emission, nm [toluene]**
6.0.2	400	610
6.0.3	396	613

The inclusion of the mesitylene shows to have little effect on the emission profile of the tetradentate complexes, but benefitted the solubility of the complex. The addition of this group did not vastly change the emission or excitation wavelengths. This suggests that the mestiylene has little contribution to the frontier molecular orbitals. Example molecular orbitals were calculated for the *tert*-butyl free compounds in the study by Pander *et al* at Durham University. The HOMO was shown to distinctly manifest on the phenolate moieties and metal centre for both the cyclopentene positions, whereas the LUMO seemed to manifest across the bipyridine structure of the ligand with a larger contribution from the central platinum ion. This is depicted in Figure 123.

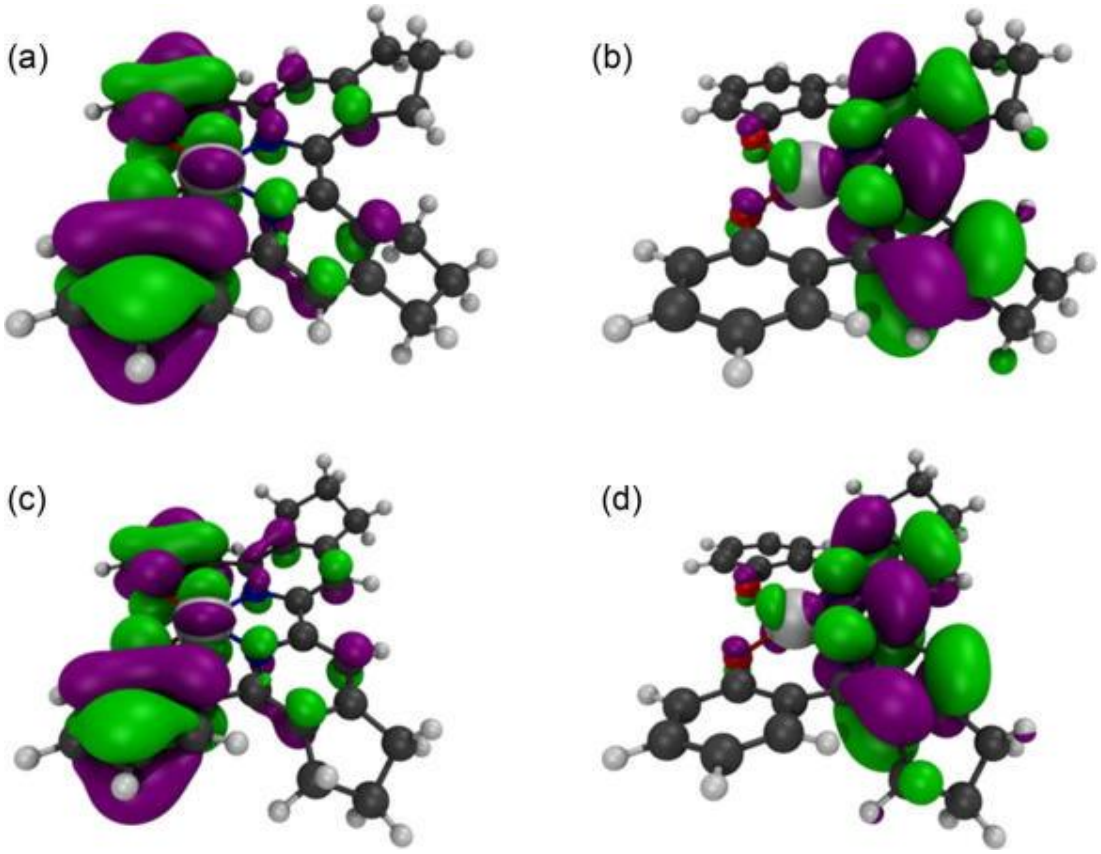

Figure 123 - The HOMO (a) and (c) and LUMO (b) and (d) of complexes **6.2.1** (top) and **6.2.3** (bottom), which shows the presence of the HOMO across the phenolate moieties and the LUMO being delocalised the bipyridine groups. The depiction is taken from the paper by Pander *et al.*[198]

The orbital projections of the tert-butyl free complexes show the probable arrangements of the HOMO and LUMO orbitals which gives insight into those synthesised in this work. In both the HOMO and LUMO there is contribution from the central platinum (II) ion.

6.2.1. OLED Device Fabrication

The complex, **6.0.2**, was used to develop and fabricate an OLED device. The solubility of the compound resulted in low dopant concentrations within the device which is not desirable for long term application. This likely decreased the efficiency of the host to dopant energy transfer, therefore resulting in a decrease in the efficiency of the device. The OLED devices fabricated in the study produced external quantum efficiencies between η_{ext}= 8.4-10.4% and current efficiencies between 22.3 cd A^{-1} and 24.9 cd A^{-1}, the photophysical data is shown in Table 17. The complex, **6.0.2**, showed the highest EQE of the devices developed showing

η_{ext}= 10.4%, however showed poor solubility. The devices fabricated from the tert-butylated products resulted in reduced values in comparison to those without tertiary butyl substituents.

It should be noted that CIE colour coordinates (0.57, 0.42), are close to that of an actual candle (0.52, 0.42), has meant that the devices only require a single emitter rather than the previously required 2 or 3.[199-200]

Table 17 - The photophysical data of the devices fabricated using complexes synthesised in the project by Pander *et al*. The data for complex **6.0.2** is highlighted in bold.

Device	**Complex**	**EQE_{max}, %**	**λ_{max}, nm**	**Max Current Efficiency, %**	**Max Brightness, cd m^{-2}**	**CIE coordinates**
Dev 1	6.2.1	10.0	590	23.2	7000	0.54, 0.46
Dev 2	6.2.2	8.5	567	24.9	3500	0.46, 0.51
Dev 3	6.2.3	5.5	603	9.9	2200	0.57, 0.42
Dev 4	**6.0.2**	**10.4**	**577**	**22.3**	**5000**	**0.52, 0.47**

The complex, **6.0.3**, has not been used to fabricate an OLED device and will require further testing.

6.3. Conclusions

The work carried out has described the synthesis of two novel tetradentate salen type ligands and their analogous complexes by 1,2,4-methodology. The complexes developed have shown encouraging photophysical results and through the optimisation of structures and conditions, the peak quantum efficiencies can be increased further.

The synthesis of **6.0.2** has shown that from commercially available starting materials such as (5-tert-butyl-2-methoxyphenyl)boronic acid, that stable complexes can be developed. These complexes show higher levels of luminescence than previous BpyBph examples described by

Che *et al* and Lin *et al* which showed quantum yield values ϕ_{lum}= 0.05-0.12 and ϕ_{lum}= 0.1-0.27 respectively.[112, 150] The study involving **6.0.2** showed a range of peak PLQY values of ϕ_{lum}= 0.12-0.34 which is in agreement with the mentioned BpyBph studies carried out prior to this study. The resulting OLED devices showed an increased level of EQE (η_{ext}= 5.5-10.4%) and only required one emitter in place of the combination previously required.

The study concluded that the inclusion of the tertiary butyl substituent did not show any benefit toward the solubility of the complex. The solubility was only distinctly affected by the positioning of cyclopentene rings on the pyridyl moieties. As a strategy to further increase the level of solubility of these complexes, further substitution of alkyl groups on these cyclopentene rings would be of benefit. The coordination of a different cycle could also benefit the level of solubility, such as changing from cyclopentene to cyclohexene (with further oxidation) could show a dramatic increase in solubility and photophysical properties.

As an alternative to the substitution of the cyclopentene ring, the substitution of the tertiary butyl with a different group, such as mesitylene and other 'bulky' substituents which improve solubility through reduced intermolecular interactions.

The synthesis of **6.0.3** showed a distinct improvement in the level of solubility however did not show any significant changes to the photophysical properties. This indicates that there is little contribution to the molecular orbitals from the solubilising groups on the phenolate moieties. The emission, λ_{max}= 613nm in toluene is only slightly red shifted in comparison to **6.0.2**, further supporting the idea that there is little contribution from the solubilising groups in the molecular orbitals. Further testing of the photophysical properties will be required in order to determine the quantum efficiency of the complex, this was not carried out at Northumbria due to limitations involving the measurable standard, an issue previously discussed.

The preparation of a series of complexes in which the specific aspects of the ligand structure are optimised would show significant advances in the production of 'candlelight' OLED

devices. This is a highly achievable prospect through the tuning of the emission wavelength as a result of simple structural changes. A major issue that needs to be addressed in further developments is the solubility of resultant complexes, at this point this is a major drawback.

6.4. Experimental

6.4.1. Tetradentate O^N^N^O Ligands

6.4.1.1. Synthesis of **6.1.0**

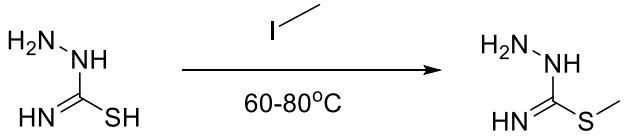

Alkyl iodide (14.94ml, 240mmol) was added to a suspension of thiosemicarbazide (18.23g, 200mmol) in ethanol (150ml). The solution was heated between 60-80°C for 30minutes and then cooled to room temperature. After cooling, a pale yellow precipitate was formed, the solid was filtered off and washed with Et_2O to give white crystalline, S-methyl thiosemicarbazide hydrogen iodide (15g, 72%). ^{1}H NMR (400MHz, DMSO, ppm), δ 10.69 (br.s, 1H), 9.25 (br.s, 1H), 5.35 (br.s, 2H), 3.50 (s, 3H).

6.4.1.2. Synthesis of **6.1.1**

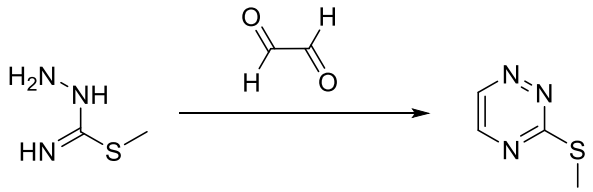

A solution of 40% glyoxal (12.2ml, 266mmol) and $NaHCO_3$ (13.98g, 166mmol) in ice water (75ml) was added to a solution of S-methyl thiosemicarbazide hydrogen iodide (7g, 67mmol) dissolved in ice water (75ml). The reaction mixture was stirred for 10minutes and time evolution of gas was observed. The reaction mixture was left in the fridge for 12 hours and the product was extracted into dichloromethane. The combined organic layers were then washed with dichloromethane (3 x 15ml), dried over Na_2SO_4, filtered and concentrated *in*

vacuo to achieve a yellow oil (3.35g, 40%). ^{1}H NMR (400MHz, $CDCl_3$, ppm), δ 8.95 (d, *J*= 4Hz, 1H), 8.39 (d, *J*= 2Hz, 1H), 2.71 (s, 3H)

6.4.1.3. Synthesis of **6.1.2**

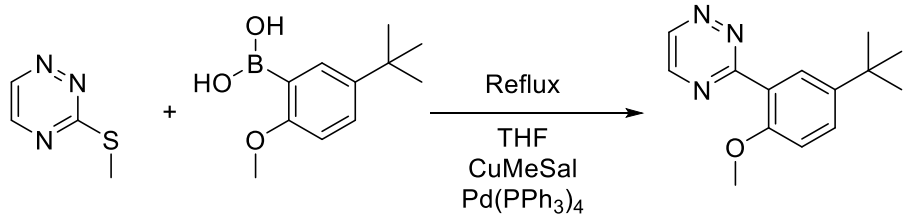

To a mixture of 3-(methylthio)-1,2,4-triazine (0.277g, 2.18mmol), 3-tertbutyl-5-methoxyphenyl boronic acid (1.00g, 4.81mmol), CuMeSal (1.03g, 4.81mmol) in dry THF (50 mL) under argon. Pd(PPh3)4 (0.281g, 0.218mmol) was added. The reaction mixture was stirred overnight at reflux. The reaction was quenched with a Na_2CO_3 saturated solution and extracted with dichloromethane. The combined organic phases were dried over MgSO4 and concentrated in vacuo. After purification by column chromatography on silica gel, (DCM/EtOAc, 2:1), the desired product was obtained as yellowish oil. Yield (0.445g, 84%). ^{1}H NMR (400MHz, $CDCl_3$, ppm), δ 9.23 (d, *J*= 2.4Hz, 1H), 8.74 (d, *J*=2Hz, 1H), 7.86 (s, *J*= 2.4Hz, 1H), 7.55 (dd, *J*= 6, 2.6Hz, 1H), 7.06 (d, *J*= 12Hz, 1H), 3.90 (s, 3H), 1.35 (s, 9H).

6.4.1.4. Synthesis of **6.1.3**

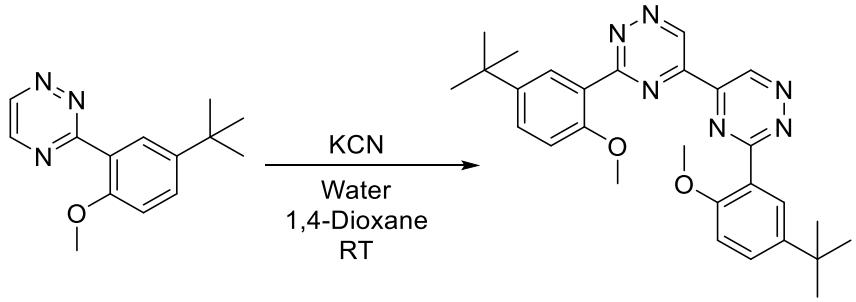

A solution of 3-(5-tert-butyl-2-methoxyphenyl)-1,2,4-triazine (0.445g, 1.83mmol) in water (10ml), 1,4-dioxane (15ml) was stirred until complete dissolution. A solution of KCN (0.12g, 1.83mmol) was added in two equal portions (2 x 3ml). The mixture was stirred overnight,

washed with water and methanol to give 3-(5-tert-butyl-2-methoxyphenyl)-5-[3-(5-tert-butyl-2-methoxyphenyl)-1,2,4-triazin-5-yl]-1,2,4-triazine. Yield (0.265g, 30%). ^{1}H NMR (400MHz, $CDCl_3$, ppm), δ 10.31 (s, 2H), 8.03 (d, *J*= 2.4Hz, 2H), 7.64 (dd, *J*=7, 2.8Hz, 2H), 7.13 (d, *J*= 8.4Hz, 2Hz), 3.75 (s, 6H), 1.38 (s, 9H). HRMS (ESI) calcd for $C_{28}H_{33}N_6O_2$ ($[M+H]^+$): m/z 485.2665. Found: m/z 485.2652.

6.4.1.5. Synthesis of **6.1.4**

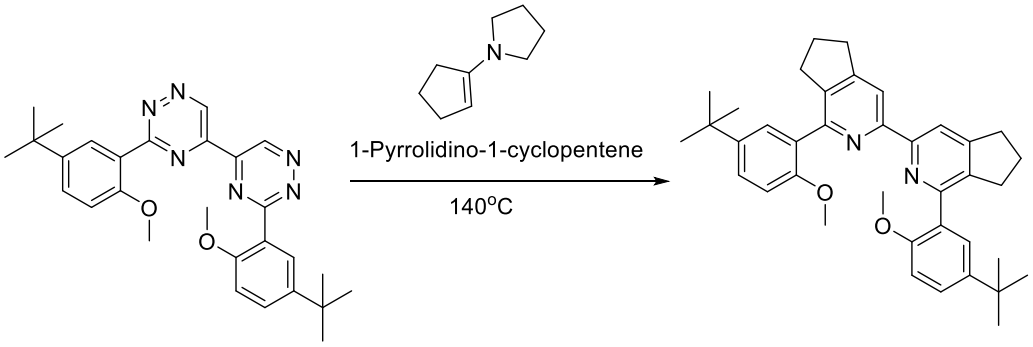

A sample of **6.1.3** (0.265g, 0.566mmol) was placed in a round bottom flask under an argon atmosphere. 1-pyrroldino-1-cyclopentene (0.291ml, 2.263mmol) was added slowly. The flask was heated at 140°C for 1 hour. Acetic acid was added (5ml) and refluxed for 30mins. The mixture was left to cool to room temperature overnight. Water (15ml) was added resulting in the formation of solid. The solid was filtered and washed with water. White solid was collected and weighed. (0.136g, 80%). ^{1}H NMR (400MHz, $CDCl_3$, ppm), δ 8.36 (s, 2H), 7.53 (d, *J*=2.4 Hz, 2H), 7.44 (dd, *J*= 6, 2.4 Hz, 2H), 6.96 (d, *J*= 8.8 Hz, 2H), 3.85 (s, 6H), 3.00 (t, *J*= 7.2 Hz, 4H), 2.82 (t, *J*= 7.2 Hz, 4H), 2.05 (quin, *J*= 7.2 Hz, 4H), 1.34 (s, 18H). ^{13}C NMR (100MHz, $CDCl_3$), δ 155.0, 154.9, 154.5, 152.5, 143.3, 139.7, 129.6, 128.7, 126.3, 116.5, 110.8, 55.7, 34.4, 33.3, 31.8, 31.5, 25.1.

6.4.1.6. Synthesis of **6.1.5**

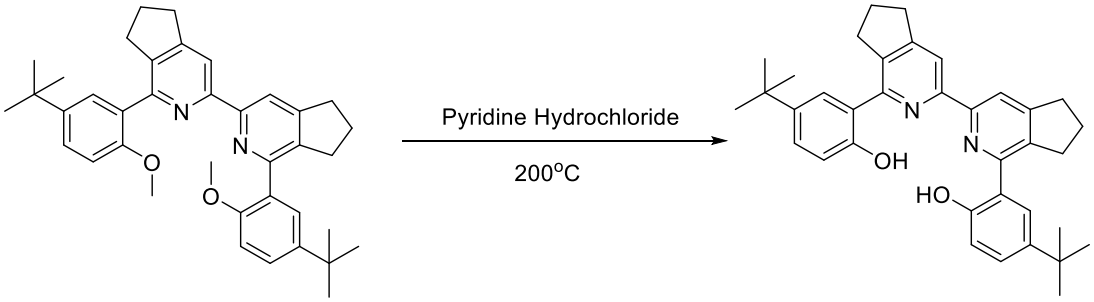

A sample of **6.1.4** (0.136g, 0.243mmol) to a round bottom flask with pyridine hydrochloride (1.99g, 17.2mmol). The reaction mixture was then heated to 200°C for 2 hours. Water (30ml) was then added to the flask and the resulting grey solid was filtered and washed with water to give **6.1.5**. Yield (0.12g, 93%). ^{1}H NMR (400MHz, $CDCl_3$, ppm), δ 8.12 (s, 2H), 7.83 (d, *J*= 2 Hz, 2H), 7.42 (dd, *J*= 6.8, 2 Hz, 2H), 7.08 (d, *J*= 8.8 Hz, 2H), 3.40 (t, *J*= 7.2 Hz, 4H), 3.15 (t, *J*= 7.4 Hz), 2.25 (quin, *J*= 7.2 Hz, 4H), 1.42 (s, 9H).^{13}C NMR (100MHz, $CDCl_3$), δ 159.0, 156.7, 153.9, 141.1, 137.8, 128.1, 125.9, 120.2, 117.4, 115.9, 34.6, 34.4, 33.6, 31.8, 25.9. HRMS (ESI) calcd for $C_{36}H_{41}N_2O_2$ ($[M+H]^+$): m/z 533.3168. Found: m/z 533.3170.

6.4.1.7. Synthesis of **6.1.8**

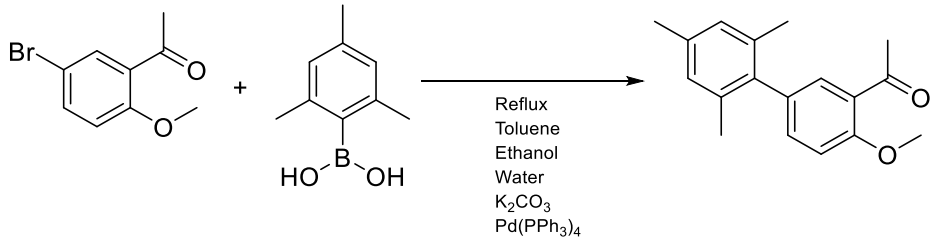

A mixture of K_2CO_3 (2.00g, 14.47mmol) and toluene (100ml) was degassed for 5minutes. Water (25ml) and ethanol (25ml) were added and degassed under argon. 1-(5-bromo-2-methoxyphenyl)ethan-1-one (5.00g, 21.8mmol) and 2,4,6-trimethylphenylboronic acid (3.93g, 24.01mmol) were added to the suspension, the reaction was degassed further. Tetrakis palladium(triphenylphosphine) (1.26g, 1.09mmol) and the reaction was heated under reflux overnight. The reaction mixture was separated with brine (20ml) and extracted into EtOAc (3 x 20ml). The organic layers were collected and dried over $MgSO_4$. The solvent was removed under reduced pressure resulting in the formation of solid. The solid was purified by column chromatography (fine silica, DCM/EtOAc, 10:1), the solvent was removed under reduced pressure resulting in a yellow/white solid. Yield (4.37g, 74%). ^{1}H NMR (400MHz, $CDCl_3$, ppm), δ 7.53 (d, *J*= 2.3Hz, 1H), 7.22 (d, *J*= 2.3Hz, 1H), 7.03 (d, *J*= 8.2Hz, 1H), 6.91 (s, 2H), 3.95 (s, 3H), 3.47 (d, *J*= 5.5Hz, 3H), 2.63 (s, 3H), 2.31 (s, 3H), 1.98 (s, 6H). ^{13}C NMR (100MHz, $CDCl_3$), δ 199.7, 157.8, 137.7, 136.8, 136.3, 134.7, 133.3, 131.4, 128.2, 128.1, 111.8, 55.7, 32.0, 21.1, 20.9.

6.4.1.8. Synthesis of **6.1.9**

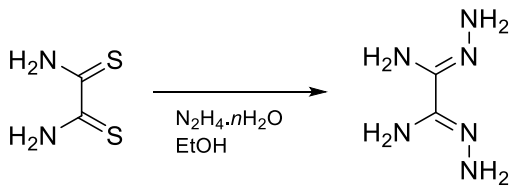

To a suspension of dithiooxamide (5.2g, 43mmol) in ethanol (50ml), hydrazine hydrate (7ml, 133mmol) was added and the mixture was stirred at room temperature for 15minutes. The red colour of the starting material faded and a beige colour formed with evolution of SH_2. The

reaction was heated under reflux for 15 minutes, the precipitate was filtered whilst hot and washed with ethanol and diethyl ether (4.45g, 88%). ^{1}H NMR (400MHz, DMSO, ppm), δ 4.97 (br.s, 4H), 3.31 (br.s, 4H).

6.4.1.9. Synthesis of **6.1.10**.

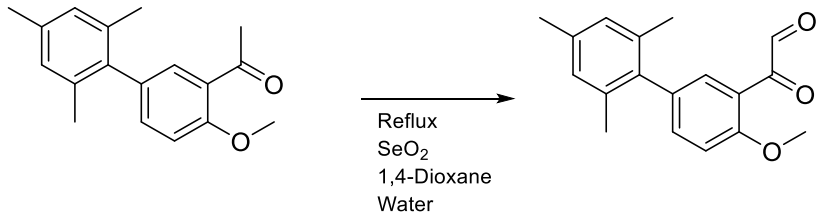

Selenium dioxide (0.484g, 4.36mmol) was dissolved in 1,4-dioxane (30ml) and H_2O (1ml). **6.1.8** (1g, 3.73mmol) in 1,4-dioxane (10ml) was added to the solution and the reaction was heated under reflux overnight. The precipitated selenium was filtered through celite and the solvent was removed under reduced pressure. The resulting brown oil was purified by column chromatography (fine silica, DCM/EtOAc, 10:1). The solvent was removed under reduced pressure yielding an orange brown oil. Yield (0.9g, 85%). ^{1}H NMR (400MHz, $CDCl_3$, ppm), δ 9.74 (s, 1H), 7.61 (d, *J*= 2.3Hz, 1H), 7.52 (d, *J*= 2.3Hz, 1H), 7.38 (dd, *J*= 8.2, 2.3Hz, 1H), 7.04 (br.d, *J*= 8.7Hz, 1H), 7.01 (br.d, *J*= 8.2Hz, 1H), 2.66 (s, 3H), 2.31 (s, 9H).

6.4.1.10. Synthesis of **6.1.11**

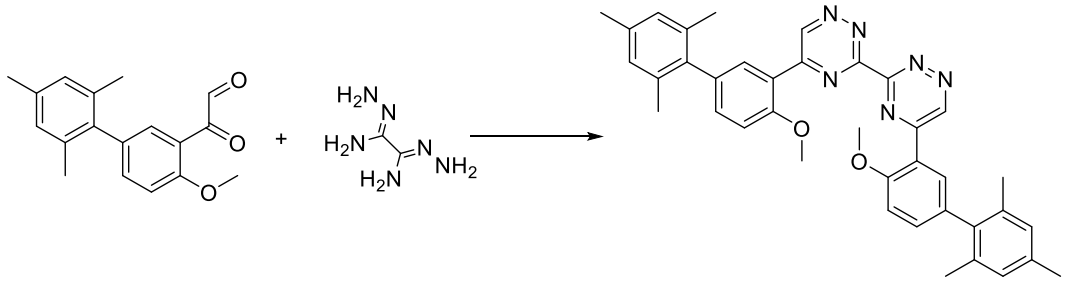

Diamidrazone (0.16g, 1.36mmol) in ethanol (40ml) was added to the oily suspension of **6.1.10** (0.90g, 2.71mmol). The reaction was heated under reflux overnight before cooling to room temperature. The precipitated solid was filtered and washed with ethanol (10ml) to leave a grey crystalline solid. Yield (0.18g, 23%). ^{1}H NMR (400MHz, $CDCl_3$, ppm), δ 10.13 (s, 2H), 8.08 (d, *J*= 1.83Hz, 2H), 7.31 (dd, *J*= 8.5, 2Hz, 2H), 7.11 (d, *J*= 8.7Hz, 2H), 6.89 (s, 4H), 4.02 (s, 6H), 2.32 (s, 6H), 2.01 (s, 12H). ^{13}C NMR (100MHz, $CDCl_3$), δ 157.5, 150.1, 136.9, 136.3, 135.1, 134.5, 132.7, 128.2, 111.8, 55.8, 21.1, 20.9.

6.4.1.11. Synthesis of **6.1.12**

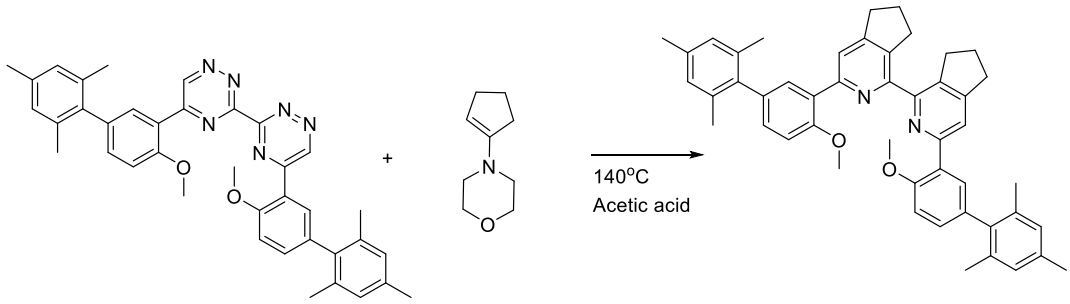

To a sample of **6.1.11** (0.15g, 0.246mmol), 1-morpholino-1-cyclopentene (0.151g, 0.985mmol) was added to the solid before being heated to 140°C for 1 hour. Acetic acid (10ml) was added to the suspension and the reaction was heated under reflux for 30minutes. Water (10ml) was added and the reaction as allowed to cool to RT. The precipitated solid was filtered and washed with water yielding a brown solid. Yield (0.12g, 71%). ^{1}H NMR (400MHz, $CDCl_3$, ppm), δ 7.65 (s, 2H), 7.55 (s, 2H), 7.08 (d, *J*= 8.7Hz, 2H), 7.02 (d, *J*=8.2Hz, 2H), 6.92 (s, 4H), 3.88 (s, 6H), 3.32 (t, *J*= 7.6Hz, 4H), 2.96 (t, *J*= 7.6Hz, 4H), 2.31 (s, 6H), 2.07-2.02 (m, 16H).

6.4.1.12. Synthesis of **6.1.13**

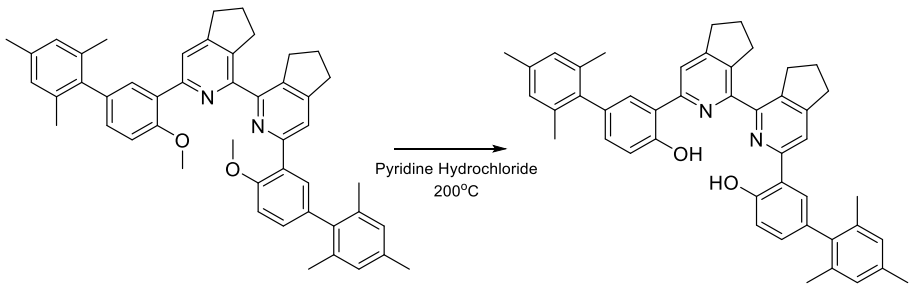

A sample of **6.1.12** (0.100g, 0.146mmol) was added to a flask with pyridine hydrochloride (1.5g, 13.00mmol), the reaction was heated to 200°C for 2 hours. Water (30ml) was added to the flask, the resulting black solid was filtered and washed with water. Yield (0.080g, 83%). ^{1}H NMR (400MHz, $CDCl_3$, ppm), δ 7.64 (s, 2H), 7.55 (d, *J*= 2.3Hz, 2H), 7.07 (m, 2H), 7.03 (t, *J*= 8.2Hz, 2H), 6.92 (s, 4H), 3.87 (s, 2H), 3.32 (t, *J*= 7.6Hz, 4H), 2.96 (t, *J*= 7.6Hz, 4H), 2.31 (s, 6H), 2.05 (s, 16H).

6.4.2. Tetradentate O^N^N^O Platinum Complexes

6.4.2.1. Synthesis of **6.0.2**

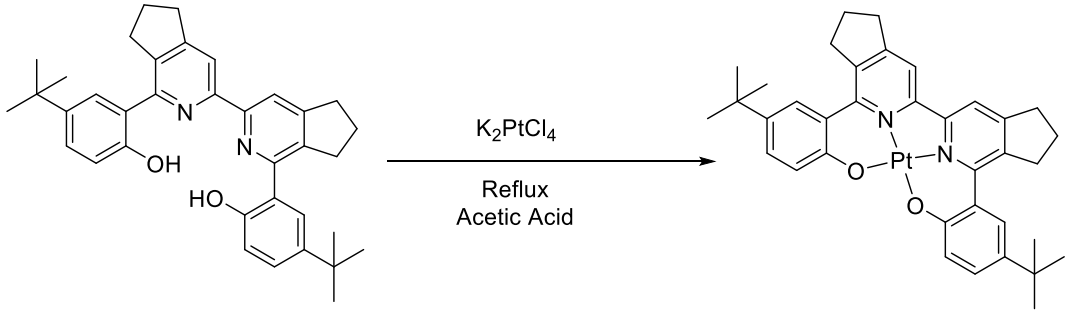

A mixture of **6.1.5** (0.06g, 0.113mmol) and potassium tetrachloroplatinate (0.046g, 0.113mmol) in acetic acid (30ml) was heated under reflux for 14 hours. Water (30ml) was added and the solid product was filtered off, washed with water and dried to give **6.0.2** (0.023g, 28%).^{1}H NMR (400MHz, DMSO, ppm), δ 8.43 (s, 2H), 7.63 (d, *J*= 2.4 Hz, 2H), 7.36 (dd, *J*= 6.4, 2.4 Hz, 2H), 7.04 (d, *J*= 8.8 Hz, 2H), 3.42 (t, *J*= 6.8 Hz, 4H), 2.95 (t, *J*= 6.8 Hz, 4H), 2.01

(m, 4H), 1.30 (s, 18H). HRMS (ESI) calcd for $C_{36}H_{39}N_2O_2Pt$ ($[M+H]^+$): m/z 725.2639. Found: m/z 725.2646.

*Due to the insolubility of the complex, the sample was unable to be characterised by ^{13}C NMR.

6.4.2.2. Synthesis of **6.0.3**

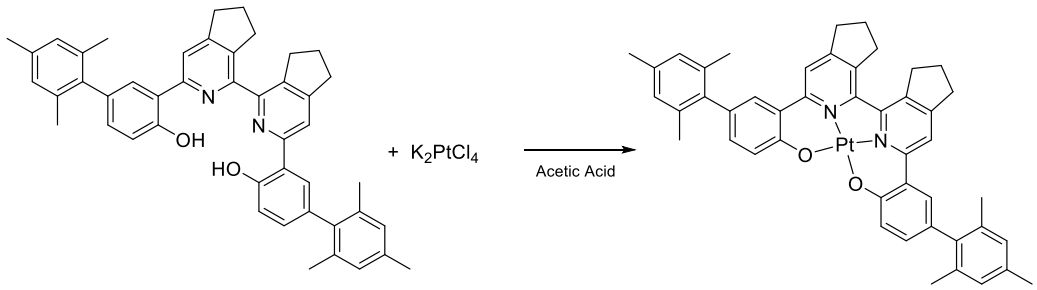

A sample of **6.1.13** (0.060g, 0.091mmol) was added to acetic acid (40ml) and heated until all solid had dissolved. Potassium tetrachloroplatinate (0.041g, 0.1mmol) was added to the suspension and the reaction was heated under reflux overnight. Water (10ml) was added and the reaction was allowed to cool to room temperature. The resulting brown solid was then purified by column chromatography (fine silica, DCM), yielding an orange solid. Yield (0.015g, 20%). ^1H NMR (400MHz, $CDCl_3$, ppm), δ 8.05 (s, 2H), 7.56 (s, 2H), 7.51 (d, *J*= 8.7Hz, 2H), 7.11 (d, *J*= 8.7Hz, 2H), 6.96 (s, 4H), 3.10 (t, *J*= 6.9Hz, 4H), 2.92 (t, *J*= 7.2Hz, 4H), 2.33 (s, 6H), 2.16-2.08 (m, 16H). HRMS (ESI) calculated for $C_{46}H_{42}N_2O_2Pt$ ($[M+H]^+$)= 850.29670. Found m/z = 850.29590.

CHAPTER 7

Conclusions & Future Work

7. Conclusions and Future Work

As a result of this project a variety of novel mono- and dinuclear cyclometalated complexes have been prepared. Although dinuclear complexes were the major target, much of new knowledge was generated for the mononuclear complexes and will the basis for two publications. For example, complexes employing phenolic O^N^C type auxiliary ligands were prepared for the first time and showed promising photophysical behaviour (manuscript in preparation). New synthetic route to neutral tetradentate complexes of ONNO type was developed based on chemistry of 1,2,4-triazines and was described as a paper in *Inorganic Chemistry*.

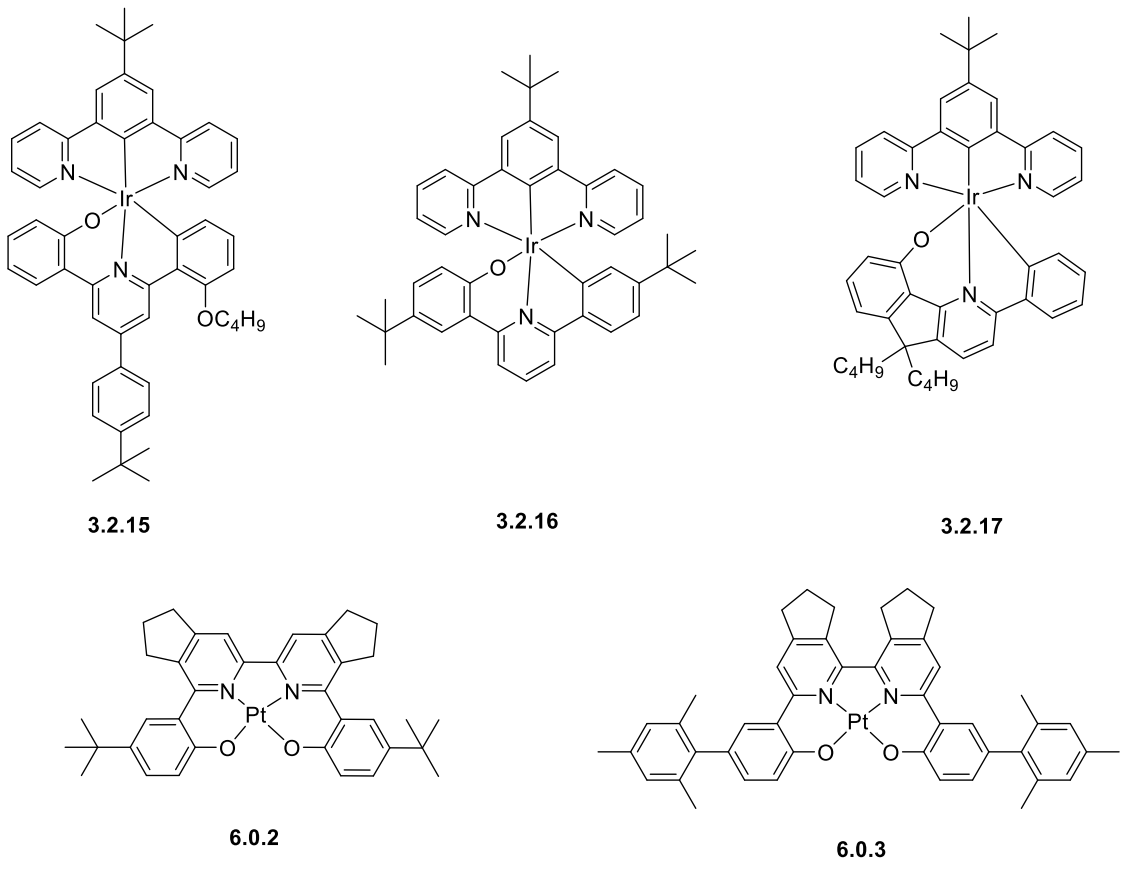

Figure 124 - The structures of the mononuclear complexes that are and will be subject for publications.

However, the most important results of this thesis were obtained for dinuclear complexes. These results will be a subject for two publications. During this project, we developed highly soluble diiridium complexes that were successfully used to prepare a solution-processible

OLEDs with external quantum efficiency of 8%. We also showed that fluorine-free complexes can be prepared although the emission maximum shift to a deeper red region.

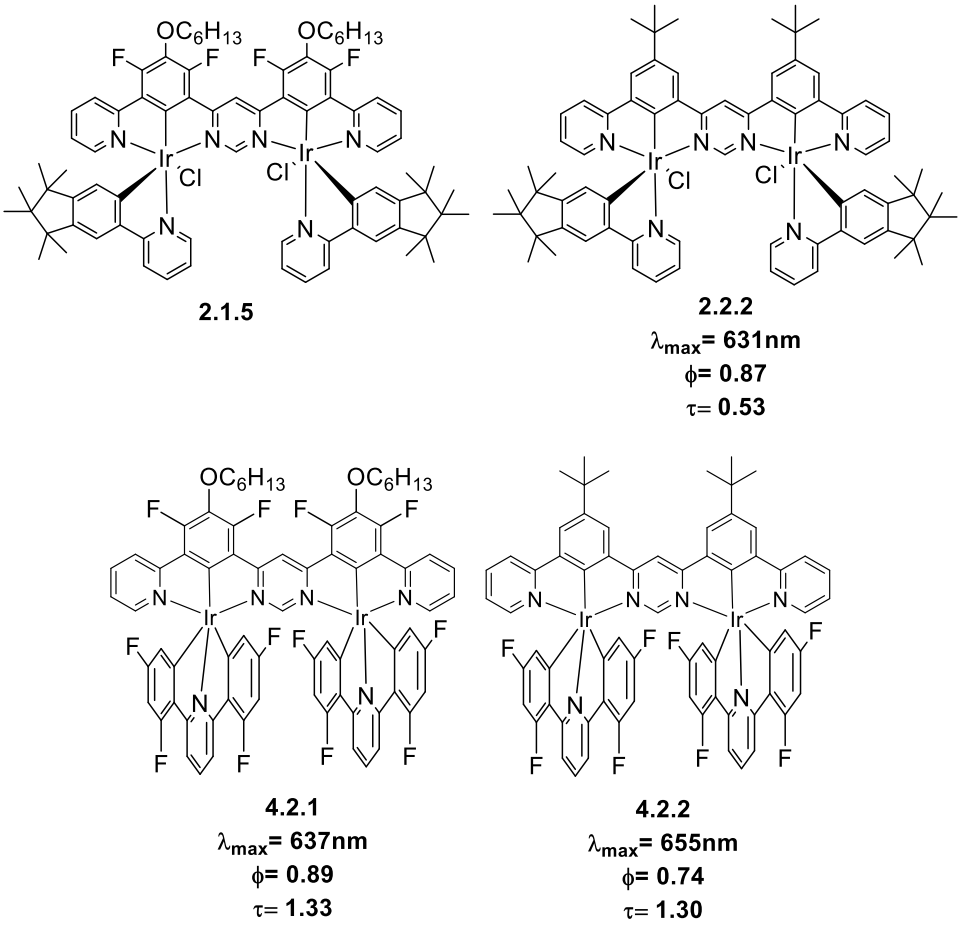

Figure 125 - The di-iridium complexes prepared and characterised during the project. Two manuscripts are currently in preparation for publication.

The most exciting results of this thesis are unprecedented dinuclear complexes **4.2.2** and **4.2.1**, which were prepared on a 1g scale and fully characterised. These complexes are one of the best deep-red emitters known to date which showed excellent performance in OLEDs with EQE of 20%. All our attempts to prepare fluorine-free analogues have failed so far, but this research will be continued.

It should be noted that in all cases, the synthesis of dinuclear complexes proved to be a very challenging task. The reaction conditions developed and optimised for mononuclear model compounds do not always translate well for the synthesis of corresponding dinuclear systems.

This is a particularly acute problem if unsymmetrical ligands are used; thus leading to formation of *rac*- and *meso*- isomers.

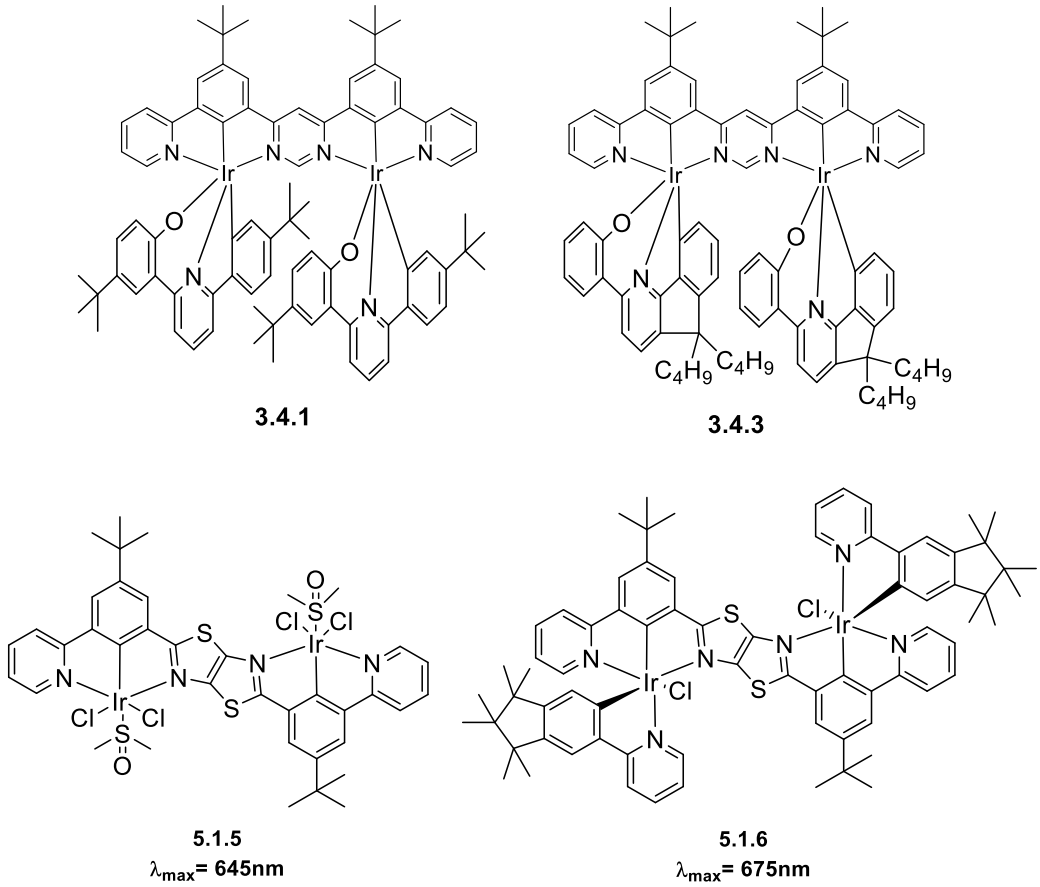

Figure 126 - The di-iridium complexes prepared during the project however a sufficiently pure sample was not isolated.

In the follow-up work, dinuclear systems that do not form mixtures of isomers will be targeted with some key-bridging ligands having already been prepared (shown in Figure 127).

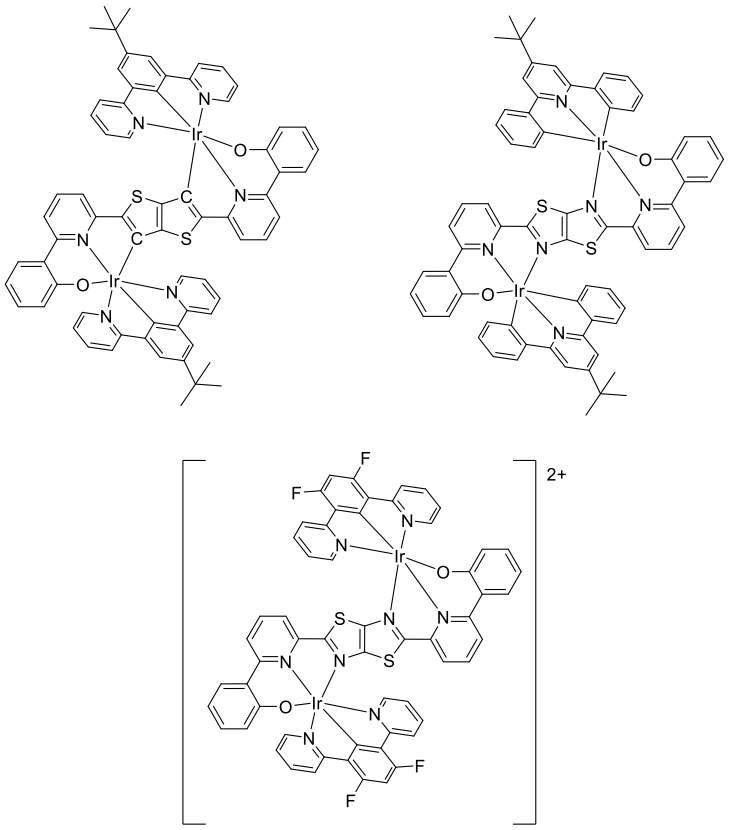

Figure 127 - Examples of charge neutral and cationic dinuclear complexes that would result in the formation of a single isomer.

This work targeted complexes exclusively for OLED application. In the future complexes of similar design but of ionic character will be prepared for bioimaging applications. This is particularly important because not only the emission but also the absorption in the red region is exceptionally high for bimetallic complexes; resulting in the high brightness of these emitters. High absorption in the red region is also of interest for application in dye-sensitised solar cells, photocatalysis and photo-dynamic therapy. There is a bright future for these bright emitters!

CHAPTER 8

Appendices

8. Appendices

8.1. Equipment and Chemicals

Reagents were purchased from Sigma Aldrich, Alfa Aesar, Fisher Scientific, Fluorochem and Apollo Scientific and were used without any further purification.

Solvents were purchased from Fisher Scientific, Sigma Aldrich and Alfa Aesar at reagent, HPLC or spectroscopic grade. When required, solvents were dried over activated 4 Å molecular sieves.

Column chromatography was carried out using Fisher Scientific silica gel 60 Å (35-70 μ). Specific complexes (**2.2.2**, **4.2.2**, **4.2.1**, **5.1.6**) were carried out with smaller particle size, Apollo Scientific ZEOprep 60 Å (15-40 μ).

NMR Spectroscopy was performed on JEOL ELS400 Delta spectrometer at frequencies of 400 MHz for ^{1}H and ^{19}F NMR and 101 MHz for ^{13}C NMR. Chemical shifts (δ) are in ppm, using tetramethylsilane (TMS) as an internal standard and coupling constants are in Hertz. Deuterated chloroform ($CDCl_3$), deuterated dimethyl sulfoxide (DMSO-d^6), deuterated dichloromethane (DCM-d^2) and deuterated acetonitrile (ACN-d^3) were used as solvents. Chemical shifts were observed with splitting, integrals and *J* values. The splitting of the signals were recorded as singlet (s), doublet (d), triplet (t), quartet (q), quintet (quin), sextet (sext) and multiplet (m). Additionally, further splitting of signals were recorded as e.g. doublet of doublets (dd) and triplet of doublets (ddd).

Mass spectrometry was carried out at the EPSRC National Mass Spectrometry Service Centre on at Swansea University using spectrometers including a Thermo Scientific LTQ Orbitrap XL Mass spectrometer, a Waters Xevo G2-S ToF spectrometer, a Bruker ultrafleXtreme spectrometer and a Finnigan MAT 9S XP spectrometer. Ionisation techniques used included low resolution electrospray (ESI), high-resolution nano-electrospray (NSI) ionisation, atmospheric solids analysis probe (ASAP) and matrix-assisted laser desorption ionisation

(MALDI).Mass spectra was carried out at Northumbria University using a Thermo Scientific Q-Exactive high resolution mass spectrometer with electrospray ionisation (ESI).

Absorption spectra recorded at Northumbria University were measured on a Varian Cary 50 Bio Uv-Visible Spectrophotometer using quartz cuvettes of 1cm path length.

Luminescence spectra recorded at Northumbria University were measured using a Horiba Jobin Yvon FluoroMax®-4 spectrofluorimeter. Samples for emission measurements were contained within quartz cuvettes of 1 cm path length.

8.2. HOMO and LUMO Orbital Calculations and Imaging for Complexes

The HOMO and LUMO calculations for the di-iridium complex **2.2.2** and the mono-iridium analogue, **2.2.1**.

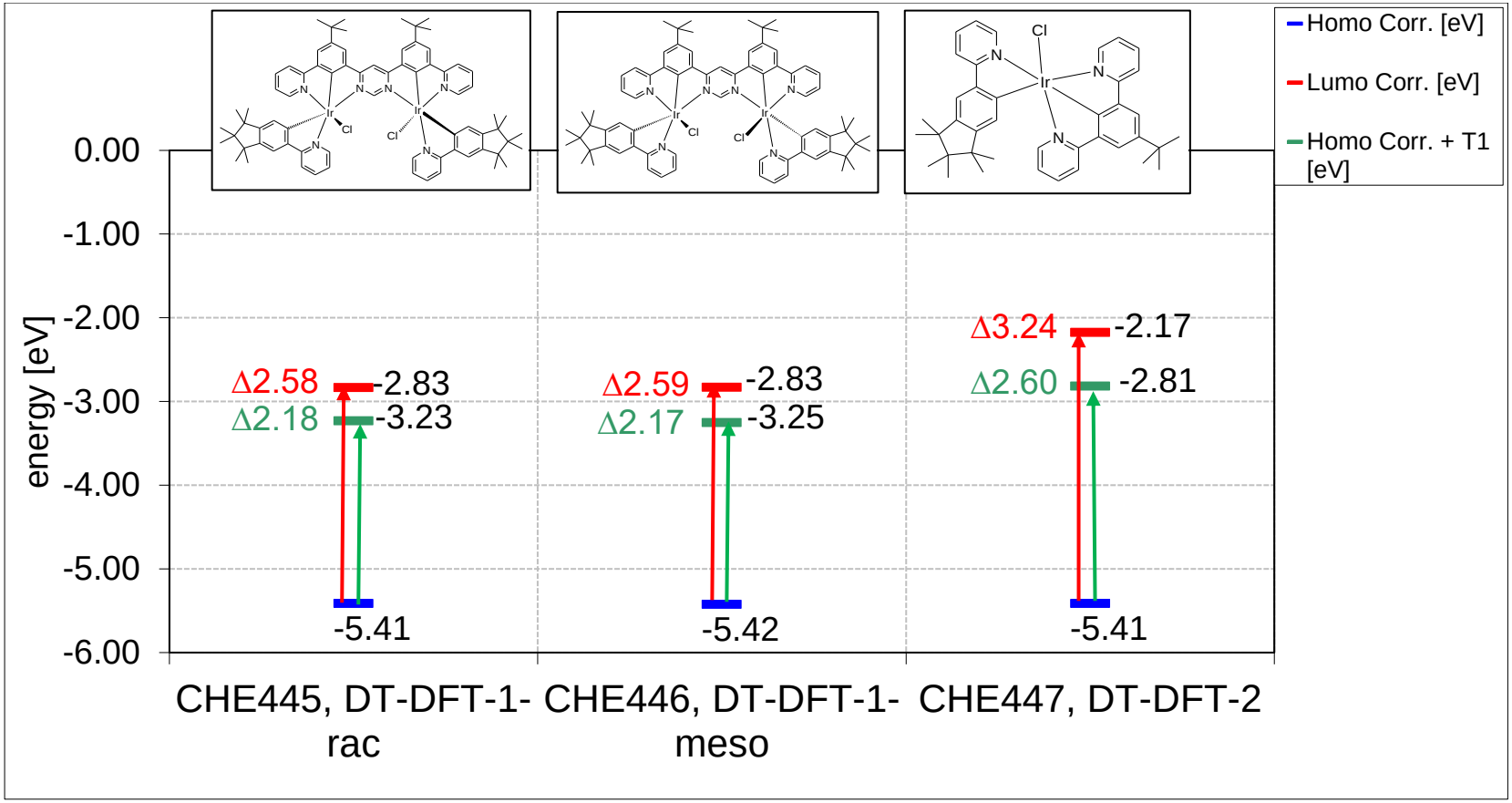

The HOMO and LUMO orbitals visualised at Merck KGaA for **2.2.1** and **2.2.2**.

Orbital Level	**2.2.1**	**2.2.2**-*meso*	**2.2.2**-*rac*
LUMO+1	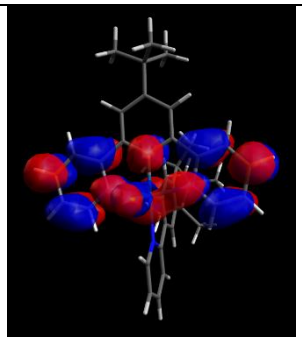	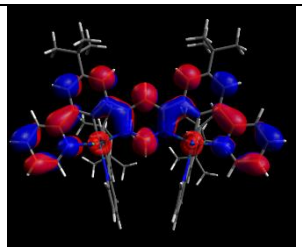	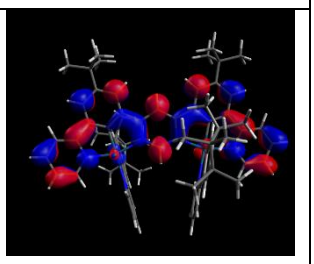
LUMO	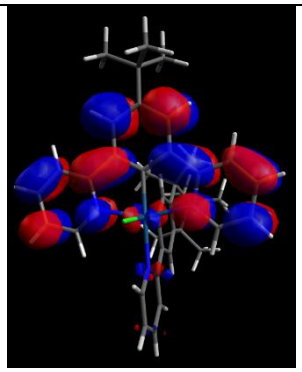	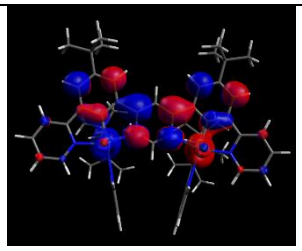	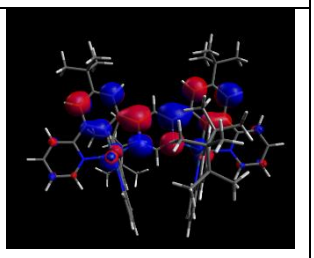
HOMO	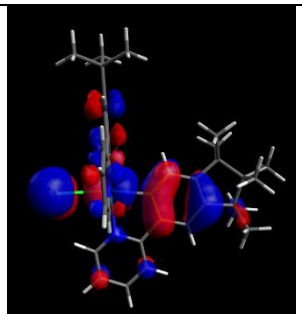	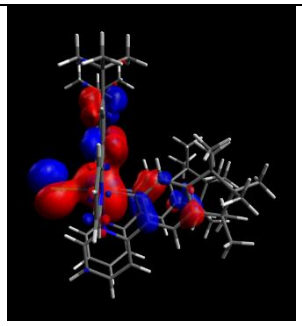	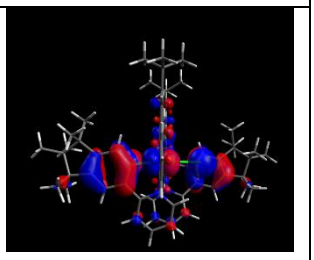
HOMO-1	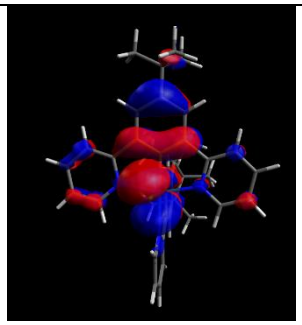	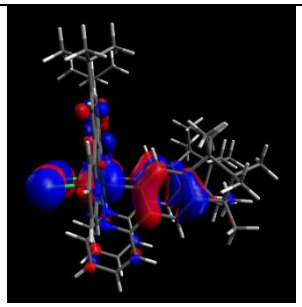	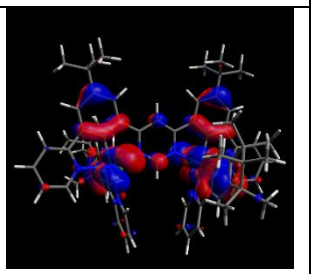

The HOMO and LUMO energy level calculations for VNK-138-2 and **4.2.3** compared to **2.2.1**, **2.2.2**, **3.1.4**, **4.1.4**, **4.1.7** and **4.1.9**.

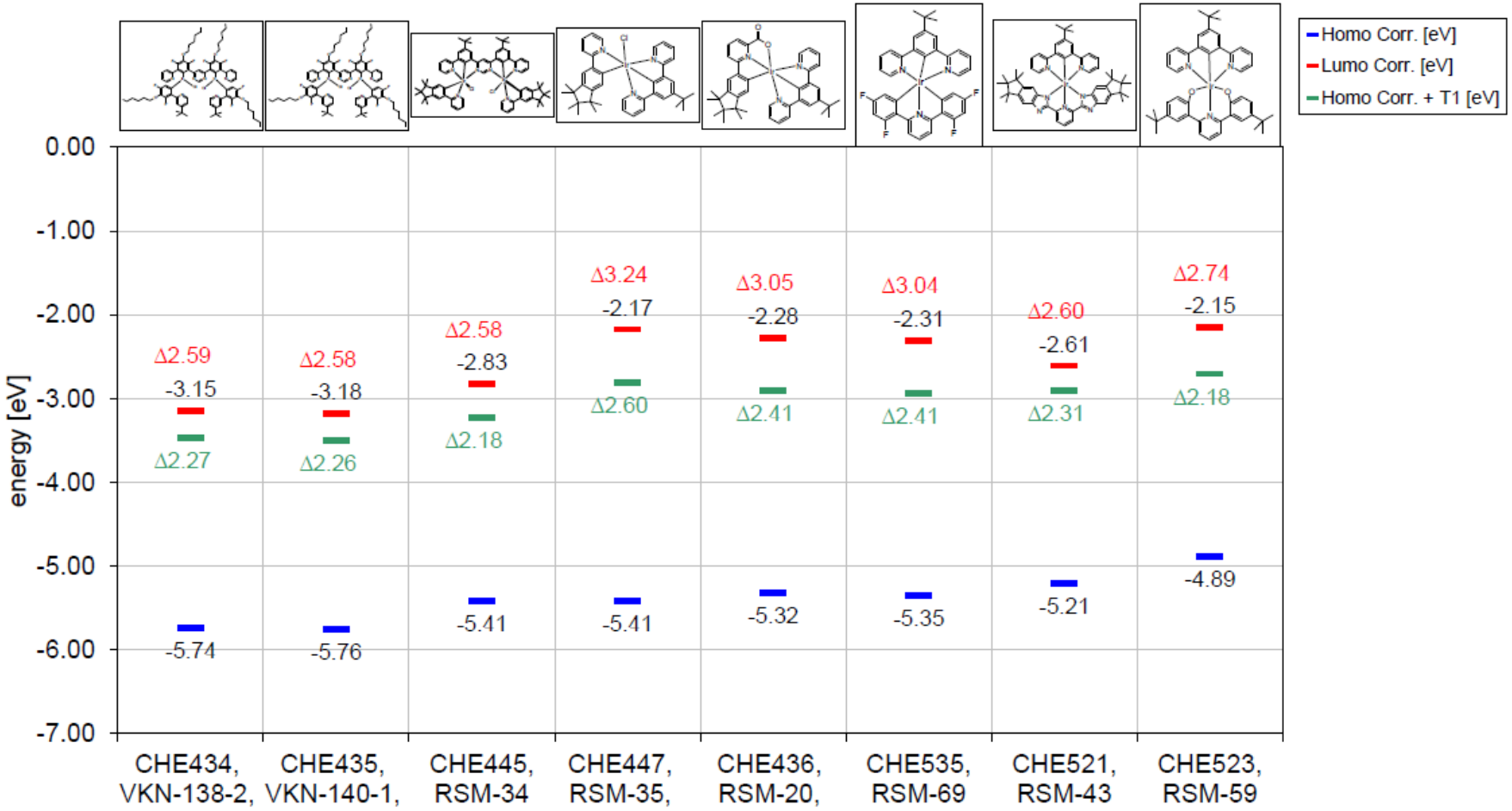

The HOMO and LUMO calculations for complexes such as **5.1.6** (CHE802) and the proposed structures of C^N^C cyclometalated complexes. A back up plan is included which involved altering the heterocycle.

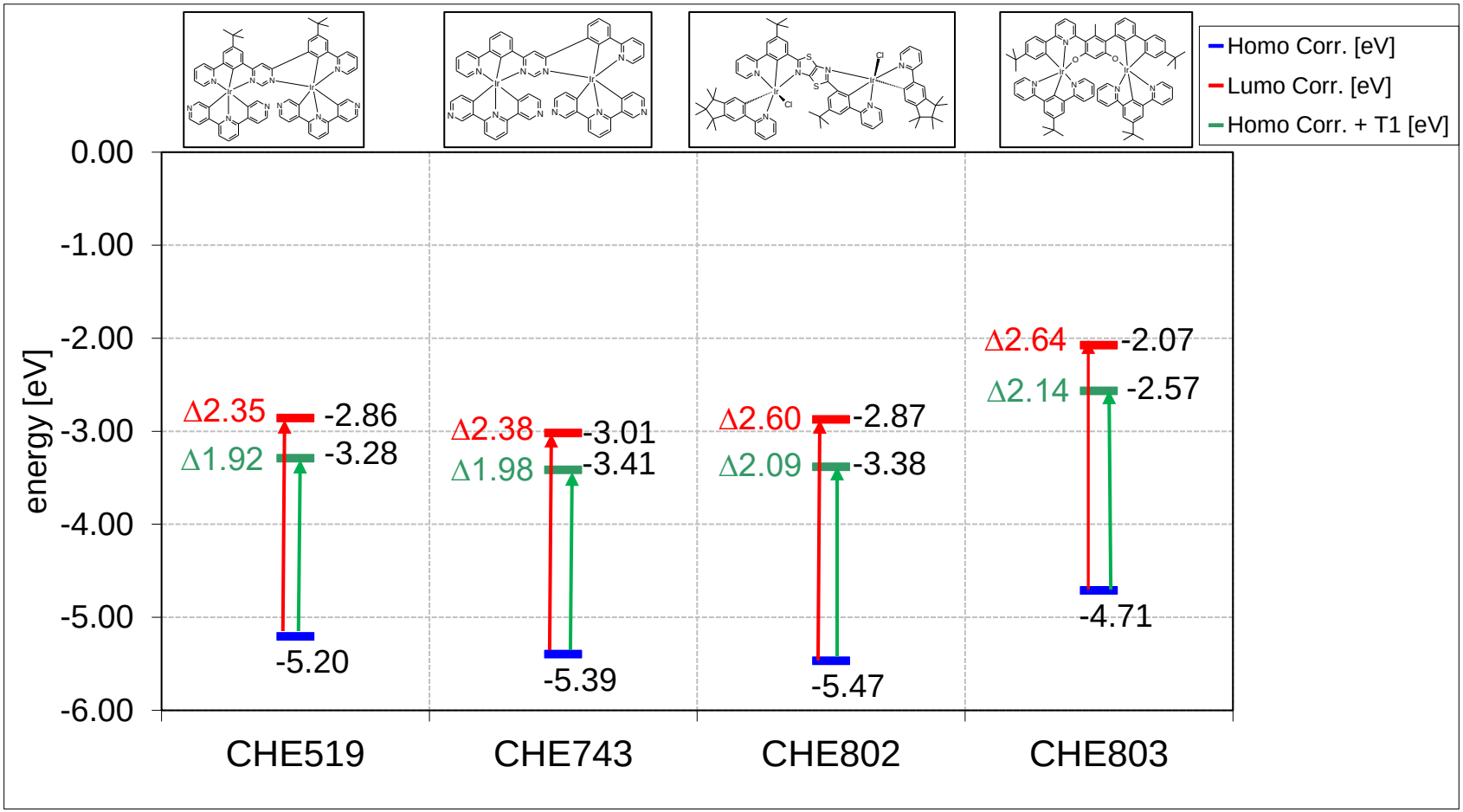

The HOMO and LUMO calculations for the proposed pyridine based C^N^C complexes, **4.1.17**. The preparation was attempted for the mono-nuclear structure however the reaction failed.

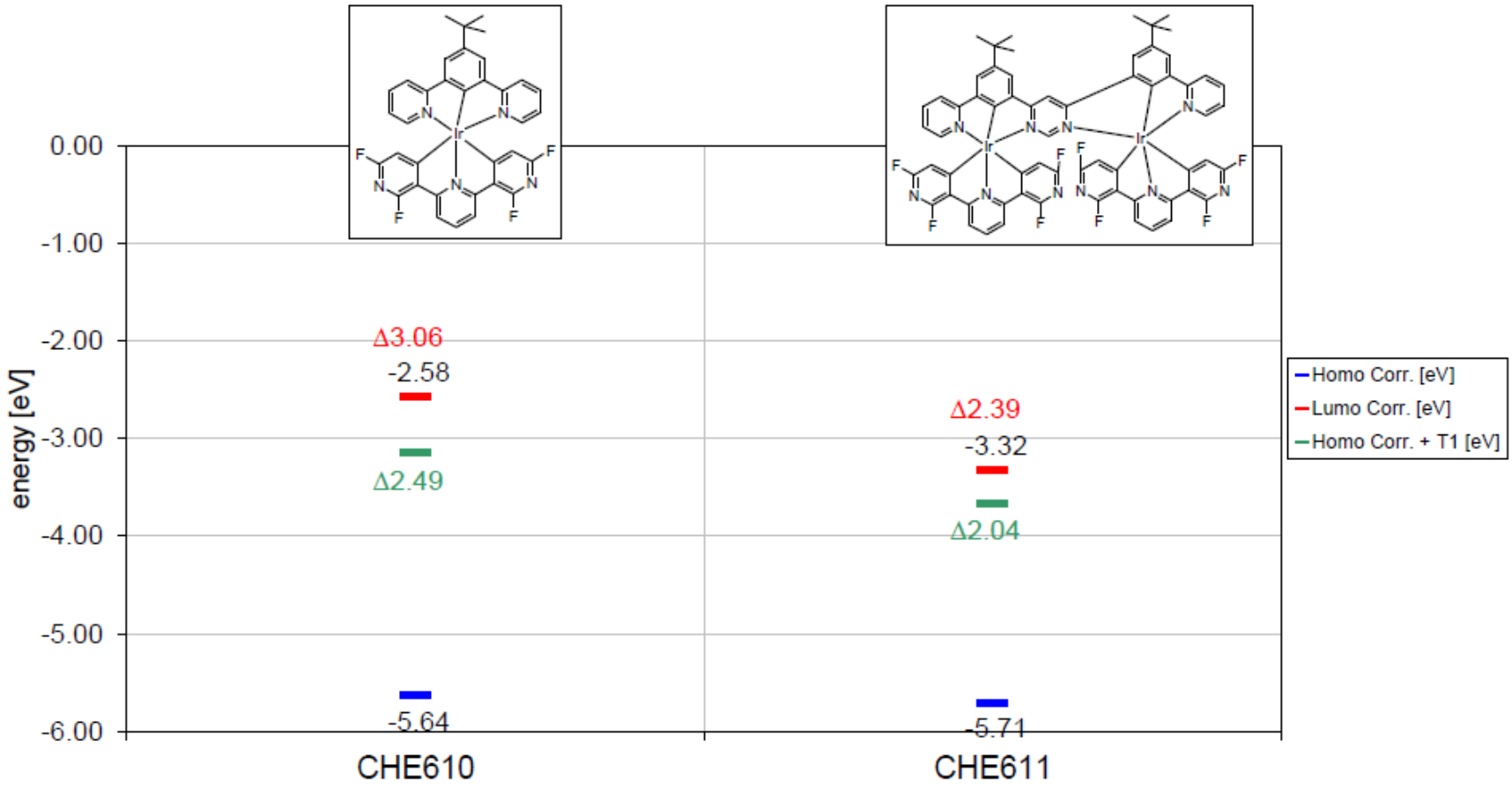

8.3. OLED Device Data for **2.2.2**

The OLED device data for **2.2.2** at different current densities (cd m^{-2}). The graphs show the effect of a changing current density on the external quantum efficiency (%). The final graph shows the LT50 values (h) for each device described. The table also describes the CIE coordinates giving an accurate depiction of the emission colour.

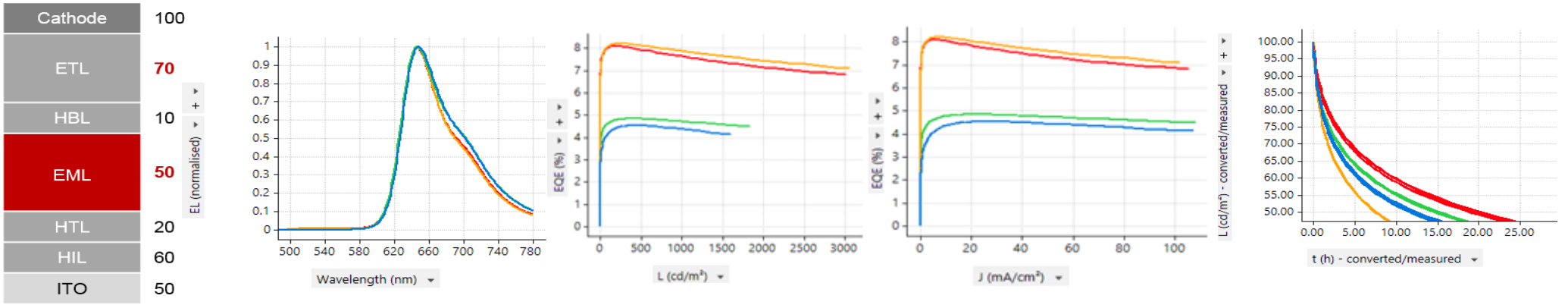

Emitter	EML mix	EL max. [nm]	CIE x/y		EQE [%] @1000 cd/m²	EQE [%] @20 mA/cm²	Eff [cd/A] @1000 cd/m²	LT50 [h] @60 mA/cm²
RSM-34	host A	648	0.71	0.29	4.3	4.5	1.6	13
RSM-34	host D / host A	646	0.71	0.29	4.7	4.9	1.8	15
RSM-34	host B / host C / co-dopant	646	0.70	0.30	7.9	7.9	3.3	8
RSM-34	host D / host C / co-dopant	646	0.70	0.30	7.7	7.8	3.2	20

8.4. OLED Device Data for **4.2.1**

The OLED device data for **4.2.1** with comparisons to **4.2.3**.

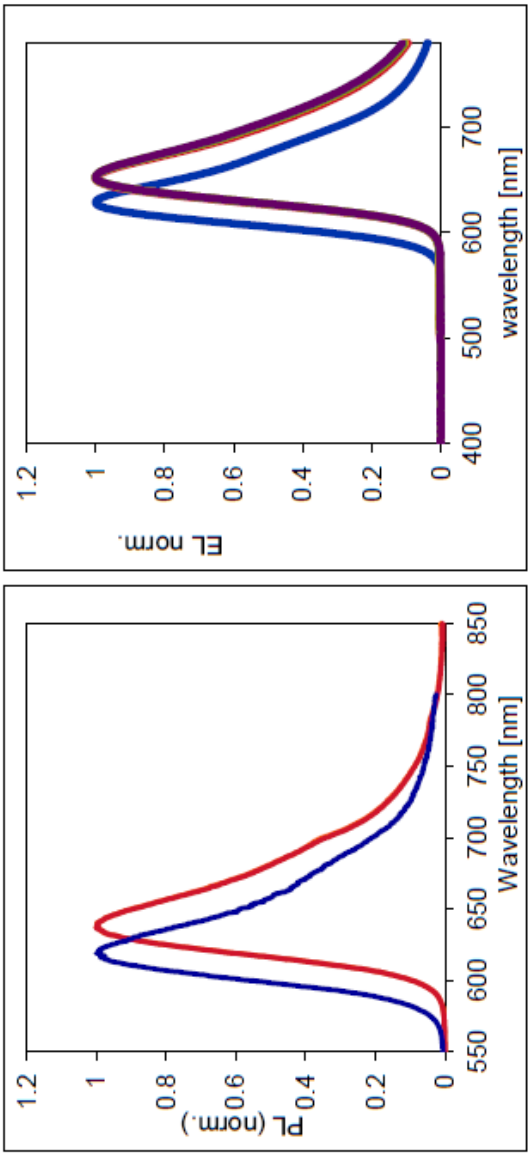

Emitter	EML mix	PL max. [nm]	EL max. [nm]	CIE x/y	
VNK-140-1	best-of (= host A)	619	629	0.68	0.32
RSM-92	host A		652	0.70	0.30
RSM-92	host D / host C / co-dopant	637	653	0.70	0.30
RSM-92	host B / host C / co-dopant		652	0.70	0.30
RSM-92	host D / host B		653	0.71	0.29

The OLED device data for **4.2.1** at different current densities (cd m^{-2}) in comparison to **4.2.3**. The graphs show the effect of a changing current density on the external quantum efficiency (%). The final graph shows the LT50 values (h) for each device described. The table also describes the CIE coordinates giving an accurate depiction of the emission colour

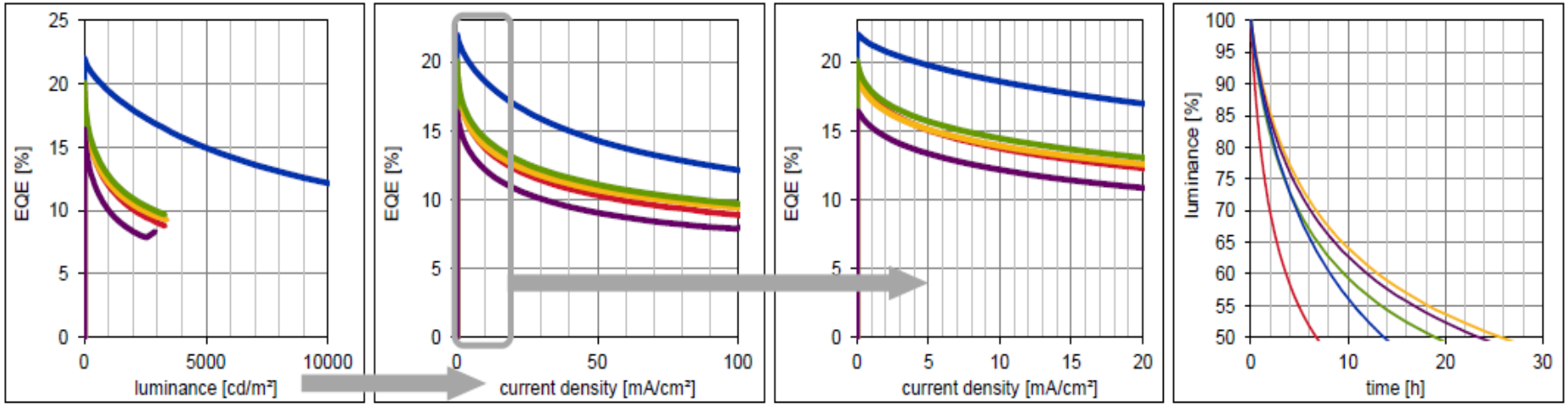

Emitter	EML mix	EL max. [nm]	CIE x/y		EQE [%] @1000 cd/m²	EQE [%] @20 mA/cm²	EQE [%] @0.1 mA/cm²	Eff [cd/A] @1000 cd/m²	LT50 [h] @60 mA/cm²
VNK-140-1	best-of (= host A)	629	0.68	0.32	19.4	17.0	22.0	16.1	15
RSM-92	host A	652	0.70	0.30	12.8	13.1	19.5	4.3	19
RSM-92	host D / host C / co-dopant	653	0.70	0.30	12.2	12.6	18.9	4.2	26
RSM-92	host B / host C / co-dopant	652	0.70	0.30	12.0	12.3	19.7	4.3	7
RSM-92	host D / host B	653	0.71	0.29	10.0	10.9	16.4	3.3	24

CHAPTER 9

References

9. References

1. Chen, Z. q.; Bian, Z. q.; Huang, C. h., Functional Ir(III) complexes and their applications. *Advanced Materials* **2010,** *22* (13), 1534-1539.
2. Nazeeruddin, M. K.; Humphry-Baker, R.; Berner, D.; Rivier, S.; Zuppiroli, L.; Graetzel, M., Highly phosphorescence iridium complexes and their application in organic light-emitting devices. *Journal of the American Chemical Society* **2003,** *125* (29), 8790-8797.
3. Lowry, M. S.; Bernhard, S., Synthetically tailored excited states: phosphorescent, cyclometalated iridium (III) complexes and their applications. *Chemistry-A European Journal* **2006,** *12* (31), 7970-7977.
4. Hedley, G. J.; Ruseckas, A.; Samuel, I. D., Ultrafast intersystem crossing in a red phosphorescent iridium complex. *The Journal of Physical Chemistry A* **2008,** *113* (1), 2-4.
5. Culham, S.; Lanoë, P.-H.; Whittle, V. L.; Durrant, M. C.; Williams, J. G.; Kozhevnikov, V. N., Highly Luminescent Dinuclear Platinum (II) Complexes Incorporating Bis-Cyclometallating Pyrazine-Based Ligands: A Versatile Approach to Efficient Red Phosphors. *Inorganic chemistry* **2013,** *52* (19), 10992-11003.
6. Daniels, R. E.; Culham, S.; Hunter, M.; Durrant, M. C.; Probert, M. R.; Clegg, W.; Williams, J. A. G.; Kozhevnikov, V. N., When two are better than one: bright phosphorescence from non-stereogenic dinuclear iridium (III) complexes. *Dalton Transactions* **2016,** *45* (16), 6949-6962.
7. Kozhevnikov, D. N.; Kozhevnikov, V. N.; Shafikov, M. Z.; Prokhorov, A. M.; Bruce, D. W.; Williams, J. A. G., Phosphorescence vs fluorescence in cyclometalated platinum (II) and iridium (III) complexes of (oligo) thienylpyridines. *Inorganic chemistry* **2011,** *50* (8), 3804-3815.
8. Kozhevnikov, V. N.; Donnio, B.; Bruce, D. W., Phosphorescent, Terdentate, Liquid-Crystalline Complexes of Platinum (II): Stimulus-Dependent Emission. *Angewandte Chemie International Edition* **2008,** *47* (33), 6286-6289.
9. Turnbull, G.; Williams, J. A. G.; Kozhevnikov, V. N., Rigidly linking cyclometallated Ir(iii) and Pt(ii) centres: an efficient approach to strongly absorbing and highly phosphorescent red emitters. *Chemical Communications* **2017,** *53* (18), 2729-2732.
10. Brulatti, P.; Gildea, R. J.; Howard, J. A.; Fattori, V.; Cocchi, M.; Williams, J. A. G., Luminescent Iridium (III) Complexes with N^ C^ N-Coordinated Terdentate Ligands: Dual Tuning of the Emission Energy and Application to Organic Light-Emitting Devices. *Inorganic chemistry* **2012,** *51* (6), 3813-3826.
11. Murphy, L.; Williams, J. G., Luminescent platinum compounds: from molecules to OLEDs. In *Molecular Organometallic Materials for Optics*, Springer: 2010; pp 75-111.
12. Wilkinson, A. J.; Goeta, A. E.; Foster, C. E.; Williams, J. A. G., Synthesis and Luminescence of a Charge-Neutral, Cyclometalated Iridium (III) Complex Containing N^ C^ N-and C^ N^ C-Coordinating Terdentate Ligands. *Inorganic chemistry* **2004,** *43* (21), 6513-6515.
13. Wilkinson, A. J.; Puschmann, H.; Howard, J. A. K.; Foster, C. E.; Williams, J. A. G., Luminescent Complexes of Iridium (III) Containing N^ C^ N-Coordinating Terdentate Ligands. *Inorganic chemistry* **2006,** *45* (21), 8685-8699.
14. Yin, B.; Niemeyer, F.; Williams, J. G.; Jiang, J.; Boucekkine, A.; Toupet, L.; Le Bozec, H.; Guerchais, V., Synthesis, structure, and photophysical properties of luminescent platinum (II) complexes containing cyclometalated 4-styryl-functionalized 2-phenylpyridine ligands. *Inorganic chemistry* **2006,** *45* (21), 8584-8596.
15. Yersin, H., *Highly efficient OLEDs with phosphorescent materials*. John Wiley & Sons: 2008.
16. Minaev, B.; Baryshnikov, G.; Agren, H., Principles of phosphorescent organic light emitting devices. *Physical Chemistry Chemical Physics* **2014,** *16* (5), 1719-1758.
17. Neve, F.; Deda, M. L.; Puntoriero, F.; Campagna, S., Ionic luminescent cyclometalated Ir(III) complexes with polypyridine co-ligands. *Inorganica Chimica Acta* **2006,** *359* (5), 1666-1672.

18. Kasha, M., Characterization of electronic transitions in complex molecules. *Discussions of the Faraday society* **1950,** *9*, 14-19.
19. Balzani, V.; Juris, A.; Venturi, M.; Campagna, S.; Serroni, S., Luminescent and Redox-Active Polynuclear Transition Metal Complexes. *Chemical Reviews* **1996,** *96* (2), 759-834.
20. Lamansky, S.; Djurovich, P.; Murphy, D.; Abdel-Razzaq, F.; Lee, H.-E.; Adachi, C.; Burrows, P. E.; Forrest, S. R.; Thompson, M. E., Highly phosphorescent bis-cyclometalated iridium complexes: synthesis, photophysical characterization, and use in organic light emitting diodes. *Journal of the American Chemical Society* **2001,** *123* (18), 4304-4312.
21. Hofbeck, T.; Yersin, H., The triplet state of fac-Ir (ppy) 3. *Inorganic chemistry* **2010,** *49* (20), 9290-9299.
22. Finkenzeller, W. J.; Yersin, H., Emission of Ir (ppy) 3. Temperature dependence, decay dynamics, and magnetic field properties. *Chemical physics letters* **2003,** *377* (3), 299-305.
23. Jansson, E.; Minaev, B.; Schrader, S.; Ågren, H., Time-dependent density functional calculations of phosphorescence parameters for fac-tris (2-phenylpyridine) iridium. *Chemical physics* **2007,** *333* (2-3), 157-167.
24. Hay, P. J., Theoretical studies of the ground and excited electronic states in cyclometalated phenylpyridine Ir (III) complexes using density functional theory. *The Journal of Physical Chemistry A* **2002,** *106* (8), 1634-1641.
25. Colombo, M. G.; Brunold, T. C.; Riedener, T.; Guedel, H. U.; Fortsch, M.; Bürgi, H.-B., Facial tris cyclometalated rhodium (3+) and iridium (3+) complexes: Their synthesis, structure, and optical spectroscopic properties. *Inorganic Chemistry* **1994,** *33* (3), 545-550.
26. Yersin, H.; Donges, D., Low-lying electronic states and photophysical properties of organometallic Pd (II) and Pt (II) compounds. Modern research trends presented in detailed case studies. In *Transition Metal and Rare Earth Compounds*, Springer: 2001; pp 81-186.
27. Hedley, G. J.; Ruseckas, A.; Samuel, I. D., Ultrafast luminescence in Ir (ppy) 3. *Chemical Physics Letters* **2008,** *450* (4-6), 292-296.
28. Yersin, H., Triplet emitters for OLED applications. Mechanisms of exciton trapping and control of emission properties. In *Transition Metal and Rare Earth Compounds*, Springer: 2004; pp 1-26.
29. Lakowicz, J. R., *Principles of fluorescence spectroscopy*. Springer Science & Business Media: 2013.
30. Tsuboyama, A.; Iwawaki, H.; Furugori, M.; Mukaide, T.; Kamatani, J.; Igawa, S.; Moriyama, T.; Miura, S.; Takiguchi, T.; Okada, S., Homoleptic cyclometalated iridium complexes with highly efficient red phosphorescence and application to organic light-emitting diode. *Journal of the American Chemical Society* **2003,** *125* (42), 12971-12979.
31. Jaffe, H.; Miller, A. L., The fates of electronic excitation energy. *Journal of Chemical Education* **1966,** *43* (9), 469.
32. Tsutsui, T.; Yang, M.-J.; Yahiro, M.; Nakamura, K.; Watanabe, T.; Tsuji, T.; Fukuda, Y.; Wakimoto, T.; Miyaguchi, S., High quantum efficiency in organic light-emitting devices with iridium-complex as a triplet emissive center. *Japanese Journal of Applied Physics* **1999,** *38* (12B), L1502.
33. de Mello, J. C.; Wittmann, H. F.; Friend, R. H., An improved experimental determination of external photoluminescence quantum efficiency. *Advanced Materials* **1997,** *9* (3), 230-232.
34. McNaught, A. D., *Compendium of chemical terminology*. Blackwell Science Oxford: 1997; Vol. 1669.
35. Arppe, R.; Hyppänen, I.; Perälä, N.; Peltomaa, R.; Kaiser, M.; Würth, C.; Christ, S.; Resch-Genger, U.; Schäferling, M.; Soukka, T., Quenching of the upconversion luminescence of NaYF4:Yb3+,Er3+ and NaYF4:Yb3+,Tm3+ nanophosphors by water: the role of the sensitizer Yb3+ in non-radiative relaxation. *Nanoscale* **2015,** *7* (27), 11746-11757.
36. Paris, J.; Brandt, W. W., Charge transfer luminescence of a ruthenium (II) chelate. *Journal of the American Chemical Society* **1959,** *81* (18), 5001-5002.

37. Juris, A.; Balzani, V.; Barigelletti, F.; Campagna, S.; Belser, P.; von Zelewsky, A., Ru(II) polypyridine complexes: photophysics, photochemistry, eletrochemistry, and chemiluminescence. *Coordination Chemistry Reviews* **1988,** *84*, 85-277.
38. Kreitner, C.; Heinze, K., The photochemistry of mono-and dinuclear cyclometalated bis (tridentate) ruthenium (II) complexes: dual excited state deactivation and dual emission. *Dalton Transactions* **2016,** *45* (13), 5640-5658.
39. Williams, J. A. G.; Wilkinson, A. J.; Whittle, V. L., Light-emitting iridium complexes with tridentate ligands. *Dalton Transactions* **2008,** (16), 2081-2099.
40. Leslie, W.; Batsanov, A. S.; Howard, J. A. K.; Williams, J. A. G., Cross-couplings in the elaboration of luminescent bis-terpyridyl iridium complexes: the effect of extended or inhibited conjugation on emission. *Dalton Transactions* **2004,** (4), 623-631.
41. Santoro, A.; Prokhorov, A. M.; Kozhevnikov, V. N.; Whitwood, A. C.; Donnio, B.; Williams, J. A. G.; Bruce, D. W., Emissive Metallomesogens Based on 2-Phenylpyridine Complexes of Iridium(III). *Journal of the American Chemical Society* **2011,** *133* (14), 5248-5251.
42. Williams, J. A. G.; Beeby, A.; Davies, E. S.; Weinstein, J. A.; Wilson, C., An alternative route to highly luminescent platinum (II) complexes: cyclometalation with N^ C^ N-coordinating dipyridylbenzene ligands. *Inorganic chemistry* **2003,** *42* (26), 8609-8611.
43. Williams, J. A. G.; Develay, S.; Rochester, D. L.; Murphy, L., Optimising the luminescence of platinum(II) complexes and their application in organic light emitting devices (OLEDs). *Coordination Chemistry Reviews* **2008,** *252* (23), 2596-2611.
44. Chi, Y.; Chou, P.-T., Transition-metal phosphors with cyclometalating ligands: fundamentals and applications. *Chemical Society Reviews* **2010,** *39* (2), 638-655.
45. Rausch, A. F.; Murphy, L.; Williams, J. A. G.; Yersin, H., Probing the Excited State Properties of the Highly Phosphorescent Pt(dpyb)Cl Compound by High-Resolution Optical Spectroscopy. *Inorganic Chemistry* **2009,** *48* (23), 11407-11414.
46. Ulbricht, C.; Beyer, B.; Friebe, C.; Winter, A.; Schubert, U. S., Recent Developments in the Application of Phosphorescent Iridium(III) Complex Systems. *Advanced Materials* **2009,** *21* (44), 4418-4441.
47. You, Y.; Park, S. Y., Phosphorescent iridium(iii) complexes: toward high phosphorescence quantum efficiency through ligand control. *Dalton Transactions* **2009,** (8), 1267-1282.
48. Kalyanasundaram, K., *Photochemistry of polypyridine and porphyrin complexes*. Academic Press: 1991.
49. Brady, R.; Miller, W. V.; Vaska, L., Luminescence of d 8 complexes of iridium and rhodium, and its quenching by molecular oxygen and other gases. *Journal of the Chemical Society, Chemical Communications* **1974,** (10), 393-394.
50. Geoffroy, G. L.; Wrighton, M. S.; Hammond, G. S.; Gray, H. B., Electronic absorption and emission spectral studies of square-planar Rhodium (I) and Iridium (I) complexes. Evidence for a charge-transfer emitting state. *Journal of the American Chemical Society* **1974,** *96* (10), 3105-3108.
51. Camassei, F. D.; Ancarani-Rossiello, L.; Castelli, F., Luminescence properties of some platinum (II) complexes. Counter-ion and molecular geometry effects. *Journal of Luminescence* **1973,** *8* (1), 71-81.
52. Maestri, M.; Sandrini, D.; Balzani, V.; Chassot, L.; Jolliet, P.; Von Zelewsky, A., Luminescence of ortho-metallated platinum (II) complexes. *Chemical physics letters* **1985,** *122* (4), 375-379.
53. Paw, W.; Cummings, S. D.; Mansour, M. A.; Connick, W. B.; Geiger, D. K.; Eisenberg, R., Luminescent platinum complexes: tuning and using the excited state. *Coordination chemistry reviews* **1998,** *171*, 125-150.
54. Chassot, L.; Mueller, E.; Von Zelewsky, A., cis-Bis (2-phenylpyridine) platinum (II)(CBPPP): a simple molecular platinum compound. *Inorganic Chemistry* **1984,** *23* (25), 4249-4253.

55. Chassot, L.; Von Zelewsky, A., Cyclometalated complexes of platinum (II): homoleptic compounds with aromatic C, N ligands. *Inorganic Chemistry* **1987,** *26* (17), 2814-2818.
56. Cho, J.-Y.; Suponitsky, K. Y.; Li, J.; Timofeeva, T. V.; Barlow, S.; Marder, S. R., Cyclometalated platinum complexes: High-yield synthesis, characterization, and a crystal structure. *Journal of Organometallic Chemistry* **2005,** *690* (17), 4090-4093.
57. Gianini, M.; Forster, A.; Haag, P.; von Zelewsky, A.; Stoeckli-Evans, H., Square planar (SP-4) and octahedral (OC-6) complexes of platinum (II) and-(IV) with predetermined chirality at the metal center. *Inorganic chemistry* **1996,** *35* (17), 4889-4895.
58. Kauffmann, T. In *In search of new organometallic reagents for organic synthesis*, Berlin, Heidelberg, Springer Berlin Heidelberg: Berlin, Heidelberg, 1980; pp 109-147.
59. Brooks, J.; Babayan, Y.; Lamansky, S.; Djurovich, P. I.; Tsyba, I.; Bau, R.; Thompson, M. E., Synthesis and characterization of phosphorescent cyclometalated platinum complexes. *Inorganic Chemistry* **2002,** *41* (12), 3055-3066.
60. Tsujimoto, H.; Yagi, S.; Honda, Y.; Terao, H.; Maeda, T.; Nakazumi, H.; Sakurai, Y., Photoluminescent properties of heteroleptic cyclometalated platinum(II) complexes bearing 1,3-bis(3,4-dibutoxyphenyl)propane-1,3-dionate as an ancillary ligand. *Journal of Luminescence* **2010,** *130* (2), 217-221.
61. Koo, C.-K.; Wong, K.-L.; Man, C. W.-Y.; Lam, Y.-W.; So, L. K.-Y.; Tam, H.-L.; Tsao, S.-W.; Cheah, K.-W.; Lau, K.-C.; Yang, Y.-Y., A bioaccumulative cyclometalated platinum (II) complex with two-photon-induced emission for live cell imaging. *Inorganic chemistry* **2009,** *48* (3), 872-878.
62. Rausch, A. F.; Homeier, H. H.; Yersin, H., Organometallic Pt (II) and Ir (III) triplet emitters for OLED applications and the role of spin–orbit coupling: A study based on high-resolution optical spectroscopy. In *Photophysics of Organometallics*, Springer: 2010; pp 193-235.
63. Koo, C.-K.; Wong, K.-L.; Man, C. W.-Y.; Tam, H.-L.; Tsao, S.-W.; Cheah, K.-W.; Lam, M. H.-W., Two-photon plasma membrane imaging in live cells by an amphiphilic, water-soluble cyctometalated platinum (II) complex. *Inorganic chemistry* **2009,** *48* (16), 7501-7503.
64. Mauro, M.; Aliprandi, A.; Septiadi, D.; Kehr, N. S.; De Cola, L., When self-assembly meets biology: luminescent platinum complexes for imaging applications. *Chemical Society Reviews* **2014,** *43* (12), 4144-4166.
65. Adachi, C.; Baldo, M. A.; Thompson, M. E.; Forrest, S. R., Nearly 100% internal phosphorescence efficiency in an organic light-emitting device. *Journal of Applied Physics* **2001,** *90* (10), 5048-5051.
66. Baldo, M.; Lamansky, S.; Burrows, P.; Thompson, M.; Forrest, S., Very high-efficiency green organic light-emitting devices based on electrophosphorescence. *Applied Physics Letters* **1999,** *75*, 4.
67. King, K.; Spellane, P.; Watts, R. J., Excited-state properties of a triply ortho-metalated iridium (III) complex. *Journal of the American Chemical Society* **1985,** *107* (5), 1431-1432.
68. Sajoto, T.; Djurovich, P. I.; Tamayo, A. B.; Oxgaard, J.; Goddard, W. A.; Thompson, M. E., Temperature Dependence of Blue Phosphorescent Cyclometalated Ir(III) Complexes. *Journal of the American Chemical Society* **2009,** *131* (28), 9813-9822.
69. Berger, R. J.; Stammler, H. G.; Neumann, B.; Mitzel, N. W., fac-Ir (ppy) 3: Structures in the Gas-Phase and of a New Solid Modification. *European Journal of Inorganic Chemistry* **2010,** *2010* (11), 1613-1617.
70. Tanaka, D.; Sasabe, H.; Li, Y.-J.; Su, S.-J.; Takeda, T.; Kido, J., Ultra high efficiency green organic light-emitting devices. *Japanese Journal of Applied Physics* **2006,** *46* (1L), L10.
71. Kawamura, Y. G., Kenichi; Brooks, Jason; Brown, Julie J; Sasabe, Hiroyuki; Adachi, Chihaya., 100% phosphorescence quantum efficiency of Ir(III) complexes in organic semiconductor films. *Applied Physics Letters* **2005,** *86* (7), 071104.
72. Sprouse, S.; King, K.; Spellane, P.; Watts, R. J., Photophysical effects of metal-carbon. sigma. bonds in ortho-metalated complexes of iridium (III) and rhodium (III). *Journal of the American Chemical Society* **1984,** *106* (22), 6647-6653.

73. Dedeian, K.; Djurovich, P.; Garces, F.; Carlson, G.; Watts, R., A new synthetic route to the preparation of a series of strong photoreducing agents: fac-tris-ortho-metalated complexes of iridium (III) with substituted 2-phenylpyridines. *Inorganic Chemistry* **1991,** *30* (8), 1685-1687.
74. Tamayo, A. B.; Alleyne, B. D.; Djurovich, P. I.; Lamansky, S.; Tsyba, I.; Ho, N. N.; Bau, R.; Thompson, M. E., Synthesis and characterization of facial and meridional tris-cyclometalated iridium (III) complexes. *Journal of the American Chemical Society* **2003,** *125* (24), 7377-7387.
75. Meyer, T. J., Photochemistry of metal coordination complexes: metal to ligand charge transfer excited states. *Pure and Applied Chemistry* **1986,** *58* (9), 1193-1206.
76. Cummings, S. D.; Eisenberg, R., Tuning the excited-state properties of platinum (II) diimine dithiolate complexes. *Journal of the American Chemical Society* **1996,** *118* (8), 1949-1960.
77. Ide, N.; Matsusue, N.; Kobayashi, T.; Naito, H., Photoluminescence properties of facial- and meridional-Ir(ppy)3 thin films. *Thin Solid Films* **2006,** *509* (1), 164-167.
78. Lamansky, S.; Djurovich, P.; Murphy, D.; Abdel-Razzaq, F.; Kwong, R.; Tsyba, I.; Bortz, M.; Mui, B.; Bau, R.; Thompson, M. E., Synthesis and Characterization of Phosphorescent Cyclometalated Iridium Complexes. *Inorganic Chemistry* **2001,** *40* (7), 1704-1711.
79. Sarada, G.; Yoon, J.; Cho, W.; Cho, M.; Cho, D. W.; Kang, S. O.; Nam, Y.; Lee, J. Y.; Jin, S.-H., Substituent position engineering of diphenylquinoline-based Ir (III) complexes for efficient orange and white PhOLEDs with high color stability/low efficiency roll-off using a solution-processed emission layer. *Journal of Materials Chemistry C* **2016,** *4* (1), 113-120.
80. Sarada, G.; Sim, B.; Cho, W.; Yoon, J.; Gal, Y.-S.; Kim, J.-J.; Jin, S.-H., New sky-blue and bluish–green emitting Ir(III) complexes containing an azoline ancillary ligand for highly efficient PhOLEDs. *Dyes and Pigments* **2016,** *131*, 60-68.
81. Yang, C. H.; Cheng, Y. M.; Chi, Y.; Hsu, C. J.; Fang, F. C.; Wong, K. T.; Chou, P. T.; Chang, C. H.; Tsai, M. H.; Wu, C. C., Blue-Emitting Heteroleptic Iridium(III) Complexes Suitable for High-Efficiency Phosphorescent OLEDs. *Angewandte Chemie* **2007,** *119* (14), 2470-2473.
82. Kessler, F.; Watanabe, Y.; Sasabe, H.; Katagiri, H.; Nazeeruddin, M. K.; Grätzel, M.; Kido, J., High-performance pure blue phosphorescent OLED using a novel bis-heteroleptic iridium(iii) complex with fluorinated bipyridyl ligands. *Journal of Materials Chemistry C* **2013,** *1* (6), 1070-1075.
83. Lee, S. Y.; Shin, D. M., Effects of the Trifluoromethyl Group on the Emission Efficiency of Red Phosphorescent Iridium(III) Complexes. *Journal of Nanoscience and Nanotechnology* **2018,** *18* (7), 5007-5012.
84. Park, S.; Sunesh, C. D.; Kim, H.; Chae, H.; Lee, J.; Choe, Y., Preparations of iridium complexes containing phenanthroline ancillary ligands and electrical properties of cationic iridium-based light-emitting electrochemical cells. *Surface and Interface Analysis* **2012,** *44* (11-12), 1479-1482.
85. Bolink, H. J.; Cappelli, L.; Cheylan, S.; Coronado, E.; Costa, R. D.; Lardiés, N.; Nazeeruddin, M. K.; Ortí, E., Origin of the large spectral shift in electroluminescence in a blue light emitting cationic iridium(iii) complex. *Journal of Materials Chemistry* **2007,** *17* (48), 5032-5041.
86. De Angelis, F.; Fantacci, S.; Evans, N.; Klein, C.; Zakeeruddin, S. M.; Moser, J.-E.; Kalyanasundaram, K.; Bolink, H. J.; Grätzel, M.; Nazeeruddin, M. K., Controlling Phosphorescence Color and Quantum Yields in Cationic Iridium Complexes: A Combined Experimental and Theoretical Study. *Inorganic Chemistry* **2007,** *46* (15), 5989-6001.
87. He, L.; Qiao, J.; Duan, L.; Dong, G.; Zhang, D.; Wang, L.; Qiu, Y., Toward Highly Efficient Solid-State White Light-Emitting Electrochemical Cells: Blue-Green to Red Emitting Cationic Iridium Complexes with Imidazole-Type Ancillary Ligands. *Advanced Functional Materials* **2009,** *19* (18), 2950-2960.
88. Di Marco, G.; Lanza, M.; Mamo, A.; Stefio, I.; Di Pietro, C.; Romeo, G.; Campagna, S., Luminescent Mononuclear and Dinuclear Iridium(III) Cyclometalated Complexes

Immobilized in a Polymeric Matrix as Solid-State Oxygen Sensors. *Analytical Chemistry* **1998,** *70* (23), 5019-5023.
89. Polson, M.; Fracasso, S.; Bertolasi, V.; Ravaglia, M.; Scandola, F., Iridium cyclometalated complexes with axial symmetry. Synthesis and photophysical properties of a trans-biscyclometalated complex containing the terdentate ligand 2, 6-diphenylpyridine. *Inorganic chemistry* **2004,** *43* (6), 1950-1956.
90. Harding, R. E.; Lo, S.-C.; Burn, P. L.; Samuel, I. D., Non-radiative decay mechanisms in blue phosphorescent iridium (III) complexes. *Organic electronics* **2008,** *9* (3), 377-384.
91. Nonoyama, M., Benzo [h] quinolin-10-yl-N Iridium (III) Complexes. *Bulletin of the Chemical Society of Japan* **1974,** *47* (3), 767-768.
92. Williams, J. A. G., Multinuclear Iridium Complexes. *Iridium (III) in Optoelectronic and Photonics Applications* **2017**, 71-109.
93. Carlson, G. A.; Djurovich, P. I.; Watts, R. J., Widely varying photophysical properties of ligand-nitrated bis (. mu.-chloro) tetrakis (2-phenylpyridinato) diiridium (III). *Inorganic Chemistry* **1993,** *32* (21), 4483-4484.
94. Flamigni, L.; Barbieri, A.; Sabatini, C.; Ventura, B.; Barigelletti, F., Photochemistry and photophysics of coordination compounds: iridium. In *Photochemistry and Photophysics of Coordination Compounds II*, Springer: 2007; pp 143-203.
95. Chandrasekhar, V.; Mahanti, B.; Bandipalli, P.; Bhanuprakash, K., Cyclometalated iridium (III) complexes containing hydroxide/chloride Ligands: isolation of heterobridged dinuclear iridium (III) compounds containing μ-OH and μ-pyrazole ligands. *Inorganic chemistry* **2012,** *51* (20), 10536-10547.
96. Fernández-Cestau, J.; Giménez, N.; Lalinde, E.; Montaño, P.; Moreno, M. T.; Sánchez, S., Synthesis, Characterization, and Properties of Doubly Alkynyl Bridging Dinuclear Cyclometalated Iridium(III) Complexes. *Organometallics* **2015,** *34* (9), 1766-1778.
97. Didier, P.; Ortmans, I.; Kirsch-De Mesmaeker, A.; Watts, R., Electrochemistry and absorption and emission spectroscopy of new orthometalated complexes of rhodium (III) and iridium (III) with the ligands 1, 4, 5, 8-tetraazaphenanthrene and 1, 4, 5, 8, 9, 12-hexaazatriphenylene. *Inorganic chemistry* **1993,** *32* (23), 5239-5245.
98. Serroni, S.; Juris, A.; Campagna, S.; Venturi, M.; Denti, G.; Balzani, V., Tetranuclear bimetallic complexes of ruthenium, osmium, rhodium, and iridium. synthesis, absorption spectra, luminescence, and electrochemical properties. *Journal of the American Chemical Society* **1994,** *116* (20), 9086-9091.
99. Chandrasekhar, V.; Rahaman, S. W.; Hajra, T.; Das, D.; Ghatak, T.; Rafiq, S.; Sen, P.; Bera, J. K., A trinuclear bright red luminophore containing cyclometallated Ir (III) motifs. *Chemical Communications* **2011,** *47* (38), 10836-10838.
100. Auffrant, A.; Barbieri, A.; Barigelletti, F.; Lacour, J.; Mobian, P.; Collin, J.-P.; Sauvage, J.-P.; Ventura, B., Bimetallic Iridium(III) Complexes Consisting of Ir(ppy)2 Units (ppy = 2-Phenylpyridine) and Two Laterally Connected NΛN Chelates as Bridge: Synthesis, Separation, and Photophysical Properties. *Inorganic Chemistry* **2007,** *46* (17), 6911-6919.
101. Donato, L.; McCusker, C. E.; Castellano, F. N.; Zysman-Colman, E., Mono- and Dinuclear Cationic Iridium(III) Complexes Bearing a 2,5-Dipyridylpyrazine (2,5-dpp) Ligand. *Inorganic Chemistry* **2013,** *52* (15), 8495-8504.
102. Tsuboyama, A.; Takiguchi, T.; Okada, S.; Osawa, M.; Hoshino, M.; Ueno, K., A novel dinuclear cyclometalated iridium complex bridged with 1, 4-bis [pyridine-2-yl] benzene: its structure and photophysical properties. *Dalton Transactions* **2004,** (8), 1115-1116.
103. Kozhevnikov, V. N.; Durrant, M. C.; Williams, J. A. G., Highly Luminescent Mixed-Metal Pt (II)/Ir (III) Complexes: Bis-Cyclometalation of 4, 6-Diphenylpyrimidine As a Versatile Route to Rigid Multimetallic Assemblies. *Inorganic chemistry* **2011,** *50* (13), 6304-6313.
104. Williams, J. A. G., The coordination chemistry of dipyridylbenzene: N-deficient terpyridine or panacea for brightly luminescent metal complexes. *Chemical Society Reviews* **2009,** *38* (6), 1783-1801.

105. Lanoë, P.-H.; Tong, C. M.; Harrington, R. W.; Probert, M. R.; Clegg, W.; Williams, J. A. G.; Kozhevnikov, V. N., Ditopic bis-terdentate cyclometallating ligands and their highly luminescent dinuclear iridium (III) complexes. *Chemical Communications* **2014,** *50* (52), 6831-6834.
106. Ho, C.-L.; Wong, W.-Y.; Gao, Z.-Q.; Chen, C.-H.; Cheah, K.-W.; Yao, B.; Xie, Z.-Y.; Wang, Q.; Ma, D.-G.; Wang, L.-X.; Yu, X.-M.; Kwok, H.-S.; Lin, Z.-Y., Red-Light-Emitting Iridium Complexes with Hole-Transporting 9-Arylcarbazole Moieties for Electrophosphorescence Efficiency/Color Purity Trade-off Optimization. *Advanced Functional Materials* **2008,** *18* (2), 319-331.
107. Hwang, F.-M.; Chen, H.-Y.; Chen, P.-S.; Liu, C.-S.; Chi, Y.; Shu, C.-F.; Wu, F.-I.; Chou, P.-T.; Peng, S.-M.; Lee, G.-H., Iridium (III) complexes with orthometalated quinoxaline ligands: subtle tuning of emission to the saturated red color. *Inorganic chemistry* **2005,** *44* (5), 1344-1353.
108. Adamovich, V.; Brooks, J.; Tamayo, A.; Alexander, A. M.; Djurovich, P. I.; D'Andrade, B. W.; Adachi, C.; Forrest, S. R.; Thompson, M. E., High efficiency single dopant white electrophosphorescent light emitting diodes. *New Journal of Chemistry* **2002,** *26* (9), 1171-1178.
109. Fleetham, T.; Huang, L.; Li, J., Tetradentate Platinum Complexes for Efficient and Stable Excimer-Based White OLEDs. *Advanced Functional Materials* **2014,** *24* (38), 6066-6073.
110. Li, K.; Guan, X.; Ma, C.-W.; Lu, W.; Chen, Y.; Che, C.-M., Blue electrophosphorescent organoplatinum(ii) complexes with dianionic tetradentate bis(carbene) ligands. *Chemical Communications* **2011,** *47* (32), 9075-9077.
111. Vezzu, D. A. K.; Deaton, J. C.; Jones, J. S.; Bartolotti, L.; Harris, C. F.; Marchetti, A. P.; Kondakova, M.; Pike, R. D.; Huo, S., Highly Luminescent Tetradentate Bis-Cyclometalated Platinum Complexes: Design, Synthesis, Structure, Photophysics, and Electroluminescence Application. *Inorganic Chemistry* **2010,** *49* (11), 5107-5119.
112. Lin, Y. Y.; Chan, S. C.; Chan, M. C. W.; Hou, Y. J.; Zhu, N.; Che, C. M.; Liu, Y.; Wang, Y., Structural, Photophysical, and Electrophosphorescent Properties of Platinum(II) Complexes Supported by Tetradentate N2O2 Chelates. *Chemistry – A European Journal* **2003,** *9* (6), 1263-1272.
113. Kui, S. C.; Chow, P. K.; Cheng, G.; Kwok, C.-C.; Kwong, C. L.; Low, K.-H.; Che, C.-M., Robust phosphorescent platinum (ii) complexes with tetradentate O∧ N∧ C∧ N ligands: high efficiency OLEDs with excellent efficiency stability. *Chemical Communications* **2013,** *49* (15), 1497-1499.
114. Kui, S. C.; Chow, P. K.; Tong, G. S. M.; Lai, S. L.; Cheng, G.; Kwok, C. C.; Low, K. H.; Ko, M. Y.; Che, C. M., Robust Phosphorescent Platinum (II) Complexes Containing Tetradentate O^ N^ C^ N Ligands: Excimeric Excited State and Application in Organic White-Light-Emitting Diodes. *Chemistry–A European Journal* **2013,** *19* (1), 69-73.
115. Baldo, M. A.; O'brien, D.; You, Y.; Shoustikov, A.; Sibley, S.; Thompson, M.; Forrest, S. R., Highly efficient phosphorescent emission from organic electroluminescent devices. *Nature* **1998,** *395* (6698), 151.
116. D'Andrade, B. W.; Thompson, M. E.; Forrest, S. R., Controlling exciton diffusion in multilayer white phosphorescent organic light emitting devices. *Advanced Materials* **2002,** *14* (2), 147-151.
117. Turner, E.; Bakken, N.; Li, J., Cyclometalated Platinum Complexes with Luminescent Quantum Yields Approaching 100%. *Inorganic Chemistry* **2013,** *52* (13), 7344-7351.
118. Fleetham, T.; Li, G.; Wen, L.; Li, J., Efficient "Pure" Blue OLEDs Employing Tetradentate Pt Complexes with a Narrow Spectral Bandwidth. *Advanced Materials* **2014,** *26* (41), 7116-7121.
119. Chen, D.; Li, K.; Guan, X.; Cheng, G.; Yang, C.; Che, C.-M., Luminescent Iridium(III) Complexes Supported by a Tetradentate Trianionic Ligand Scaffold with Mixed O, N, and C Donor Atoms: Synthesis, Structures, Photophysical Properties, and Material Applications. *Organometallics* **2017,** *36* (7), 1331-1344.

120. Rani, S.; Kumar, S.; Chandra, S., Synthesis of NNNN Tetradentate Macrocyclic Ligand and its Pd(II), Pt(II), Ru(III), and Ir(III) Complexes: Spectroscopic, Thermal, and Antimicrobial Studies. *Synthesis and Reactivity in Inorganic, Metal-Organic, and Nano-Metal Chemistry* **2010,** *40* (10), 940-946.
121. Laskar, I. R.; Chen, T.-M., Tuning of Wavelengths: Synthesis and Photophysical Studies of Iridium Complexes and Their Applications in Organic Light Emitting Devices. *Chemistry of Materials* **2004,** *16* (1), 111-117.
122. Murphy, L.; Brulatti, P.; Fattori, V.; Cocchi, M.; Williams, J. A. G., Blue-shifting the monomer and excimer phosphorescence of tridentate cyclometallated platinum(ii) complexes for optimal white-light OLEDs. *Chemical Communications* **2012,** *48* (47), 5817-5819.
123. Bernanose, A., Electroluminescence of organic compounds. *British Journal of Applied Physics* **1955,** *6* (S4), S54.
124. Tang, C. W.; VanSlyke, S. A., Organic electroluminescent diodes. *Applied physics letters* **1987,** *51* (12), 913-915.
125. Caspar, J. V.; Meyer, T. J., Photochemistry of tris(2,2'-bipyridine)ruthenium(2+) ion (Ru(bpy)32+). Solvent effects. *Journal of the American Chemical Society* **1983,** *105* (17), 5583-5590.
126. Baldo, M. A.; Thompson, M. E.; Forrest, S. R., High-efficiency fluorescent organic light-emitting devices using a phosphorescent sensitizer. *Nature* **2000,** *403*, 750.
127. Köhler, A.; Wilson, J. S.; Friend, R. H., Fluorescence and Phosphorescence in Organic Materials. *Advanced Materials* **2002,** *14* (10), 701-707.
128. Karzazi, Y., Organic light emitting diodes: Devices and applications. *J. Mater. Environ. Sci* **2014,** *5* (1), 1-12.
129. Dodabalapur, A., Organic light emitting diodes. *Solid State Communications* **1997,** *102* (2-3), 259-267.
130. Geffroy, B.; le Roy, P.; Prat, C., Organic light-emitting diode (OLED) technology: materials, devices and display technologies. *Polymer International* **2006,** *55* (6), 572-582.
131. Joseph, S.; Ruth, S., Organic light-emitting devices (OLEDs) and OLED-based chemical and biological sensors: an overview. *Journal of Physics D: Applied Physics* **2008,** *41* (13), 133001.
132. Helfrich, W.; Schneider, W., Recombination radiation in anthracene crystals. *Physical Review Letters* **1965,** *14* (7), 229.
133. Li, W.; Li, J.; Wang, F.; Gao, Z.; Zhang, S., Universal host materials for high-efficiency phosphorescent and delayed-fluorescence OLEDs. *ACS applied materials & interfaces* **2015,** *7* (47), 26206-26216.
134. Tao, Y.; Yang, C.; Qin, J., Organic host materials for phosphorescent organic light-emitting diodes. *Chemical Society Reviews* **2011,** *40* (5), 2943-2970.
135. Tsai, M. H.; Lin, H. W.; Su, H. C.; Ke, T. H.; Wu, C. c.; Fang, F. C.; Liao, Y. L.; Wong, K. T.; Wu, C. I., Highly Efficient Organic Blue Electrophosphorescent Devices Based on 3,6-Bis(triphenylsilyl)carbazole as the Host Material. *Advanced Materials* **2006,** *18* (9), 1216-1220.
136. Zhang, T.; Liang, Y.; Cheng, J.; Li, J., A CBP derivative as bipolar host for performance enhancement in phosphorescent organic light-emitting diodes. *Journal of Materials Chemistry C* **2013,** *1* (4), 757-764.
137. Evans, R. C.; Douglas, P.; Winscom, C. J., Coordination complexes exhibiting room-temperature phosphorescence: evaluation of their suitability as triplet emitters in organic light emitting diodes. *Coordination chemistry reviews* **2006,** *250* (15-16), 2093-2126.
138. Hisamatsu, Y.; Aoki, S., Design and Synthesis of Blue-Emitting Cyclometalated Iridium (III) Complexes Based on Regioselective Functionalization. *European Journal of Inorganic Chemistry* **2011,** *2011* (35), 5360-5369.
139. Holmes, R.; Forrest, S.; Sajoto, T.; Tamayo, A.; Djurovich, P.; Thompson, M.; Brooks, J.; Tung, Y.-J.; D'andrade, B.; Weaver, M., Saturated deep blue organic electrophosphorescence using a fluorine-free emitter. *Applied Physics Letters* **2005,** *87* (24), 243507.

140. Sivasubramaniam, V.; Brodkorb, F.; Hanning, S.; Loebl, H. P.; van Elsbergen, V.; Boerner, H.; Scherf, U.; Kreyenschmidt, M., Fluorine cleavage of the light blue heteroleptic triplet emitter FIrpic. *Journal of Fluorine Chemistry* **2009,** *130* (7), 640-649.
141. Byun, Y.; Jeon, W. S.; Lee, T.-W.; Lyu, Y.-Y.; Chang, S.; Kwon, O.; Han, E.; Kim, H.; Kim, M.; Lee, H.-J., Study on a set of bis-cyclometalated Ir (iii) complexes with a common ancillary ligand. *Dalton Transactions* **2008,** (35), 4732-4741.
142. Jeon, S. O.; Jang, S. E.; Son, H. S.; Lee, J. Y., External Quantum Efficiency Above 20% in Deep Blue Phosphorescent Organic Light-Emitting Diodes. *Advanced Materials* **2011,** *23* (12), 1436-1441.
143. Tsuzuki, T.; Shirasawa, N.; Suzuki, T.; Tokito, S., Color tunable organic light-emitting diodes using pentafluorophenyl-substituted iridium complexes. *Advanced Materials* **2003,** *15* (17), 1455-1458.
144. Ho, C.-L.; Li, H.; Wong, W.-Y., Red to near-infrared organometallic phosphorescent dyes for OLED applications. *Journal of Organometallic Chemistry* **2014,** *751*, 261-285.
145. Wu, C.; Tao, S.; Chen, M.; Wong, F.-L.; Yuan, Y.; Mo, H.-W.; Zhao, W.; Lee, C.-S., Efficient and Stable Deep-Red Phosphorescent Organic Light-Emitting Diodes Based on an Iridium Complex Containing a Benzoxazole-substituted Ancillary Ligand. *Chemistry – An Asian Journal* **2013,** *8* (11), 2575-2578.
146. Kamtekar, K. T.; Monkman, A. P.; Bryce, M. R., Recent Advances in White Organic Light-Emitting Materials and Devices (WOLEDs). *Advanced Materials* **2010,** *22* (5), 572-582.
147. Schanda, J., *Colorimetry: understanding the CIE system*. John Wiley & Sons: 2007.
148. Kanno, H. S., Yiru; Forrest, SR, High-efficiency top-emissive white-light-emitting organic electrophosphorescent devices. *Applied Physics Letters* **2005,** *86* (26), 263502.
149. Sun, Y. F. S. R., High-efficiency white organic light emitting devices with three separate phosphorescent emission layers. *Applied Physics Letters* **2007,** *91* (26), 263503.
150. Li, K.; Tong, G. S. M.; Wan, Q.; Cheng, G.; Tong, W.-Y.; Ang, W.-H.; Kwong, W.-L.; Che, C.-M., Highly phosphorescent platinum (II) emitters: photophysics, materials and biological applications. *Chemical Science* **2016,** *7* (3), 1653-1673.
151. Zhang, J.; Zhao, F.; Zhu, X.; Wong, W.-K.; Ma, D.; Wong, W.-Y., New phosphorescent platinum(ii) Schiff base complexes for PHOLED applications. *Journal of Materials Chemistry* **2012,** *22* (32), 16448-16457.
152. Ephraim, J., Ueber die einwirkung von aldehyden auf thioamide I. *Berichte der deutschen chemischen Gesellschaft* **1891,** *24* (1), 1026-1031.
153. Johnson, J. R.; Ketcham, R., Thiazolothiazoles. I. The Reaction of Aromatic Aldehydes with Dithioöxamide1. *Journal of the American Chemical Society* **1960,** *82* (11), 2719-2724.
154. Auffrant, A.; Barbieri, A.; Barigelletti, F.; Collin, J.-P.; Flamigni, L.; Sabatini, C.; Sauvage, J.-P., Dinuclear Iridium (III) Complexes Consisting of Back-to-Back tpy−(ph) n−tpy Bridging Ligands (n= 0, 1, or 2) and Terminal Cyclometallating Tridentate N− C− N Ligands. *Inorganic chemistry* **2006,** *45* (26), 10990-10997.
155. Whittle, V. L.; Williams, J. A. G., A New Class of Iridium Complexes Suitable for Stepwise Incorporation into Linear Assemblies: Synthesis, Electrochemistry, and Luminescence. *Inorganic Chemistry* **2008,** *47* (15), 6596-6607.
156. Shin, C. H.; Huh, J. O.; Baek, S. J.; Kim, S. K.; Lee, M. H.; Do, Y., Dinuclear Iridium(III) Complexes Linked by a Bis(β-diketonato) Bridging Ligand: Energy Convergence versus Aggregation-Induced Emission. *European Journal of Inorganic Chemistry* **2010,** *2010* (23), 3642-3651.
157. Neve, F.; Crispini, A.; Serroni, S.; Loiseau, F.; Campagna, S., Novel Dinuclear Luminescent Compounds Based on Iridium(III) Cyclometalated Chromophores and Containing Bridging Ligands with Ester-Linked Chelating Sites. *Inorganic Chemistry* **2001,** *40* (6), 1093-1101.
158. Steel, P. J.; Caygill, G. B., Cyclometallated compounds V. Double cyclopalladation of diphenyl pyrazines and related ligands. *Journal of Organometallic Chemistry* **1990,** *395* (3), 359-373.

159. Rausch, A. F.; Murphy, L.; Williams, J. G.; Yersin, H., Probing the excited state properties of the highly phosphorescent Pt (dpyb) Cl compound by high-resolution optical spectroscopy. *Inorganic chemistry* **2009,** *48* (23), 11407-11414.
160. Rausch, A. F.; Murphy, L.; Williams, J. G.; Yersin, H., Improving the performance of Pt (II) complexes for blue light emission by enhancing the molecular rigidity. *Inorganic chemistry* **2011,** *51* (1), 312-319.
161. Yutaka, T.; Obara, S.; Ogawa, S.; Nozaki, K.; Ikeda, N.; Ohno, T.; Ishii, Y.; Sakai, K.; Haga, M.-a., Syntheses and Properties of Emissive Iridium(III) Complexes with Tridentate Benzimidazole Derivatives. *Inorganic Chemistry* **2005,** *44* (13), 4737-4746.
162. Gildea, L. F.; Batsanov, A. S.; Williams, J. A. G., Bright orange/red-emitting rhodium (III) and iridium (III) complexes: tridentate N^ C^ N-cyclometallating ligands lead to high luminescence efficiencies. *Dalton Transactions* **2013,** *42* (29), 10388-10393.
163. Stoessel, P. Metal Complexes. WO2014094961A1, 26/06/2014, 2014.
164. Dixon, I. M.; Collin, J.-P.; Sauvage, J.-P.; Flamigni, L.; Encinas, S.; Barigelletti, F., A family of luminescent coordination compounds: iridium() polyimine complexes. *Chemical Society Reviews* **2000,** *29* (6), 385-391.
165. Yao, S.-Y.; Ou, Y.-L.; Ye, B.-H., Asymmetric synthesis of enantiomerically pure mono-and binuclear bis (cyclometalated) iridium (III) complexes. *Inorganic chemistry* **2016,** *55* (12), 6018-6026.
166. Powell, D. A.; Maki, T.; Fu, G. C., Stille cross-couplings of unactivated secondary alkyl halides using monoorganotin reagents. *Journal of the American Chemical Society* **2005,** *127* (2), 510-511.
167. Mee, S. P. H.; Lee, V.; Baldwin, J. E., Significant Enhancement of the Stille Reaction with a New Combination of Reagents—Copper(I) Iodide with Cesium Fluoride. *Chemistry - A European Journal* **2005,** *11* (11), 3294-3308.
168. Baird, M. S.; de Meijere, A.; Chessum, N.; Couty, S.; Dzielendziak, A., *Science of Synthesis: Houben-Weyl Methods of Molecular Transformations Vol. 48: Alkanes*. Georg Thieme Verlag: 2014; Vol. 48.
169. Wei, X.; Peng, J.; Cheng, J.; Xie, M.; Lu, Z.; Li, C.; Cao, Y., High Performance Polymer Electrophosphorescent Devices with tert-Butyl Group Modified Iridium Complexes as Emitters. *Advanced Functional Materials* **2007,** *17* (16), 3319-3325.
170. Ishiyama, T.; Murata, M.; Miyaura, N., Palladium (0)-catalyzed cross-coupling reaction of alkoxydiboron with haloarenes: a direct procedure for arylboronic esters. *The Journal of Organic Chemistry* **1995,** *60* (23), 7508-7510.
171. Ammermann, S.; Daniliuc, C.; Jones, P. G.; du Mont, W.-W.; Kowalsky, W.; Johannes, H.-H., A unique six-membered chelated iridium complex. *Dalton Transactions* **2008,** (31), 4095-4098.
172. Alessio, E., Synthesis and reactivity of Ru-, Os-, Rh-, and Ir-halide− sulfoxide complexes. *Chemical reviews* **2004,** *104* (9), 4203-4242.
173. Yao, J. H.; Zhen, C.; Loh, K. P.; Chen, Z.-K., Novel iridium complexes as high-efficiency yellow and red phosphorescent light emitters for organic light-emitting diodes. *Tetrahedron* **2008,** *64* (48), 10814-10820.
174. Lin, C. H.; Chang, Y. Y.; Hung, J. Y.; Lin, C. Y.; Chi, Y.; Chung, M. W.; Lin, C. L.; Chou, P. T.; Lee, G. H.; Chang, C. H.; Lin, W. C., Iridium(III) Complexes of a Dicyclometalated Phosphite Tripod Ligand: Strategy to Achieve Blue Phosphorescence Without Fluorine Substituents and Fabrication of OLEDs. *Angewandte Chemie International Edition* **2011,** *50* (14), 3182-3186.
175. Wang, B.; Liang, F.; Hu, H.; Liu, Y.; Kang, Z.; Liao, L.-S.; Fan, J., Strongly phosphorescent platinum (ii) complexes supported by tetradentate benzazole-containing ligands. *Journal of Materials Chemistry C* **2015,** *3* (31), 8212-8218.
176. Ishiyama, T.; Ishida, K.; Miyaura, N., Synthesis of pinacol arylboronates via cross-coupling reaction of bis(pinacolato)diboron with chloroarenes catalyzed by palladium(0)–tricyclohexylphosphine complexes. *Tetrahedron* **2001,** *57* (49), 9813-9816.

177. Acharyya, R.; Basuli, F.; Wang, R.-Z.; Mak, T. C. W.; Bhattacharya, S., Iridium(III) Complexes Formed by O−H and/Or C−H Activation of 2-(Arylazo)phenols. *Inorganic Chemistry* **2004,** *43* (2), 704-711.
178. Miyaura, N.; Suzuki, A., Palladium-catalyzed cross-coupling reactions of organoboron compounds. *Chemical reviews* **1995,** *95* (7), 2457-2483.
179. Miyaura, N.; Yanagi, T.; Suzuki, A., The Palladium-Catalyzed Cross-Coupling Reaction of Phenylboronic Acid with Haloarenes in the Presence of Bases. *Synthetic Communications* **1981,** *11* (7), 513-519.
180. Li, K.; Ming Tong, G. S.; Wan, Q.; Cheng, G.; Tong, W.-Y.; Ang, W.-H.; Kwong, W.-L.; Che, C.-M., Highly phosphorescent platinum(ii) emitters: photophysics, materials and biological applications. *Chemical Science* **2016,** *7* (3), 1653-1673.
181. Narine, A. A.; Wilson, P. D., Synthesis and evaluation of 7-hydroxyindan-1-one-derived chiral auxiliaries. *Canadian Journal of Chemistry* **2005,** *83* (5), 413-419.
182. Goldring, W. P. D.; Bouazzaoui, S.; Malone, J. F., A rearrangement–cycloaddition approach to spiro-fused indanones. *Tetrahedron Letters* **2011,** *52* (9), 960-963.
183. Levy, J.-N.; Latham, C. M.; Roisin, L.; Kandziora, N.; Fruscia, P. D.; White, A. J. P.; Woodward, S.; Fuchter, M. J., The design and synthesis of novel IBiox N-heterocyclic carbene ligands derived from substituted amino-indanols. *Organic & Biomolecular Chemistry* **2012,** *10* (3), 512-515.
184. Parada, G. A.; Glover, S. D.; Orthaber, A.; Hammarström, L.; Ott, S., Hydrogen Bonded Phenol-Quinolines with Highly Controlled Proton-Transfer Coordinate. *European Journal of Organic Chemistry* **2016,** *2016* (20), 3365-3372.
185. Walker, S. E.; Lamb, C. J. C.; Beattie, N. A.; Nikodemiak, P.; Lee, A. L., Oxidative Heck desymmetrisation of 2,2-disubstituted cyclopentene-1,3-diones. *Chemical Communications* **2015,** *51* (19), 4089-4092.
186. Tao, R.; Qiao, J.; Zhang, G.; Duan, L.; Wang, L.; Qiu, Y., Efficient Near-Infrared-Emitting Cationic Iridium Complexes as Dopants for OLEDs with Small Efficiency Roll-off. *The Journal of Physical Chemistry C* **2012,** *116* (21), 11658-11664.
187. Slater, J. W.; Steel, P. J., Syntheses of new binucleating heterocyclic ligands. *Tetrahedron letters* **2006,** *47* (39), 6941-6943.
188. Zampese, J. A.; Keene, F. R.; Steel, P. J., Diastereoisomeric dinuclear ruthenium complexes of 2, 5-di (2-pyridyl) thiazolo [5, 4-d] thiazole. *Dalton Transactions* **2004,** (24), 4124-4129.
189. Beves, J. E.; Danon, J. J.; Leigh, D. A.; Lemonnier, J. F.; Vitorica-Yrezabal, I. J., A Solomon link through an interwoven molecular grid. *Angewandte Chemie International Edition* **2015,** *54* (26), 7555-7559.
190. Gras, M.; Therrien, B.; Süss-Fink, G.; Casini, A.; Edafe, F.; Dyson, P. J., Anticancer activity of new organo-ruthenium, rhodium and iridium complexes containing the 2-(pyridine-2-yl)thiazole N,N-chelating ligand. *Journal of Organometallic Chemistry* **2010,** *695* (8), 1119-1125.
191. Bevk, D.; Marin, L.; Lutsen, L.; Vanderzande, D.; Maes, W., Thiazolo [5, 4-d] thiazoles–promising building blocks in the synthesis of semiconductors for plastic electronics. *RSC Advances* **2013,** *3* (29), 11418-11431.
192. Chambron, J.-C.; Sauvage, J.-P., Topologically complex molecules obtained by transition metal templation: it is the presentation that determines the synthesis strategy. *New Journal of Chemistry* **2013,** *37* (1), 49-57.
193. Cukurovali, A.; Yilmaz, İ.; Kirbag, S., Spectroscopic Characterization and Biological Activity of Salicylaldehyde Thiazolyl Hydrazone Ligands and their Metal Complexes. *Transition Metal Chemistry* **2006,** *31* (2), 207-213.
194. Srivastava, A.; Yang, J.; Zhao, B.; Jiang, Y.; Blackmon, W.; Kraemer, B., Highly Efficient and Scalable Process for Demethylation of 6-(2,4-Dimethoxybenzoyl)chromen-2-one and Other Aryl Methyl Ethers. *Synthetic Communications* **2010,** *40* (12), 1765-1771.
195. Daniels, R. E. Multimetallic Emitters for Bioimaging and Display Applications. Northumbria University, Northumbria University, 2017.

196. Dessi, A.; Calamante, M.; Mordini, A.; Zani, L.; Taddei, M.; Reginato, G., Microwave-activated synthesis of thiazolo[5,4-d]thiazoles by a condensation/oxidation sequence. *RSC Advances* **2014,** *4* (3), 1322-1328.
197. Jensen, M. P.; Lange, S. J.; Mehn, M. P.; Que, E. L.; Que, L., Biomimetic Aryl Hydroxylation Derived from Alkyl Hydroperoxide at a Nonheme Iron Center. Evidence for an FeIVO Oxidant. *Journal of the American Chemical Society* **2003,** *125* (8), 2113-2128.
198. Pander, P.; Bulmer, R.; Martinscroft, R.; Thompson, S.; Lewis, F.; Penfold, T.; Dias, F.; Kozhevnikov, V., 1, 2, 4-Triazines in the Synthesis of Bipyridine Bisphenolate ONNO Ligands and Their Highly Luminescent Tetradentate Pt (II) Complexes for Solution-Processable OLEDs. *Inorganic Chemistry* **2018,** *57* (7), 3825-3832.
199. Jou, J.-H.; Hsieh, C.-Y.; Chen, P.-W.; Kumar, S.; Hong, J. H. In *Candlelight style organic light-emitting diode: a plausibly human-friendly safe night light*, SPIE: 2014; p 8.
200. Jou, J.-H.; Su, Y.-T.; Liu, S.-H.; He, Z.-K.; Sahoo, S.; Yu, H.-H.; Chen, S.-Z.; Wang, C.-W.; Lee, J.-R., Wet-process feasible candlelight OLED. *Journal of Materials Chemistry C* **2016,** *4* (25), 6070-6077.
201. Kempf, B.; Hampel, N.; Ofial, A. R.; Mayr, H., Structure–Nucleophilicity Relationships for Enamines. *Chemistry–A European Journal* **2003,** *9* (10), 2209-2218.
202. Zhou, Q.-Q.; Yuan, X.; Xiao, Y.-C.; Dong, L.; Chen, Y.-C., Aminocatalytic asymmetric Diels–Alder reaction of phosphorus dienophiles and 2,4-dienals. *Tetrahedron* **2013,** *69* (48), 10369-10374.
203. Holligan, B. M.; Jeffery, J. C.; Norgett, M. K.; Schatz, E.; Ward, M. D., The co-ordination chemistry of mixed pyridine-phenol ligands; spectroscopic and redox properties of mononuclear ruthenium complexes with (pyridine)6-(phenolate) donor sets (x= 1 or 2). *Journal of the Chemical Society, Dalton Transactions* **1992,** (23), 3345-3351.